Monitoring of Passive Optical Networks Utilising an Optical Coding Technique

A thesis submitted in fulfillment of the requirements for the degree of Doctor of Philosophy by

Huda Saleh Abbas
MEng, BCS

School of Engineering
College of Science, Engineering and Health
RMIT University

September 2017

Statement

I certify that except where due acknowledgement has been made, the work is that of the author alone; the work has not been submitted previously, in whole or in part, to qualify for any other academic award; the content of the thesis is the result of work which has been carried out since the official commencement date of the approved research program; any editorial work, paid or unpaid, carried out by a third party is acknowledged; and, ethics procedures and guidelines have been followed.

Huda Saleh Abbas

12 September 2017

Acknowledgements

This thesis is dedicated to my parents, brothers and sisters, my husband, and my children for their support, patience and love.

I wish to acknowledge the important contributions of Associate Professor Mark A Gregory, my primary supervisor, who advised and supported me. I thank him for trusting in my capabilities. Also, I thank my second supervisor Professor Michael Austin for his guidance. I acknowledge the opportunity given to me by the government of Saudi Arabia and The Custodian of the Two Holy Mosques Scholarship for financial support, which provided the opportunity to further my education. By undertaking this PhD, I have an opportunity to contribute to my country, the education sector and society.

Abstract

Passive Optical Networks (PONs) have become the most popular fibre based access networks over the last decade. They are widely deployed for use in Fibre-to-the-Premises (FTTP) scenarios. PON is a point-to-multipoint connection (P2MP) between an optical line terminal (OLT) located at the central office (CO) and multiple optical network units (ONU) at the customer premises. The next generation of PONs (NG-PON) are likely to deploy a ring-and-spur long reach PON (LR-PON). NG-PON aims to accommodate more ONUs, extend the network coverage out to 100 km, minimize complexity and improve operational outcomes. An all fibre access network, operating over extended distances, presents a reliability risk, thereby increasing the need for a reliable and cost-effective monitoring system to enhance protection and reduce restoration time. Among existing monitoring techniques, attention is focused on approaches that use optical code division multiplexing (OCDM), also known as optical coding (OC). The OC is applied to a signal that is sent from the network management system (NMS) to the ONUs. The monitoring signal is transmitted onto a fibre and split into a number of sub-signals that are equal in number to the ONUs. Each one of the ONUs receives a sub-signal, encodes it, and then reflects it back to the NMS. The NMS has the capability to identify faulty ONUs by examining the code received from the ONUs. A review of the literature has shown that the use of OCs does improve system performance, especially in the timely detection of faults. Many of the studies, found in the literature, focus on how to implement optical spreading codes that are used in OCDM Access (OCDMA) systems and currently the optical orthogonal code (OOC) is the dominant code implemented for time-domain coding. Although the OOC code performs well, its construction is relatively complex. The available code-words (cardinality) that are offered by OOC are proportional to the code length. Implementing OOC in a high capacity PON requires a long code length causes an inevitable degradation of system performance. Therefore, an improved optical coding

technique for PONs should provide code-words that conform to PON split ratios.

The main objective of the research was to develop an optical spreading code, based on a prime code family for OCDMA systems, that has the capability to accommodate different PON split ratios and with characteristics that improve transmission system performance when compared to existing prime code families. The novel code presented in this thesis is identified as the *extended grouped new modified prime code* (EG-nMPC). The number of code-words generated by the proposed codes are substantially higher than those generated by the existing code families and more compatible to the different PON splitting ratios. In addition, with a low code weight, both power consumption and hardware complexity decreases.

The code performance was evaluated using mathematical models for two transmission formats - pulse position modulation (PPM) and on-off keying (OOK) modulation. The performance of EG-nMPC was compared to other prime codes, and the results show that the proposed code improves the performance of OCDMA in terms of bit-error rate (BER).

As PON is a point-to-multipoint connection oriented access network, downstream traffic is encrypted and broadcast to all ONUs, while the unencrypted upstream traffic from each ONU terminal occurs in a burst mode. The OLT carries out a ranging process to determine transmission delays between ONUs, to prevent collisions between the burst mode traffic from each of the ONUs. In this research, the burst mode traffic ranging process has been replicated in the monitoring system, with this replication providing a fixed equalization delay time for the monitoring transmissions.

To investigate the ring-and-spur LR-PON reliability several protection architectures were evaluated, in term of cost and availability, to determine the optimal protection architecture. In this thesis, the reliability parameter Failure Impact Robustness (FIR), has been used to calculate the failure impact of the different components in ring-and-spur LR-PON, hence selecting the optimal protection scheme.

A PON-based optical communication system model was developed and the proposed EG-nMPC code was incorporated. Fibre split ratios of 32, 64 and 128, were considered in this study. The simulation results show that the EG-nMPC code improves the performance, efficiency and accuracy of the PON transmission monitoring system.

To conclude, this research aims to enhance the PON performance by a fast detection of the fault and quick restoration. This research has contributed to knowledge by identifying a new and novel spreading code that is compatible with the different PON splitting ratios for OC monitoring techniques. By using the ranging process, a fixed equalization delay time has been assigned to each ONU to manage the upstream burst traffic. The spreading code has been implemented in a real-time simulation to show the status of each fibre link. The implementation was carried out based on 1-D tree topology system. However, the proposed EG-nMPC can be exploited to enable network monitoring that is based on hybrid 1D/2D coding. This coding is complementary with the structure of LR-PON as explained in section 8.2.3. In addition, with the use of the FIR parameter for the different components in the ring-and-spur architecture, an optimal protection scheme for both OLT and the ring (feeder fibre), has been nominated. This protection scheme ensures that protection, availability and cost are at their optimal values.

Table of Contents

List of Figures

List of Tables

List of Acronyms and Abbreviations

ABD	availability block diagrams
Alloc-ID	Allocation Identifier
APON	Asynchronous transfer mode passive optical network
ATM	Asynchronous transfer mode
AWG	Array waveguide grating
BER	Bit-error rate
BFSA	Brillouin frequency shift assignment
BPON	Broadband passive optical network
BW map	Bandwidth map
CO	Central Office
CoS	Classes of Service
CWDM	Coarse wavelength division multiplexing
DBA	Dynamic bandwidth allocation
DBWA	Dense bandwidth and wavelength allocation
DPMPC	Double-padded modified prime code
DPSK	Differential phase-shift keying
DRA	Distributed Raman amplifier
DS-OCDM	Direct Sequence OCDM
DWDM	Dense wavelength division multiplexing
EDFA	Erbium doped fibre amplifier
EG-nMPC	extended grouped new modified prime code
EPC	Extended prime code

EPON	Ethernet PON
FBG	Fibre Bragg grating
FIR	Failure Impact Robustnes
FSAN	Full service access network group
FTTP	Fibre-to-the-Premises
Gbps	Gigabyte per second
GEM	GPON Encapsulation Method
GF	Galois field
GPMPC	Group padded modified prime code
GPON	Gigabit passive optical network
GTC	the GPON Transmission Convergence
IEEE	Institute of Electrical and Electronic Engineers
ITU	International Telecommunications Union and its standards (ITU-T)
IP	Internet Protocol
IPPC	Incrementally Pulse Positioned Code
LAG	Link Aggregation
LAN	Local area network
LR-PON	Long reach PON
MAI	Multiple access interference
MCIP	Multiple-Customers Interference Probability
ML-OOC	Multilevel-Optical Orthogonal Code
MPC	Modified prime code
NG-PON1	Next generation PON stage 1
NG-PON2	Next generation PON stage 2
n-MPC	New modified prime code

NMS	Network Management System
OBS	Optical burst switching
OC	Optical coding
OCDM	Optical code division multiplexing
OCDMA	Optical code division multiple access system
ODN	Optical distribution network
OFDM	Optical frequency division multiplexing
OLT	Optical line terminal
ONU	Optical network unit
OOC	Optical orthogonal codes
OOK	On–off keying
ODL	Optical tapped delay line
OTDR	Optical time domain reflectometer
P	Prime number
P2MP	Point to multi-point
PC	Prime code
PCBd	Physical Control Block downstream
PLOu	Physical Layer Overhead
PMPC	Padded modified prime code
PON	Passive optical networks
PPM	Pulse position modulation
PSC	Power Splitter/Combiner
QCC	Quadratic congruence code
QoS	Quality of service
RN	Remote node

SIR	Signal to Interference Ratio
SLA	Service Level Agreement
SL-RSOA	Self-injection locked reflective semiconductor optical amplifier
SMAC	Slotted Medium Access Control
SNI	Server Node Interface
SNR	Signal-to-Noise Ratio
SNIR	Signal-to-Noise-and-Interference Ratio
SOA	Semiconductor optical amplifier
SPON	Slotted-PON
T-CONT	traffic containers
TDM	Time division multiplexing
TDMA	Time division multiple access
T-MPC	Transposed modified prime code
T-SPMPC	Transposed sparse-padded modified prime code
TWDM	Time/wavelength division multiplexing
UNI	User Network Interface
WDM	Wavelength division multiplexing
XG-PON	10 Gigabit-capable passive optical network
XGS-PON	10-gigabit symmetrical passive optical network
X-TDM	Hybrid time division multiplexing
X-WDM	Hybrid wavelength division multiplexing

Chapter 1 INTRODUCTION

The research carried out relates to the monitoring of Passive Optical Networks (PON), utilizing the Optical Coding (OC) technique. In the introductory chapter, an overview of PON monitoring is provided followed by the research problem, research objectives, contribution, and methodology. The introductory chapter ends with a thesis summary.

1.1 Introduction

PON is defined as a broadband access network technology that offer advantages, when employed to provide Fibre-to-the-Premises (FTTP), including cost-effectiveness; a point to multi-point architecture; high quality triple-play service capabilities for data, voice and video; reduced maintenance and operational costs; and high speed internet access [1]. The International Telecommunications Union (ITU) and the Institute of Electrical and Electronic Engineers (IEEE) developed the Asynchronous Transfer Mode (ATM) technology in the 1980s, and this was utilised as the basis for early PON versions including ATM PON (APON), Broadband PON (BPON) and the more recent variation Gigabit PON (GPON); and a second group named Ethernet PON (EPON) [2, 3]. Of these, EPON and GPON are now ubiquitous. A conventional PON architecture is presented in Figure 1-1 [4].

Figure 1-1 shows the PON architecture which consists of an Optical Line Terminal (OLT), Optical Distribution Network (ODN), and Optical Network Units (ONU). The PON Point to Multi-Point (P2MP) architecture includes an OLT that is located in the Central Office (CO), ONUs that are located in premises within a region around the CO and fibre distribution that utilises optical splitters to connect the feeder fibre from the OLT to multiple ONUs using drop fibres [5].

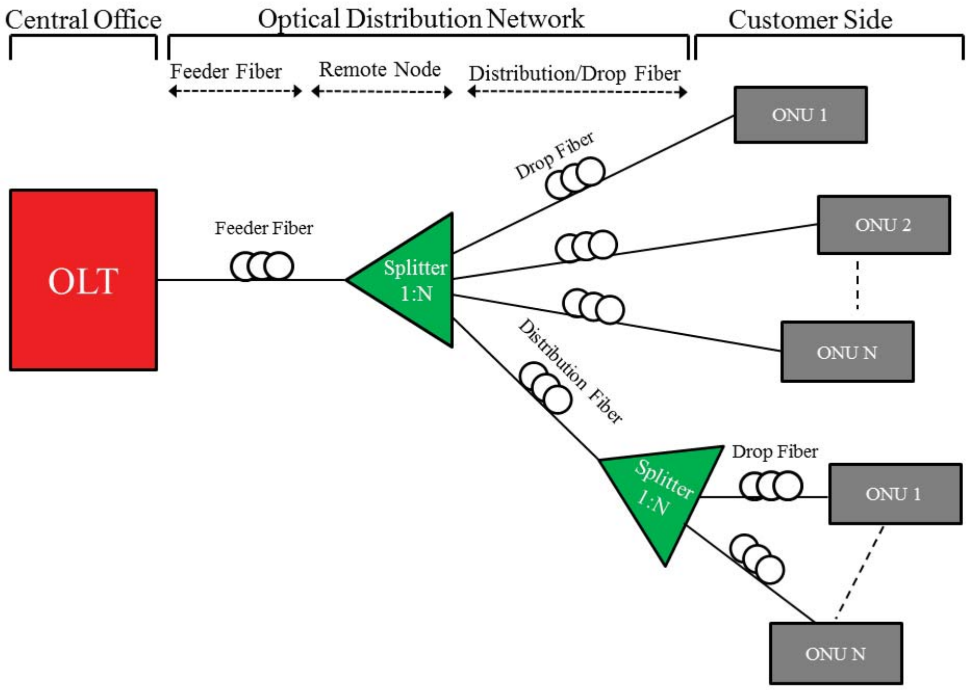

Figure 1-1 PON architecture [4]

The first PON generation was based on Time Division Multiple Access (TDMA), and provided an EPON downstream rate of one gigabit per second (Gbps) and a GPON downstream rate of 2.4 Gbps. The next generation PON stage 1 (NG-PON1) increased the data rate to up to 10 Gbps for both variants. With the rapid expansion of high bandwidth applications and internet services, however, the NG-PON1 was found to be insufficient to meet the demand for more bandwidth and an improved Quality of Service (QoS). To determine an acceptable upgrade pathway, research was conducted to investigate options for the next generation PON stage 2 and one implementation has now occurred (NG-PON2) [4].

PON technologies are classified as either pure or hybrid technologies [6] [7]. Pure technologies include high speed Time Division Multiplexing PON (TDM-PON), Wavelength Division Multiplexing PON (WDM-PON), Optical Code Division Multiplexing PON (OCDM-PON), and Orthogonal Frequency Division Multiplexing PON (OFDM-PON) [8]. Hybrid technologies include hybrid TDM and WDM (TWDM), X-WDM and X-TDM [4, 9, 10].

The predominant methods for implementing PON use either WDM-PON or time TDM-PON, or a combination of the two techniques [11]. Although TDM-PON is a cost-effective technology, it was found to be restrictive in terms of security and bandwidth. WDM-PON provides high bandwidth to multiple ONUs. It is, however, more expensive due to the need for additional equipment [12]. OFDM-PON is scalable and the current implementation has a higher capacity (40 Gbps). It is also efficient and flexible, with dynamic bandwidth allocations for downstream and upstream transmissions [13]. Its flexibility and optical transmission complexity, however, requires more power, setup and may be less secure [14-16]. OCDM-PON makes efficient use of bandwidth and is more secure. However, with an increasing number of ONUs, issues such as multiple access and noise interference could occur [17].

Hybridised TDM-PON and WDM-PON combine the advantages of both technologies [12, 18]. Over time, a TWDM-PON design emerged as standard for NG-PON2 [19], based on performance (40Gbps/10Gbps), power and cost [20].

In terms of topology, ring-and-tree, identified in some of the literature as ring-and-spur, is the dominant topology for NG-PON [21-23]. The ring, feeder fibre, is based on WDM and connects the OLT to a number of Remote Nodes (RN), each of which serves a spur that is based on TDM. A ring-and-spur topology meets the requirements of the NG-PON as it aims to support more than 1000 ONUs over distances up to 100 km and to optimize the fibre infrastructure utilization, enhance scalability, and increase distribution flexibility as additional RNs could be added [24].

The general structure of an OCDM Access (OCDMA) system is based on a star topology as shown in Figure 1-2 [25]. Each communication channel in the system is composed of both transmission and receiver sides connected by a star coupler. The main components of the transmission side are ‘information source’ and ‘encoder’. The main components of the receiver side are ‘decoder’ and ‘receiver’ [26]. Each transmitter on the OCDMA system has been allocated a unique code-word. Transmitted data is based on a binary number to represent the presence or absence of the light (1= presence, 0 = absence) [27]. If the data is a 1, the encoding process will be executed and if it is a 0, the encoded process will not be executed [25]. Each transmitter encodes the data with its corresponding code-word. The decoding process is a reverse operation of the encoding process.

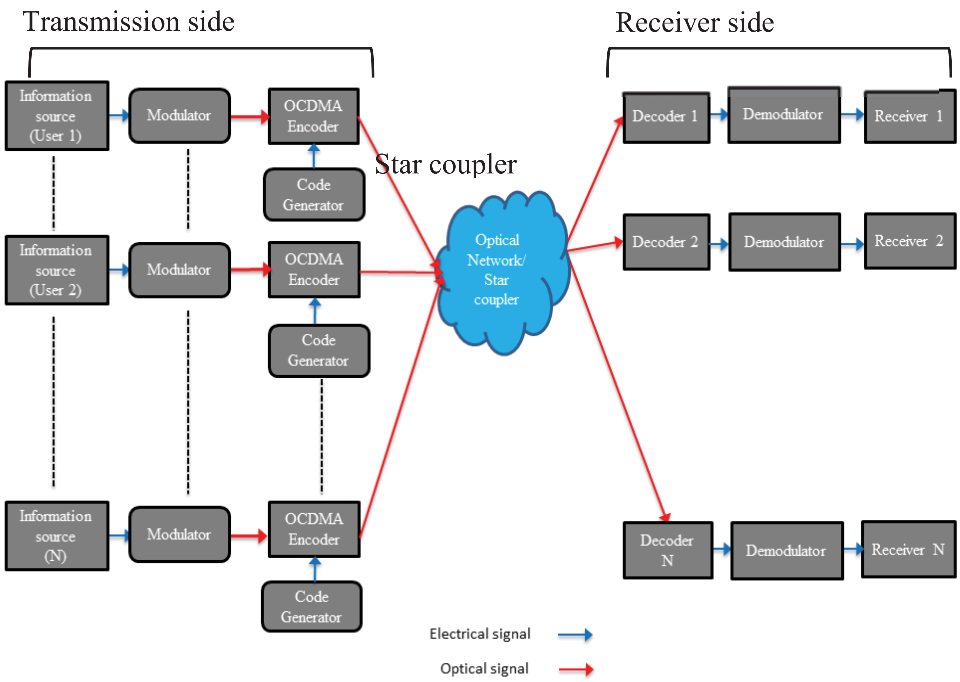

Figure 1-2 OCDMA system [25]

Of the two OCDMA systems, one utilises a coherent approach while the other has an incoherent approach. Incoherent OCDMA is more popular than coherent OCDMA because of the simplicity and robustness of its encoding and decoding processes [28]. Encoding and decoding systems that are based on incoherent OCDMA utilise unipolar codes, due to improved performance compared to the bipolar codes that have been used in radio frequency CDMA [27]. As a result, research has focused on developing new codes. Common unipolar codes include optical orthogonal/pseudo-orthogonal codes (OOC), prime codes (PC), and quadratic congruence codes (QCC). The OOC is quite common due to its performance when compared to other codes utilising measures such as the correlation functions (auto-and cross correlation). However, the construction of an OOC is complex. Several studies have been proposed to improve the performance of PC and QCC. The construction of a PC that is based on congruence techniques is less complex than the construction of OOC [27].

Code-words can be formed by utilizing a one-dimensional (1-D) encoding scheme in either the time or frequency domains. In the case of 1-D coding, the code cardinality (number of available code-words) will be limited. It requires a longer code length to provide more code-words. A two-dimensional (2-D) encoding scheme is a combination of both domains. 2-D encoding has been proposed to solve the limitation associated with code cardinality in 1-D encoding. A three-dimensional (3-D) encoding scheme that uses space or polarization as the third domain, provides a further increase in the code cardinality [29].

The aims of an OCDMA system are, firstly, to accommodate a large number of communication channels in the system and, secondly, to distinguish the signal of the intended transmitter from other transmitters' signals. Increasing the number of communication channels leads to an increase in the Multiple Access Interference (MAI), an undesirable outcome as it leads to system performance degradation. Therefore, implementing an orthogonal code with high auto correlation and low cross-correlation is highly recommended to make the required distinction between signals [30].

Ensuring service reliability is one of the most important requirements for end-users [31]. With the NG-PON architecture, its high capacity and large coverage area, fault management has gained in importance. Network providers aim to reduce failure impact, which refers to minimizing the number of ONUs that are affected by a single failure in the network [31]. Thus, a reliability parameter named Failure Impact Robustness (FIR) has been introduced by

Dixit et al. in [31].

Four types of protection schemes, known as Type A to D, have been standardized in the ITU, Series G, Supplement 51 “Passive optical network protection considerations” to protect sections of the network.

Besides network protection, monitoring the network is another important factor that ensures service continuity. PON monitoring was standardised for surveillance, testing and control by the ITU as either pre- or post-fault [32]. Monitoring techniques are classified as either based on Optical Time Domain Reflectometry (OTDR), or based on non-OTDR. OTDR is based on Fresnel reflection and Rayleigh backscattering, therefore it is a promising technique for monitoring point-to-point connections [33]. Examples of non-OTDR based monitoring techniques are Brillouin Frequency Shift Assignment (BFSA), reference reflector–broadband source, reflected signal, Self-Injection Locked Reflective Semiconductor Optical Amplifier (SL-RSOA), and monitoring based on OCDM, which is referred to as an OC technique [34]. Amongst these techniques, OC has received considerable attention due to its simplicity and cost-effectiveness. This technique overcomes the limitations associated with OTDR and provides a favourable solution to monitor PON with its potentially large number of ONUs connected to each feeder fibre [33]. Several studies have been proposed for PON monitoring based on OC and are discussed in more detail in the literature review.

As discussed in above, the standard OCDMA system requires a code with a high correlation to recognize the intended signal [25]. However, in PON, the OLT performs a ranging process to assign an equalization delay for each ONU to avoid burst collision. Monitoring based OC can apply this ranging process into the monitoring layer; hence the condition of high auto-correlation and low cross-correlation has become less important. The main objective is to provide a number of code-words that are compatible with the PON splitting ratio with smaller

Prime number (P). There is no mention in the literature of a monitoring system that uses codes based on OCDMA codes other than OOC. The use of a PC in this research provides a new and innovative approach that is shown to have several benefits over alternate approaches.

1.2 Research Problem

The aim of PON technologies is to increase data throughput to 40 Gbps and beyond, extend the access network reach, and accommodate more ONUs. This architecture leads to challenges in network monitoring and thus a cost-effective management system is required. The challenges have led to a substantial amount of research being carried out in this area [35]. The ITU L66 recommendation 'Optical fibre cable maintenance criteria for in-service fibre testing in access networks' recommended the standardization of PON maintenance and monitoring functions. According to this recommendation, OTDR has been picked up as the optimal technique for in-service monitoring, testing and measurement. OTDR is a reliable technique that detects and locates the exact location of a fault. However, standard OTDR cannot be implemented in a PON, as PON utilises a P2MP architecture; therefore, research has been carried out to modifying standard OTDR in order to cope with the PON P2MP architecture. The modifications led to limitations in network capacity and an increase in the system complexity [33].

The cost of design, installation and establishment, or the capital cost, for monitoring each fibre link, and the total ongoing system maintenance costs are calculated and provide a life cycle cost for a monitoring system. Thus, monitoring systems should be simplified to reduce costs. Constant monitoring of the ONU links enhances reliability. Utilizing OTDR, however, is not economically feasible for a PON network with a large number of ONUs. The monitoring system should be designed for a large and increasing number of ONUs so there is scope for further research [4]. Monitoring utilising an OC technique is preferred over other techniques due to its simplicity and low cost. This technique utilizes the OOC and PC codes that have been used in OCDMA systems [36].

PON accommodates a potentially large and increasing number of ONUs as new PON versions are developed. The address code chosen must be compatible with the maximum number of ONUs supported by the PON version. The existing families of PC include: basic prime code (PC), extended PC (EPC), modified PC (MPC), new-MPC (n-MPC), padded MPC (PMPC), group PMPC (GPMPC), double PMPC (DPMPC), Transposed-MPC (T-MPC), and transposed-sparse padded MPC (T-SPMPC). Characteristics such as cardinality ($|C|$), length (L), and weight (w) (number of the digit 1 in the code-word) are a function of the prime number (P), hence this number plays an important role in determining those characteristics. Basic PC provides P code-word with length of P^2 and weight of P. MPC, n-MPC, PMPC, DPMPC, and GPMPC provide P^2 code-words with lengths of P^2, P^2+P, P^2+P, P^2+2P, and P^2+2P, respectively, and weights *of* P, $P+1$, $P+1$, $P+2$, and $P+2$, respectively. T-MPC and T-SPMPC provide $2P^2$ code-words with length of P^2 and weight of P and (P+1)/2, respectively.

Considering the existing PC families that support the PON architecture, Table 1-1 below shows the characteristics of different PC families that support the different PON splitting ratios.

It can be observed that there are issues with the current codes to accommodate the different PON splitting ratios. Firstly, the code-words are far more than what is required in many PON networks, which results in a large number of unused codes, leading to an inefficient system. Secondly, increasing the prime number leads to an increase in the weight , which leads to an increase in the hardware (encoder/decoder) complexity, hence power consumption. In addition, increasing the prime number will increase length, resulting in, understandably, an increase in processing time and a drop in efficiency [37].

Table 1-1 The characteristics of different Prime code families

	32				**64**				**128**			
PC family	***P***	**|*C*| (unused codes)**	***L***	***W***	***P***	**|*C*| (unused codes)**	***L***	***W***	***P***	**|*C*| (unused codes)**	***L***	***w***
Basic PC	33	33 (1)	1089	33	67	67 (1)	4486	67	131	131 (3)	17161	131
MPC	7	49 (17)	49	7	11	121 (57)	121	11	13	169 (41)	169	13
n-MPC	7	49 (17)	56	8	11	121 (57)	132	12	13	169 (41)	182	14
PMPC	7	49 (17)	56	8	11	121 (57)	132	12	13	169 (41)	182	14
DPMPC	7	49 (17)	63	9	11	121 (57)	143	13	13	169 (41)	195	15
GPMPC	7	49 (17)	63	9	11	121 (57)	143	13	13	169 (41)	195	15
T-MPC	5	50 (18)	25	5	7	98 (34)	49	7	11	242 (114)	121	11
T-SPMPC	5	50 (18)	25	3	7	98 (34)	49	4	11	242 (114)	121	6

The objective of this research is to develop a spreading code that is suitable for the different PON splitting ratios, and that also possesses improved characteristics in terms of cardinality, length, weight, correlation functions, and BER performance [5].

In terms of protection, the protection types demonstrated in the ITU-T standard are for a PON with a typical tree topology [38]. The literature shows the performance of three protection schemes for a ring-and-spur topology in terms of cost and availability. However, according to ring-and-spur architecture that supports a large number of ONUs, it is important to examine the FIR parameter for every component in the network and, hence, select the appropriate protection schemes.

The research questions are:

1. Can the existing codes implemented in OCDMA systems be modified to

accommodate, with better characteristics, the number of ONUs supported in PON?

2. How would the new application of the FIR parameter improve system performance?
3. What advantages would be achieved when applying PON ranging into the monitoring layer?

These research questions are formulated in such a way so that, when investigated and answered, PON system performance will be enhanced, which leads to faster detection and traffic restoration. Enhancing the monitoring system can be realized by utilizing a proper spreading code with improved characteristics coupled with valuable information gathered from the ranging process that helps to distinguish between codes coming from multiple ONUs. Quick restoration is dependant on selecting the optimal protection scheme, selected by evaluating the FIR parameter. Responses to those questions, when put together, will result in an improvement in the overall performance of PON and a reduction in the outage time.

1.3 Research Objectives

The objective of this research was to improve the design of OCDMA system codes by reducing the prime number used. The smaller prime number should accommodate the number of ONUs in the PON with enhanced characteristics. In addition, the FIR parameter will be used to determine the protection scheme, in terms of cost and availability, for ring-and-spur PON.

Additional research objectives include:

- Modifying the existing code in OCDMA systems, based on the PC family, to achieve a cardinality that has a lower number of unused codes and supports the different PON splitting ratios (32, 64, and 128) with improved characteristics.
- Simplifying encoder and decoder hardware design, based on an optical tapped delay

line by reducing the code weight, hence the number of optical tapped delay lines.

- Gaining an energy-efficient code with a lower code weight where the code sequences are patched with blocks of zeros.

- Using the concept of the PON upstream transmission ranging process found at the data layer, in the monitoring layer as well thereby taking advantage of the fixed upstream transmission interval at the monitoring layer to provide an equalization delay for each ONU.

- Calculating the FIR of the different components in the ring-and-spur system to select the optimal protection scheme, and evaluate its performance.

1.4 Research Contribution

Although there is no shortage of literature on research conducted on OC for PON monitoring, the research in the literature focuses on OOC and related enhanced coding schemes. By focusing on the use of a PC, rather than an OOC, the research carried out, and presented in this thesis, provides a new and innovative approach to improve PON monitoring outcomes. Although PC has been used in OCDMA schemes found in the literature, the outcomes were non-optimal. The proposed PC and monitoring approach is suitable for the different PON splitting ratios and provides the basis for an improvement to the overall monitoring outcomes for PON networks. The modified PC is identified by variations to the code-word numbers, length, and weight. Improved performance was obtained for the three splitting ratios studied (32, 64 and 128) using a PC with a smaller prime number, reduced number of unused codes, shorter length and reduced weight. In addition, FIR was used to determine the components with a high probability of failure thereby potentially affecting a large number of ONUs in a ring-and-spur architecture. The resulting monitoring technique was found to be cost efficient, reliable and suitable for typical PON implementations. The research was modelled and simulations of typical configurations demonstrated the effectiveness of the proposed approach in providing the Network Management System (NMS) with accurate information about the fibre links.

1.5 Research Methodology

The research methodology was designed to permit a logical consideration of the research questions and to build upon the research carried out for each of the research questions. The research outcome was a new approach in the design of spreading codes for PON monitoring based OC techniques.

The methodology adopted for Research Question 1 was to identify code families that might be suitable candidates that could modified to improve monitoring outcomes. The investigation identified that by combining the two coding techniques, padding and extension, that were used in the n-MPC and EPC, respectively, it would be possible to design a new code that could satisfy the research objectives. The resulting code-words were doubled to provide the number of code-words needed and the next step was to build a network model and to carry out simulations to gather results for analysis. The performance of the proposed code was compared to that of the most recent code reported in the literature (T-SPMPC) and to MPC which is the basis of most of the codes identified in the literature.

MATLAB was utilized to evaluate the performance of the codes in an on-off keying model and a pulse position modulation model.

Research Question 2 was approached with the objective to add to what had been found so far by improving the measurement of the reliability of the protection scheme. A variety of protection schemes for ring-and-spur have been utilized to find the optimal design in relation to both cost and reliability. By calculating the FIR of the different components in the ring-and-spur system to select the optimal protection scheme it was possible to evaluate its performance and the outcomes identified that the protection scheme (OLT-Ring) presented in this thesis provides an improvements.

The methodology adopted for Research Question 3 was to consider an improved fibre monitoring technique suitable for PON that could be adopted with future PON systems. A critical aspect of the design was to ensure that upstream monitoring signals would not clash with the monitoring signals from other ONUs. To achieve this objective a fixed delay time was introduced into the monitoring system by taking the advantage of both the fixed burst interval at the monitoring layer, and the concept of the PON ranging process at the data layer. The outcome of this approach was to improve the monitoring system design, efficiency and reliability.

The industry standard VPITransmissionMaker tool was used to evaluate the status of each ONU's link for the three scenarios corresponding to PON splitting ratios (32, 64, 128).

1.6 Publications

Peer reviewed journal and conference publications are listed below:

Journal

1. H. S. Abbas and M. A. Gregory, "Passive optical network survivability: protection, detection and restoration," International Journal of Information, Communication Technology and Applications, vol. 1, pp.128-142, 2014. doi: https://doi.org/10.17972/ajicta20151115.
2. H. S. Abbas and M. A. Gregory, " The Next Generation of Passive Optical Networks: A Review " Journal of Network and Computer Applications (JNCA), 2016. doi: https://doi.org/10.1016/j.jnca.2016.02.015
3. H. S. Abbas, M. A. Gregory and M. Austin, "A New Family of Prime Codes for

Synchronous Optical Code Division Multiple-Access Networks" (submitted to Journal of Computer Networks and Communications – Scopus indexed)

4. H. S. Abbas and M. A. Gregory, "Implementation of OC Monitoring System in PON Networks" (progressing will submitted to Journal of Computer Networks and Communications – Scopus indexed)

Conference

1. H. S. Abbas and M. A. Gregory, "Feeder fibre and OLT protection for ring-and-spur long-reach passive optical network," in Telecommunication Networks and Applications Conference (ATNAC), 2013 Australasian, 2013, pp. 63-68. doi: 10.1109/ATNAC.2013.6705358

2. H. S. Abbas and M. A. Gregory, "OCDM network implementation of 1-D OOC and passive correlation receiver," in Artificial Intelligence with Applications in Engineering and Technology (ICAIET), 2014 4th International Conference on, 2014, pp. 311-316.doi:10.1109/ICAIET.2014.58

1.7 Structure of Thesis

Chapter 1 outlines the significance of this research and briefly introduces its objectives and methodology.

The literature review presented in Chapter 2 is divided into three sections; PON network, OCDMA systems, and a summary of the current research on PON monitoring optical coding techniques.

Chapter 3 focuses on a review and provides a comparative table of different PC families. This is done in order to introduce the proposed code extended grouped new modified prime code (EG-nMPC), which is the subject of this research.

In Chapter 4, the proposed code is introduced. The construction steps and the code parameters are detailed. The performance of the code is analyzed in an incoherent system using both OOK and PPM systems.

Chapter 5 introduces three protection schemes for long-reach PON (LR-PON) based on a ring-and-spur topology. The three protection schemes were examined in terms of availability and cost and then compared to the existing protection schemes.

Chapter 6 presents a definition for the fixed equalization delay for the monitoring layer with an explanation of the overall monitoring system. In addition, it analyses the effect of the pulse width on the different noise sources and on the system performance for the different PON splitting ratios.

Chapter 7 presents the design and implementation of the monitoring system in VPItransmissionMaker. Three scenarios compatible with GPON splitting ratios (32, 64, 128) were simulated. The outcome of implementing the monitoring system does provide the network management with crucial information about the status of each drop fibre link.

The thesis ends with a conclusion, suggestions for future work, appendix and a bibliography.

Chapter 2 LITERATURE REVIEW

The literature review chapter is composed of three main sections; NG-PONs, OCDMA, and PON monitoring based on OC. The first section, NG-PONs, comprises four sub-sections, which are: a review of the different multiplexing techniques of NG-PON including pure, and hybrid TDM and WDM design; an overview of LR-PON; an overview of GPON physical and data link layers; and finally, a review of the reliability aspects of the systems, including protection, and monitoring.

The second section on OCDMA systems includes the encoding process, the devices of encoder and decoder, challenges associated with OCDMA system, design issues of the spreading code, code types, and modulation schemes.

The third section on PON monitoring reviews the most recent work performed on PON monitoring based on OC.

1.1 Next Generation-PON

NG-PON is divided into two stages; NG-PON1 and NG-PON2 [8]. The first standardized NG-PON1 was XG-PON1 (X=10 G=Gigabit PON) that delivers 10 Gbps downstream and 2.5 Gbps upstream (10/2.5G). It uses a single fixed wavelength in each direction [39]. Details about the XG-PON physical layer have been described in ITU-T G.987.2 [40]. The second standardized NG-PON1was XG-PON2, which can be referred to as XGS-PON (X=10, G = Gigabit, S = symmetrical PON) [40]. The latest XGS-PON delivers 10 Gbps in both directions and has a dual rate transmission capability [41].

The most advanced NG-PON2, that has been introduced by the Full Service Access Network Group (FSAN), delivers a minimum of 40 Gbps in the downstream and 10 Gbps in the upstream direction [8]. It aims to extend the coverage, increase both bandwidth and transmission speed, support high capacity and ensures efficiency of both energy and cost [42]. Several enabling technologies have been proposed for NG-PON2. However, TWDM-

PON has been selected as the primary technology for NG-PON2 as it meets the requirements [8].

2.2 Multiplexing Techniques

2.2.1Pure Techniques

This section reviews the pure techniques in terms operations, advantages and disadvantages.

2.2.1.1 Time Division Multiplexing- Passive Optical Network

Using a single wavelength, TDM-PON allows multiple ONUs to share the same bandwidth [43]. TDM-PON structure is shown in Figure 2-1 [13].

The downstream traffic is broadcast from the OLT to all ONUs and a specific time is assigned by the OLT to each ONU to control upstream transmissions. These time slots are allocated in downstream and upstream frames where an algorithm assigns the bandwidth timing to avoid collision [4, 11]. Although TDM-PON is simple and cost effective, the number of ONUs in the system is limited due to the splitter attenuation as well as the available bitrate of the transmitter and receiver at the CO and ONUs [44]. Standard TDM operates over a maximum of 20 km from the OLT with typically 32 ONUs, and a maximum distance of 10 km from OLT typically permits 64 ONUs [44]. In addition, shared bandwidth compromises security through attack or eavesdropping [45].

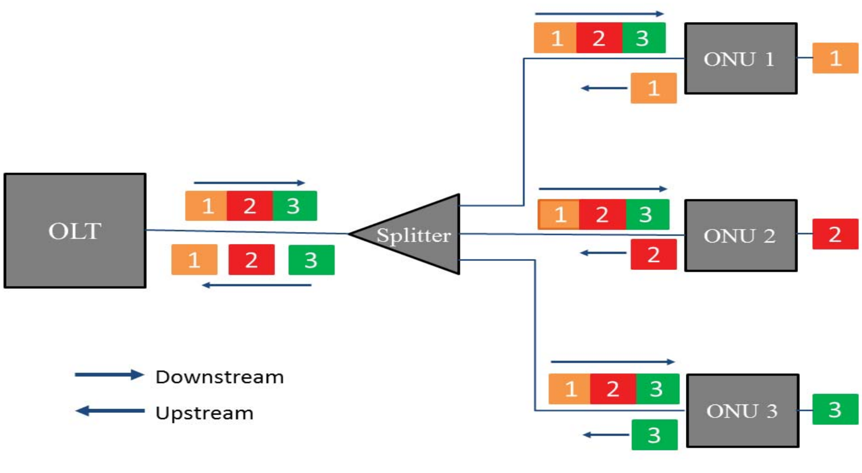

Figure 2-1 Design of TDM-PON [13]

To meet the NG-PON2 standards of 40 Gbps for TDM-PON, system architecture variations were proposed. The first of these variations is a conventional on-off key (OOK). However, it requires a 40 Gbps burst-mode receiver, high-cost 40 GHz electronics and photonics, and highly sensitive receivers [46]. The other system to achieve a bitrate of 40 Gbps is duo-binary modulation [43, 47]. It is similar to a deployed PON system, but uses one wavelength for downstream and another for upstream. In duo-binary modulation, phase and amplitude modulations permit ONUs to have 20 GHz bandwidth and reduce delivery issues such as dispersion [48].

In summary, time division multiplexing was not found to be conducive to upgrading to meet the ITU standards for future technologies.

2.2.1.2 Wavelength Division Multiplexing-Passive Optical Networks

WDM-PON has been considered as an alternative technology to TDM-PON. It provides a virtual point-to-point connection between the OLT and several ONUs; where, each ONU is assigned a different wavelength for upstream and downstream transmission [44].

Several architectures have been introduced to enable WDM-PON implementation. One of the architectures is based on legacy TDM-PON with the use of a band pass splitter at each ONU in order to distinguish between the wavelengths of upstream and downstream transmission. This architecture is shown in Figure 2-2. It does, however, exhibit the power loss drawback that is due to the use of the splitter, reduced security, and difficulties in implementing colorless ONUs [12]. The standard structure of WDM-PON is shown in Figure 2-3 [44]. This design differs from a TDM-PON system by using devices such as an Array Waveguide Grating (AWG) in place of the TDM-PON power splitter [43].

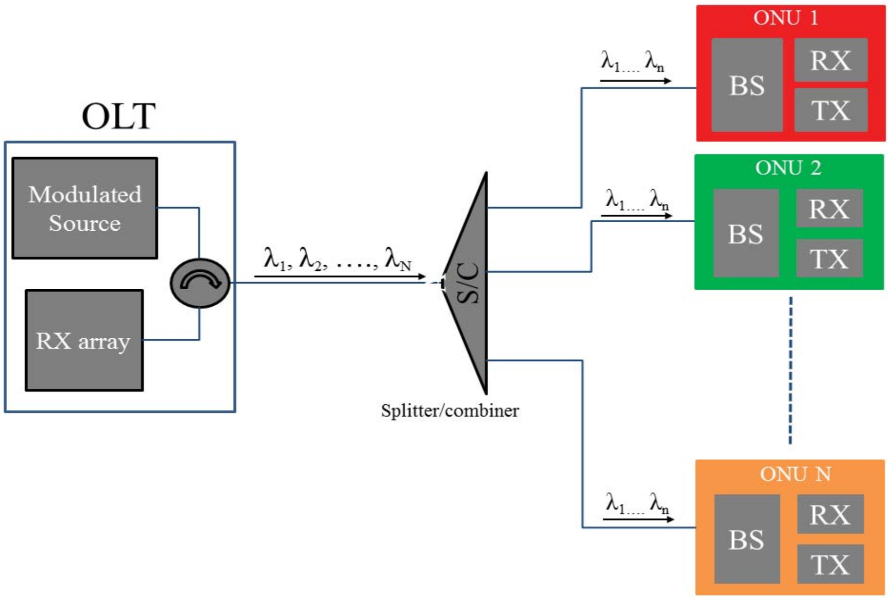

Figure 2-2 WDM-PON based legacy TDM-PON [12]

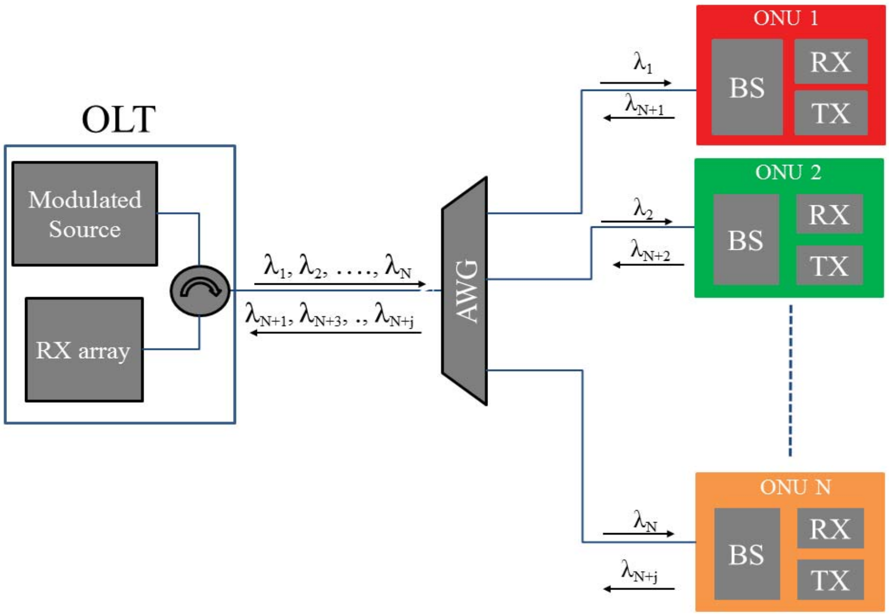

Figure 2-3 Standard WDM-PON [44]

In the downstream transmission, the wavelength channels are routed using a specified port at the AWG from the OLT to the ONUs. ONUs are based on the colored component and each ONU employs a transmitter and receiver to transmit and receive on its specified channel. For upstream transmission, a WDM de-multiplexer and receiver array are equipped at the OLT to process the upstream transmission [44].

WDM-PON is classified into two classes based on the number of wavelengths supported and the wavelength spacing between the individual wavelengths transmitted over a single fibre.

The first class is Dense WDM (DWDM) and its wavelength plan is defined by ITU-T G.694.1, and the second class is Coarse WDM (CWDM) that has its wavelength plan defined by ITU-T G.694.2. The main objective of DWDM is to increase the network capacity by minimizing the wavelength spacing; CWDM aims to reduce the cost where the wavelength spacing is sufficiently high to permit the transmitters to be more accurately controlled [4] [12].

The multiple-wavelength characteristic in WDM-PON offers several unique features. WDM-PON allows every ONU to transmit at the peak speed as the OLT bandwidth is not shared [49, 50]. Additionally, wavelengths are able to support different bitrates and, consequently, different services can be supported for each ONU [44]. Moreover, security is improved and the potential eavesdropping issue is eliminated [50], [51]. Despite these features, a few restrictions make WDM-PON an inappropriate technology to apply to NG-PON2. As a result of the limitation of the number of wavelengths allowed in the system and the large bandwidth requirement, the utilization of the bandwidth is rendered inefficient [10]. Moreover, WDM-PON is cost-ineffective because of the need for extra equipment such as colored ONUs and a transceiver for every wavelength at the OLT [46, 51].

2.2.1.3 Optical Frequency Multiplexing PON

OFDM-PON is an enabling technology that is based on digital signal processing offering high speed and flexible system [52].

The OFDM-PON architecture is similar to the standard PON. It uses a wavelength for downstream transmission and another wavelength for upstream transmission [13]. The OLT generates multiple orthogonal subcarriers that are assigned to different ONUs and each subcarrier is timed. The OLT partitions and distributes the total bandwidth over subcarriers, timeslots, or both, according to ONU demand [15, 16].

OFDM-PON improves the bandwidth flexibility and it is an applicable technology for future PON [8]. Drawbacks of OFDM-PON are its complex receivers reliant on high speed digital signal processors and field programmable gate arrays. The architecture also has a high peak average power ratio from sinusoidal signals for subcarriers in the time domain, generating a higher than average amplitude value [14, 15]. Frequency offset from mismatch of carrier frequencies may also occur [53].

2.2.1.4 Optical Code Division Multiplexing PON

OCDM-PON is an efficient means of offering high data rate, asynchronous transmission, flexibility of ONU allocation, low signal processing latency, symmetric bandwidth and improved network security over other designs [54] [17]. Each ONU in OCDM-PON implements an encoder and a decoder with a unique fixed optical code. The OLT must have all encoders and decoders information to enable its communication with each ONU [8].

Figure 2-4 shows an example of the OCDM-PON network structure using multi-port encoder/decoder at the OLT. The main function of the multi-port encoder/decoder is to generate and recognize the different optical code in a device, this has been developed to support 40-G OCDMA system [54].

The two main limitations of OCDM-PON are the use of encoder and decoder for each ONU as well as at the OLT which increase the overall system cost, and the increase of interference as a result of increasing the number of ONUs [55].

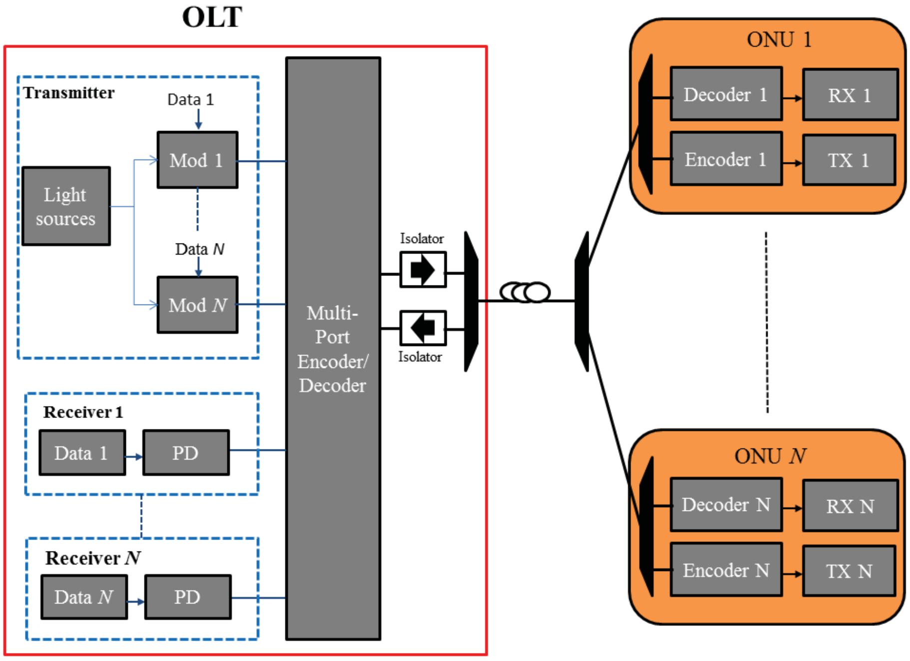

Figure 2-4 Design of OCDM-PON [54]

2.2.2Hybrid TDM and WDM-PON

In 2012, an influential and dispersed international lobby group that operates under the pseudonym of FSAN, selected a TWDM-PON design as the multiplexing technique for NG-PON2 [19]. Their decision was based on the maturity of design's technology, system performance, power consumption and cost [20]. The design was confirmed in 2013 by ITU-T under its G.989 series [56].

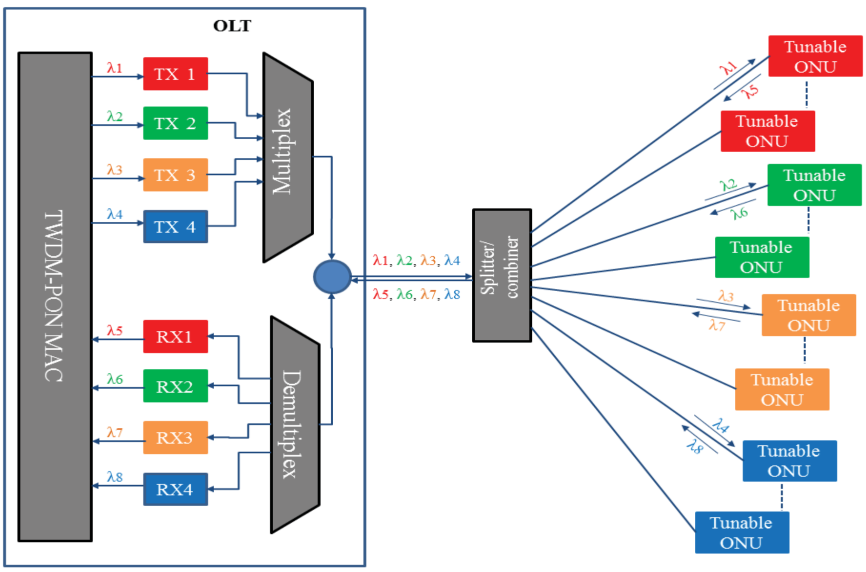

Figure 2-5 Design of TWDM-PON [57]

TWDM-PON combines the simplicity and cost efficiency offered by TDM and the high number of wavelength provided by WDM into one architecture, by transmitting TDM frames to several ONUs over several wavelengths [10, 12]. Standard TWDM-PON consists of four sets of XG-PON1 stacked as four pairs of wavelengths [48].

Figure 2-5 shows TWDM-PON and the wavelength pairs "{λ1, λ5}, {λ2, λ6}, {λ3, λ7} and {λ4, λ8}" [48]. Each XG-PON1 provides 10 Gbps and 2.5 Gbps of data in downstream and upstream transmissions, respectively. Thus, TWDM-PON increases the bit rate up to 40 Gbps for downstream transmission and 10 Gbps for upstream transmission [19]. In a basic network, programmable transmitters and receivers can be tuned to any wavelength. The system remains passive when the OLT has an amplifier, a multiplexor, and the de-multiplexor [48].

Another design that combines power splitters AWG is shown in Figure 2-6. This configuration makes use of identical colourless ONUs and supports a higher number of wavelengths than stacked PON [58].

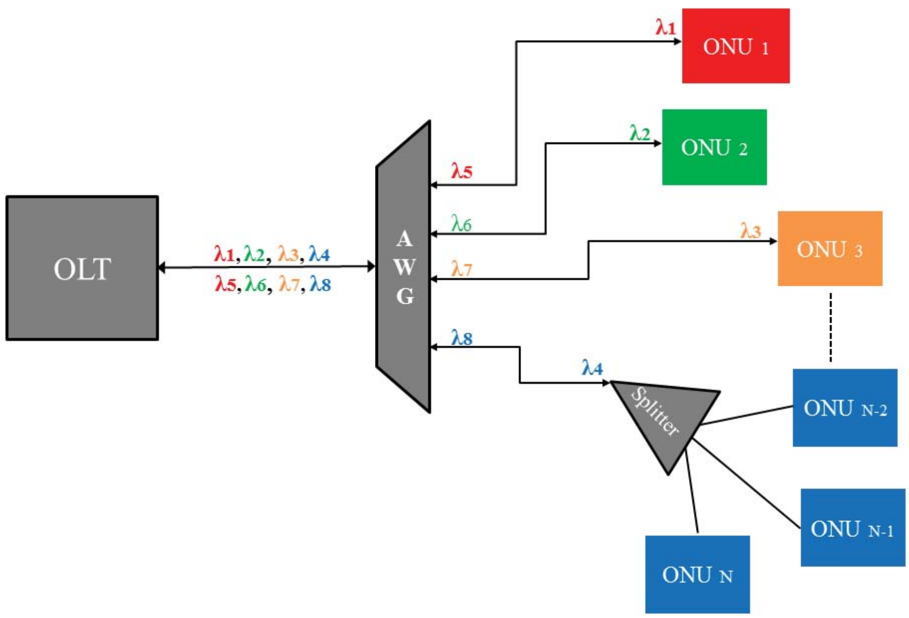

Figure 2-6 TWDM-PON, utilizes a combination of AWG and power splitters [58]

A major limitation of the TWDM-PON is the cross-talk, which occurs at the OLT receiver due to the multiple wavelength channels and dynamic power ranging at the upstream transmission [59]. This issue engenders significant debate in the literature, as researchers identify sources of crosstalk in the upstream transmission and establish mitigation devices at the OLT receiver. To mitigate cross-talk between upstream channels in TWDM-PON, low cost options are offered, such as transmitter bias current and/or modulation current, or placing semiconductor optical amplifiers or variable optical attenuators in the transmitter [60].

Efficient dynamic bandwidth and wavelength allocation maximises performance in TWDM-PON systems. Of the algorithms discussed in the literature, earliest finish time, earliest finish time with void filling [61, 62], off-DBWA and on-DBWA (described as DBWA) [63] were investigated. Other DBWA algorithms, such as Optical Burst Switching Dynamic Bandwidth Allocation (OBS-DBA), were designed for particular network architecture. This algorithm was designed for SARDANA network [64], Slotted Medium Access Control (SMAC) for Slotted PON (SPON) [65], and STARGATE EPON [66].

TWDM-PON has been receiving significant attention and many proposals have been submitted to evaluate its performance [24, 57, 67-72].

2.3 Long-reach PON

Extended reach is an important requirement for NG-PON2 [73]. LR-PON refers to studies of the consolidation of metro and regional access networks [74] (see Figure 2-7).

Figure 2-7 shows the aims of LR-PON. It aims to extend PON's domain up to 100 km. It reduces the number of active elements in the network, minimizes network planning efforts, and reduces the capital expenditure (CAPEX) and OPEX. Several techniques have been studied to realize this objective.[74].

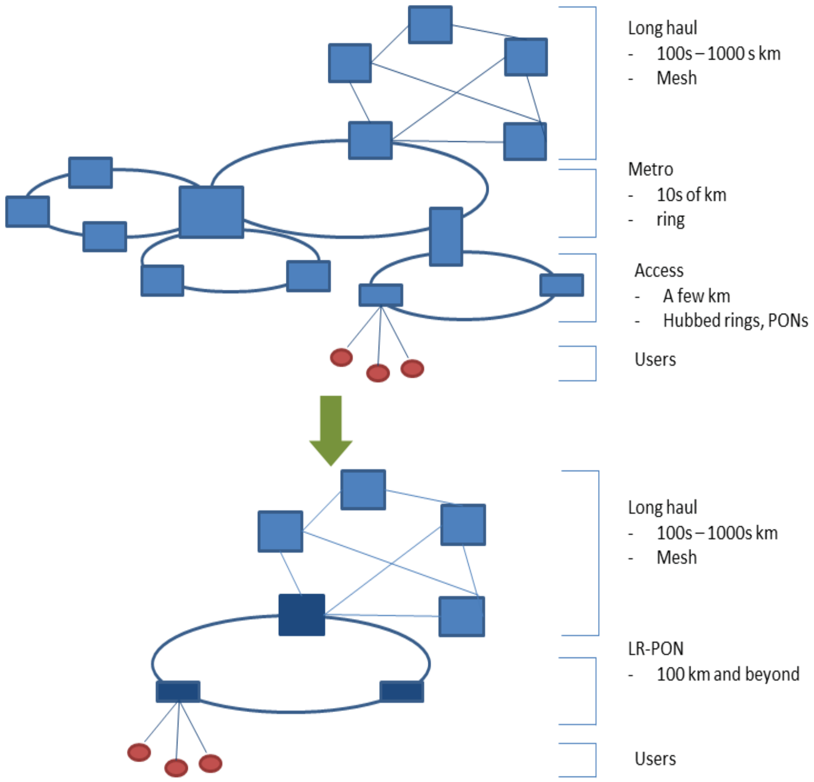

Figure 2-7 Long reach PON [74]

The most common practices to extend the reach of PON are discussed below [9].

Optical amplification. The use of optical amplifiers is widespread. It enables LR-PONs to achieve the target power distribution quotas. There are several types of optical amplifiers including, Erbium Doped Fibre Amplifier (EDFA), Semiconductor Optical Amplifiers (SOA), and Distributed Raman Amplification (DRA). Whilst EDFA is power saving and noise attenuation efficient, it is confined to C and L transmission bands; which renders it unsuitable to cope with the burst of an upstream transmission [9]. Compared to EDFA, SOA has better gain dynamics, simplified wavelength conversion and all-optical regeneration. In addition, it can operate in the O band (1310 nm), C band (1550 nm), and S band (1490 nm) ranges. However, SOA's wavelengths limit simultaneous amplification across multiple wavelengths [9]. DRA supports bidirectional amplification on flat optical gain bandwidth including channels that override those of common optical amplifiers [9].

Electrical Repeater-based networks. Using an Electrical Repeater at a local exchange is another option for optical amplification. Electrical repeaters are useful in retransmission (1R) or re-time and re-transmit (2R) of downstream and upstream signals [9]. Electronic repeaters however, require bit-rate specific burst mode receivers of a wide dynamic range. They also require power, which is not indicative in a passive optical network.

Developed modulation formats and digital coherent detection. With the optical amplification and the electronic repeater it is necessary to provide power in the local exchange, this eliminates one aspect of the passive nature of the network. An alternative option is to keep the distribution network purely passive by using developed modulation formats as well as digital coherent detection [75].

Extending the reach creates issues of medium access control as the round-trip time increases and the DBA control loop is impacted, reducing performance [76]. Although LR-PON is of value amongst PON designs, large propagation delays occur on upstream channels [77].

2.4 PON Reliability

As part of ITU standard requirements, NG-PON2 aims to include high component reliability [48]. As this includes LR-PON, there is a higher probability of fibre damage. This section discusses the reliability aspects of PON including protection schemes and monitoring techniques.

2.4.1PON Protection Schemes

The ITU-T G series recommendations supplement 51, states that there are cases where special PON redundancy and protection switching are required: mobile backhaul, business services and high-density residential complexes [38].

The ITU-T in its recommendation G.984.1 has identified four types of protection systems known as Type A, Type B, Type C, and Type D. Since that time, several studies have considered PON redundancy and protection switching. The variance between the four protection types depends on which part is being protected. Each part in the system has different effects on the system availability and total cost.

The ITU also pointed out that protection of the access network is expensive because the cost is shared only amongst a few ONUs, as compared to the larger number of ONUs serviced by transport networks. Hence, there is a general lack of attention to protection in the access networks.

As the bulk of a PON, the ODN itself constitutes the highest risk factor often due to a requirement for a Service Level Agreement (SLA) meeting 0.99999 availability. However, extending the SLA past 0.99999 means that risk reduction becomes cost prohibitive and arguably unachievable. Operators and providers offer a range of services at and below this capability [38]. An ODN constitutes above-ground cabling susceptible to tree, animal, weather and adverse event damage; underground cabling may be damaged during infrastructure installation (digging) or perhaps by burrowing animals.

Type A duplicates the feeder fibre and a fault requires operator intervention or the use of voltage-controlled optical switch to bypass the fault by connecting the spare fibre between the splitter and the OLT. Type A does not need an additional PON port at the OLT.

Type B protection provides redundancy to the OLT and the feeder fibre. With an additional PON port on the OLT, type B provides automated switching capability with the use of 2 x N optical power splitter. In standard Type B protection, both OLTs are located at the same location. However, to provide protection against catastrophic failures, the two OLTs are located at different locations. Each ONU is attached to both OLTs (primary and secondary) through a 2 x N optical splitter. In normal operation, the ONUs are connected to the primary OLT. In the case of OLT failure, the secondary OLT takes charge of controlling the PON.

This type of protection is referred to as dual-parented protection. Type B represents a simple and inexpensive, as it cost is shared among multiple ONUs.

A Type C redundancy is delivered in the OLT, ODN and ONUs. It combines two fully redundant services connected to the customers' premises as linear 1 + 1 or linear 1:1. In protection based linear 1 + 1, signals are copied and fed to both PONs. Each ONU can select one of the two signals based on some determined conditions (e.g. server defect indication). In the linear 1:1 option, the signal is delivered on one or the other PON, with the OLTs automated in case of failure of one or the other. The duplication, besides offering redundancy, can be used as extra bandwidth by the customer, but extra traffic will not be protected. There may be separate ONUs; with the option that one ONU will have two optical interfaces. Using Link Aggregation (LAG), the PONs are duplicated throughout, including OLTs and separate ONUs. In this type, protection is performed using LAG, a User Network Interface (UNI) and a Server Node Interface (SNI) interfaces. PON in this protection system, presents simple Ethernet links. Extra traffic available on the system is not protected.

Type D redundancy allowed a combination of both protected and non-protected ONUs. In another word, it allowed a combination between type B and Type C redundancy [78]. Type D redundancy, however, has been abandoned (deprecated) [38].

2.4.2Protection for ring-and-spur LR-PON

NG-PON2 is based on ring-and-spur LR-PON [80]. A LR-PON system is described below [81].

Figure 2-8 [81] shows a ring that is based on WDM connecting the OLT to a number of RNs. A Power Splitter/Combiner (PSC) is implemented to each RN to serve the tree (ONUs). Data coming downstream in a waveband Λ_D, is transmitted in a counter-clockwise direction from the CO. At RN_i, Λ_i sub-waveband of n wavelengths is de-multiplexed and dropped to the

PSC, and then to the ONUs. The upstream data flow is multiplexed in RN_i and transmitted counter-clockwise to CO.

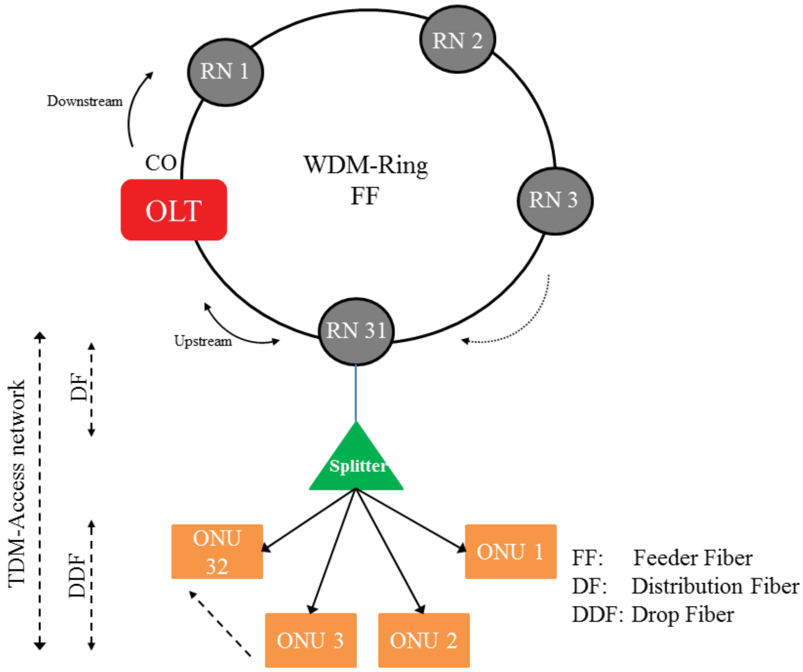

Figure 2-8 Ring-and-spur long reach PON design [81]

As shown in Figure 2-8, the downstream data flow is transmitted from the OLT in a counter-clockwise direction. The upstream data flow is transmitted in both directions. In this scenario, there are 31 RNs, each with a mean 19.5 km link to one splitter. A splitter supports 32 ONUs at a mean 0.5 km distance. Thus, there is a total of 992 ONUs. If a fault occurred along the fibre or at an OLT, all 992 ONUs would be affected. A fault in an RN, distribution fibre or a splitter would affect 32 ONUs, while a fault in ONU or its drop fibre will have an effect on only that ONU. In [82], three protection systems are discussed for such a scenario: access only protection; ring only protection, and full protection. These protection schemes are shown in Figure 2-9 (b), (c), and (d) respectively, where (a) represents a system without protection. Esmail and Fathallah in [82] have evaluated the performance of these systems taking into account the availability and the cost. The analysis has shown that protection that is based on ring duplication is the most optimal scheme when it comes to both reliability and cost.

Some implementations of protection schemes for PON are given in literature. In [79] a protection scheme for PON, that aims to protect the feeder fiber, is presented. In this demonstration, two optical switches are used to switch the traffic between the faulty and working fiber paths. The system implemented obtained a BER of 10^{-15} with feeder fiber length of 20 km. A surviving PON with simple ONUs and switchable OLTs are reported. The survivability was achieved by utilizing a protected-path switching scheme that is based on employing bidirectional colorless *N*x2 and 2x*N* AWGs. The affected traffic can be restored promptly under fiber feeder and distribution link failures, as well as the failure at the remote node. The system achieved a BER of 10^{-9} and a restoration time of 3 ms. The implementation of this work can be found in VPI transmission maker.

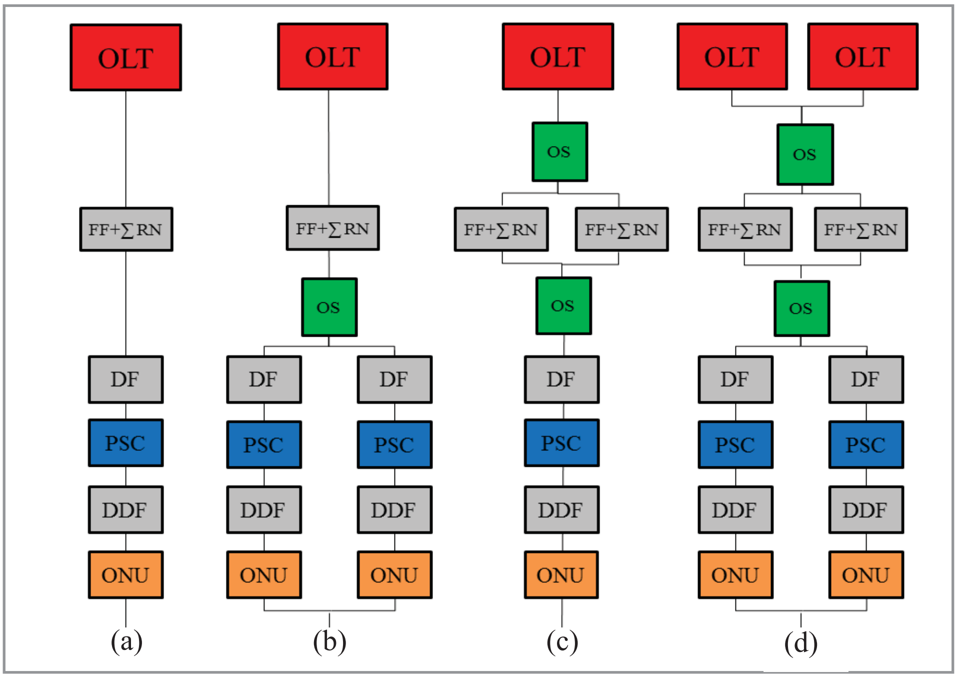

Figure 2-9 Protection systems based on [82]

2.5 PON Monitoring

The ITU has recommendations for maintenance of cable fibre networks [32]. Maintenance in ITU-T categorised into: preventative maintenance and post-fault maintenance. Each maintenance category comprises of three main functions which are: surveillance, testing and control. For post-fault, the functions are usually required. Whereas for the preventative maintenance category, the functions are optional and they are selected based on maintenance rules set by the telecommunication providers. [32]. The recommendations are shown at Table 2-1.

In a recent discussion of optical distribution networks monitoring/checking by the ITU [32], the importance of a distinction between network and system failures within the context of the ONU being connected or not was made. The Union recommended OTDR for diagnosing faults in the network, using a power meter and a light source. OTDR results in a functional relationship between fibre length and power, that contains information about the fibre (see Figure 2-10) [84]. The Union hypothesized that XG-PON2 systems would autonomously detect and locate ODN faults especially between the CO and the first-stage splitter. Monitoring end-to-end performance enables operators to identify dropouts or throttling, and for this higher layer, technology like Ethernet performance monitoring can be used for monitoring and verifying data flows through PON network elements [40].

Standard OTDR cannot be used to monitor all of the PON branches, as PON is a point to multi-point architecture, where the reflected signal would comprise all backward signals coming from multiple branches. Other issues include short range connection points on the fibres, and lack of reliability due to complexity through many ONUs, and the need for high dynamic range for the reflectometer [11, 84].

Table 2-1 ITU PON maintenance recommendations [32]

Maintenance category	Maintenance Activity	Functions	Status
Preventative maintenance	Surveillance (e.g, periodic testing)	Detection of fibre loss increase	Optional
		Detection of fibre deterioration	Optional
		Detection of water penetration	Optional
	Testing (e.g, fibre degradation testing)	Measurement of fibre fault location	Optional
		Measurement of fibre strain distribution	Optional
		Measurement of water location	Optional
	Control (e.g, network element	Fibre identification	Optional

	control)	Fibre transfer	Optional
Post-fault maintenance	Surveillance (e.g, reception of transmission system alarm or customer trouble report)	Interface with transmission operation system Interface with customer service operation	Required Required
	Testing (e.g, fibre fault testing)	Fault distribution between transmission equipment and fibre network Measurement of fibre fault location Confirmation of fibre condition	Required Required Optional
	Control (e.g, cable repair, removel)	Restoration/permanent repair Fibre identification Fibre transfer	Required Required Required

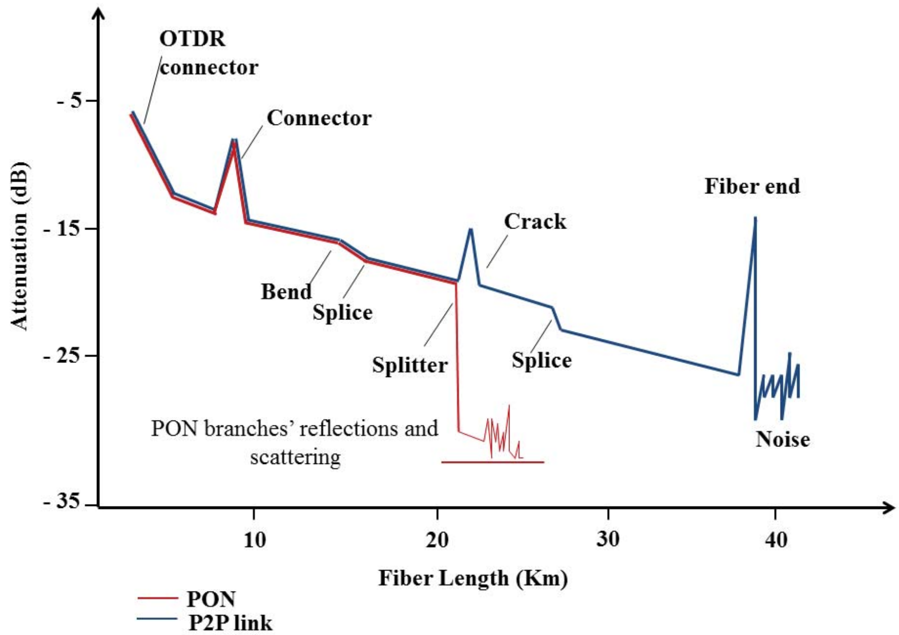

Figure 2-10 OTDR fault trace [84]

Table 2-2 Monitoring techniques shows other optional monitoring techniques that are different from the standard OTDR. One of the techniques that is of interest to this thesis is the OC monitoring technique. This system is scalable, less complex and, consequently, has lower construction costs. However, a reliable fault locating feature has yet to be established, although there are solutions being sought in current research [84, 85].

In OC, monitoring signals are transmitted over the U-band while data signals are transmitted over the L band. At the NMS, located at the CO, an optical downstream monitoring signal is generated. The signal splits at the RN to sub-pulses that are equal in number to the number of branches. A passive encoder, at the extremity of each drop fibre, encodes its sub-pulse by a unique code and then reflects the encoded sub-pulses back to the NMS at the CO. The NMS can detect the faulty branch by checking its corresponding code. The presence of the code denotes a healthy link and the absence of the code denotes broken link [86], (see Figure 2-11).

Table 2-2 Monitoring techniques [87]

Monitoring technique		**Cost**	**Capacity**	**Scalable**	**Complex**	**Reliable**	**Transparent**	**Centralized**	**Automated**
Single wavelength OTDR	Upstream OTDR	High	Low	No	Low	Low	No	No	No
	Active bypass	Low	High	No	Low	Low	Yes	Yes	Yes
	Semi-passive bypass	Low	High	No	Low	Low	Yes	Yes	Yes
	Reference reflector	Low	High	No	Low	Low	Yes	Yes	Yes
	Switchable reflective element	High	High	Yes	Medium	Low	Yes	Yes	Yes
Tunable OTDR	Wavelength routing	High	Low	No	High	High	Yes	Yes	Yes
	Reference reflector	High	Low	No	Medium	High	Yes	Yes	Yes
Brillouin OTDR		High	High	No	Medium	Medium	Yes	Yes	Yes
Embedded OTDR		Medium	High	Yes	High	Low	No	No	Yes
OFDR+IF units		Low	High	Yes	Low	Medium	Yes	Yes	Yes
Optical coding		Low	High	Yes	Low	Medium	Yes	Yes	Yes
SL-RSOA		Low	High	Yes	Medium	Low	Yes	No	Yes
Reflected signal		High	High	Yes	Low	Medium	Yes	Yes	Yes

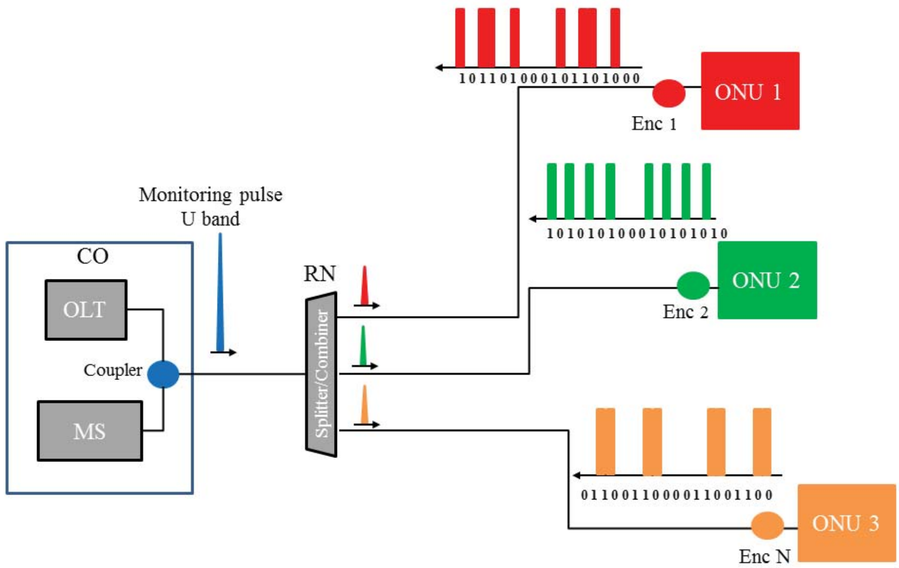

Figure 2-11 Optical coding monitoring technique [84]

2.6 GPON

Gigabit PON supports different downstream and upstream transmission rates. For downstream transmission, GPON defines rates of 1.2 Gbps or 2.4 Gbps, whereas bitrate of 1.5 Gbps, 6.2 Gbps, 1.2 Gbps or 2.4 Gbps have been identified for upstream transmission. Typically, GPON operates using 1.2 Gbps for upstream transmission and 2.4 Gbps for downstream transmission [88]. Wavelength bands that are allocated to downstream transmission are in the range 1480-1500 nm. For the upstream wavelength bands, GPON uses a wavelength band of 1290-1330 nm [89]. GPON provides a 1550 nm wavelength band for the video signal. GPON supports spilt ratios of 32, 64, and 128 ONUs [90].

GPON, an ITU standard defined in recommendation series G.984.1 – G.984.4, is characterized by dynamic bandwidth allocation, reliable timing and high quality service through its traffic containers (T-CONT). Internet Protocol (IP) or Ethernet elements are configured by GPON Encapsulation Method (GEM). The GEM comprises of the GEM header and GEM payload. GEM header includes information about ONU address. The GEMs are encapsulated into the GPON Transmission Convergence (GTC) payload [91].

GPON downstream frame is 125 μn long and it uses TDM to divide the available bandwidth among the ONUs [92]. The downstream frame is showing in Figure 2-12. It consists of Physical Control Block downstream (PCBd), and a payload that includes ATM section and GEM section [93]. The data is broadcast to all ONUs, whereupon individual units extract the appropriate data using information in the PCBd. In addition, the Bandwidth map (BW map) within the downstream data flow allocates upstream time for each ONU to transmit its upstream traffic [93], (see Figure 2-14).

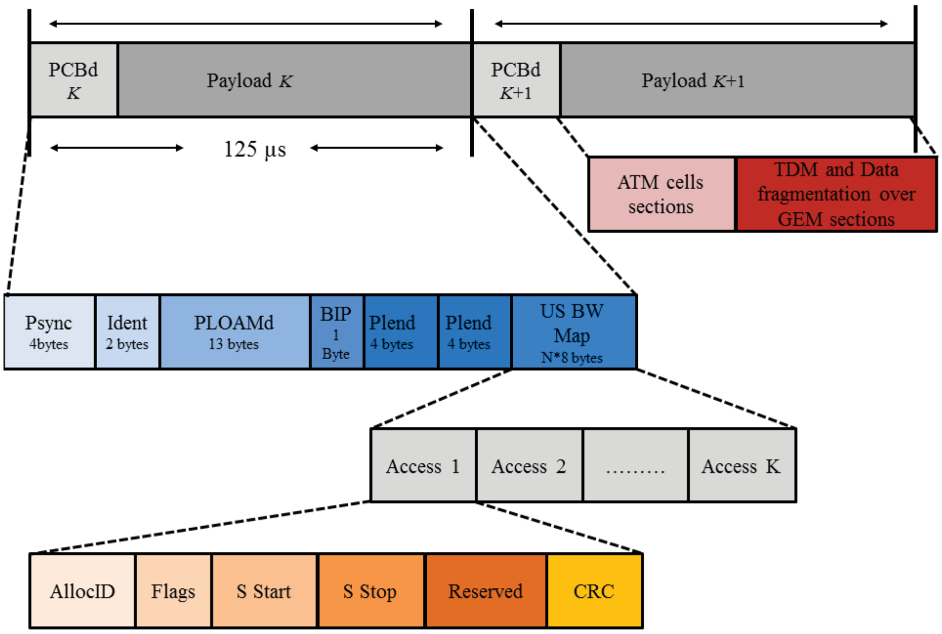

Figure 2-12 Downstream frame [93]

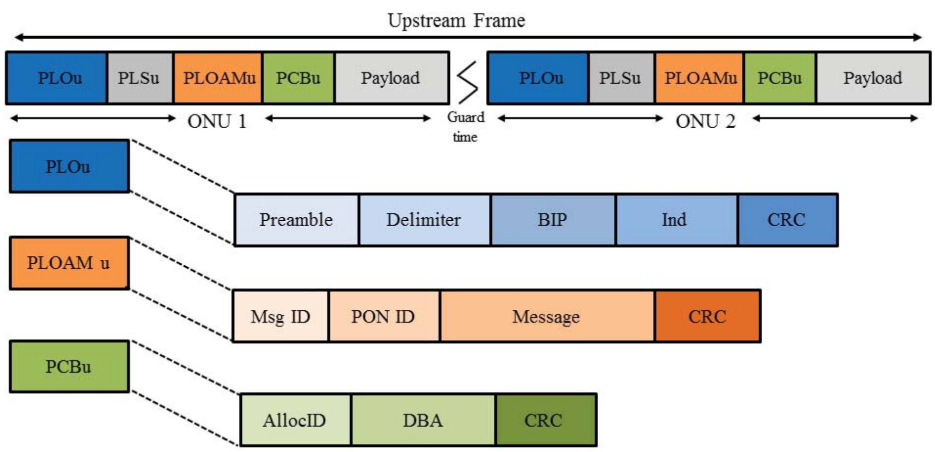

Figure 2-13 Upstream frame [93]

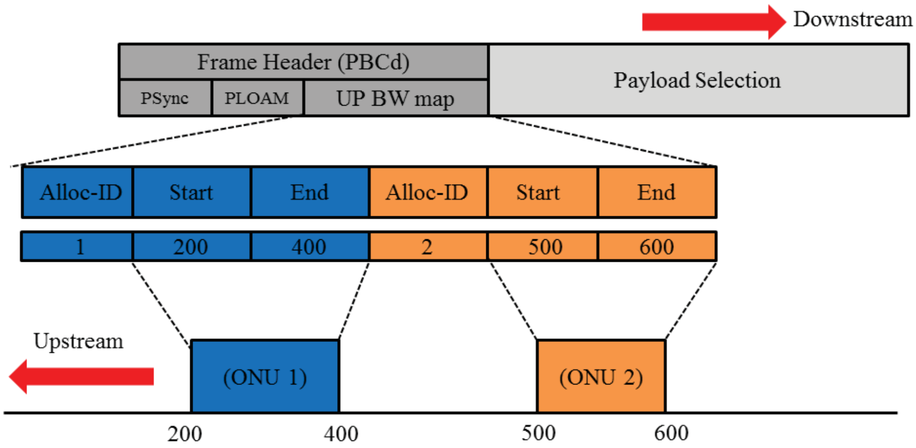

Figure 2-14 Upstream and downstream [94]

The upstream frame is 125 μn based on TDMA. It contains multiple transmission bursts arriving from the ONUs [92]. The upstream frame is shown in Figure 2-13. Each of the upstream burst frames consists of a Physical Layer Overhead (PLOu) and a payload [92]. When traffic reaches the OLT, ONU traffic is queued based on Classes of Service (CoS) with a diverse QoS dependent on the type of the T-CONTs that is specified in the Allocation Identifier (Alloc-ID) in the PCBd . The OLT classifies and ranks the data flow needs of each ONU according to ITU-T Recommendation G.983.4 for T-CONT types:

- T-CONT 1: Supports time-sensitive fixed bandwidth
- T-CONT 2: Supports assured and shared bandwidth with less time sensitive and quality data
- T-CONT 3: Supports bandwidths providing a guaranteed minimum Committed Information
- T-CONT 4: Supports 'best-effort', average need services.

The OLT controls the assignment of the time frame for each ONU based on its identified load. When each ONU transmits its upstream traffic during the assigned time slot, there is a possibility that frames from different ONUs will collide at some point due to the difference in propagation delay [95, 96].

In order to guarantee that the upstream transmissions do not collide, a ranging process is performed by the OLT during the activation and registration of the ONUs. The ranging process is based on calculating a specific delay time for each ONU according to its logical distance from the OLT to equalize its transmission delay with other ONUs [96]. Each ONU will store and apply its delay to all the upstream transmissions. The delay values are broadcast to other ONUs using PLOAM messages and each ONU resumes its transmission based on the delay [97] [95].

The accuracy of the ranging process to control the upstream bursts is limited, thus a Guard Time (T_g) is a very significant concept in the upstream transmission. T_g is the time that is assigned to the period between two consecutive bursts to avoid packet collision [98]. The number of bits assigned to the guard time depends on the data rate, and increases with it. For example, a data rate of 1.244 Gbps consumes 32 bits, while that of 2.48 Gbps consumes 64 bits [98].

2.7 OCDMA Systems

The OCDM-PON configuration was discussed in Section 2.2.1.4. This section focuses on OCDMA system encoding principles, encoder and decoder devices, OCDMA system challenges, spreading code design issues, and the different optical spreading codes.

2.7.1 Encoding Principle

In OCDMA systems, each communication channel is assigned a unique code. The transmitter encodes each data bit by multiplying it by its unique code before transmission [99]. The coding processes are performed using one-dimensional coding (1-D), two-dimensional coding (2-D), or three-dimensional coding (3-D).

1-D spreads codes on either the time or frequency domains. For encoding in the time domain, a light source produces short optical pulses. Then by using a fibre delay time, and an electrical modulator, each data bit generated by the laser source is encoded [100]. In the frequency domain, an ultra-short broadband light pulse passes through a diffraction grating scattering in multiple wavelengths [100]. In time based encoding, the bit time is divided into smaller chips that are equal to the code length, whereas in wavelength based encoding, the code is formed by dividing the transmitted bits into a number of unique subset of wavelengths [99]. The principle of encoding using time and wavelength domains is shown in Figure 2-15. The decoding operation is based on using a reverse operation to encoding (reverse time/wavelength) [99].

2-D spreads the code using both time and wavelength domains, simultaneously by placing pulses in different chips over a bit interval, each with a different wavelength, (see Figure 2-15) [99]. Consequently, 2-D coding possess better flexibility and security characteristics than 1-D coding [100].

3-D is executed in space, time, and wavelength; or in polarisation, time, and wavelength domains. Such codes support more cardinality than 2-D, improve the code performance; as well as minimizing the code length [101]. The Local Area Network (LAN) of an OCDMA system is based on a broadcast method. Multiple encoders at the transmission side encode the data with unique codes. All the encoded signals are coupled at the star coupler and broadcast to the receiver side. Each receiver receives the sum of the encoded signals. The decoding operation at the receiver side is based on the correlation function [30]. If an intended encoder transmits a signal, only the associated decoder (that is applying the revers encoding process) is able to recover the signal by representing an auto-correlation peak of the code.

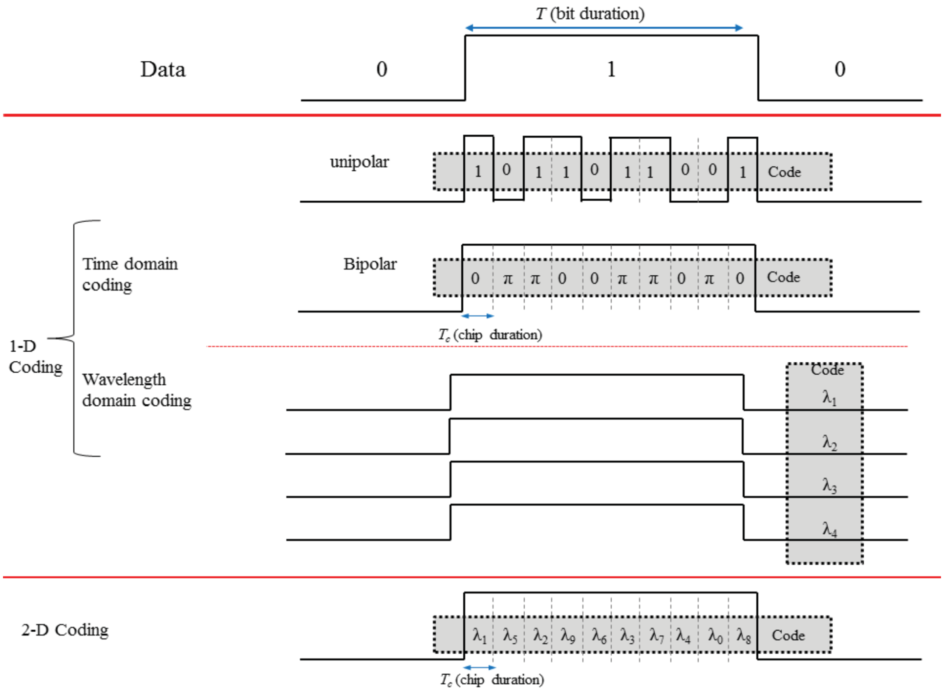

Figure 2-15 Coding dimensions [99]

Table 2-3 Coding domain and relevant devices [99]

Coding domain	Encoding device
Time	Optical delay line
	Mach-Zehnder interferometer
	External phase modulator
	Phase modulator and local oscillator
	Planar lightwave circuits with delay and phase modulators
	Segmented fibre grating
	Uniform Bragg grating
Wavelength	Liquid crystal modulator
	Broadband source
	AWG and phase-plates
	AWG and holograms
	Superstructured Bragg grating
2-D	Fibre Bragg grating
	Integrated laser source-encoder

Other signals detected as interference or noise and are represented by cross-correlation [30, 99]. The correlation function can be implemented using several schemes. One scheme is based on multiplying the optical pulse sequence by a reference signal that is stored at the receiver. This process is performed in real time. Another approach is to perform the correlation by using passive optical means. An example of the encoding and decoding of this approach is the use of ODL (explained in Section 0).

2.7.2 Encoder/Decoder Devices

Devices used for encoding and decoding and their corresponding coding scheme are presented in Table 2-3 [99]. The most common devices are reviewed in this section.

2.7.2.1 Optical Delay Line

The Optical Delay Line (ODL) is used as an encoder and a decoder for both 1-D and 2-D domains as shown in Figure 2-16 and Figure 2-17, respectively.

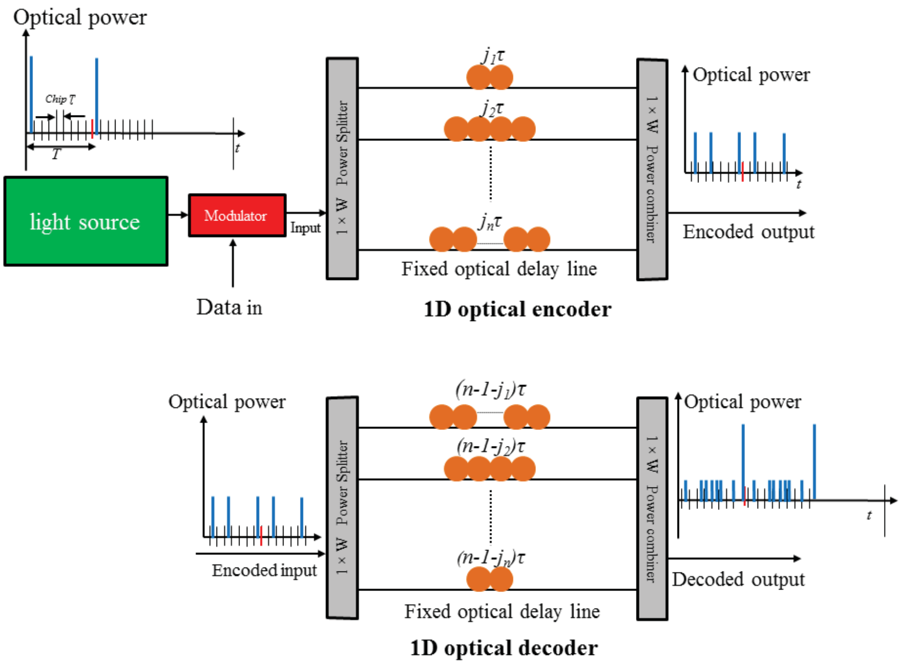

Figure 2-16 1-D ODL-based encoder/decoder [27]

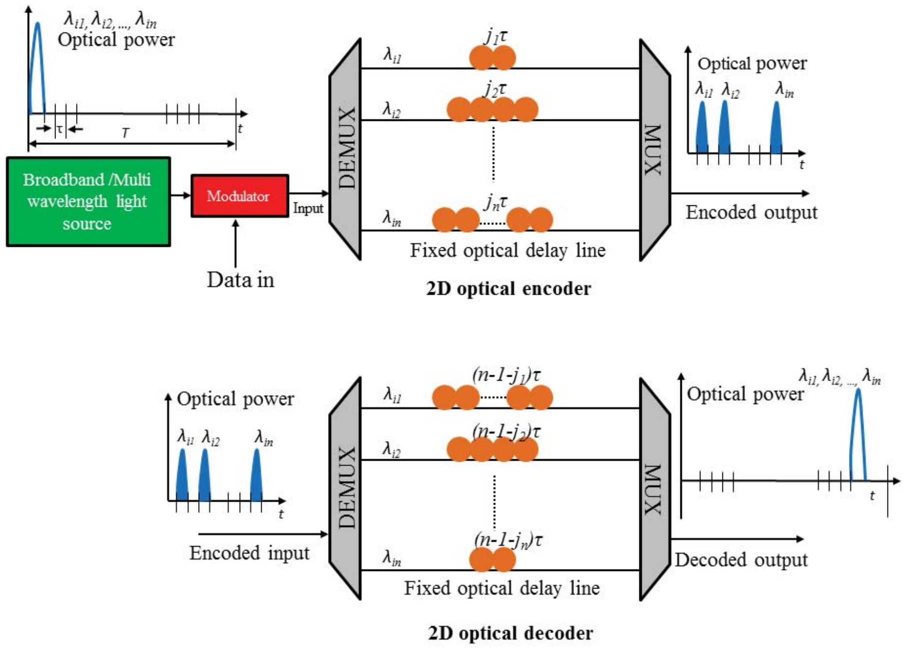

Figure 2-17 2-D ODL-based encoder/decoder [27]

In Figure 2-16, the encoder consists of an optical splitter, several ODLs, equal in number to the code weight, and a power combiner. The light source sends an optical pulse for time T composed of chips, each represented by $\mathcal{T}$, and in total equal to the code length. This signal is then split into w sub-signals, each of which is assigned a delay line according to the code-word. The delay assigned is $ji\mathcal{T}$, where $0 \leq j.i \geq L$. The sub-signals are combined by the power combiner. The decoder design is the same as the encoder except for the values assigned to the delay line. The delay lines for the decoder are changed to $(L\ \text{-}1\text{-}\ j)\ \mathcal{T}$. The output of the decoder represents an auto-correlation function of the code-word [29].

Example: Consider OOC, represented with length of 32 and weight of 4, this code can generate two code-words {1 0 (9) 1 0 (2) 1 0 (14) 1 0 (3)} and {1 0 (4) 1 0 (6) 1 0 (18) 1}, where the internal bracketed figures denote the number of 0s for each series. The code-words can be represented by {(0, 10, 13, 28) mod 32} and {(0, 5, 12, 31) mod 32} [102]. The delay lines for both encoder and decoder are shown in Table 2-4.

For 2-D encoding, see Figure 2-17, the light source is replaced with a multi-wavelength light source or with a broadband light source that produces a train of short pulses [27]. In addition, the power splitter/combiner are replaced by a wavelength division de-multiplexer/multiplexer respectively.

Table 2-4 Encoder/decoder delay lines [103]

Encoder/Decoder	Parameter	Value
Encoder 1	Delay line 1	0*TimeChip
	Delay line 2	10*TimeChip
	Delay line 3	13*TimeChip
	Delay line 4	28*TimeChip
Encoder 2	Delay line 1	0*TimeChip
	Delay line 2	5*TimeChip
	Delay line 3	12*TimeChip
	Delay line 4	31*TimeChip
Decoder 1	Delay line 1	31*TimeChip
	Delay line 2	21*TimeChip
	Delay line 3	18*TimeChip
	Delay line 4	3*TimeChip
Decoder 2	Delay line 1	31*TimeChip
	Delay line 2	26*TimeChip
	Delay line 3	19*TimeChip
	Delay line 4	0*TimeChip

The de-multiplexer splits the optical pulse into w sub-pulses, each of which represents a wavelength. These sub-pulses are assigned a specified delay, similar to 1-D encoding. The delay lines for $(\lambda_1, \lambda_2, \ldots, \lambda_w)$ are $(j1\mathcal{T}, j2\mathcal{T}, \ldots, jw\,\mathcal{T})$. The decoder for 2-D is the same as the encoder except for the delay line values which are $(n - 1 - j1)$, $(L - 1 - j2)\,\mathcal{T}$, …, $(L - 1 - jw)\,\mathcal{T}$. The sub-signals are combined at the multiplexer and they produce an auto-correlation corresponding to the assigned code-word [27].

2.7.2.2 Fibre Bragg Grating

Encoder/decoders based on Fibre Bragg Grating (FBG) have a wavelength selective filter to reflect the optical signal [29]. These encoder/decoders can be designed either in series or parallel forms. A 2-D serial FBG architecture is shown at Figure 2-18 [104].

The encoder shown in Figure 2-18 consists of a three-port based circulator, FBG and ODL both qual to *w*. The broadband light source generates a short optical pulse which is modulated by data. The output pulse is fed into the optical circulator through port 1. The output signals from port 2 are reflected through FBGs in different wavelengths. Each two FBGs are joined together using ODL with differing delay times. The reflected optical pulse signals for port 2 of the circulator (including different wavelengths and delay times) comprise output from port 3. The decoder structure based on serial FBGs is the same as the encoder except that the FBGs are in reverse order and the values of the ODL are changed to be complementary to the delay assigned to the encoder [27].

The parallel 2-D form of the FBG structures is presented in Figure 2-19. The encoder/decoder in Figure 2-19 have a three-port based circulator, AWG, FBGs and ODL, with the latter two being, each, equal to *w* [104]. The broadband light source generates a short optical pulse which is modulated by data and fed to port 1 of the circulator. The AWG splits the pulse into *w* wavelength sub-pulses each with a pre-defined delay time, and reflected to the AWG through FBG. The reflected pulses are multiplexed and fed into the circulator port 2, and output is obtained from port 3. The decoder for parallel FBGs follows the design of the encoder except its delay time values, that should complement those of the encoder ODLs [27].

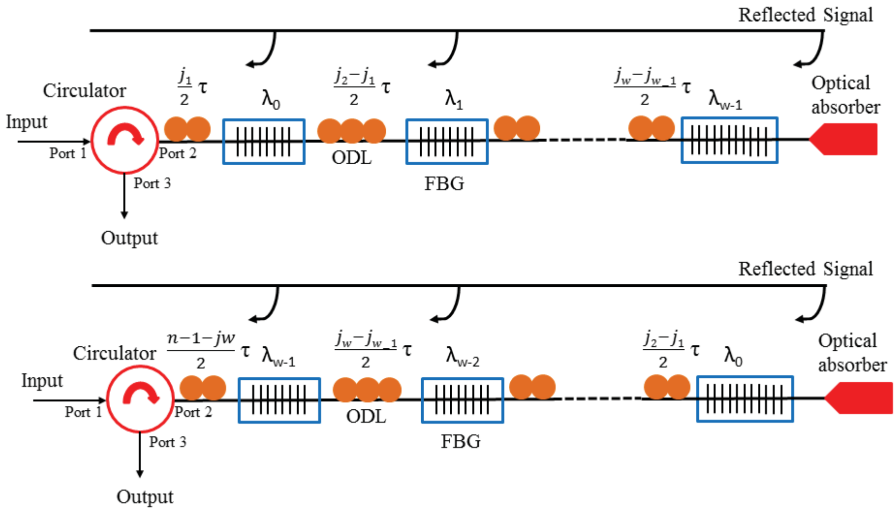

Figure 2-18 2-D FBG-based serial encoder/decoder [104]

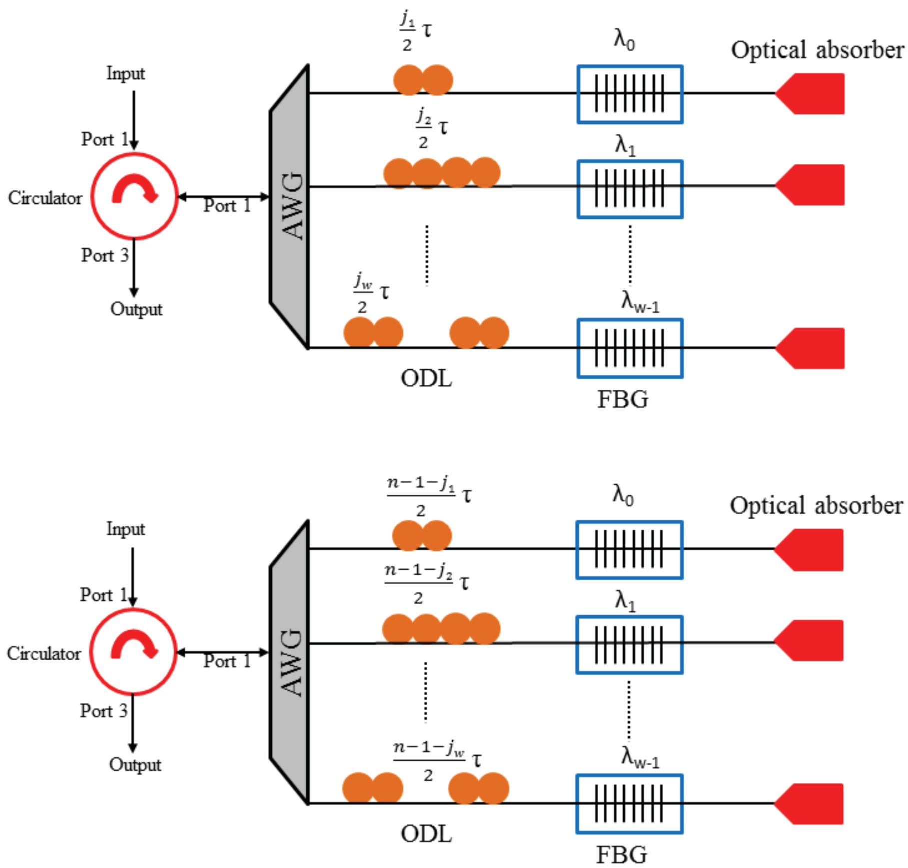

Figure 2-19 2-D FBG-based parallel encoder/decoder [104]

2.7.2.3 Arrayed Waveguide Grating

Arrayed Waveguide Grating (AWG) based feedback ODL is shown in Figure 2-20.

In this design, the input optical pulses are divided by AWG into small sub-pulses at different wavelengths, each of which delayed by a pre-assigned delay time and fed back into the

AWG. The sub-pulses are combined at the AWG output port, providing an encoded signal. The decoder structure follows the encoder with delay time values in a reverse order, so that the encoder wavelength with the highest delay value forms the shortest for the decoder feedback [104].

An AWG with mirrored ODL is shown in Figure 2-21. The design of an encoder based on AWG with mirrored ODL is similar to the previous encoder. The difference is that the ODLs are mirrored to reduce the feedback structure [27] [104].

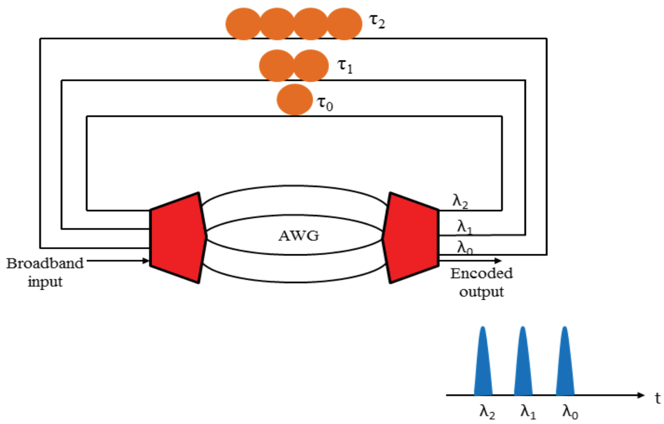

Figure 2-20 AWG with ODL feedback [104]

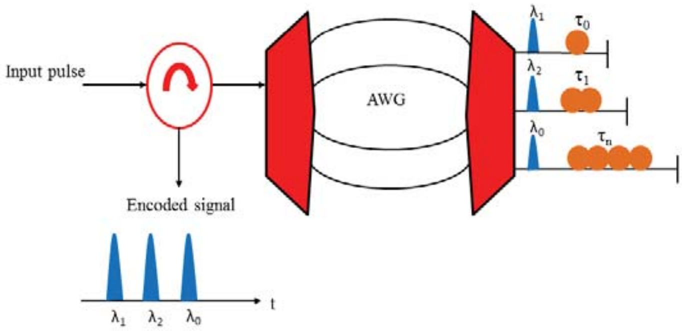

Figure 2-21 AWG with mirrored ODL [104]

2.7.3OCDMA System Challenges

There are several challenges for OCDMA systems. The most critical challenges are discussed in this section [25].

- **Coding Schemes.** Codes in OCDMA systems have parameters such as auto and cross-correlation functions, weight, length, and cardinality. These parameters are the main factors affecting the performance of OCDMA, as estimated by the probability of MAI. MAI increases as the number of transmitted communication channels increases. Hence the importance of knowing the number of the active communication channels that are able to transmit asynchronously. Researchers have proposed codes that generate the required code-words.

- **Network Architecture.** Network architecture can refer to the network topology that based on the scalability of the network, the integrated device, the cost of the system, and the robustness of the environment. For star based networks, the number of connection channels can exceed the number of input/output ports. One suggestion to increase the number of connection channels by employing the optical splitter and combiner, beside the coupler. Another suggestion is to use multiplexers and demultiplexers. The star topology is limited to local area networks with limited coverage. A solution to increase the coverage is the use of ring topology. The ring makes use of add/drop multiplexer which is the main component. The multipoint-to-multipoint connection provided by the star topology is not efficient to deploy in access networks because of the nature of traffic. Therefore, another alternative of optimal topology is tree topology.

- **Hardware Design.** Each channel in OCDMA systems has to implement an encoder and a decoder to encode/decode its data. Several devices can be used for the coding process, and there may be a need for advanced optical processing components, which will result in an increase in the total cost.

2.7.4 Spreading Code Design Issues

As discussed in the Section 2.6.3, identifying a coding scheme is one of the most important challenges affecting the performance of OCDMA. Thus, the following issues have to be considered when designing an effective spreading code [25].

The length of spreading codes is constrained by increasing code cardinality (the number of available communication channels). This is particularly relevant to 1-D codes, to support a large cardinality, the length of the code increases exponentially, resulting in a code that is inefficient to implement. As stated in coding principles, 1-D time encoding is based on dividing the bit time into smaller chips (equal to code length). The chip width is, therefore, an important aspect to consider. It has been stated in [105] and in [106] that the state of the art photodiodes at the receiver are able to detect a chip time of the order of 100 ps. In addition, the authors predicted that chip times may drop to the order of 10 ps, and may even reach the order of femtosecond with the use of the fast-nonlinear optical element, e.g Kerr effect.

Code cardinality can be, assisted by 2-D and 3-D coding [27]. The code weight refers to the pulses represented by 1 in the code-word. Although, increasing the weight improves the correlation properties, it increases the power consumption as well as the hardware complexity (e.g. increasing the number of ODL in time encoding scheme). Construction mechanism is also of concern in designing the address codes. Simplifying the construction mechanism of the code renders it more popular for implementation.

2.7.5Optical Spreading Codes

Spreading code sets attributed to OCDMA systems can be classified into bipolar codes, those that have sequences of (-1, 1), and unipolar codes, those that have sequences of (1, 0). The optical spreading codes, their characteristics in relation to coding dimension, polarisation, and light types are summarised in Table 2-5 . The following are the most common optical spreading codes.

Bipolar codes

- maximum length sequence (*m*-sequence) codes have lengths of 2^L-1, where L is the number of shift registers from a Linear Feedback Shift Register (LFSR) generator necessary to initiate the sequence

- Gold code sequences [107] are constructed from two m-sequences of the same length and rate with modulo-2 addition; for a Gold sequence of length $m = 2^L$-1, two LFSR each of length 2^L-1 are required

- Hadamard–Walsh codes are bipolar, perfectly orthogonal used to separate transceivers on the downlink channel [30].

Unipolar code

- Optical orthogonal code.

- Prime code sets.

- Quadratic Congruence Codes.

Table 2-5 OCDM codes and protocols [27]

Code-dimensions	Title	Polarisation	Light type	Attributed codes
1-D code	Pulse amplitude	Unipolar	Incoherent	OOC PC QCC HCC
	Pulse phase	Bipolar	Coherent	M-sequence Gold code Walsh-Hadamard codes
	Spectral amplitude	Unipolar	Incoherent	
	Spectral phase	Bipolar	Coherent	
2-D code	Wavelength-hopping time spreading	Unipolar	Incoherent	2D WH/TS OOC
	Space encoding	Unipolar	Incoherent	2D space codes
3-D code	3-dimension encoding	Unipolar codes	Incoherent	Space/time/wavelength or polarisation/time/wavelength codes

2.7.6OCDMA Modulation Schemes

On-off keying (OOK) and pulse position modulation (PPM) are the most popular modulation schemes used in OCDMA systems [108]. In OOK modulation, a data bit is denoted by two symbols based on binary numbers. If the data bit is equal to 1, the bit time is divided into L chips of width (T_c). Thus the frame duration can be expressed as $T_s = L.T_c$. (see Figure 2-22 , (a)) [109].

In the case of M-array PPM modulation, a data bit is denoted by M symbols, thus, every symbol signifies log_2^m data bits. As shown in Figure 2-22 (b), a frame of duration T_s is divided into M symbols (M = 4 symbols), each symbol represents two data bits. Each symbol is divided into L chips of width T_c, thus the symbol duration can be expressed as $\tau = L.T_c$, the frame duration can, therefore, be expressed as $T_s = M.\ \tau$ [109].

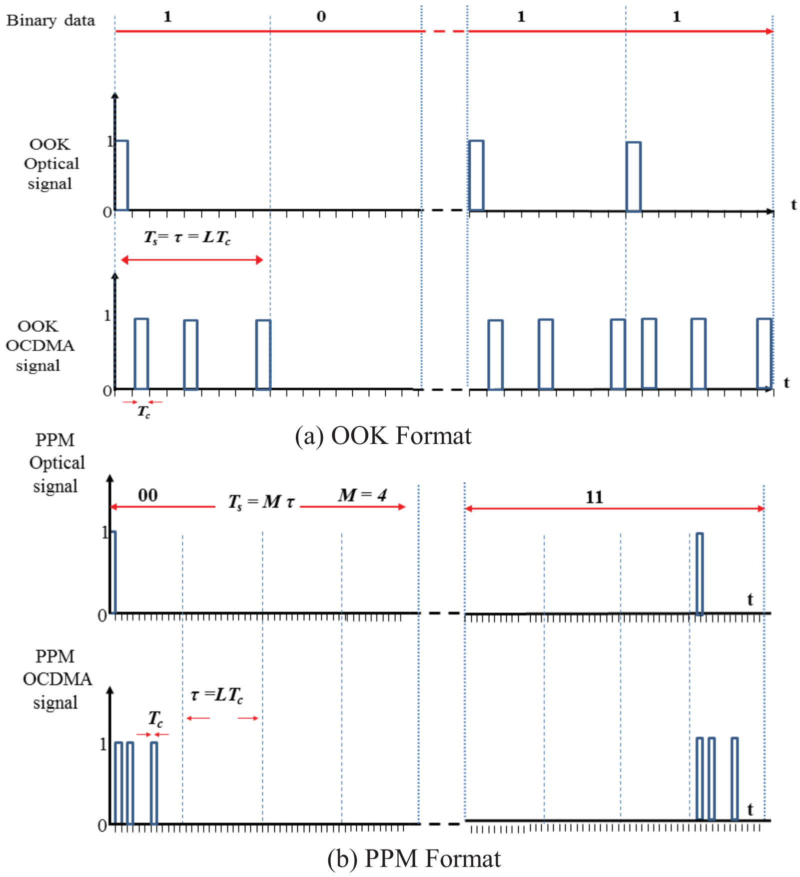

Figure 2-22 Signalling format, (a) OOK-OCDMA, (b) PPM-OCDMA [109]

The PPM-OCDMA approach has been shown to be an energy efficient scheme. This is because, for a given bit-error-rate, PPM-OCDMA can increase the number of communication channels by increasing the pulse-position multiplicity (M) for the same average power, whereas OOK-OCDMA cannot [110]. On the other hand, however, the OOK-OCDMA system has a simpler signaling format than the PPM-OCDMA, as its chip width is larger than that in the PPM format (see Figure 2-22). In addition, the hardware used for the PPM modulation format is complex [109].

2.8 PON Monitoring based OC Technique Research

In [84] and [111], a number of the required features that must be fulfilled in the monitoring system were discussed. The first feature is for the system to be centralized; the NMS at the CO must be able to obtain monitoring information from the system without intervention by the ONU. In addition, the monitoring system must be able to automatically detect the fault without any intervention from the technicians. This feature leads to minimizing the measurement time and reducing the cost of operational expenditure. Transparency is another must feature in monitoring systems. The monitoring process should not interrupt the transmission/receiving of the data. To achieve this, a monitoring pulse must be transmitted in the U-band and a wavelength selector should ensure data flows [111]. Simplification and cost-effectiveness of the monitoring system are highly desired. NG-PON accommodates high capacity and monitoring based TDM (utilizing one wavelength) is a simple and cost-effective way to monitor high network capacity (64, 128+), which is suitable for NG-PON.

Although the efficiency of the monitoring PON based OC technique is largely dependant on the spreading code, investigation of ways to enhance that code has been overlooked by researchers. The importance of the current work stems from the fact that this thesis places a heavy weight on ways to enhance the spreading code, rather than the coding scheme.

A proposed monitoring system based on Direct Sequence OCDM (DS-OCDM) can be found in [112]. In this system, each ONU implements a fixed encoder based on OOC to encode its signal. The encoded signals are combined at the RN and sent to the NMS. The decoder at the NMS is based on a switch and fixed decoders. In the case of a healthy branch, the decoder represents an auto-correlation peak; otherwise, a cross-correlation will be represented. The monitoring system is able to monitor TDM-PON, WDM-PON or TWDM-PON systems with around 1000 ONUs using a single wavelength in the U-band.

One approach to detect a faulty TDM-PON branch was described in [113] where the code implemented is an OOC, and the encoders used to distinguish between branches are based on five FBGs, that are, implemented outside the ONUs. The simulation monitoring signal was transmitted over the C-band (data band) and was trialled on a 1×16 TDM-PON with 20 km of optical fibre. The system was able to support up to 120 m branch length with 3 m spatial resolution.

In [111], a modified monitoring system that meets most of the features required for monitoring PON has been proposed. In this system, the encoder is simple and cost-effective and is based on FBG with 100% reflectivity, a coupler, and a patch cord. The code implemented is Multilevel-Optical Orthogonal Code (ML-OOC).

A mathematical model for PON monitoring based on a 2-D OOC has been developed in [33]. The mathematical model includes three modules: monitoring pulse generator modules, encoding and transmission modules, and decoding and identification modules. The system performance was evaluated in terms of Signal-to-Noise Ratio (SNR), Signal to Interference Ratio (SIR), and optimal decision probability.

Periodic coding was introduced in [114] with two FBG on the same waveband. The main function of the first FBG is to perform partial reflectivity (38%). The second FBG functions as a frequency selective mirror. The length of the patch cord between the two FBG has been increased to form the optical cavity. However, partial reflectivity of the first FBG has an effect on the impulse response sensitivity. In addition, increasing the number of ONUs has led to an inefficient increase in the length of the patch cords. The system was able to support up to 64 ONUs and its performance was tested using SNR. The limitations were resolved by the introduction of an Incrementally Pulse Positioned Code (IPPC) coding scheme [115]. In this scheme, each grating works to reflect the different wavelengths with 100% reflectivity, thus resulting in the construction of a 2-D code. The monitoring system performance was examined using SIR.

A different approach for PON monitoring with a periodic optical encoder was proposed in [116] where each periodic optical encoder produces a unique periodic code with the use of a FBG, with 100% reflectivity and a fibre ring with a different length for each distribution or drop fibre. The proposed encoder improved system performance by reducing the monitoring cost, and was able to accommodate a large number of ONUs (256). The performance of the encoder was evaluated mathematically using SNR.

Another two encoders that implemented 1-D unipolar codes were suggested in [117]. The encoders were implemented using a couple of FBGs to form a cavity with the use of multi-level periodic codes (similar to [116]). The encoders produce a code with a weight of 2 and 3 that enhance the correlation properties of multi-level periodic codes. The performance has been evaluated in terms of Signal-to-Noise-and-Interference Ratio (SNIR).

A centralized monitoring system using a 2-D optical frequency time-hopping/periodic code was investigated in [118]. A low-cost encoder was used for each ONU based on two FBGs with 59% reflectivity. The system was simulated for 4 ONUs to check the status of the fibre (healthy/broken). In addition, the system was evaluated in terms of Multiple-Customers Interference Probability (MCIP). The result showed an improvement in the overall interference.

A remote coding scheme for PON monitoring was presented in [119] with the system based on a cascaded encoder that uses a 1 x 2 optical power splitter and combiner, and an FBG at the RN. The monitoring pulse consists of *P* wavelengths transmitted via U-band into the RN. The encoder reflects the wavelengths and produces a specific combination of wavelength for every ONU. The monitoring pulses are reflected with the use of an identical reflector and transmitted back to the receiver. The received signal is demultiplexed into *P* wavelengths, and then passed to a detector which checks the power received against a set value.

Another 2-D time/wavelength OCDMA physical layer PON monitoring system uses reflective encoders at the ONU based on FBG serial arrays [87]. This system makes use of a broadband source with a M sub-bands in the C band. An encoder that is based on incoherent

2-D coding is set to each ONU to reflect M pulses, a pulse for each sub-band, in different time slots. At the receiver side, a demultiplexer works to demultiplex the M sub-bands. The concept was verified in a PON with five sub-bands and four closely spaced ONUs with a very high user density. Parameters including beat noise, false alarm and misdetection were tested [87].

A set of coding schemes for monitoring PON have been analysed by Fathallah and Esmail in [86] where they show the different coding scheme designs and evaluate their performance in relation to SNR, probabilities of false alarm and misdetection. The coding schemes are based on either ODL, that uses a power splitter/combiner, FBG, or ring coding. PON monitoring based on OC for a tree topology was reported in [86]. Fathallah and Esmail discussed an approach for monitoring a ring using an OC technique. Their approach was based on dividing the ring into a number of segments and then installing an encoder based on 1-D for each segment. In this approach, the ring is bidirectional fibre, where the monitoring pulse is transmitted from the NMS in the counter-clockwise direction, and received in the clockwise direction. In this way, if a code is missing, the NMS will detect the fault location. This, however, will not be the case if another simultaneous fault occurs behind the faulty segment. The strategy proposed to overcome this problem is based on transmitting another monitoring signal in the opposite direction to enable the NMS to monitor the segment located after the first fault. However, this approach requires a large number of advanced encoders.

A hybrid 1-D/2-D OCDMA coding scheme was introduced for the first time by Rad et al. in [120]. The main purpose of 1-D/2-D was to eliminate the beat noise that resulted from 1-D coding. The system combined both the simplicity and cost effectiveness offered by 1-D coding and the beat noise cleaning provided by 2-D coding. In this system, the optical transmitter is a multi-wavelength laser, the encoders for distribution fibres are based on 1-D coding, and the decoding is based on 2-D coding using standard multi-FBG with 95%

reflectivity at the NMS. The performance of the system has been analysed using receiver operating characteristics. The proposed coding reduced the cost and achieved SNR higher than 16dB for 256 ONUs.

2.9 Summary

This chapter provides a literature survey of the systems and structures that form current and future designs for PON. PON multiplexing technologies were investigated, and the restrictions on numbers of ONUs, security, bandwidth, interference, and costs discussed. The ITU offers guidelines for developing effective systems; however, researchers take the liberty to address issues by building hybrid schemes. TWDM-PON, selected as the optimal scheme, is the subject of this study.

In addition, OCDMA systems are thoroughly investigated to identify coding principles, and the design of the devices used for encoding and decoding. An analysis and investigation of OCDMA have proven to be challenging. The issues associated with spreading codes, including increasing the cardinality to accommodate the number of active communication channels, has led to the conclusion that there is a need for a code that is suitable for PON.

Moreover, studies focusing on PON monitoring based upon an OC technique were analysed. It is important to note that, most of these studies are based on developing a coding scheme and evaluating the system performance based on mathematical models in terms of SNR, SIR, MCIP, probability of false alarm, or probability of misdetection. This thesis takes another direction for PON monitoring; it aims to design a code that provides code-words compatible with the different splitting ratios commonly found in PONs. The proposed code is designed in such a way as to increase the code-words, reduce the prime number and, hence, reducing the hardware complexity and energy consumption. This is followed by the implementation of the code in different PON scenarios using VPItransmissionMaker. The purpose of the implementation is to provide the NMS with useful information about the status of each fibre (either healthy or faulty).

Chapter 3 OPTICAL SPREADING CODE

Chapter 3 analyses and investigates the most common address codes for OCDMA designs, OOC, QCC, and PCs with a focus on PCs. The importance of this chapter stems from the fact that the code designed in this thesis has its background and origins imbedded in the existing OCDMA codes.

3.1 Optical Orthogonal Code

OOC, or time-based coding [121], is one of the most important temporal codes [122]. An OOC has a low weight resulting in low encoding and decoding efficiency. The number of possible code-words is low in comparison to the same code length in radio communication techniques, such as Walsh–Hadamard codes. Code length is also constrained by an OOC characteristic to have a short pulse with a pulse-width smaller than the bit duration [123]. OOC is a family of binary sequences represented by (*N, w, λa, λc*), where *N* is the length of the code and *w* is the Hamming-weight (number of single digits (1) in each code-word) that satisfies the following auto and cross correlation properties [30]:

$$R_{C_iC_j}(m) = \sum_{n=0}^{N-1} C_i(n)\, C_j(n+m) \le \lambda_c, \qquad \text{for}, \forall m \tag{3-1}$$

$$R_{C_iC_j}(m) = \sum_{n=0}^{N-1} C_i(n)\, C_j(n+m) \le \lambda_a, \qquad \text{for}, \qquad [m]_n \neq 0 \tag{3-2}$$

An (*N*, *w*, λ*a*, λ*c*) OOC, is a constant-weight symmetric OOC, when *λa* = *λc*, represented as (*N*, *w*, λ) OOC. When *λa* ≠ *λc*, an (*N*, *w*, λ*a*, λ*c*) OOC is a constant-weight asymmetric OOC [25, 27] [124]. Otherwise, the OOC code is a variable-weight OOC represented by (*N*, *w*, λ*a*, λ*c*, *Q*), where *w* denotes a set of code weight, defined as $w = \{ w_1, w_2, \ldots w_P\}$, and *Q* denotes a set of code-words defined as $Q = \{q_1, q_2, .., q_P\}$ [125].

A special case of OOC, referred to as optimal OOC, is when λ*a* = λ*c* = λ, which is represented by *(N, w, λ).* The maximum number of code-words of *(n, w, λ)* is represented by *Φ(N, w, λ)* and is defined by [30]:

$$\Phi(N, w, \lambda) \leq \frac{(N-1)(N-2)\ldots(N-\lambda)}{w(w-1)(w-2)\ldots(w-\lambda)} \tag{3-3}$$

Another case of OOC is referred to as strict OOC when $\lambda a = \lambda c = 1$, where the cardinality is given by [30]:

$$|C| \leq \left\lfloor \frac{(N-1)}{w(w-1)} \right\rfloor \tag{3-4}$$

OOC code construction is complex, and methods to construct it include combinational construction, algebraic construction, and construction of finite projective geometrics [27]. Table 3-1 shows sequence indexes of OOC code with different *N* [30].

Table 3-1 OOC (*N*, 3, 1) sequence indexes of various lengths [30]

N	Sequence index, $N \leq 49$
7	{1, 2, 4}
13	{1, 2, 5} {1, 3, 8}
19	{1, 2, 6} {1, 3, 9} {1, 4, 11}
25	{1, 2, 7} {1, 3, 10} {1, 4, 12} {1, 5, 14}
31	{1, 2, 8} {1, 3, 12} {1, 4, 16} {1, 5, 15}{1, 6, 14}
37	{1, 2, 12} {1, 3, 10} {1, 4, 18} {1, 5, 13}{1, 6, 19}{1, 7, 13}
43	{1, 2, 20} {1, 3, 23} {1, 4, 16} {1, 5, 14}{1, 6, 17}{1, 7, 15}{1, 8, 19}

Table 3-2 presents the OOC sequence codes (31, 3, 1).

Table 3-2 Sequence codes of OOC (31, 3, 1) [30]

Index	Sequence Codes
{1, 2, 8}	1 1 0 0 0 0 0 1 0 0 0 0 0 0 0 0 0 0 0 0 0 0 0 0 0 0 0 0 0 0 0
{1, 3, 12}	1 0 1 0 0 0 0 0 0 0 0 1 0 0 0 0 0 0 0 0 0 0 0 0 0 0 0 0 0 0 0
{1, 4, 16}	1 0 0 1 0 0 0 0 0 0 0 0 0 0 0 1 0 0 0 0 0 0 0 0 0 0 0 0 0 0 0
{1, 5, 15}	1 0 0 0 1 0 0 0 0 0 0 0 0 0 1 0 0 0 0 0 0 0 0 0 0 0 0 0 0 0 0
{1, 6, 14}	1 0 0 0 0 1 0 0 0 0 0 0 0 1 0 0 0 0 0 0 0 0 0 0 0 0 0 0 0 0 0

3.2 Quadratic Congruence Code

QCC is constructed in two steps.

Step 1.

Select a prime number, *P*, and construct a quadratic congruence sequence based on the Galois field (*GF*) [27].

$$S_i = \left(S_{i,0}, S_{i,1}, \dots, S_{i,j}, \dots, S_{i,(P-1)}\right), \qquad i = 1,2, \dots , P-1 \tag{3-5}$$

where, the elements of S_i are:

$$S_{i,j} = \left\{i.\frac{j(j+1)}{2}\right\} (mod\ P), \qquad 1 \le i \le P-1, \qquad 0 \le i \le P-1 \tag{3-6}$$

where,

$$S_{i,j} \in GF(P) = \{0,1, \dots, P-1\} \tag{3-7}$$

Step 2.

Construct a binary sequence from the quadratic congruence sequence.

$$C_i = \left(C_{i,0}, C_{i,1}, \dots, C_{i,k}, \dots, C_{i,(n-1)}\right), \qquad i = 1,2, \dots , P-1 \tag{3-8}$$

where,

$$C_{i,k} = \begin{cases} 1, & if\ k = s_{i,j} + j.P, for\ j = \{0,1, \dots, P-1\} and\ j = \left\lfloor \frac{k}{P} \right\rfloor, for\ k = 0,1, \dots, P^2 - 1 \\ 0, & elsewhere \end{cases} \tag{3-9}$$

where, [x] is an integer ≤ x. QCC has a length of $n = P^2$, a weight of $w = P$ and a cardinality of $|C| = P\text{-}1$. The maximum auto and cross-correlation functions are $\lambda a = 2$, $\lambda a = 4$, respectively. Table 3-3 is an example of QCC code sequences for $P = 7$ [27].

Table 3-3 QCC code sequences for *P* = 7 [27]

i	S_i	C_i
1	S_1 = 0 1 3 6 3 1 0	1000000 0100000 0001000 0000001 0001000 0100000 1000000
2	S_2 = 0 2 6 5 6 2 0	1000000 0010000 0000001 0000010 0000001 0010000 1000000
3	S_3 = 0 3 2 4 5 3 0	1000000 0001000 0010000 0000100 0010000 0001000 1000000
4	S_4 = 0 4 5 3 5 4 0	1000000 0000100 0000010 0001000 0000010 0000100 1000000
5	S_5 = 0 5 1 2 1 5 0	1000000 0000010 0100000 0010000 0100000 0000010 1000000
6	S_6 = 0 6 4 1 4 6 0	1000000 0000001 0000100 0100000 0000100 0000001 1000000

3.4 Prime Code

PCs are simpler to construct than other code types, and are able to be modified to increase the cardinality [30]. This section considers prime codes families.

3.4.1Basic Prime Code

Basic PC was introduced in [126, 127] and is constructed sequentially;

First select a prime number and build a set of prime sequences based on a Galois field *GF*(*P*).

$$S_i = \left(S_{i,0}, S_{i,1}, \dots, S_{i,j}, \dots, S_{i,(P-1)}\right), \qquad i = 0, 1 \, \dots, P-1 \tag{3-10}$$

where,

$$S_{i,j} = \{i \,.\, j\} \; (\text{mod } P) \tag{3-11}$$

i and j are elements over $GF(P) = \{0,1,2,\dots,P\text{-}1\}$. The prime sequences S_i for 5, as a prime number, are shown as an example in Table 3-4.

Table 3-4 Basic prime code sequences for *P* = 5 [27]

Index	S_i				
	j = 0	***j = 1***	***j = 2***	***j = 3***	***j = 4***
S_0	0	0	0	0	0
S_1	0	1	2	3	4
S_2	0	2	4	1	3
S_3	0	3	1	4	2
S_4	0	4	3	2	1

Secondly, map S_i into a binary sequence C_i as follows:

$$C_i = \left(C_{i,0}, C_{i,1}, \dots, C_{i,k}, \dots, C_{i,(N-1)}\right), \qquad i = 0, 1 \, \dots, P-1, N = P^2 \tag{3-12}$$

where,

$$C_{i,k} = \begin{cases} 1, & if\ k = s_{i,j} + j.P, for\ j = \{0,1,\dots,P-1\} \\ 0, & elsewhere \end{cases} \tag{3-13}$$

A binary prime sequence is generated as in For $n_1,n_2 \in \{1, 2, \dots, P\}$. The cross-correlation value of the basic PC could reach 2 and the auto-correlation value could be reduced to (P - 1) in the case of non-zero shift [128]. However, these changes in PC correlation properties complicate the receiver detection process, therefore, the maximum cross-correlation cannot exceed 1 and the auto-correlation must be equal to the weight [128].

Table 3-5 [27]. As shown in For n_1,n_2 ∊ {1, 2, … , P}. The cross-correlation value of the basic PC could reach 2 and the auto-correlation value could be reduced to (P - 1) in the case of non-zero shift [128]. However, these changes in PC correlation properties complicate the receiver detection process, therefore, the maximum cross-correlation cannot exceed 1 and the auto-correlation must be equal to the weight [128].

Table 3-5 Binary sequence of basic PC, P = 5 the basic PC support cardinality of P with weight (w) of P and length (L) of P^2. The correlation function of any two code sequences C_n and C_m can be defined as:

$$C_{n1}.C_{n2} = \begin{cases} P, & m = n; Auto - correlation \\ 1, & m \neq n; Cross - correlation \end{cases} \tag{3-14}$$

For n_1,n_2 ∊ {1, 2, … , P}. The cross-correlation value of the basic PC could reach 2 and the auto-correlation value could be reduced to (P - 1) in the case of non-zero shift [128]. However, these changes in PC correlation properties complicate the receiver detection process, therefore, the maximum cross-correlation cannot exceed 1 and the auto-correlation must be equal to the weight [128].

Table 3-5 Binary sequence of basic PC, *P* = 5 [27]

Index	*C*				
	***j* = 0**	***j* = 1**	***j* = 2**	***j* = 3**	***j* = 4**
C_0	10000	10000	10000	10000	10000
C_1	10000	01000	00100	00010	00001
C_2	10000	00100	00001	01000	00010
C_3	10000	00010	01000	00001	00100
C_4	10000	00001	00010	00100	01000

3.4.2 Extended Prime Code

Extended prime code (EPC) was proposed by Yang and Kwong in [126] and is used to overcome changes in correlation properties associated with basic PC [126, 129]. EPC is constructed in a similar way to the basic PC, but with each subsequence padded with ($P - 1$) or more zeros. Mapping S_i into binary sequence C_i can be modified:

$$C_{i,k} = \begin{cases} 1, & if\ k = s_{i,j} + j(2P-1), for\ j = \{0,1,\dots,P-1\} \\ 0, & elsewhere \end{cases} \quad (3\text{-}15)$$

The EPC increases the length up to $2P - 1$, thus improving the correlation functions. It supports a weight of P and cardinality of P^2. Table 3-6, shows sequences of EPC when $P = 5$.

Table 3-6 Extended prime code sequences, *P* = 5 [126]

Index	*C*				
	***j* = 0**	***j* = 1**	***j* = 2**	***j* = 3**	***j* = 4**
C_0	100000000	100000000	100000000	100000000	100000000
C_1	100000000	010000000	001000000	000100000	000010000
C_2	100000000	001000000	000010000	010000000	000100000
C_3	100000000	000100000	010000000	000010000	001000000

3.4.3 Modified Prime Code

A modified prime code (MPC) is applicable with increasing numbers of network transceivers, as it is an address code with low weight and large cardinality. MPC has been proposed in [27]. It can increase cardinality up to P^2 with weight and length of P and P^2, respectively [127, 130]. Code construction is performed on the basic PC, and then every code sequence is time shifted P times. The auto- and cross-correlation of MPC are:

$$C_{n1}.C_{n2} = \begin{cases} 1, & n1 \neq n2, n1\ and\ n2\ in\ different\ groups \\ 0, & n1 \neq n2, n1\ and\ n2\ in\ same\ group \\ P, & n1 = n2 \end{cases} \quad (3\text{-}16)$$

where, n_1, $n_2 \in \{1, 2, \dots, P\}$. An example of MPC is shown in Table 3-7, when $P = 5$.

An example of MPC is shown in Table 3-7, when $P = 5$.

Table 3-7 Modified prime code sequences, *P* = 5 [127]

Index		MPC sequences
	C_{00}	10000 10000 10000 10000 10000
	C_{01}	01000 01000 01000 01000 01000
C_0	C_{02}	00100 00100 00100 00100 00100
	C_{03}	00010 00010 00010 00010 00010
	C_{04}	00001 00001 00001 00001 00001
	C_{10}	10000 01000 00100 00010 00001
	C_{11}	01000 00100 00010 00001 10000
C_1	C_{12}	00100 00010 00001 10000 01000
	C_{13}	00010 00001 10000 01000 00100
	C_{14}	00001 10000 01000 00100 00010
	C_{20}	10000 00100 00001 01000 00010
	C_{21}	01000 00010 10000 00100 00001
C_2	C_{22}	00100 00001 01000 00010 10000
	C_{23}	00010 10000 00100 00001 01000
	C_{24}	00001 01000 00010 10000 00100
	C_{30}	10000 00010 01000 00001 00100
	C_{31}	01000 00001 00100 10000 00010
C_3	C_{32}	00100 10000 00010 01000 00001
	C_{33}	00010 01000 00001 00100 10000
	C_{34}	00001 00100 10000 00010 01000
	C_{40}	10000 00001 00010 00100 01000
	C_{41}	01000 10000 00001 00010 00100
C_4	C_{42}	00100 01000 10000 00001 00010
	C_{43}	00010 00100 01000 10000 00001
	C_{44}	00001 00010 00100 01000 10000

3.4.4New Modified Prime Code

A new modified prime code (n-MPC) has been introduced by Liu et al. in [108] and it aims to improve BER by increasing the weight and enhancing system security by increasing the length. n-MPC is constructed as MPC, with the last subsequence repeated at the end the following code sequence in the same group and rotating it in the same group [108] (presented in **bold in** Table 3-8). In n-MPC, the cardinality is P^2, the weight is $P + 1$ and the length is $P^2 + P$. The cross- and auto-correlation functions are:

$$C_{n1}.C_{n2} = \begin{cases} \leq 2, & n1 \neq n2, n1 \; and \; n2 \; in \; different \; groups \\ 0, & n1 \neq n2, n1 \; and \; n2 \; in \text{ the } same \; group \\ P+1, & n1 = n2 \end{cases} \quad (3\text{-}17)$$

where, $n_1, n_2 \in \{1, 2, \ldots, P\}$. An example of n-MPC is shown in Table 3-8, where $P = 5$.

Table 3-8 New modified prime code sequences, P = 5 [108]

Index		MPC sequence	Padded sequence
	C_{00}	10000 10000 10000 10000 10000	**01000**
	C_{01}	00001 00001 00001 00001 00001	10000
C_0	C_{02}	00010 00010 00010 00010 00010	00001
	C_{03}	00100 00100 00100 00100 00100	00010
	C_{04}	01000 01000 01000 01000 **01000**	00100
	C_{10}	10000 01000 00100 00010 00001	00010
	C_{11}	01000 00100 00010 00001 10000	00001
C_1	C_{12}	00100 00010 00001 10000 01000	10000
	C_{13}	00010 00001 10000 01000 00100	01000
	C_{14}	00001 10000 01000 00100 00010	00100
	C_{20}	10000 00100 00001 01000 00010	01000
	C_{21}	00100 00001 01000 00010 10000	00010
C_2	C_{22}	00001 01000 00010 10000 00100	10000
	C_{23}	01000 00010 10000 00100 00001	00100
	C_{24}	00010 10000 00100 00001 01000	00001
	C_{30}	10000 00010 01000 00001 00100	00001
	C_{31}	01000 01000 00001 00100 10000	00100
C_3	C_{32}	00100 00001 00100 10000 00010	10000
	C_{33}	00010 00100 10000 00010 01000	00010
	C_{34}	00001 00100 00010 01000 00001	01000
	C_{40}	10000 00001 00010 00100 01000	10000
	C_{41}	00001 00010 00100 01000 10000	01000
C_4	C_{42}	00010 00100 01000 10000 00001	10000
	C_{43}	00100 01000 10000 00001 00010	00001
	C_{44}	01000 10000 00001 00010 00100	00010

3.4.5Padded Modified Prime Code

A padded modified prime code (PMPC) has been proposed by Liu and Tsao in [131]. It increases the auto-correlation peak to identify a single signal from the flow. Codes are constructed from MPC and then each group is padded with a sub-sequence stream of P length. The padded sub-sequence is constant within sequences in the same group and time shifted for other groups. PMPC cardinality is P^2 and the length and weight increased to (P^2 + P) and (P+1) respectively.

The auto-correlation and cross-correlation functions are [131]:

$$C_{n1}.C_{n2} = \begin{cases} P+1, & n1 = n2; auto-correlation \\ 1, & n1 \neq n2; cross-correlation \end{cases} \quad (3\text{-}18)$$

where, n_1, n_2 ∈{1, 2, …. , P}. The code-words of PMPC where P = 5 are listed in .

Table 3-9.

Table 3-9 Padded modified prime code sequences, *P* = 5 [30]

Index		MPC sequence	Padded sequence
	C_{00}	10000 10000 10000 10000 10000	10000
	C_{01}	00001 00001 00001 00001 00001	10000
C_0	C_{02}	00010 00010 00010 00010 00010	10000
	C_{03}	00100 00100 00100 00100 00100	10000
	C_{04}	01000 01000 01000 01000 01000	10000
	C_{10}	10000 01000 00100 00010 00001	01000
	C_{11}	01000 00100 00010 00001 10000	01000
C_1	C_{12}	00100 00010 00001 10000 01000	01000
	C_{13}	00010 00001 10000 01000 00100	01000
	C_{14}	00001 10000 01000 00100 00010	01000
	C_{20}	10000 00100 00001 01000 00010	00100
	C_{21}	00100 00001 01000 00010 10000	00100
C_2	C_{22}	00001 01000 00010 10000 00100	00100
	C_{23}	01000 00010 10000 00100 00001	00100
	C_{24}	00010 10000 00100 00001 01000	00100
	C_{30}	10000 00010 01000 00001 00100	00010
	C_{31}	01000 01000 00001 00100 10000	00010
C_3	C_{32}	00100 00001 00100 10000 00010	00010
	C_{33}	00010 00100 10000 00010 01000	00010
	C_{34}	00001 00100 00010 01000 00001	00010
	C_{40}	10000 00001 00010 00100 01000	00001
	C_{41}	00001 00010 00100 01000 10000	00001
C_4	C_{42}	00010 00100 01000 10000 00001	00001
	C_{43}	00100 01000 10000 00001 00010	00001
	C_{44}	01000 10000 00001 00010 00100	00001

3.4.6Group padded Modified Prime Code

The group padded modified prime code (GPMPC) expands the process used in n-MPC, where the last two sub-sequences are repeated and rotated at the end of the code sequence in the same group. Available codes are P^2 and the length and weight are increased up to (P + 2) and (P^2 + 2P), respectively. The auto- and cross-correlations functions follow [30]:

$$C_{n1}.C_{n2} = \begin{cases} \leq 2, & n1 \neq n2, n1 \; and \; n2 \; in \; different \; groups \\ 0, & n1 \neq n2, n1 \; and \; n2 \; in \text{ the } same \; group \\ P+2, & n1 = n2 \end{cases} \quad (3\text{-}19)$$

where, n_1, n_2 ∈{1, 2, …. , P}. The code-words of GPMPC with P = 5 are shown in Table 3-10.

Table 3-10 Double padded modified prime code sequences, *P* = 5 [30]

Index		MPC sequences	Double padded sequence
	C_{00}	10000 10000 10000 10000 10000	00001 00001
	C_{01}	01000 01000 01000 01000 01000	10000 10000
C_0	C_{02}	00100 00100 00100 00100 00100	01000 01000
	C_{03}	00010 00010 00010 00010 00010	00100 00100
	C_{04}	00001 00001 00001 00001 00001	00010 00010
	C_{10}	10000 01000 00100 00010 00001	00001 10000
	C_{11}	01000 00100 00010 00001 10000	10000 01000
C_1	C_{12}	00100 00010 00001 10000 01000	01000 00100
	C_{13}	00010 00001 10000 01000 00100	00100 00010
	C_{14}	00001 10000 01000 00100 00010	00010 00001
	C_{20}	10000 00100 00001 01000 00010	00001 01000
	C_{21}	01000 00010 10000 00100 00001	10000 00100
C_2	C_{22}	00100 00001 01000 00010 10000	01000 00010
	C_{23}	00010 10000 00100 00001 01000	00100 00001
	C_{24}	00001 01000 00010 10000 00100	00010 10000
	C_{30}	10000 00010 01000 00001 00100	00001 00100
	C_{31}	01000 00001 00100 10000 00010	10000 00010
C_3	C_{32}	00100 10000 00010 01000 00001	01000 00001
	C_{33}	00010 01000 00001 00100 10000	00100 10000
	C_{34}	00001 00100 10000 00010 01000	00010 01000
	C_{40}	10000 00001 00010 00100 01000	00001 00010
	C_{41}	01000 10000 00001 00010 00100	10000 00001
C_4	C_{42}	00100 01000 10000 00001 00010	01000 10000
	C_{43}	00010 00100 01000 10000 00001	00100 01000
	C_{44}	00001 00010 00100 01000 10000	00010 00100

3.4.7Double padded Modified Prime Code

The double padded modified prime code (DPMPC) has been proposed by Karbassian and Ghafouri-Shiraz in [132]. The generation of DPMPC is based on the following three steps:

Step 1. Generating MPC sequence.

Step 2. The first padded sub-sequence is based on padding the last sub-sequence of MPC in the same group (similarly to n-MPC), (presented in underline in Table 3-11).

Step 3. The second padded sub-sequence is based on routing the final sub-sequence of the last MPC in same group, (presented in **bold** in Table 3-11).

Table 3-11 Double padded modified prime code, *P* = 5 [132]

Index		MPC sequences	Double padded sequence
	C_{00}	10000 10000 10000 10000 10000	10000 01000
	C_{01}	01000 01000 01000 01000 01000	01000 00100
C_0	C_{02}	00100 00100 00100 00100 00100	00100 00010
	C_{03}	00010 00010 00010 00010 00010	00010 00001
	C_{04}	00001 00001 00001 00001 00001	00001 01000
	C_{10}	10000 01000 00100 00010 00001	00001 **00010**
	C_{11}	01000 00100 00010 00001 10000	10000 00001
C_1	C_{12}	00100 00010 00001 10000 01000	01000 10000
	C_{13}	00010 00001 10000 01000 00100	00100 01000
	C_{14}	00001 10000 01000 00100 **00010**	00010 00100
	C_{20}	10000 00100 00001 01000 00010	00010 00100
	C_{21}	01000 00010 10000 00100 00001	00001 00010
C_2	C_{22}	00100 00001 01000 00010 10000	10000 00001
	C_{23}	00010 10000 00100 00001 01000	01000 10000
	C_{24}	00001 01000 00010 10000 00100	00100 01000
	C_{30}	10000 00010 01000 00001 00100	00100 01000
	C_{31}	01000 00001 00100 10000 00010	00010 00100
C_3	C_{32}	00100 10000 00010 01000 00001	00001 00010
	C_{33}	00010 01000 00001 00100 10000	10000 00001
	C_{34}	00001 00100 10000 00010 01000	01000 10000
	C_{40}	10000 00001 00010 00100 01000	01000 10000
	C_{41}	01000 10000 00001 00010 00100	00100 01000
C_4	C_{42}	00100 01000 10000 00001 00010	00010 00100
	C_{43}	00010 00100 01000 10000 00001	00001 00010
	C_{44}	00001 00010 00100 01000 10000	10000 00001

Available codes are P^2 and the length and weight are increased up to (P + 2) and (P^2 + 2P), respectively compared to MPC. The auto- and cross-correlations functions follow:

$$C_{n1}.C_{n2} = \begin{cases} 1, & n1 \neq n2, n1\ and\ n2\ in\ different\ groups \\ 0, & n1 \neq n2, n1\ and\ n2\ in\ \text{the}\ same\ group \\ P+2, & n1 = n2 \end{cases} \quad (3\text{-}20)$$

where, n_1, n_2 ∈{1, 2, …. , P}.

3.4.8 Transposed Modified Prime Code

The OCDMA system aims for a large number of transceivers and efficient receiver recognition. To increase cardinality, P must grow, creating an inefficient code due to increasing length [133]. Transposed-MPC (T-MPC) doubles cardinality and improves the spectral efficiency [134]. The code construction aims at constructing an MPC, then using a full padded technique similar to n-MPC and DPMPC, where the last code sequence is repeated at the end the following code sequence and rotated in the same group. (See Table 3-12). T-MPC has cardinality of P^2, length of $2P^2$ and weight of $2P$. The auto-correlation and cross-correlation functions are:

$$C_{n1}.C_{n2} = \begin{cases} \leq 2, & n1 \neq n2, n1\ and\ n2\ in\ different\ groups \\ 0, & n1 \neq n2, n1\ and\ n2\ in\ \text{the}\ same\ group \\ 2P, & n1 = n2 \end{cases} \tag{3-21}$$

Table 3-12 Full padded modified prime code, *P* = 5 [135]

Index		MPC sequences	Padded sequences
C_0	C_{00}	10000 10000 10000 10000 10000	00001 00001 00001 00001 00001
	C_{01}	01000 01000 01000 01000 01000	10000 10000 10000 10000 10000
	C_{02}	00100 00100 00100 00100 00100	01000 01000 01000 01000 01000
	C_{03}	00010 00010 00010 00010 00010	00100 00100 00100 00100 00100
	C_{04}	00001 00001 00001 00001 00001	00010 00010 00010 00010 00010
C_1	C_{10}	10000 01000 00100 00010 00001	00001 10000 01000 00100 00010
	C_{11}	01000 00100 00010 00001 10000	10000 01000 00100 00010 00001
	C_{12}	00100 00010 00001 10000 01000	01000 00100 00010 00001 10000
	C_{13}	00010 00001 10000 01000 00100	00100 00010 00001 10000 01000
	C_{14}	00001 10000 01000 00100 00010	00010 00001 10000 01000 00100
C_2	C_{20}	10000 00100 00001 01000 00010	00001 01000 00010 10000 00100
	C_{21}	01000 00010 10000 00100 00001	10000 00100 00001 01000 00010
	C_{22}	00100 00001 01000 00010 10000	01000 00010 10000 00100 00001
	C_{23}	00010 10000 00100 00001 01000	00100 00001 01000 00010 10000
	C_{24}	00001 01000 00010 10000 00100	00010 10000 00100 00001 01000
C_3	C_{30}	10000 00010 01000 00001 00100	00001 00100 10000 00010 01000
	C_{31}	01000 00001 00100 10000 00010	10000 00010 01000 00001 00100
	C_{32}	00100 10000 00010 01000 00001	01000 00001 00100 10000 00010
	C_{33}	00010 01000 00001 00100 10000	00100 10000 00010 01000 00001
	C_{34}	00001 00100 10000 00010 01000	00010 01000 00001 00100 10000
C_4	C_{40}	10000 00001 00010 00100 01000	00001 00010 00100 01000 10000
	C_{41}	01000 10000 00001 00010 00100	10000 00001 00010 00100 01000

C_{42}	00100 01000 10000 00001 00010	01000 10000 00001 00010 00100
C_{43}	00010 00100 01000 10000 00001	00100 01000 10000 00001 00010
C_{44}	00001 00010 00100 01000 10000	00010 00100 01000 10000 00001

The third step is to consider Table 3-12, as a matrix and apply a 'transpose function' to produce a new matrix. The new matrix comprises the T-MPC sequences in Table 3-13 which shows that the cardinality of T-MPC is doubled with the same length and weight of MPC ($w = P$, $L = P^2$), using the following correlation functions:

$$C_{n1}.C_{n2} = \begin{cases} \leq 2, & n1 \neq n2, n1\ and\ n2\ in\ different\ groups \\ 0, & n1 \neq n2, n1\ and\ n2\ in\ \text{the}\ same\ group \\ P, & n1 = n2 \end{cases} \tag{3-22}$$

Table 3-13 Transposed modified prime code sequences, *P* = 5 [135]

Index		TMPC sequences	Index		TMPC sequences
	C_{00}	10000 10000 10000 10000 10000		C_{50}	01000 00100 00100 00100 00100
	C_{01}	00001 01000 00010 00100 00001		C_{51}	10000 00010 10000 00001 01000
0	C_{02}	00010 00100 01000 00001 00010	**5**	C_{52}	00001 00001 00010 01000 10000
	C_{03}	00100 00010 00001 01000 00100		C_{53}	00010 10000 01000 00010 00001
	C_{04}	01000 00001 00100 00010 01000		C_{54}	00100 01000 00001 10000 00010
	C_{10}	10000 00001 00001 00001 00001		C_{60}	00100 00010 00010 00010 00010
	C_{11}	00001 10000 00100 01000 00010		C_{61}	01000 00001 01000 10000 00100
1	C_{12}	00010 01000 10000 00010 00100	**6**	C_{62}	10000 10000 00001 00100 01000
	C_{13}	00100 00100 00010 10000 01000		C_{63}	00001 01000 00100 00001 10000
	C_{14}	01000 00010 01000 00100 10000		C_{64}	00010 00100 10000 01000 00001
	C_{20}	10000 00010 00010 00010 00010		C_{70}	00010 00001 00001 00001 00001
	C_{21}	00001 00001 01000 10000 00100		C_{71}	00100 10000 00100 01000 00010
2	C_{22}	00010 10000 00001 00100 01000	**7**	C_{72}	01000 01000 10000 00010 00100
	C_{23}	00100 01000 00100 00001 10000		C_{73}	10000 00100 00010 10000 01000
	C_{24}	01000 00100 10000 01000 00001		C_{74}	00001 00010 01000 00100 10000
	C_{30}	10000 00100 00100 00100 00100		C_{80}	00001 10000 10000 10000 10000
	C_{31}	00001 00010 10000 00001 01000		C_{81}	00010 01000 00010 00100 00001
3	C_{32}	00010 00001 00010 01000 10000	**8**	C_{82}	00100 00100 01000 00001 00010
	C_{33}	00100 10000 01000 00010 00001		C_{83}	01000 00010 00001 01000 00100
	C_{34}	01000 01000 00001 10000 00010		C_{84}	10000 00001 00100 00010 01000
	C_{40}	10000 01000 01000 01000 01000		C_{90}	11111 00000 00000 00000 00000
	C_{41}	00001 00100 00001 00010 10000		C_{91}	00000 11111 00000 00000 00000
4	C_{42}	00010 00010 00100 10000 00001	**9**	C_{92}	00000 00000 11111 00000 00000
	C_{43}	00100 00001 10000 00100 00010		C_{93}	00000 00000 00000 11111 00000
	C_{44}	01000 10000 00010 00001 00100		C_{94}	00 0 00000 00000 11111

3.4.9 Transposed Sparse-padded Modified Prime Code

Transposed sparse-padded MPC (T-SPMPC) is constructed in four steps.

Step 1. Generates a MPC sequence.

Step 2. Generates a sparse padded sequence (SP_{xy}) as follows:

$$SP_{xy} = \{SP_{xyi} | i = 0, 1, \dots, P - 1\} \quad (3\text{-}23)$$

where, each SP_{xyi} sequence consists of M_{xyi} (MPC sequences), and L_{xyi}, defined as follows:

$$M_{xyi} = \begin{cases} S_{xi}, & y = 0 \\ M_{x(y\ominus 1)(i\oplus 1)}, & elsewhere \end{cases} \quad (3\text{-}24)$$

where, $\ominus$ denotes subtraction mod P, and $\oplus$ denotes addition mod P.

$$L_{xyi} = \begin{cases} x, & if\ M_{xyi} = x \\ N, & elsewhere \end{cases} \quad (3\text{-}25)$$

where, x denotes the number of the group and N refers to "Null" sequence. The resulting code-words are shown in Table 3-14 [136].

Step 3. Exchange between M_{xyi} and L_{xyi} sequences. Cross-correlations in Table 3-14 occur through M_{xyi}.; however, L_{xyi} sequences are sparse and avoid cross-correlation. The exchange process follows:

$$\begin{aligned} M_{xyi}(new) &= L_{xyi}(old) \\ L_{xyi}(new) &= M_{xyi}(old) \end{aligned} \quad (3\text{-}26)$$

By applying the following condition:

$$x \ominus M_{xyi} < \frac{P+1}{2} \quad (3\text{-}27)$$

Table 3-15, shows the intermediate table for SPMPC. Table 3-16 shows the binary sequences.

Table 3-14 Sparse padded sequence, SP, P = 5 [136]

Group	Sequence	SP_{xy0}		SP_{xy1}		SP_{xy2}		SP_{xy3}		SP_{xy4}	
		M_{xyi}	L_{xyi}	M_{xyi}	L_{xyi}	M_{xyi}	L_{xyi}	M_{xyi}	L_{xyi}	M_{xyi}	L_{xyi}
0	SP_{00}	0	0	0	0	0	0	0	0	0	0
	SP_{01}	4	N	4	N	4	N	4	N	4	N
	SP_{02}	3	N	3	N	3	N	3	N	3	N
	SP_{03}	2	N	2	N	2	N	2	N	2	N
	SP_{04}	1	N	1	N	1	N	1	N	1	N
1	SP_{10}	0	N	1	1	2	N	3	N	4	N
	SP_{11}	1	1	2	N	3	N	4	N	0	N
	SP_{12}	2	N	3	N	4	N	0	N	1	1
	SP_{13}	3	N	4	N	0	N	1	1	2	N
	SP_{14}	4	N	0	N	1	1	2	N	3	N
2	SP_{20}	0	N	2	2	4	N	1	N	3	N
	SP_{21}	2	2	4	N	1	N	3	N	0	N
	SP_{22}	4	N	1	N	3	N	0	N	2	2
	SP_{23}	1	N	3	N	0	N	2	2	4	N
	SP_{24}	3	N	0	N	2	2	4	N	1	N
3	SP_{30}	0	N	3	3	1	N	4	N	2	N
	SP_{31}	3	3	1	N	4	N	2	N	0	N
	SP_{32}	1	N	4	N	2	N	0	N	3	3
	SP_{33}	4	N	2	N	0	N	3	3	1	N
	SP_{34}	2	N	0	N	3	3	1	N	4	N
4	SP_{40}	0	N	4	4	3	N	2	N	1	N
	SP_{41}	4	4	3	N	2	N	1	N	0	N
	SP_{42}	3	N	2	N	1	N	0	N	4	4
	SP_{43}	2	N	1	N	0	N	4	4	3	N
	SP_{44}	1	N	0	N	4	4	3	N	2	N

Table 3-15 Intermediate sparse padded MPC [136]

Group	Sequence	SP_{xy0}		SP_{xy1}		SP_{xy2}		SP_{xy3}		SP_{xy4}	
		M_{xyi}	L_{xyi}	M_{xyi}	L_{xyi}	M_{xyi}	L_{xyi}	M_{xyi}	L_{xyi}	M_{xyi}	L_{xyi}
0	*SP00*	0	0	0	0	0	0	0	0	0	0
	SP01	N	4	N	4	N	4	N	4	N	4
	SP02	N	3	N	3	N	3	N	3	N	3
	SP03	2	N	2	N	2	N	2	N	2	N
	SP04	1	N	1	N	1	N	1	N	1	N
1	*SP10*	N	0	1	1	2	N	3	N	N	4
	SP11	1	1	2	N	3	N	N	4	N	0
	SP12	2	N	3	N	N	4	N	0	1	1
	SP13	3	N	N	4	N	0	1	1	2	N
	SP14	N	4	N	0	1	1	2	N	3	N
2	*SP20*	N	0	2	2	4	N	N	1	3	N
	SP21	2	2	4	N	N	1	3	N	N	0

	SP22	4	N	N	1	3	N	N	0	2	2
	SP23	N	1	3	N	N	0	2	2	4	N
	SP24	3	N	N	0	2	2	4	N	N	1
	SP30	0	N	3	3	N	1	4	N	N	2
	SP31	3	3	N	1	4	N	N	2	0	N
3	*SP32*	N	1	4	N	N	2	0	N	3	3
	SP33	4	N	N	2	0	N	3	3	N	1
	SP34	N	2	0	N	3	3	N	1	4	N
	SP40	0	N	4	4	N	3	N	2	1	N
	SP41	4	4	N	3	N	2	1	N	0	N
4	*SP42*	N	3	N	2	1	N	0	N	4	4
	SP43	N	2	1	N	0	N	4	4	N	3
	SP44	1	N	0	N	N	4	N	3	N	2

Table 3-16 Sparse padded MPC, P = 5 [136]

Group	Sequence	SP_{xy0}		SP_{xy1}		SP_{xy2}		SP_{xy3}		SP_{xy4}	
		M_{xyi}	L_{xyi}	M_{xyi}	L_{xyi}	M_{xyi}	M_{xyi}	L_{xyi}	M_{xyi}	L_{xyi}	M_{xyi}
	SP_{00}	10000	10000	10000	10000	10000	10000	10000	10000	10000	10000
	SP_{01}	00000	00001	00000	00001	00000	00001	00000	00001	00000	00001
0	SP_{02}	00000	00010	00000	00010	00000	00010	00000	00010	00000	00010
	SP_{03}	00100	00000	00100	00000	00100	00000	00100	00000	00100	00000
	SP_{04}	01000	00000	01000	00000	01000	00000	01000	00000	01000	00000
	SP_{10}	00000	10000	01000	01000	00100	00000	00010	00000	00000	00001
	SP_{11}	01000	01000	00100	00000	00010	00000	00000	00001	00000	10000
1	SP_{12}	00100	00000	00010	00000	00000	00001	00000	10000	01000	01000
	SP_{13}	00010	00000	00000	00001	00000	10000	01000	01000	00100	00000
	SP_{14}	00000	00001	00000	10000	01000	01000	00100	00000	00010	00000
	SP_{20}	00000	10000	00100	00100	00001	00000	00000	01000	00010	00000
	SP_{21}	00100	00100	00001	00000	00000	01000	00010	00000	00000	10000
2	SP_{22}	00001	00000	00000	01000	00010	00000	00000	10000	00100	00100
	SP_{23}	00000	01000	00010	00000	00000	10000	10000	00100	00001	00000
	SP_{24}	00010	00000	00000	10000	00100	00100	00001	00000	00000	01000
	SP_{30}	10000	00000	00010	00010	00000	01000	00001	00000	00000	00100
	SP_{31}	00010	00010	00000	01000	00001	00000	00000	00100	10000	00000
3	SP_{32}	00000	01000	00001	00000	00000	00100	10000	00000	00010	00010
	SP_{33}	00001	00000	00000	00100	10000	00000	00010	00010	00000	01000
	SP_{34}	00000	00100	10000	00000	00010	00010	00000	01000	00001	00000
	SP_{40}	10000	00000	00001	00001	00000	00010	00000	00100	01000	00000
	SP_{41}	00001	00001	00000	00010	00000	00100	01000	00000	10000	00000
4	SP_{42}	00000	00010	00000	00100	01000	00000	10000	00000	00001	00001
	SP_{43}	00000	00100	01000	00000	10000	00000	00001	00001	00000	00010
	SP_{44}	01000	00000	10000	00000	00001	00001	00000	00010	00000	00100

Step 4. Apply the transpose function for T-MPC in Table 3-16 to generate the T-SPMPC code sequences as shown in Table 3-17.

The cardinality, length and weight are $2P^2$, P^2 and $(P+1)/2$, respectively. The auto-correlation and cross-correlation functions of T-SPMPC are as follows:

$$Cn.Cm = \begin{cases} 0, & \dfrac{3p^3 - p^2 - 3p + 1}{4p^3 - 2p} probability \\ 1, & \dfrac{p^3 + p^2 + p - 1}{4p^3 - 2p} probability \end{cases} \quad (3\text{-}28)$$

Table 3-17 Transposed sparse-padded modified prime code, *P* = 5 [136]

Index		TMPC sequences	Index		TMPC sequences
	C_{00}	10000 00000 00000 10000 10000		C_{50}	10000 00010 00010 00000 00000
	C_{01}	00001 01000 00000 00000 00001		C_{51}	00000 00001 01000 10000 00000
0	C_{02}	00010 00100 01000 00000 00000	**5**	C_{52}	00000 00000 00001 00100 01000
	C_{03}	00000 00010 00001 01000 00000		C_{53}	00100 00000 00000 00001 10000
	C_{04}	00000 00000 00100 00010 01000		C_{54}	01000 00100 00000 00000 00001
	C_{10}	10000 10000 10000 00000 00000		C_{60}	10000 00000 00000 00100 00100
	C_{11}	00000 01000 00010 00100 00000		C_{61}	00001 00010 00000 00000 01000
1	C_{12}	00000 00000 01000 00001 00010	**6**	C_{62}	00010 00001 00010 00000 00000
	C_{13}	00100 00000 00000 01000 00100		C_{63}	00000 10000 01000 00010 00000
	C_{14}	01000 00001 00000 00000 01000		C_{64}	00000 00000 00001 10000 00010
	C_{20}	10000 00000 00000 00001 00001		C_{70}	10000 00100 00100 00000 00000
	C_{21}	00001 10000 00000 00000 00010		C_{71}	00000 00010 10000 00001 00000
2	C_{22}	00010 01000 10000 00000 00000	**7**	C_{72}	00000 00000 00010 01000 10000
	C_{23}	00000 00100 00010 10000 00000		C_{73}	00100 00000 00000 00010 00001
	C_{24}	00000 00000 01000 00100 10000		C_{74}	01000 01000 00000 00000 00010
	C_{30}	10000 00001 00001 00000 00000		C_{80}	10000 00000 00000 01000 01000
	C_{31}	00000 10000 00100 01000 00000		C_{81}	00001 00100 00000 00000 10000
3	C_{32}	00000 00000 10000 00010 00100	**8**	C_{82}	00010 00010 00100 00000 00000
	C_{33}	00100 00000 00000 10000 01000		C_{83}	00000 00001 10000 00100 00000
	C_{34}	01000 00010 00000 00000 10000		C_{84}	00000 00000 00010 00001 00100
	C_{40}	10000 00000 00000 00010 00010		C_{90}	10000 01000 01000 00000 00000
	C_{41}	00001 00001 00000 00000 00100		C_{91}	00000 00100 00001 00010 00000
4	C_{42}	00010 10000 00001 00000 00000	**9**	C_{92}	00000 00000 00100 10000 00001
	C_{43}	00000 01000 00100 00001 00000		C_{93}	00100 00000 00000 00100 00010
	C_{44}	00000 00000 10000 01000 00001		C_{94}	01000 10000 00000 00000 00100

3.5 Summary

This chapter provides a broad background of the most common codes applied into OCDMA system including OOC, QCC and PC families. It gives details about the construction of the codes, the parameters and an example of the resulted code-words

.

Chapter 4 EXTENDED GROUPED NEW MODIFIED PRIME CODE

This chapter answers Research Question 1" Can the existing codes implemented in OCDMA systems be modified to accommodate, with better characteristics, the number of ONUs supported in PON?. This chapter introduces the proposed code "EG-nMPC", with steps of code construction detailed in section 4.1.1, and the parameters of the code are given in section 4.1.2. In addition, the code performance is evaluated in term of BER in an incoherent system using OOK and PPM modulations. Furthermore, the performance of the proposed code is compared to other prime codes and a discussion of the improvements achieved by the proposed code are highlighted in section 4.3

4.1 Proposed Code

This section contains a description of the code construction and parameters.

4.1.1EG-nMPC Construction

The EG-nMPC construction is described in the following seven steps:

Step 1. Choose the prime number, for example *P = 3*

Step 2. Generate the prime sequence based on a Galois Field *GF (P)*

$$S_{\mathrm{i}} = \left(S_{i,0}, S_{i,1}, \dots, S_{i,j}, \dots, S_{i,(P-1)}\right), i = 0,1, \dots, P-1 \tag{4-1}$$

where the element of the sequence is

$$S_{i,j} = \{i \,.\, j\}\,(mod\ P) \tag{4-2}$$

where *i* and *j* are elements over *GF(P) = {0,1,2,…,P-1}*.

Step 3. Map S_i into a binary sequence C_i as follows:

$$C_i = \left(C_{i,0}, C_{i,1}, \dots, C_{i,k}, \dots, C_{i,(n-1)}\right), i = 0,1, \dots, P-1, n = P^2 \tag{4-3}$$

where

$$C_{i,k} = \begin{cases} 1, & if\ k = S_{i,j} + j.P, for\ j = \{0,1,\ldots,P-1\} \\ 0, & elsewhere \end{cases} \tag{4-4}$$

Step 4. Extend the prime code by patching each sub-sequence by P of $0s$.

Step 5. For each code sequence, apply the time-shifting method described in MPC. Table 4-1 shows the resulting code-words with P = 3.

Table 4-1 Time shifting of extended prime code, *P* = 3

Group	Binary Code C_i			
0	C_{00}	100000	100000	100000
	C_{01}	010000	010000	010000
	C_{02}	001000	001000	001000
	C_{03}	000100	000100	000100
	C_{04}	000010	000010	000010
	C_{05}	000001	000001	000001
1	C_{10}	100000	010000	001000
	C_{11}	010000	001000	000100
	C_{12}	001000	000100	000010
	C_{13}	000100	000010	000001
	C_{14}	000010	000001	100000
	C_{15}	000001	100000	010000
2	C_{20}	100000	001000	010000
	C_{21}	010000	000100	001000
	C_{22}	001000	000010	000100
	C_{23}	000100	000001	000010
	C_{24}	000010	100000	000001
	C_{25}	000001	010000	100000

Step 6. Apply the method used in n-MPC which is based on repeating the last sequence stream of the earlier code-word and rotating within the same group [30]. Table 4-2 shows the result of this step. In the table, the padded sequence stream of the first code and the last sequence stream of the earlier code are presented in **bold**.

Step 7. From each group, generate two groups where:

- Group 1: Consists of the $S_{i,j}$ where $i = 0, \ldots, P\text{-}1$ and j can take the values of zero or any even number. Other sub-sequences are patched with blocks of zeros.

- Group 2: Consists of the $S_{i,j}$ where $i = 0, \ldots, P-1$ and j is an odd number. Other sub-sequences are patched with blocks of zeros.

The final code-words are presented in

Table 4-3. The code is represented by C_{xyz}, where x denotes the group (0 to $P-1$), y denotes the sub-group (1 or 2) and z denotes the code sequence (0 to $2P-1$).

Table 4-2 Binary sequence of extended new modified prime code

Group		Binary Code C_i			Padded sequence
0	C_{00}	100000	100000	100000	**000001**
	C_{01}	010000	010000	010000	100000
	C_{02}	001000	001000	001000	010000
	C_{03}	000100	000100	000100	001000
	C_{04}	000010	000010	000010	000100
	C_{05}	000001	000001	**000001**	000010
1	C_{10}	100000	010000	001000	010000
	C_{11}	010000	001000	000100	001000
	C_{12}	001000	000100	000010	000100
	C_{13}	000100	000010	000001	000010
	C_{14}	000010	000001	100000	000001
	C_{15}	000001	100000	010000	100000
2	C_{20}	100000	001000	010000	100000
	C_{21}	010000	000100	001000	010000
	C_{22}	001000	000010	000100	001000
	C_{23}	000100	000001	000010	000100
	C_{24}	000010	100000	000001	000010
	C_{25}	000001	010000	100000	000001

Table 4-3 Binary sequence of extended grouped new modified prime code

Group		Binary Code C_i				
0	**1**	C_{010}	000000	100000	000000	000001
		C_{011}	000000	010000	000000	100000
		C_{012}	000000	001000	000000	010000
		C_{013}	000000	000100	000000	001000
		C_{014}	000000	000010	000000	000100
		C_{025}	000000	000001	000000	000010
	2	C_{020}	100000	000000	100000	000000
		C_{021}	010000	000000	010000	000000
		C_{022}	001000	000000	001000	000000
		C_{023}	000100	000000	000100	000000

		C_{024}	000010	000000	000010	000000
		C_{025}	000001	000000	000001	000000
1	**1**	C_{110}	000000	010000	000000	010000
		C_{111}	000000	001000	000000	001000
		C_{112}	000000	000100	000000	000100
		C_{113}	000000	000010	000000	000010
		C_{114}	000000	000001	000000	000001
		C_{115}	000000	100000	000000	100000
	2	C_{120}	100000	000000	001000	000000
		C_{121}	010000	000000	000100	000000
		C_{122}	001000	000000	000010	000000
		C_{123}	000100	000000	000001	000000
		C_{124}	000010	000000	100000	000000
		C_{125}	000001	000000	010000	000000
2	**1**	C_{210}	000000	001000	000000	100000
		C_{211}	000000	000100	000000	010000
		C_{212}	000000	000010	000000	001000
		C_{213}	000000	000001	000000	000100
		C_{214}	000000	100000	000000	000010
		C_{215}	000000	010000	000000	000001
	2	C_{220}	100000	000000	010000	000000
		C_{221}	010000	000000	001000	000000
		C_{222}	001000	000000	000100	000000
		C_{223}	000100	000000	000010	000000
		C_{224}	000010	000000	000001	000000
		C_{225}	000001	000000	100000	000000

4.1.2Code Parameters

The length L, weight w, cardinality $|C|$, autocorrelation λ_{xyz}, and cross-correlation $\lambda_{x1y1z1,x2y2z2}$ of EG-nMPC are given by:

$$L = 2P^2 + 2P \quad (4\text{-}5)$$

$$w = \frac{(P+1)}{2} \quad (4\text{-}6)$$

$$|C| = 4P^2 \quad (4\text{-}7)$$

$$\lambda_{xyz} = w \quad (4\text{-}8)$$

$$\lambda_{x_1y_1z_1,x_2y_2z_2} = \begin{cases} 0, & \frac{P^2-1}{8P^2-2}\ probability \\ 1, & \frac{7P^2-1}{8P^2-2}\ probability \end{cases} \quad (4\text{-}9)$$

Equation (4-9) is obtained as follows:

Each code-word causes $w(P - 1)$ pairs of cross-correlations. Thus the cross-correlation value of 1 for a one communication channel and for all communication channels can be formed respectively as follow:

$$\lambda_{1\,(\text{one C-channel})} = \frac{P^2 - 1}{2} \tag{4-10}$$

$$\lambda_{1\,(\text{all C-channels})} = 2P^4 - 2P^2 \tag{4-11}$$

The total number of correlation pairs of EG-nMPC is:

$$\lambda_{Corr-pairs} = 4P^2.(4P^2 - 1) = 16\,P^4 - 4P^2 \tag{4-12}$$

The probability of a cross-correlation value of 1 is given by:

$$Pb_{\lambda 1} = \frac{\lambda_{1\,(all\,users)}}{\lambda_{corr-pairs}} = \frac{P^2 - 1}{8P^2 - 2} \tag{4-13}$$

The probability of a cross-correlation value of 0 is given by:

$$Pb_{\lambda 0} = 1 - Pb_{\lambda 1} = \frac{7P^2 - 1}{8P^2 - 2} \tag{4-14}$$

Taking the code C_{010} as an example, the code will not cause any cross-correlation with any code in the same group, either in the same or different subgroups. In addition, the code will not cause any cross correlation with any code in a different group and in different sub-group, as a consequence of step 7 in section 2.1. Each code- weight (w) in the code causes a cross-correlation with only one code from other groups (P – 1 group). Thus the code C_{010} will cause a cross correlation with the codes C_{114}, C_{115}, C_{214}, and C_{215}.

A system that uses an incoherent OCDMA is based on the binary *1* and *0*, where, *1* represents the presence of light and hence the encoding process executes and generates a waveform $s(n)$. The code sequence represents the destination address $f(n)$. The *0* on the other hand, represents the absence of light which means the encoding process will not be executed. After the encoding process and transmission to the communication channel, the receiver correlates the received signal with the destination address. This correlation function is denoted by *r(n)* and expressed as [136]:

$$r\,(n) = \sum_{i=1}^{N} s(i) f\,(i - n) \tag{4-15}$$

where, N is the number of communication channels. If the signal arrives correctly, then the received signal is equal to the destination address with $s(n) = f(n)$ and 1 signifies an auto-correlation function. Otherwise, 1 signifies a cross-correlation function [136].

In a synchronous OCDMA system, time synchronization T is performed at the end of each bit duration, where $T = L$ chip width [136]. For a “1 1 0 1” data stream, and synchronization time T, the correlation values of alternate codes are presented in Figure 4-1 and Figure 4-6. Figure 4-1 shows the auto-correlation value of C_{010} at each time interval T and it is equal to w (2 in Fig. 1). Figure 4-2 and Figure 4-3 show the cross-correlation value between two codes in a different group and same sub-group respectively. Figure 4-2 shows the case when the cross-correlation value is 1 and Figure 4-3 shows the case when the cross-correlation value is 0. Figure 4-4 to Figure 4-6 present the cross-correlation values of two codes from the same group and same sub-group, same group different sub-group and different group different sub-group respectively. As shown in these Figures, the value of the cross-correlation at time T is 0.

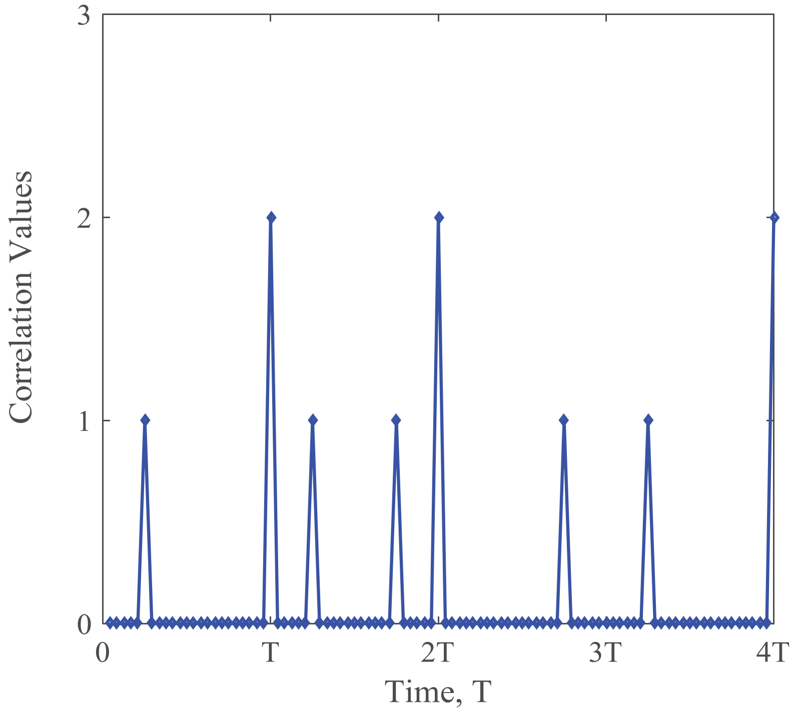

Figure 4-1 Auto-correlation of EG-nMPC of C_{010}, at synchronization time, *T*

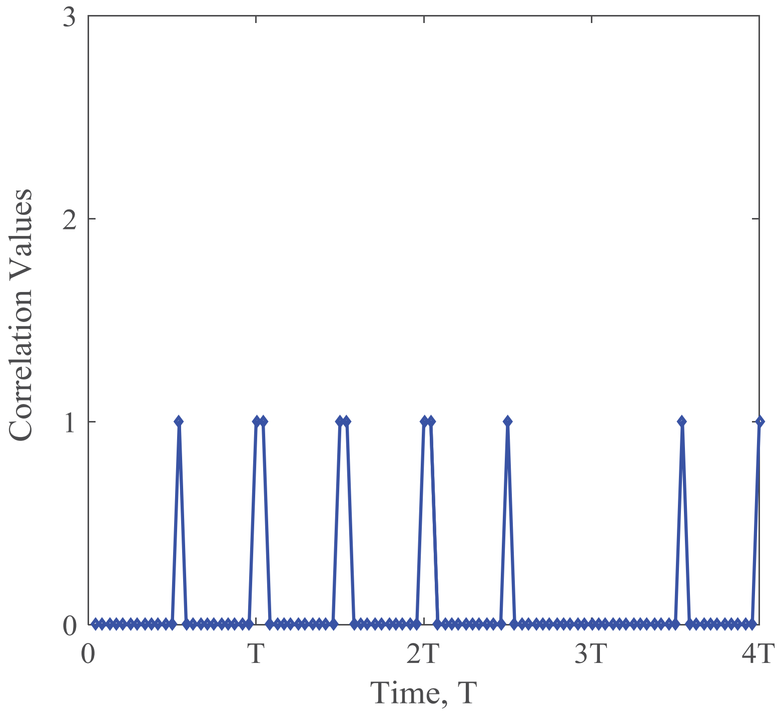

Figure 4-2 Cross-correlation of EG-nMPC of C_{014} and C_{112}, at synchronization time, *T*

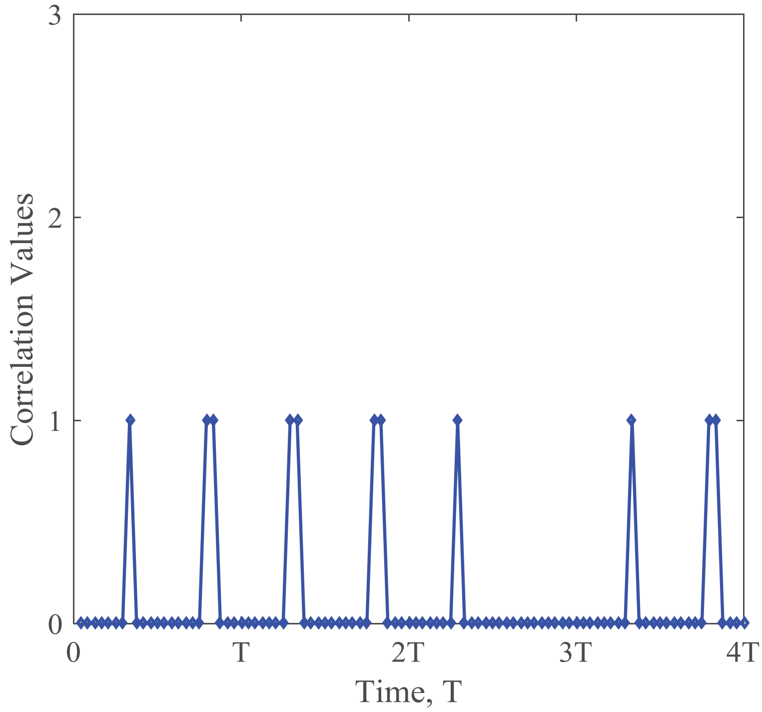

Figure 4-3 Cross-correlation of EG-nMPC of C_{022} and C_{125}, at synchronization time, T

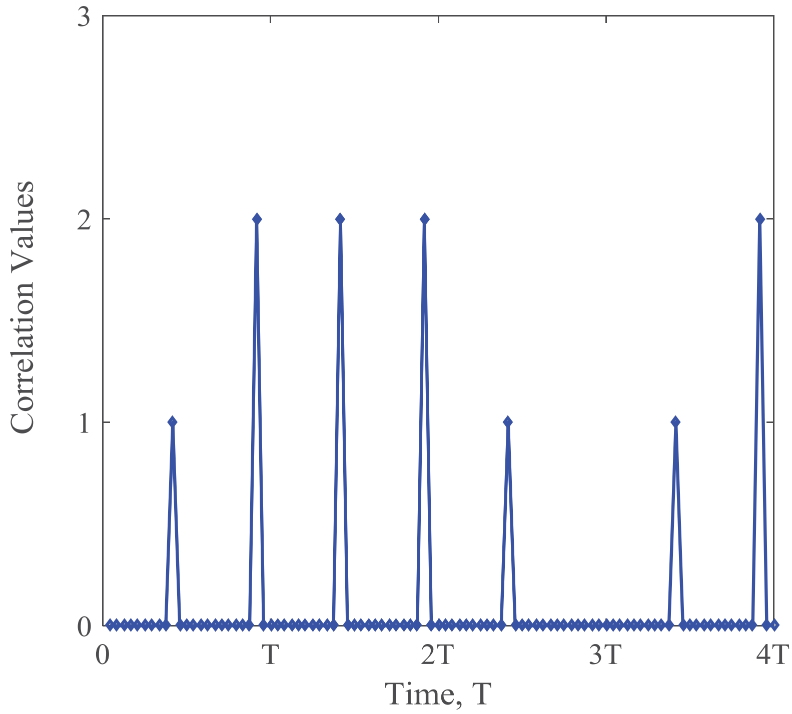

Figure 4-4 Cross-correlation of EG-nMPC of C_{110} and C_{112}, at synchronization time, T

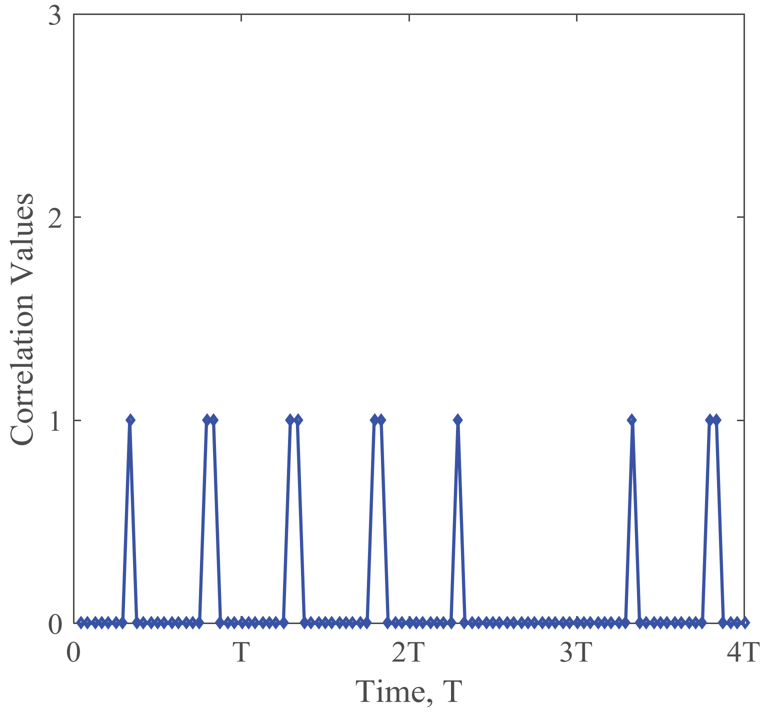

Figure 4-5 Cross-correlation of EG-nMPC of C_{024} and C_{013}, at synchronization time, T

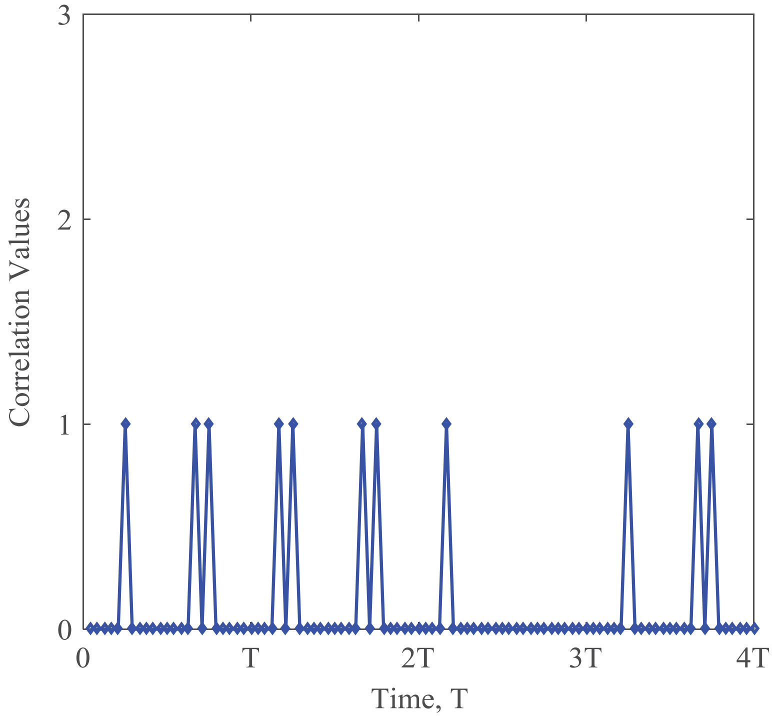

Figure 4-6 Cross-correlation of EG-nMPC of C_{020} and C_{210}, at synchronization time, T

4.2 Performance Analysis

In this section, the code performance analysis is provided.

4.2.1Performance Analysis of OOK-OCDMA System

The BER of the one dimensional time spreading code using an incoherent OOK modulation system relies on three main factors: the binary stream, the threshold range and the probability of 'hits' between '1s' within different code-words [134]. The BER can be formed as:

$$BER = \frac{1}{2}\sum_{i=0}^{w}(-1)^i \binom{w}{i}\left(1-\frac{iq}{w}\right)^{N-1} \tag{4-16}$$

In (4-16), w is the weight, N is the number of active communication channels s and q is the hit possibility of 1 between a particular communication channels and the intended communication channel which given by:

$$q = \frac{w^2}{2L} \tag{4-17}$$

However, q in (4-17) is for asynchronous OCDMA applying the OOC. For synchronous OCDMA system, q depends on the correlation expectation (E_λ) between two codes which can be expressed as [136]:

$$E_\lambda = \frac{\sum \lambda_{x1y1,x2y2}}{|C|.(|C|-1)} \tag{4-18}$$

The BER probability of MPC and T-SPMPC can be obtained from [136]. The BER of EG-nMPC can be formulated as:

$$BER = \frac{1}{2}\sum_{i=0}^{w}(-1)^i \binom{w}{i}\left(1-\frac{i}{2w}.\frac{P^2-1}{8P^2-2}\right)^{N-1} \tag{4-19}$$

4.2.2Performance Analysis of PPM-OCDMA System

EG-nMPC provides $4P^2$ code sequences, thus the number of communication channels is $4P^2$. By assuming N is the number of active communication channels, $4P^2$ - N is the number of idle communication channels. Y_n is defined as a random variable where:

$$Y_n, n \in \{1, 2, \dots, 4P^2\} \quad (4\text{-}20)$$

$$Y_n = \begin{cases} 1, & \text{if communication channel } n \text{ is active} \\ 0, & \text{if communication channel } n \text{ is idle} \end{cases} \quad (4\text{-}21)$$

thus,

$$N = \sum_{n=1}^{4P^2} Y_n \quad (4\text{-}22)$$

By assuming communication channel *1* is the desired communication channel, the random variable T is defined to represent the number of active communication channels that are not causing cross correlation with communication channel 1 and t is the realization of T. According to (4-10), T can be defined as:

$$T \overset{\text{def}}{=} \sum_{n=1}^{(7P^2+1)/2} Y_n \quad (4\text{-}23)$$

The probability distribution of the random variable T can be obtained as:

$$P_T(t) = \frac{\binom{(P^2-1)/2}{N-t} \cdot \binom{(7P^2-1)/2}{t-1}}{\binom{4P^2-1}{N-1}} \quad (4\text{-}24)$$

where $t \in \{t_{\min}, \dots, t_{\max}\}$

$$t_{min} = \max(2N - P^2 + 1)/2), 1)$$
$$t_{max} = \min(N, (7P^2 + 1)/2)$$

Let the photon count collection be denoted by the vector Y_n for communication channel n, where $Y_n = (Y_{n,0}, Y_{n,1}, \dots, Y_{n,M-1})$. Let the interference denoted by the random vector k, where $k = (k_0, k_1, \dots, k_{m-1})^T$. Let the vector u denote the realization of k, where $u = (u_0, u_1, \dots, u_{M-1})^T$. By assuming $T = t$, k can be defined as a multinomial random vector with the following probability:

$$P_{k|T}(u_0, u_1, \dots, u_{M-1}|t) = \frac{1}{M^{N-t}} \cdot \frac{(N-t)!}{u_0!, u_1!, \dots, u_{M-1}!} \quad (4\text{-}25)$$

where,

$$N - t = \sum_{i=0}^{M-1} u_i \quad (4\text{-}26)$$

Then the BER of can be given by [132]:

$$P_b = \frac{M}{2(M-1)} \sum_{t=t_{min}}^{t_{max}} P_E . P_t(t) \quad (4\text{-}27)$$

where M denotes the multiplicity and P_E denotes the error probability [132].

Similarly to (9) in [132], the lower bounded BER can be obtained in (4-30) by modifying (5) in [110] based on EG-nMPC properties. By taking $Q \rightarrow \infty$, where Q defined as:

$$\mathrm{Q} = \frac{\mu \, . (\ln M)}{w} \quad (4\text{-}28)$$

μ in (4-28) is the average photons count per pulse (photons/nat) , nat can be expressed as follow [137] [138]:

$$1\, nat = log_2 e \;\; bits \quad (4\text{-}29)$$

$$P_E \geq \sum_{u1=(\frac{P+1}{2}+1)}^{N-t} \binom{N-t}{u_1} \frac{1}{M^{u1}} . \left(1 - \frac{1}{M}\right)^{N-t-u_1} . \sum_{u_0=0}^{\min(u_1-(\frac{P+1}{2}+1),N-t-u_1)} \binom{N-t-u_1}{u_0} . \frac{1}{(M-1)^{u_0}} . \left(1 - \frac{1}{M-1}\right)^{N-t-u_0-u_1} + 0.5 \sum_{u_1=\frac{P+1}{2}}^{\frac{N-t+\frac{P+1}{2}}{2}} \binom{N-t}{u_1} \frac{1}{M^{u_1}} . \left(1 - \frac{1}{M}\right)^{N-t-u_1} . \binom{N-t-u_1}{u_1 - \left(\frac{P+1}{2}\right)} . \frac{1}{(M-1)^{u_1-\left(\frac{P+1}{2}\right)}} . \left(1 - \frac{1}{M-1}\right)^{N-t-2u_0+\frac{P+1}{2}} \quad (4\text{-}30)$$

4.3 Discussion

A comparison of the results for EG-nMPC and MPC, the basis for many of the standard codes found today, highlights the performance advantages of EG-nMPC. When EG-nMPC is compared with T-SPMPC, a recently developed code that supports a large number of communication channels with a low weight, the result shows that EG-nMPC provides an improvement.

In Figure 4-7, the correlation expectation of the MPC, T-SPMPC, and EG-nMPC are presented and as shown in the figure, the correlation expectation of MPC is the highest. With $P = 5$ the correlation expectation is 0.83 and it increases to 0.96 as P increases to 23. T-SPMPC shows a lower correlation expectation. With $P = 5$ the correlation expectation is 0.32 and decreases to 0.29 as P increases to 23. EG-nMPC shows the lowest correlation expectation compared to the other codes. With $P = 5$, the correlation expectation is 0.1212 and increases slightly to 0.1248 with P increasing to 23.

The low value of correlation expectation is a result of Step 7 in the code construction. This step aims to duplicate the number of available code-words at the same time it minimizes the correlation between the codes by replacing some of the sub-sequences with block of zeros.

Figure 4-8 presents the BER performance versus the number of communication channels of an OOK-OCDMA system. It compares the performance of the three codes with $P = 11$, and $P = 13$. The figure shows that at the BER of 10^{-9}, the performance of the three codes are similar with a slight improvement for MPC, followed by EG-nMPC and then T-SPMPC. However, with an increasing number of the communication channels, the performance of the EG-nMPC has improved and its performance with $P = 11$ and $P = 13$ is superior. In addition, this improvement can be seen clearly in Figure 4-9 with $P = 23$ and $P = 37$. The figure shows that EG-nMPC was achieved the required BER with more communication channels.

Figure 4-10 illustrates the BER performance versus the number of communication channels of a PPM-OCDMA system. The figure compares the performance of MPC and EG-nMPC, with, μ= 150, M = 16, P = 11, and P = 13. It is important to note that the comparison is made between EG-nMPC and MPC only. This is due to the absence of mathematical expressions to evaluate the BER of T-SPMPC, in the case of a PPM-OCDMA system without interference cancellation. The figure shows that at the BER value of 10^{-9}, MPC accommodates a slightly higher number of communication channels when compared to EG-nMPC. However, as the number of communication channels increases, the BER of EG-nMPC reduces, pointing to an improved performance. The smaller BER values are attributed to the EG-nMPC capability to accommodate a larger number of communication channels. The capability of EG-nMPC to accommodate more communication channels with the same average photons/nat, is also evident from Figure 4-10, an outcome that points to the code being energy-efficient.

It is important to note the significant role played by the multiplicity, M, in improving the system performance, as shown in Figure 4-11. The figure shows the performance of BER versus the number of communication channels, with M = 16 and M = 8, P = 13, and μ =150. As shown in the figure, an increase in the value of M results in an improvement in system performance, however, larger values of M lead to an increase in system cost and complexity.

EG-nMPC increases the cardinality of the code with a smaller P, as shown in Figure 4-12. For a large number of communication channels, EG-nMPC has a lower BER overall compared to the other code families with both modulation systems as shown in Figure 4-8, Figure 4-9, and Figure 4-10. Therefore, it is effective to implement EG-nMPC over GPON thereby supporting a high number of ONUs.

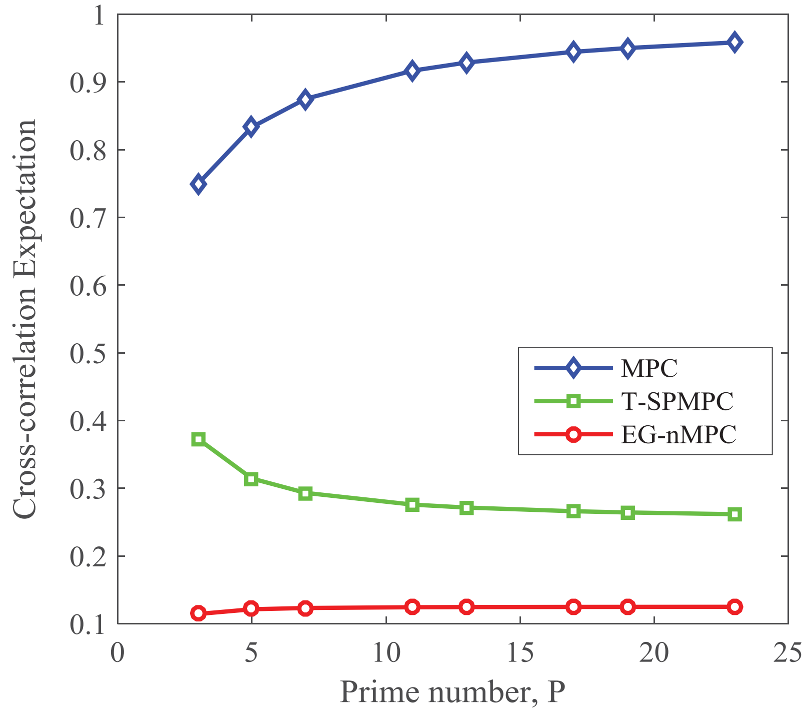

Figure 4-7 Cross-correlation expectations of MPC, T-SPMPC and EG-nMPC

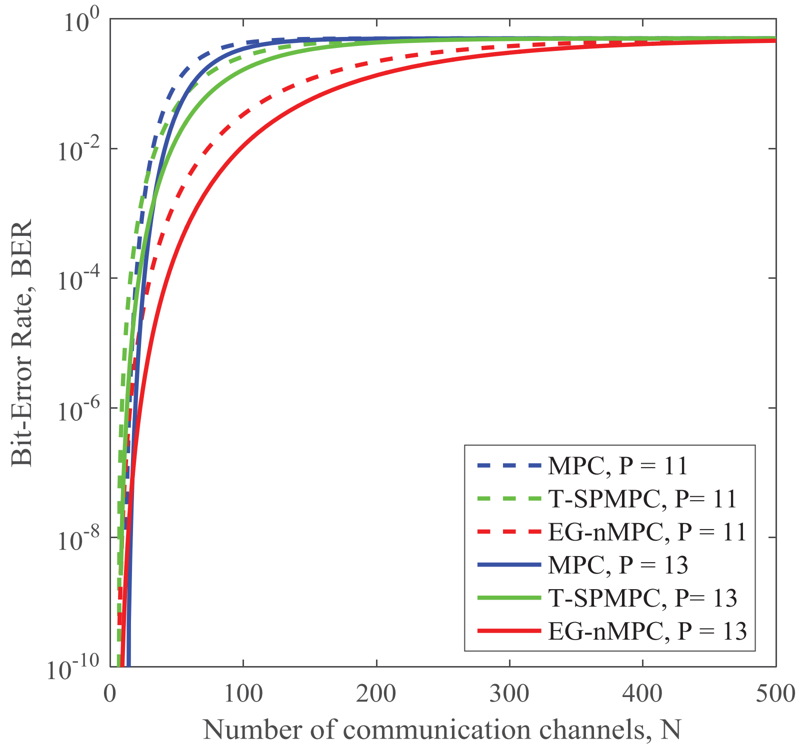

Figure 4-8 BER versus number of communication channels, for MPC, T-SPMPC, and EG-nMPC, using OOK system for *P* = 11 and *P* = 13

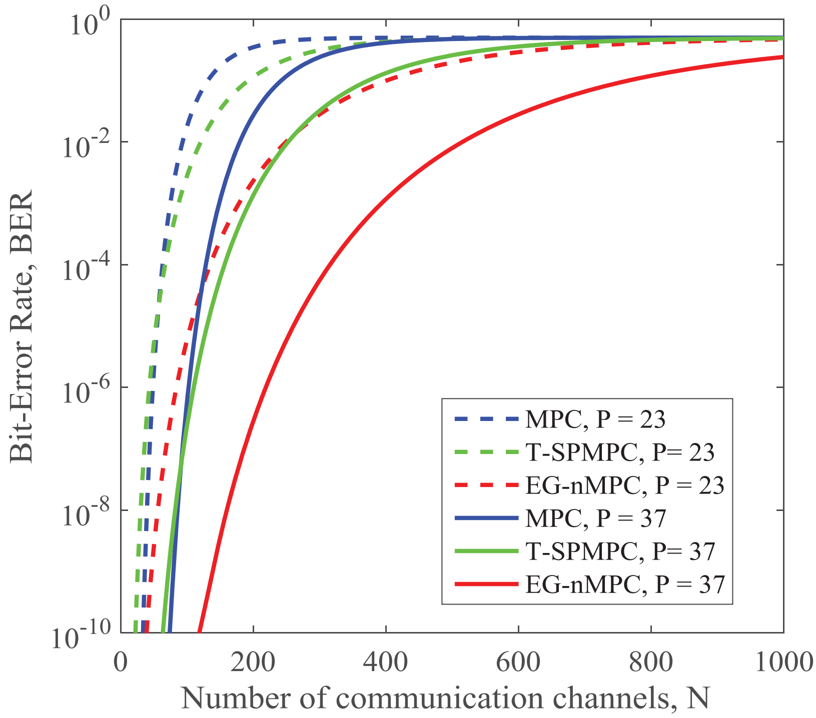

Figure 4-9 BER versus number of communication channels, for MPC, T-SPMPC, and EG-nMPC using OOK system, for *P* = 23 and *P* = 37

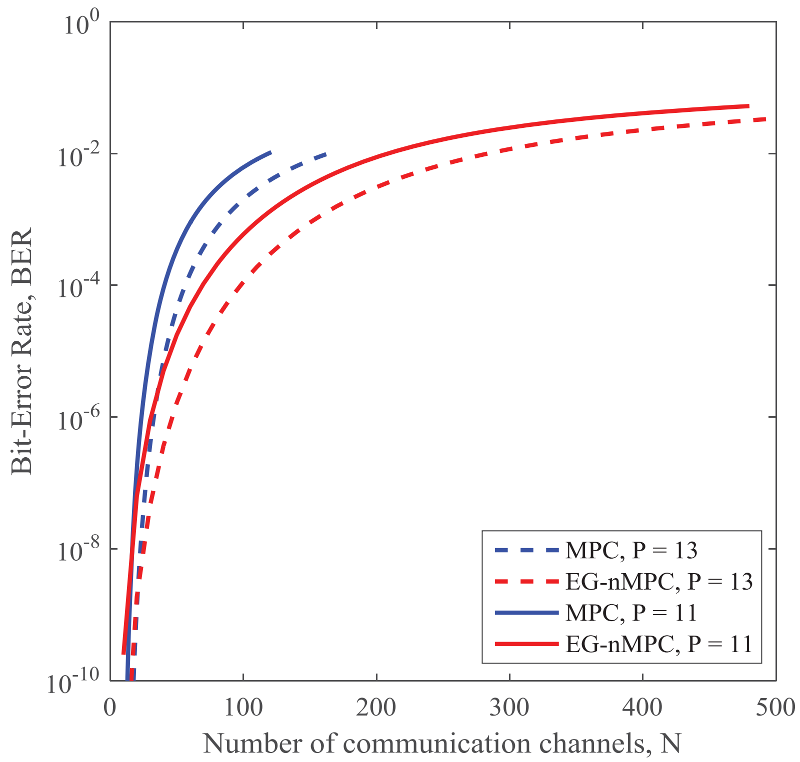

Figure 4-10 BER versus number of communication channels, for MPC, and EG-nMPC using PPM-OCDMA system, for *P* = 11, and *P* = 13

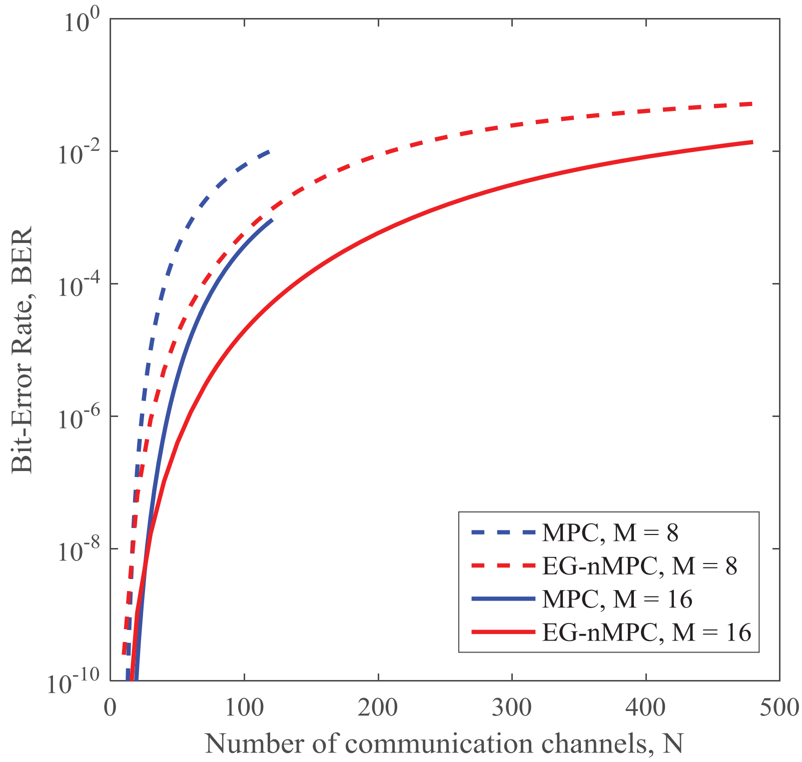

Figure 4-11 BER versus number of communication channels, for MPC, and EG-nMPC using PPM-OCDMA system, for *P* = 11, *M* = 8 and *M* = 16

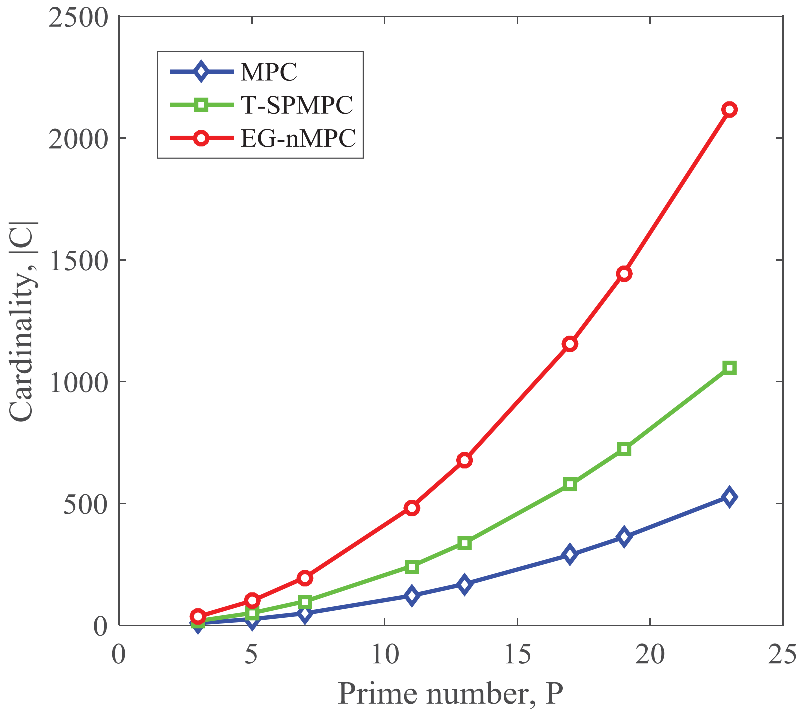

Figure 4-12 Cardinality of MPC, T-SPMPC and EG-nMPC

4.4 Code Comparison for GPON Splitting Ratios

As stated in Chapter 1, the spreading code of an OCDMA system can be used in a monitoring system for PON networks. For 1-D coding, a 1-D OOC has improved performance over prime codes in terms of correlation. Its construction mechanism, however, is relatively complex, in addition to its cardinality being bound by its length and weight [30]. Therefore, an OOC can only support a limited number of code-words. To increase the number of code-words, the length needs to be increased. Table 4-4 shows examples of optimal OOC codes [27]. On the other hand, 1-D PC is characterized by a simple construction mechanism, in addition to its cardinality not being subject to an upper bound and there are no mathematical limitations on the way the code is used, other than matching the code used with the optical transmission system capabilities [27, 30]. The correlation probabilities of OOC are higher than those of PCs, however, this feature has become less important in PON due to the use of TDMA and the ranging process performed by the OLT and ONU to avoid upstream burst collision. The selection of the spreading code implemented in OC techniques is determined by the cardinality of the spreading code selected [36]. Hence, the main objective is to provide the number of code-words that are compatible with PON splitting ratios (32, 64, and 128).

Table 4-4 Examples of optimal OOC code [27]

Weight, w	Length, n	Cardinality, $\|C\|$
3	31	5
3	255	42
3	511	85
3	1023	170
4	40	3
4	364	30
4	1093	91
5	85	4
5	341	17
5	1365	68
6	156	5
6	631	21
6	3156	105

The proposed code can be implemented in OC techniques as it provides compatible cardinality with lower unused code-words when compared to other PCs, thereby leading to an increase in the code utilization factor that is defined as the number of active communication channels at a given BER [133].

EG-nMPC increases the cardinality of the code with a smaller value of *P*, as shown in Figure 4-12. Implementing EG-nMPC as a spreading code for an OC technique to monitor PON networks that support splitting ratios of 32, 64, and 128 could be seen to be an improved solution. Table 4-5 shows a comparison of the code parameters for the different PON splitting ratios. For a splitting ratio of 32, EG-nMPC has been shown to have the lowest weight, length and unused codes, i.e. 2, 24, 4, respectively. This renders EG-nMPC a superior code for supporting a splitting ratio of 32, as compared to other codes. T-SPMPC ranks second in superiority, with MPC being the least desirable code among the three. The very slight increase in the number of unused codes exhibited by T-SPMPC as compared to MPC, does not carry any significant weight on this superiority ranking. The inferiority of MPC, for a splitting ratio of 32, is evidenced by the values of its weight, its length, and the number of unused codes, i.e. 7, 49, 17 respectively.

For a splitting ratio of 64, MPC shows the least desirable option with largest values for weight, length, and unused codes, i.e. 11, 121 and 57 respectively. When it comes to code length and the number of unused codes, T-SPMPC is shown to be a better option when compared to EG-nMPC, with a length of 49, as compared to 60, and the number of unused codes being 34 as compared to 36. However, EG-nMPC possesses a lower weight when compared to T-SPMPC, i.e. 3 and 4, respectively. For a splitting ratio of 128, although MPC has the lowest number of unused codes, its weight is far larger and the length is far longer than other codes. EG-nMPC exhibits lower weight, length, and a smaller number of unused codes compared to T-SPMPC. Consequently, it could be concluded that EG-nMPC possesses improved numerical values for weight, length and number of unused codes.

Table 4-5 Code Parameter Comparison

32					64				128			
PC	*P*	Cardinality (unused codes)	*L*	*w*	*P*	Cardinality (unused codes)	*L*	*w*	*P*	Cardinality (unused codes)	*L*	*w*
MPC	7	49 (17)	49	7	11	121 (57)	121	11	13	169 (41)	169	13
T-SPMPC	5	50 (18)	25	3	7	98 (34)	49	4	11	242 (114)	121	6
EG-nMPC	3	36 (4)	24	2	5	100 (36)	60	3	7	196 (68)	112	4

4.5 Summary

In this chapter, the construction of the proposed code for a PON monitoring based OC technique has been described and its parameters have been defined. In addition, the performance of the proposed code has been evaluated using an incoherent OOK-OCDMA system, and then compared to both MPC and T-SPMPC. In incoherent PPM-OCDMA systems, however, performance of the proposed code was evaluated and compared to MPC only. In addition, it has been shown that, the use of EG-nMPC as a spreading code for a monitoring-based OC technique is valid as it possesses overall superior characteristics, when compared to the other two codes, and that is in regard to weight, length, and the number of unused codes.

Chapter 5 NG-PON PROTECTION

This chapter answers Research Question 2 "How would the new application of the FIR parameter improve system performance? ". To answer this question, the chapter starts with an overview of NG-PON architecture that is based on LR-PON in section 5.1. It then followed by evaluation of the FIR parameter for the different network components in section 5.2 . Based on this parameter, three protection schemes for LR-PON were proposed as shown in section 5.3. The performance of the proposed protection schemes were then evaluated in term of cost and availability, and compared to the existing protection schemes.

5.1 NG-PON Architecture

The LR-PON architecture is an optimal solution that meets the requirements of NG-PON [12]. It aims to extend coverage and to accommodate 1024 ONUs [8]. This can be achieved by implementing optical amplifiers in the field [139]. Depending on GPON splitting ratios and the architecture of LR-PON, that is based on ring-and spur, NG-PON that support 1024 ONUs, at least, can be realized by implementing one of the following scenarios:

- Scenario A: 32 RNs each with a splitting ratio of 32
- Scenario B: 16 RNs each with a splitting ratio of 64
- Scenario C: 8 RNs each with a splitting ratio of 128

The calculations in this chapter are based on Figure 5-1 and the follwing asumptions.

The feeder fibre (FF), 100 km long, is connected to a number of K RNs, where $K \in \{32, 16, 8\}$. Hence, there are a (K+1) fibre segments (L_{FS}). Each RN connects to a splitter using a distribution fibre (DF) with a length of 20 km each. The splitter is connected to N ONUs, where, $N \in \{32, 64, 128\}$. In the calculations, presented in this chapter, the ONU is assumed to be at a distance of 1 km from the splitter, which is connected to (K/2) RN.

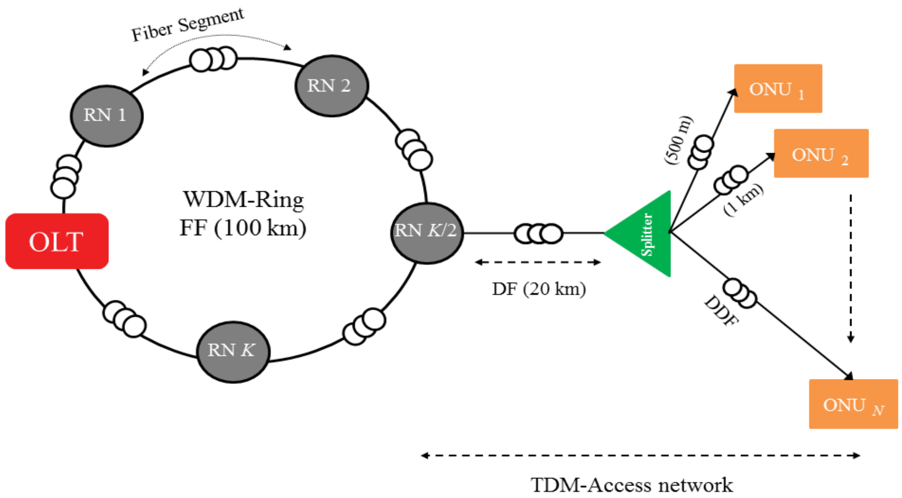

Figure 5-1 LR-PON

5.2 FIR for Network Components

FIR is an important parameter that is used to quantify the resistance of a component or a connection to a single failure [140]. There is an inverse relationship between FIR and the number of affected ONUs. So, as the value of FIR decreases, the number of affected ONUs increases [31]. The FIR for a network component can be calculated from the following equation [31]:

$$FIR_{component} = \frac{1}{(CAF * Un_{component})} \quad (5\text{-}1)$$

where *CAF* is the number of ONUs affected by a failure in the component, and $Un_{\text{component}}$ is the unavailability of that component [31]. The parameters used to find the FIR for the different compnents are presented in Table 5-1.

Table 5-1 FIR parameters

Components	Unavailablity	Availablity	CAF
OLT	5.12E-7	0.999999488	*K*x*N*
FF	3.42E-4	0.999658	*K*x*N*
DF	6.4E-5	0.999936	*N*
DDF	3.42E-6	0.99999658	1
RN	4.00E-7	0.9999996	*N*
Splitter	1.00E-7	0.9999999	*N*
ONU	5.12E-7	0.999999488	1

Figure 5-2 shows the FIR of different network components for a ring-and-spur LR-PON. It should be noted that the FIR of the OLT, FF, ONU, and DDF have the same numerical value for the different scenarios. This is due to the fact that a fault in the OLT or FF will affect 1024 ONUs, while a fault in an ONU or DDF will affect only one ONU. FIR values for DF, splitter, and RN, however, affect different numbers of ONUs based on the splitting ratios. It is evident from Figure 5-2 that the FIR values of the ONU and DDF are the highest. This is due to the fact that only one ONU is affected by that fault. The ONU acquires a higher FIR value, compared to the DDF, due to its higher availability. The FIR values of the splitter and the RN are lower than those of ONU and DDF, as the number of users affected by a single fault in these components is $N \epsilon$ (32, 64, or 128) for scenarios A, B, and C respectively. The ranking of the FIR of those components is based on their availability, where the splitter has higher availability than the RN. Although a fault in the OLT would affect 1024 ONUs and a fault in DF would affect N ONUs, the FIR of the OLT is larger than that of DF because of its higher availability. It is evident also that the FIR of the FF is the lowest because of its low availability as well as the fact that a faulty FF would affect 1024 ONUs.

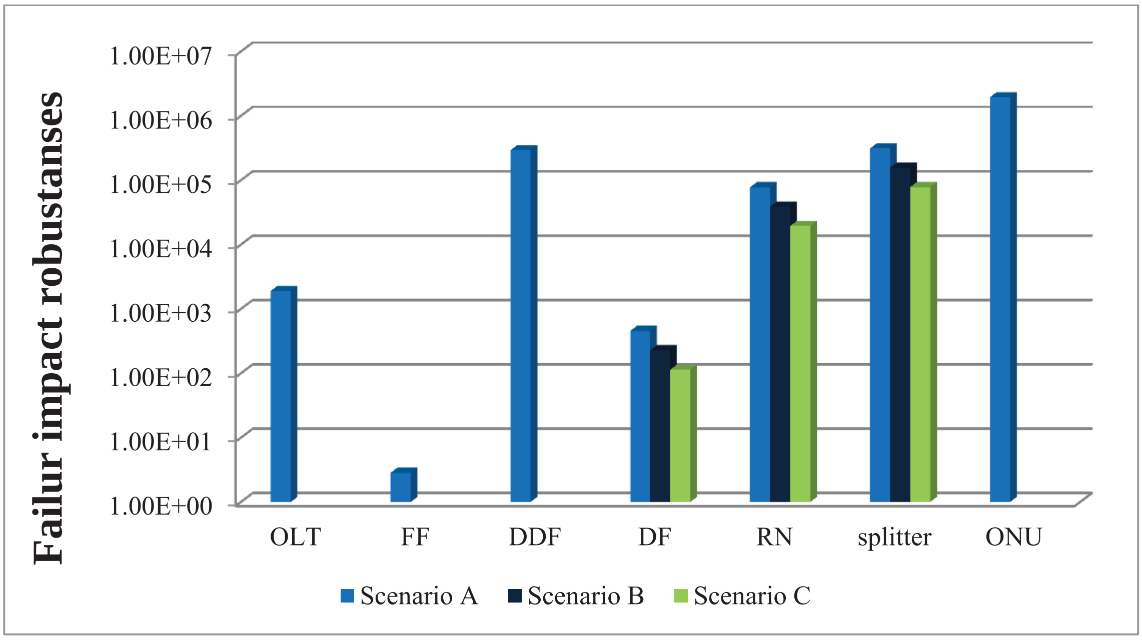

Figure 5-2 FIR for different network components in ring-and-spur

5.3 Protection Schemes for LR-PON

Based on the numerical FIR values, three protection schemes are proposed for LR-PON, i.e. Ring-DF protection, OLT-Ring-DF protection and OLT-Ring protection schemes.

Figure 5-3 presents the availability block diagrams (ABD) based on the ring-and-spur LR-PON architecture, a sketch diagram that is similar in design to that reported in the literature, see Section 2.4.2. In the ABD above, blocks are used to represent components, and lines are used to represent connections between components.

Figure 5-3 (a) shows an OLT-Ring protection scheme. In this scheme, the protection of the ring is carried out by duplicating the RNs and using a spare FF fibre, where, two OSs are used to re-route the traffic from the faulty FF fibre to the spare one. The protection of the OLT is performed by duplicating the OLT. In case of a faulty primary OLT, the secondary OLT is activated to take control of the PON. The switching process is entirely within the OLT, hence, no need for a switching protocol [141].

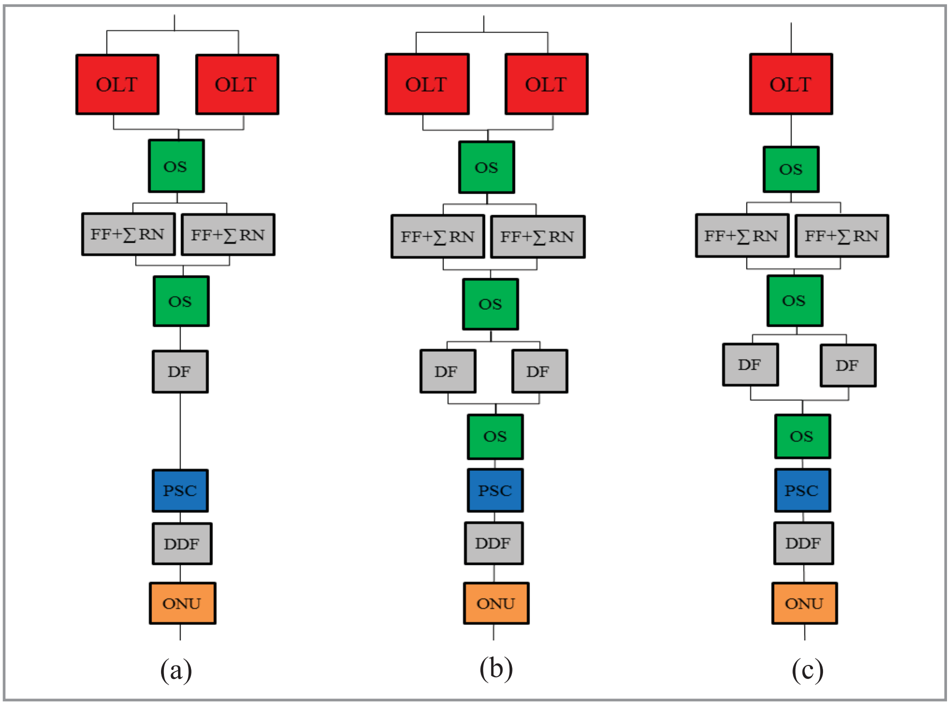

Figure 5-3 ABD for the proposed protection schemes, (a) OLT-Ring protection, (b) OLT-Ring-DF protection, (c) Ring-DF protection

Figure 5-3 (b) shows an OLT-Ring-DF protection scheme. In this scheme, OSs are used to re-route traffic in case of a fault detected in the operational FF, DF or both.

Figure 5-3 (c) shows a Ring-DF protection scheme. This type of protection is similar to Type D protection, an independent duplication of feeder and branch fibre that was discussed in ITU-T Recommendation G.983.1 [142]. This protection was proposed for a typical tree topology, where each distribution fibre was protected by a spare fibre, as well as each ONU being connected to an OS to switch between the faulty distribution fibre and the spare one [142, 143]. However, for Ring-DF protection based LR-PON, the DF connects RN and splitter together; hence, the duplication of the DF requires only two OSs.

5.3.1 Availability

The network availability is the collective availability of all the network components, and is calculated based on the assumption that the components are able to provide services and perform functions in a predetermined period of time without any failure [82]. The availability can be defined as [81]:

$$A = 1 - \left(\frac{MTTR}{MTBF}\right) \tag{5-2}$$

Where, MTTR denotes the mean time to repair and MTBF denotes the mean time between failures. The unavailability is the "complement of availability" that can be derived as follows:

$$Un = MTTR.FIT_s/10^9 \tag{5-3}$$

Where, FIT denotes failure in time, with 1 FIT signifying a failure in 10^9 h. The values of MTTR and FIT for network components are found in [82].

The unavailability of non-protection, access protection, ring protection and fully protection schemes have been defined in [82]. Non-protection scheme provides a single path between the OLT and the ONUs. Access protection scheme duplicates the path between the RN and the ONUs. Ring protection is based on duplicating the ring which includes the RNs. Full protection aims to duplicate each part in the LR-PON. The proposed protection schemes that include OLT-ring protection, ring-DF protection and OLT-ring-DF aim to duplicate the ring and the OLT, the ring and the distribution fibers, and the OLT, ring, and the distribution fibers, respectively. In the following equations, the duplicated parts of each protection scheme are squared, that is raised to power 2. The abbreviation of the formulas (5-4) - (5-10) are given in Table 5-2.

The unavailability of non-protection, access protection, ring protection, fully protection, OLT-Ring protection, Ring-DF protection, and OLT-Ring-DF protection schemes, respectively, are defined as follow:

$$Un_{non\text{Prot.}} = Un_{OLT} + \frac{K}{2}.L_{FS}.Un_F + \frac{K}{2}.Un_{RN} + L_{DF}.Un_F + Un_S + L_{DDF}.Un_F + Un_{ONU} \quad (5\text{-}4)$$

$$Un_{Access\ \text{Prot.}} = Un_{OLT} + \frac{K}{2}.L_{FS}.Un_F + \frac{K}{2}.Un_{RN} + Un_{OS} + [L_{DF}.Un_F + Un_S + L_{DDF}.Un_F + Un_{ONU}]^2 \quad (5\text{-}5)$$

$$Un_{Ring\ \text{Prot.}} = Un_{OLT} + Un_{OS} + \left[\frac{K}{2}.L_{FS}.Un_F + \frac{K}{2}.Un_{RN}\right]^2 + Un_{OS} + L_{DF}.Un_F + Un_S + L_{DDF}.Un_F + Un_{ONU} \quad (5\text{-}6)$$

$$Un_{Fully\ \text{Prot.}} = [Un_{OLT}]^2 + Un_{OS} + \left[\frac{K}{2}.L_{FS}.Un_F + \frac{K}{2}.Un_{RN}\right]^2 + Un_{OS} + [L_{DF}.Un_F + Un_S + L_{DDF}.Un_F + Un_{ONU}]^2 \quad (5\text{-}7)$$

$$Un_{OLT-Ring\text{Prot.}} = [Un_{OLT}]^2 + Un_{OS} + \left[\frac{K}{2}.L_{FS}.Un_F + \frac{K}{2}.Un_{RN}\right]^2 + Un_{OS} + L_{DF}.Un_F + Un_S + L_{DDF}.Un_F + Un_{ONU} \quad (5\text{-}8)$$

$$Un_{Ring-DF\ \text{Prot.}} = Un_{OLT} + Un_{OS} + \left[\frac{K}{2}.L_{FS}.Un_F + \frac{K}{2}.Un_{RN}\right]^2 + Un_{OS} + [L_{DF}.Un_F]^2 + Un_{OS} + Un_S + L_{DDF}.Un_F + Un_{ONU} \quad (5\text{-}9)$$

$$Un_{OLT-Ring-DF\ \text{Prot.}} = [Un_{OLT}]^2 + Un_{OS} + \left[\frac{K}{2}.L_{FS}.Un_F + \frac{K}{2}.Un_{RN}\right]^2 + Un_{OS} + [L_{DF}.Un_F]^2 + Un_{OS} + Un_S + L_{DDF}.Un_F + Un_{ONU} \quad (5\text{-}10)$$

Table 5-2 Abbrevation of unavailablity evaluation

Abbreviations	
$Un_{\text{non prot.}}$	Unavailability of non-protected scheme
$Un_{Access\ prot.}$	Unavailability of access protected scheme
$Un_{Ring\ prot.}$	Unavailability of ring protected scheme
$Un_{Fully\ Prot.}$	Unavailability of fully protected scheme
$Un_{OLT\text{-}Ring\ Prot.}$	Unavailability of OLT and ring protected scheme
$Un_{Ring\text{-}DF\ Prot.}$	Unavailability of ring and distribution fibers protected scheme
$Un_{OLT\text{-}Ring\text{-}DF\ Prot.}$	Unavailability of OLT, ring and distribution protected scheme
$Un_{\text{OLT.}}$	Unavailability of OLT
$Un_{\text{F.}}$	Unavailability of the fiber
Un_{RN}	Unavailability of the RN
Un_s	Unavailability of the splitter
Un_{ONU}	Unavailability of the ONU
Un_{OS}	Unavailability of the optical switch
L_{FS}	Length of the fibre segments
L_{DF}	Length of the distribution fiber

L_{DDF}	Length of the ddrop fiber

5.3.2 Cost

Similar to the availability, and in each equation of the protection scheme, the costs of the duplicated parts are doubled. The cost of non-protection, access protection, ring protection, fully protection, OLT-Ring protection, Ring-DF protection, and OLT-Ring-DF protection schemes, respectively, are defined similar to [82] as follows:

$$C_{non\ Prot.} = C_{OLT} + L_{FF}(C_F + C_B) + K.C_{RN} + \mathrm{K}.C_S + K.L_{DF}(C_F + C_B) + K.N[(L_{DDF}(C_F + C_B) + C_{ONU})] \quad (5\text{-}11)$$

$$C_{\mathrm{Access}\ Prot.} = C_{OLT} + L_{FF}(C_F + C_B) + K.C_{RN} + K.C_{OS} + 2K.L_{DF}(C_F + C_B) + 2K.C_S + 2K.N[(L_{DDF}(C_F + C_B) + C_{ONU})] \quad (5\text{-}12)$$

$$C_{Ring\ Prot.} = C_{OLT} + C_{OS} + 2L_{FF}(C_F + C_B) + 2K.C_{RN} + K.C_{OS} + K.L_{DF}(C_F + C_B) + K.C_S + K.N[(L_{DDF}(C_F + C_B) + C_{ONU})] \quad (5\text{-}13)$$

$$C_{\mathrm{Fully}\ Prot.} = 2C_{OLT} + C_{OS} + 2L_{FF}(C_F + C_B) + 2K.C_{RN} + 2K.C_{OS} + 2K.[L_{DF}(C_F + C_B)] + 2K.C_S + 2K.N[(L_{DDF}(C_F + C_B) + C_{ONU})] \quad (5\text{-}14)$$

$$C_{OLT-Ring\ Prot.} = 2C_{OLT} + C_{OS} + 2L_{FF}(C_F + C_B) + 2K.C_{RN} + K.C_{OS} + K.L_{DF}(C_F + C_B) + K.C_S + K.N[(L_{DDF}(C_F + C_B) + C_{ONU})] \quad (5\text{-}15)$$

$$C_{Ring-DF\ Prot.} = C_{OLT} + C_{OS} + 2L_{FF}(C_F + C_B) + 2K.C_{RN} + K.C_{OS} + 2K.L_{DF}(C_F + C_B) + K.C_{OS} + K.C_S + K.N[(L_{DDF}(C_F + C_B) + C_{ONU})] \quad (5\text{-}16)$$

$$C_{OLT-Ring-DF\ Prot.} = 2C_{OLT} + C_{OS} + 2L_{FF}(C_F + C_B) + 2K.C_{RN} + K.C_{OS} + 2K.L_{DF}(C_F + C_B) + K.C_{OS} + K.C_S + K.N[(L_{DDF}(C_F + C_B) + C_{ONU})] \quad (5\text{-}17)$$

The cost of the components can be found in [82, 144]. The abbreviation of the formulas (5-11) - (5-17) are given in Table 5-3.

Table 5-3 Abbrevation of cost evaluation

Abbreviations	
$C_{\mathrm{non\ prot.}}$	Cost of non-protected scheme

$C_{Access\ prot.}$	Cost of access protected scheme
$C_{Ring\ prot.}$	Cost of ring protected scheme
$C_{Fully\ Prot.}$	Cost of fully protected scheme
$C_{OLT\text{-}Ring\ Prot.}$	Cost of OLT and ring protected scheme
$C_{Ring\text{-}DF\ Prot.}$	Cost of ring and distribution fibers protected scheme
$C_{OLT\text{-}Ring\text{-}DF\ Prot.}$	Cost of OLT, ring and distribution protected scheme
$C_{OLT.}$	Cost of OLT
$C_{F.}$	Cost of the fiber (/km)
C_B	Cost of burying fiber (/km)
C_{RN}	Cost of the RN
C_s	Cost of the splitter
C_{ONU}	Cost of the ONU
C_{OS}	Cost of the optical switch
L_{FF}	Length of the feeder fiber
L_{DF}	Length of the distribution fiber
L_{DDF}	Length of the drop fiber

5.3.3Discussion

Figure 5-4 and Figure 5-5 represent statistical analysis and comparison of all protection schemes in terms of both cost and availability, respectively. The parameters used are presented in Table 5-4. It can be seen that the fully protected architecture is the most reliable scheme because of its high availability, as compared to other protection schemes. It is, however, the most expensive one. The access protection scheme is an inefficient solution as it is very costly and with low availability, when compared to its counterparts. The cost of each of OLT-Ring-DF and Ring-DF protection schemes, which is very comparable as can be seen in Figure 5-5, is lower than that of the full and access protection schemes. The availability of OLT-Ring-DF and Ring-DF schemes is comparable, and is higher than that of access protection. The cost of ring protection and OLT-Ring protection are slightly higher than the corresponding techniques with no protection. Likewise, the availability of the schemes are higher than the corresponding techniques with no protection. Therefore, those schemes are the more satisfactory schemes.

The main contribution of this chapter is the selection of the optimal protection scheme.While [82] recommends ring only protection scheme as it achieves high availability (99.992), this research recommends the use of an OLT-Ring protection scheme that achieves a similar availability (99.993) at a similar cost becoming an improved protection scheme. This recommendation is based on the results of the FIR analysis and *CAF* values for the different components. In addition, the cost per user of the OLT-Ring protection scheme is minimal.

Table 5-4 Parameters used in the simulation of Cost and availability

Components	FIT	MTTR	Unavaliablity	Cost US $
OLT	256	2	5.12E-7	500
Fibre (km)	570	6	3.42E-6	1
Remote node	200	2	4E-7	600
Splitter 1x32	50	2	1E-7	13
Splitter 1x64	50	2	1E-7	37
Splitter 1 x 128	50	2	1E-7	190
ONU	256	2	5.12E-7	150
Burying Fibres (km)	-	-	-	250

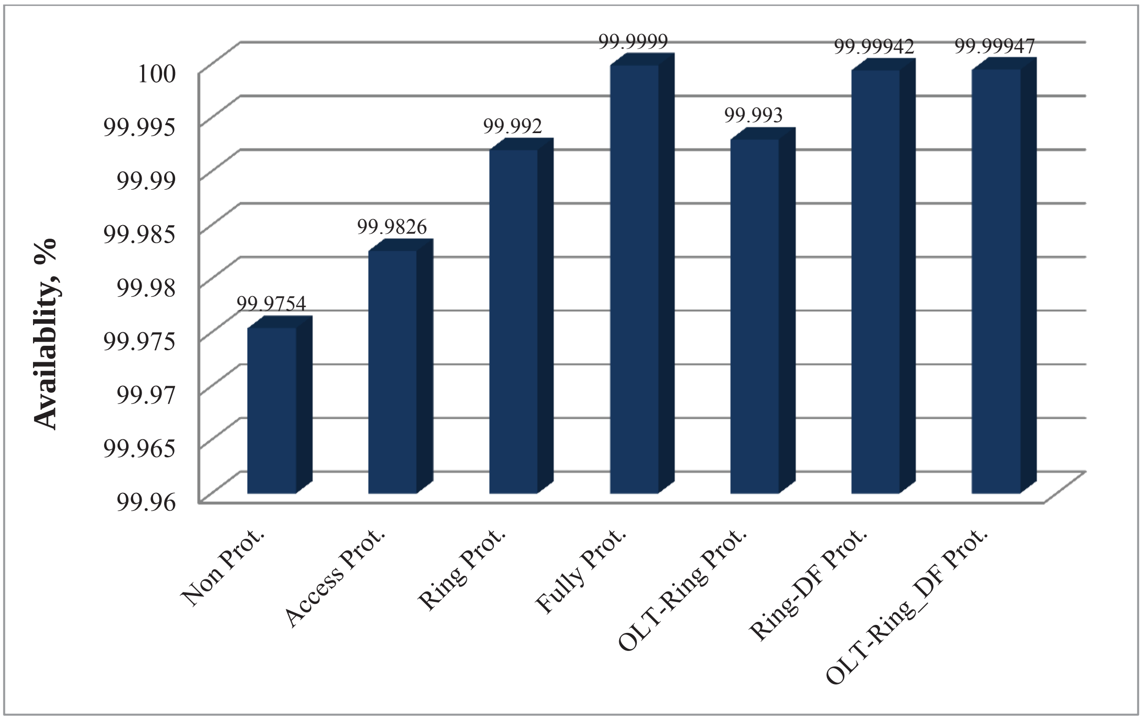

Figure 5-4 Availability of different protection schemes of LR-PON

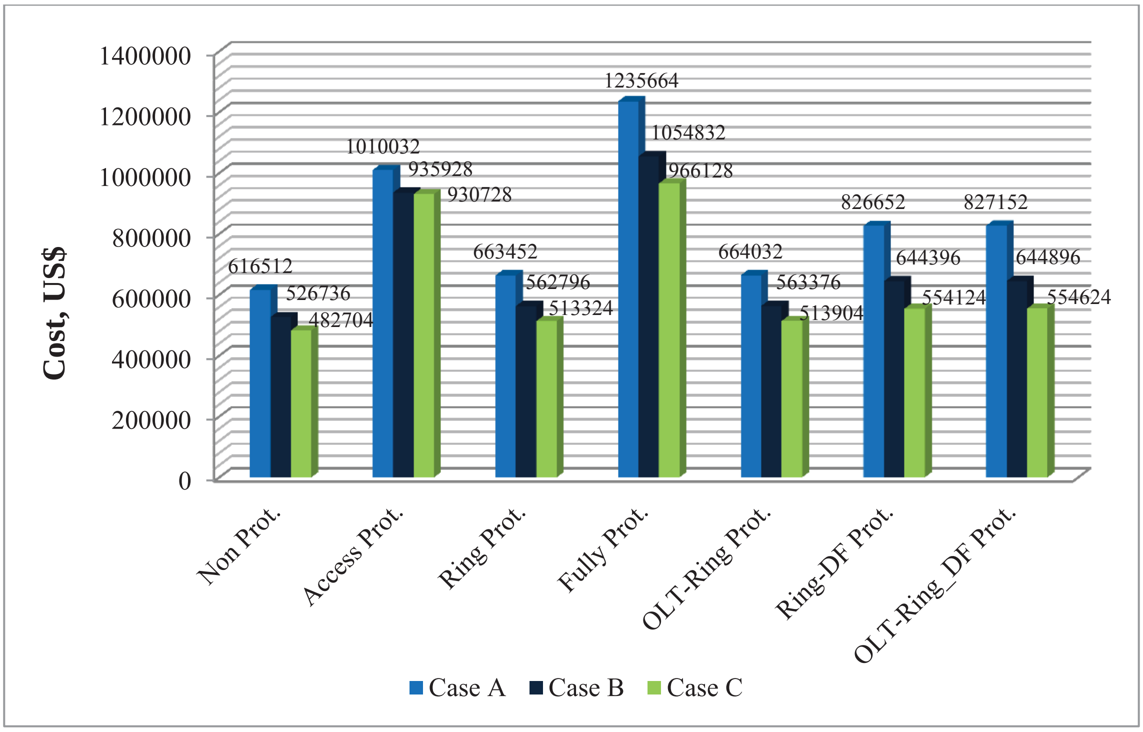

Figure 5-5 Cost of different protection schemes of LR-PON

5.4 Summary

This chapter introduces three protection schemes for LR-PON. The performance of the protection schemes has been investigated in terms of both availability and cost, and then compared to the existing protection schemes. It has been shown that an OLT-Ring protection scheme is a superior scheme for LR-PON.

Chapter 6 NG-PON MONITORING

This chapter answers Research Question 3, “What advantages would be achieved when applying PON ranging into the monitoring layer”. This chapter focuses on GPON network monitoring system. To answer this research question, the chapter starts with an explanation of the use of the GPON ranging process in the monitoring layer and the benefits gained in eliminating interference between upstream bursts from different ONUs. This is followed by an explanation of the proposed GPON monitoring system in a 1-D scenario. In addition, the chapter mathematically analyses the effect of the pulse width on the different noise sources in terms of SNR. Furthermore, there is an analysis of the effect of reducing the pulse width on reduced interference in terms of SIR.

6.1 GPON Ranging Process for the Monitoring Layer

The OLT measures the distance to each ONU and then calculates the differences in distance between two successive ONUs in order to assign an equalization delay for each ONU. The process is as follows.

The OLT measures the distance to ONU_i and ONU_{i+1} as follows: (see Figure 6-1)

$$D_{ONU_i} = 2D_s + 2D_{ONU_i} \tag{6-1}$$

$$D_{ONU_{i+1}} = 2D_s + 2D_{ONU_{i+1}} \tag{6-2}$$

where D_s is the distance between the OLT and the splitter. D_{ONUi} and D_{ONUi+1} are the distances between the splitter and ONU_i, and ONU_{i+1}, respectively. The OLT calculates the distance, (D_{Δ}), between ONU_{i+1} and ONU_i as follows:

$$D_{\Delta} = 2(D_{ONU_{i+1}} - D_{ONU_i}) \tag{6-3}$$

Based on this distance, the equalization time (T_{Δ}) can be calculated as follows:

$$T_{\Delta} = D_{\Delta}/\mathrm{v} \tag{6-4}$$

where v is the velocity defined as:

$$v = C/\eta \tag{6-5}$$

where C is the speed of the light and η is the refractive index.

The OLT sends the T_Δ to each ONU to equalize its traffic with the other ONUs. In the case where each ONU suspends its traffic by a period of time that is equal to T_Δ, the probability of interference at the optical combiner between upstream bursts will be eliminated as shown in Figure 6-1 (A: No interference). However, there is a probability of interference between bursts if an ONU suspends its upstream burst by a period of time that is less than T_Δ, as shown in Figure 6-1 (B: interference).

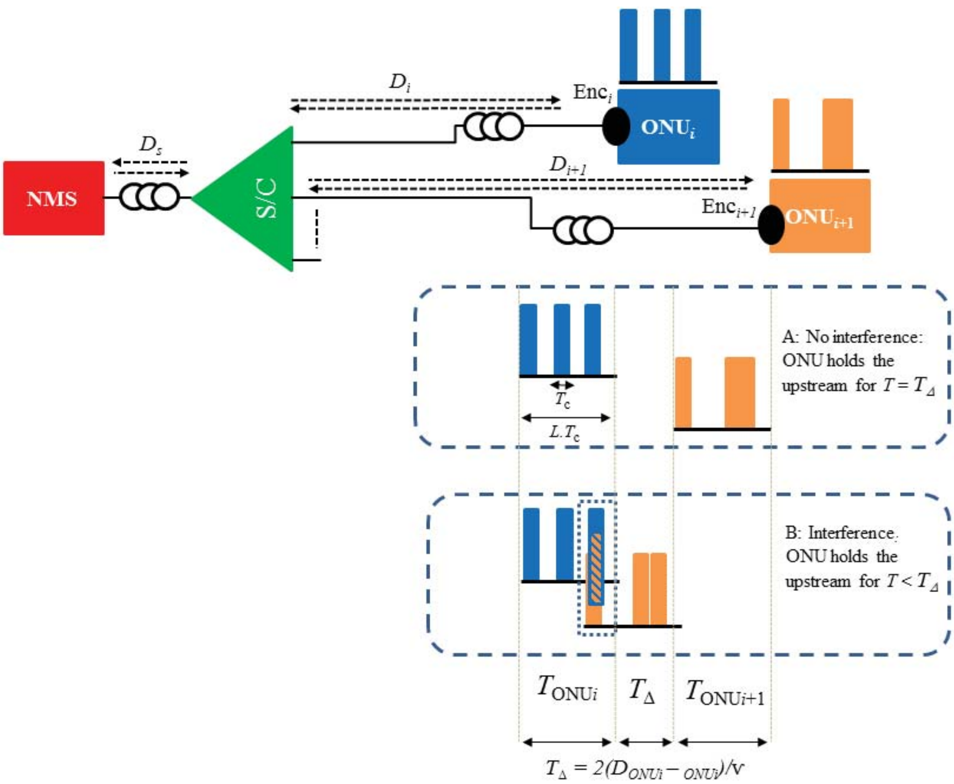

Figure 6-1 Principle of upstream transmission using equalization delay

6.2 Principle of Monitoring System

The principle of the GPON monitoring system based 1-D scenario is shown in Figure 6-2. 1-D system is based on tree topology where the OLT is located at the CO and connected to multiple ONUs over different distances. In this scenario, a pulse using one wavelength in the U-band is generated from the NMS and launched into the feeder fibre. The pulse is split into

N sub-pulses, where $N \epsilon$ (32, 64, or 128), each of which travels through a unique fibre length. Encoders are placed outside the ONUs. Each encoder encodes the monitoring sub-signal by its unique code using EG-nMPC. Encoders are based on 1-D ODLs. Each ONU suspends the transmission of its upstream burst for a time that is equal to its assigned T_Δ. All encoded sub-pulses from ONUs are combined at the RN by the combiner and then transmitted to the NMS. This monitoring system does not require implementing a decoder at the receiving side at NMS; instead, the NMS stores a reference signal that generates a time reference of the expected time of receiving each chip of each code. This time reference can be easily stored by knowing the code-word and the T_Δ of each encoder. The NMS works to compare the received chips of each code to the time reference. If a code for a specific ONU has been received correctly at the assigned time, the fiber status for that fiber will be healthy (case 1 in the Figure); otherwise the fiber will be detected as faulty (case 2 in the Figure).

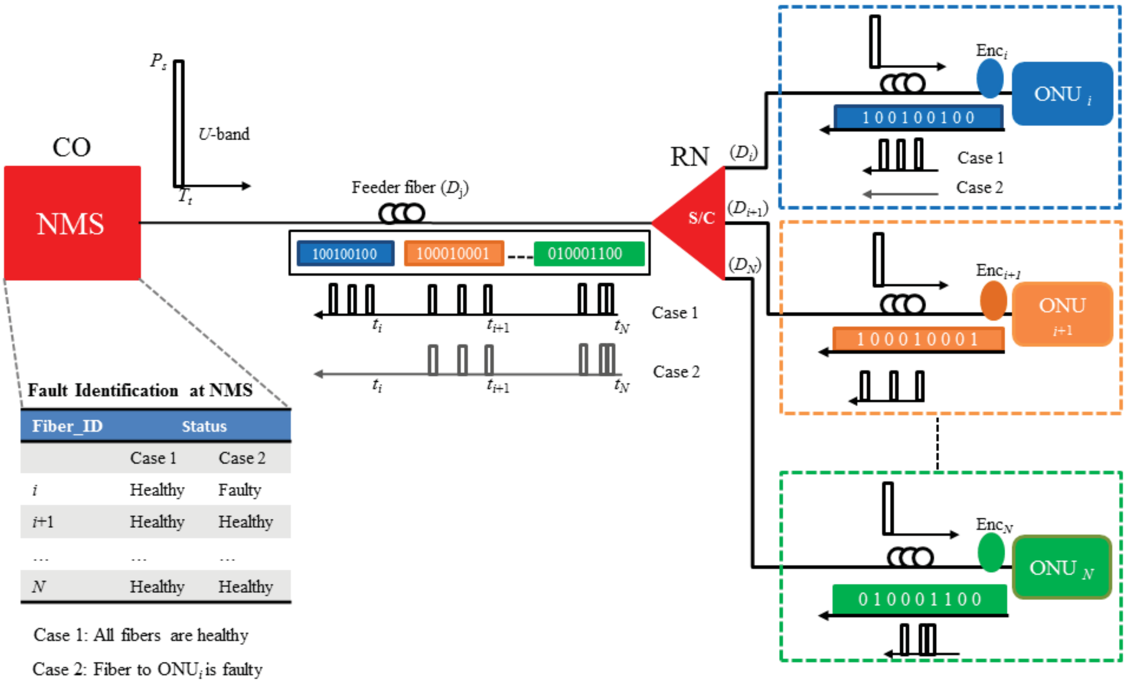

Figure 6-2 Monitoring system (1-D)

6.3 Monitoring pulse width

The pulse width has a major impact on the performance of the monitoring system. In this section, the effect of the different noise sources, including shot, beat, dark and thermal noises, on the pulse width in terms of SNR is evaluated. In addition, the effects of the pulse width on the performance of SNR and SIR for the different GPON splitting ratios are analysed.

The SNR and SIR are expressed as follows [33]:

$$SNR = \frac{E(\mu_{sig}^2)}{E(\alpha_{Noises}^2)} \tag{6-6}$$

$$SIR = \frac{E(\mu_{sig}^2)}{E(\mu_{\text{int}}^2)} \tag{6-7}$$

where, $E(\mu_{sig}^2)$ is the expectation of the desired signal power, $E(\alpha_{Noises}^2)$ is the expectation of all noises power, and $E(\mu_{int}^2)$ is the expectation of the interference signal power. μ_{sig} is derived as follows [33]:

$$\mu_{sig} = G\alpha_T \xi_i e^{-2\alpha_a l_i} \sum_{n=1}^{w} \frac{1}{T_c} \int_{t \in Tc} | Q_{in}(t_i, \lambda) |^2 \, dt \tag{6-8}$$

where G is the photodiode gain, α_T is the total loss budget, ζ_i is the fibre status, which is equal to "1" for a healthy fibre, and "0" otherwise. α_a is the fibre attenuation coefficient, li is the distance between OLT and ONU_i, w is the weight, T_c is the pulse width, Q_{in} (t, λ) is the generated monitoring pulse with a width of T_c and a power of P_s. Details of mathematical modelling of the encoding, decoding and the detection process can be found in [33]. This chapter focuses on selecting the optimal pulse width for the different GPON scenarios. Equation (6-8) can now be written as [33]:

$$\mu_{sig} = G\alpha_T w P_s \xi_i \; e^{-2\alpha_a l_i} \tag{6-9}$$

μ_{int} is defined as:

$$\mu_{\text{int}} = G\alpha_T \sum_{n=2}^{N} \rho P_s n e^{-2\alpha_a l_n} \tag{6-10}$$

where N is the number of ONUs, ρ is the interference probability given in (4-13), and l_n is the distance between OLT and ONU_N. The probability of interference between two transmission bursts can be eliminated by the use of a ranging process. The interference probability can be redefined as:

$$\rho = \lambda_C . T_\Delta \tag{6-11}$$

The noise sources i_{Noises} in the system can be defined as:

$$i_{Noises}(t) = i_{ShotN}(t) + i_{DarkN}(t) + i_{ThermalN}(t) + i_{BeatN}(t) \tag{6-12}$$

where i_{ShotN}, i_{DarkN}, i_{ThermalN}, and i_{BeatN}, are shot noise, dark noise, thermal noise, and beat noise, respectively. The power of the noises (α^2_{Noises}) can be calculated by adding the power of all noise components. It is given as follows [33]:

$$\alpha^2_{Noises} = \alpha^2_{ShotN} + \alpha^2_{DarkN} + \alpha^2_{ThermalN} + \alpha^2_{BeatN} \tag{6-13}$$

where the power of shot noise (α^2_{ShotN}) is given by:

$$\alpha^2_{ShotN} = qG(1+\varsigma)(\mu_{sig} + \mu_{\text{int}})B_e \tag{6-14}$$

where q is the electron charge, 1+ ς is photodiode excess noise factor, and B_e is the electrical bandwidth. B_e is defined as follows:

$$B_e = \frac{1}{T_C} \tag{6-15}$$

The power of dark noise ($\alpha^2_{Dark\ N}$) is given by:

$$\alpha_{DarkN}^{2} = qGI_{DarkN}B_{e} \tag{6-16}$$

where, I_{DarkN} is the dark noise current.

The power of thermal noise ($\alpha_{ThermalN}^2$) is given by:

$$\alpha_{ThermalN}^{2} = I_{thermalN}B_{e} \tag{6-17}$$

where I_{ThermalN} is the thermal noise current. The power of beat noise (α_{BeatN}^2) is given by:

$$\alpha_{BeatN}^{2} = 2\xi_{i}.\beta(1+\varsigma)(\alpha_{T}GP_{s})^{2}.we^{-2\alpha_{a}l_{i}}\sum_{n=2}^{N}2\rho ke^{-2\alpha_{a}l_{n}}{}^{2} \tag{6-18}$$

where β is defined as:

$$\beta = \frac{B_{e}}{B_{o}} \tag{6-19}$$

where B_o is the optical bandwidth.

6.4 Numerical results

For the different noise sources, plots of the SNR versus the pulse width for PON splitting ratios, 32, 64, and 128, are presented in Figure 6-3, Figure 6-4, and Figure 6-5 respectively. The parameters used for the MATLAB are presented in Table 6-1.

Figure 6-3 shows the effect of dark noise and thermal noise on the SNR for different pulse widths. The values of SNR are inversely proportional to pulse widths; as shown in (6-16) and (6-17). In addition, according to those equations, the code parameters chosen, i.e. weight, length, and available cardinality, are irrelevant, hence one figure to represent the three different splitting ratios.

Figure 6-4 presents the effect of the pulse width on the SNR for shot noise for splitting ratios of 32, 64, and 128. As can be seen, there is an inverse relationship between the shot noise and the pulse width as stated in (6-14) and (6-15). In this figure, the effect of the splitting ratios on the results can be seen. The shot noise is affected by $\mu_{sig,}$ which, in turn, is affected by the weight as well as μ_{int}, with the latter acquiring different values of interference probabilities.

Figure 6-5, illustrates the performance of the SNR versus different pulse widths for beat noise for splitting ratios of 32, 64, and 128. There is a proportional relationship between pulse width and probability of interference, which leads to higher values of SNR, see (6-18) and (6-11). However, the SNR reaches a steady state value as the pulse width reaches 10^{-6} for 32 users, and 10^{-7} for 64 and 128 users. This is due to the inverse relationship between the beat noise and the pulse width as shown in (6-18), (6-19) and (6-15)

From the discussion, it can be seen that only the shot and beat noises have an impact on the SNR and SIR. Thus, the selected pulse width should consider these noises. From Figure 6-6, it is noted that the optimal pulse width for a splitting ratio of 32, (a) in the figure, is 10^{-10} while the optimal pulse for splitting ratios of 64 and 128, (b) and (c) in the Figure, respectively, is 10^{-11}.

Figure 6-7, shows the impact of different pulse widths on the SIR. Once again, the inverse relationship could be noted.

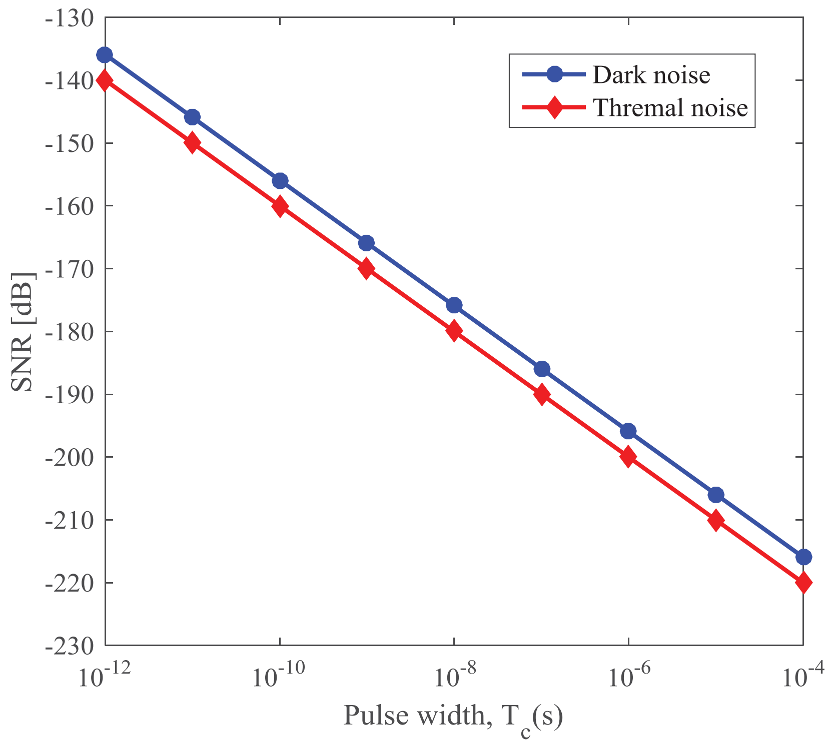

Figure 6-3 SNR versus pulse width for dark and thermal noises for all splitting ratios of 32, 64, and 128

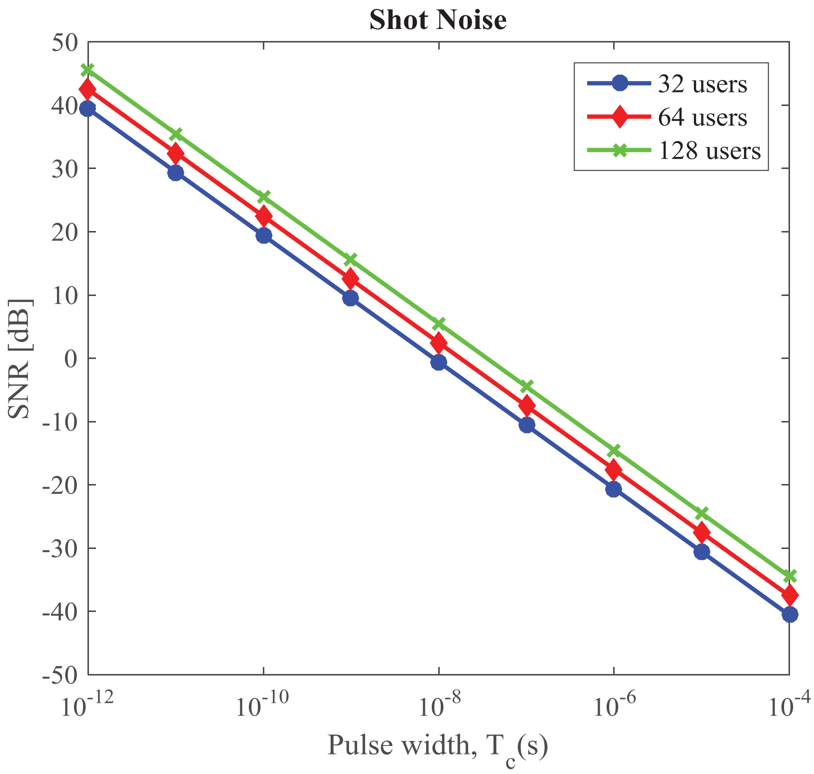

Figure 6-4 SNR versus pulse width for shot noise for splitting ratios of 32, 64, and 128

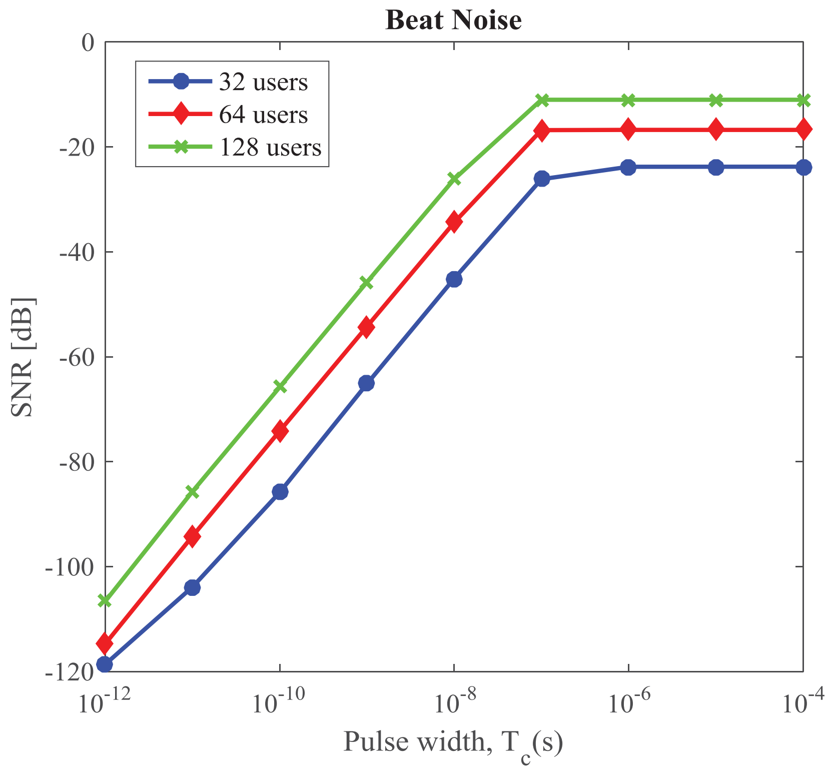

Figure 6-5 SNR versus pulse width for beat noise for splitting ratios of 32, 64, and 128

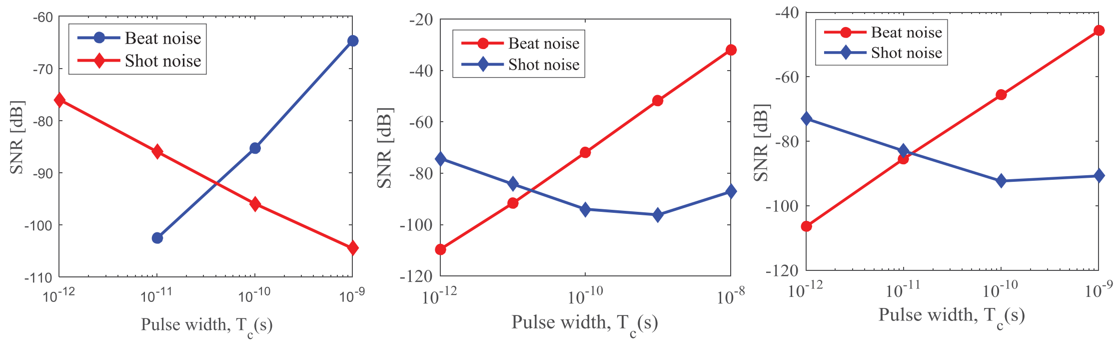

32 Splitting ratio   64 Splitting ratio   128 Splitting ratio

Figure 6-6 Beat and Shot noises for different splitting ratios

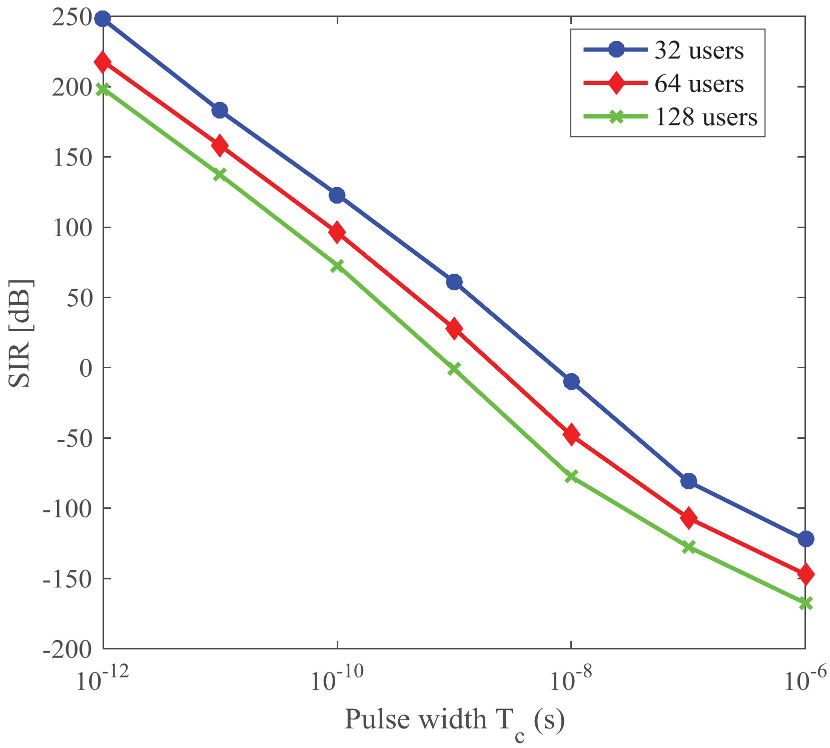

Figure 6-7 SIR versus T_c, for N = 32, 64 and 128

Table 6-1 Simulation parameters

Parameter	Value		Parameter	Value
N	Case 1	32	$1+\varsigma$	2.97
	Case 2	64	G	100
	Case 3	128	α_a	0.3 dB/km
W	Case 1	2	α_L	5 dB
	Case 2	3	$I_{Thermal\ N}$	160 nA
	Case 3	4	$I_{Dark\ N}$	10^{26} A^2/Hz
L	Case 1	24	P_s	4 dBm
	Case 2	60	T_C	$T_c\,[10^{-12}:10^{-6}]$
	Case 3	112	λ	1650 nm
B_e	$1/T_C$		L_{FF}	20 km
B_o	1 THz		c	299,792,458 m\s

6.5 Summary

This chapter exhibits the significance of utilizing the information gathered from the GPON ranging process at the data layer in eliminating the interference between upstream bursts in the monitoring layer. In addition, it explains the overall system principle for a 1-D scenario. In addition, this chapter has analysed the effect of the pulse width in the system performance in terms of SNR and SIR using a mathematical model.

Chapter 7 IMPLEMENTATION

This chapter provides an overview of VPI TransmissionMaker simulation tool including its hierarchy and parameters. It followed by implementation of 1-D EG-nMPC using VPI TransmissionMaker. For simplicity and readability, the chapter provides a description of a network simulation with four ONUs. The results for networks with capacities of 32, 64, and 128 splitting ratios are then presented based on the results obtained for 4 ONUs.

7.1 VPI TransmissionMAker overview

VPI transmissionMaker is one of the most robust tools to model and simulate photonic systems and networks such as microwave photonics application and optical fiber networks. It combines the advantages of a powerful graphical interface and a reliable simulation scheduler with flexibility in representing the optical signal. In addition, VPI provides advanced tools such as interactive simulation, data import with automatic file, and co-simulation utilizing some of the standard programming languages including Python and MATLAB [145].

VPI is hierarchically organized in a such way to permits the user to manage the modules easily. The hierarchy is divided into three levels and every level can be processed independently. These levels can be referred to as: universe, galaxy and star [146]. An example of the hierarchy is shown in Figure 7-1. As shown in the Figure, the star level is the lowest level of the simulation interface. It represents a single module with a certain function. The galaxy level represents the second level and it constructed of a combination of interconnected stars or other galaxies. This level requires at least one input and/or output port. The universe level is the highest level in the hierarchy and it may include stars and/or galaxies. The universe level shows the simulation scheme where the scheme can be executed [146].

The parameters of the modules of the VPI is divided into global and specific parameters. The global parameters impact all the modules while the specific parameter impact a specific module [146].

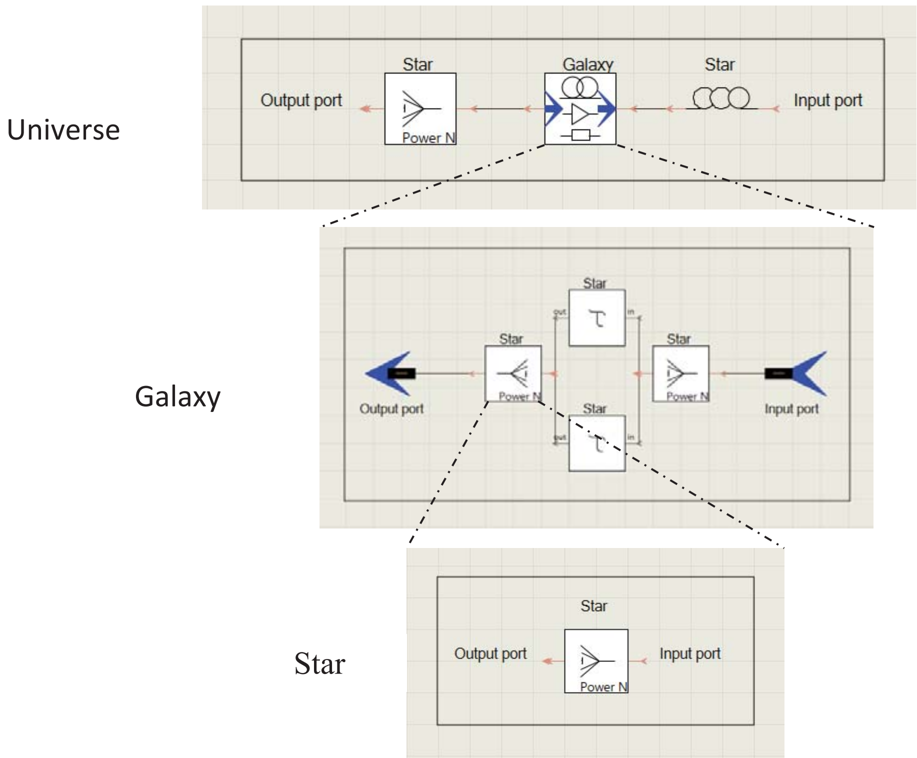

Figure 7-1 VPI Hierarchy

7.2 Network Simulation with Four ONUs

The monitoring system simulation model consists of four main parts; monitoring signal generator, RN, encoding, and decoding and fault identification. The simulation model with four ONUs is shown in

Figure **7-2**. The module parameters used in this simulation are presented in the Appendix, while the parmeters for the undefined modules are set to their default values.

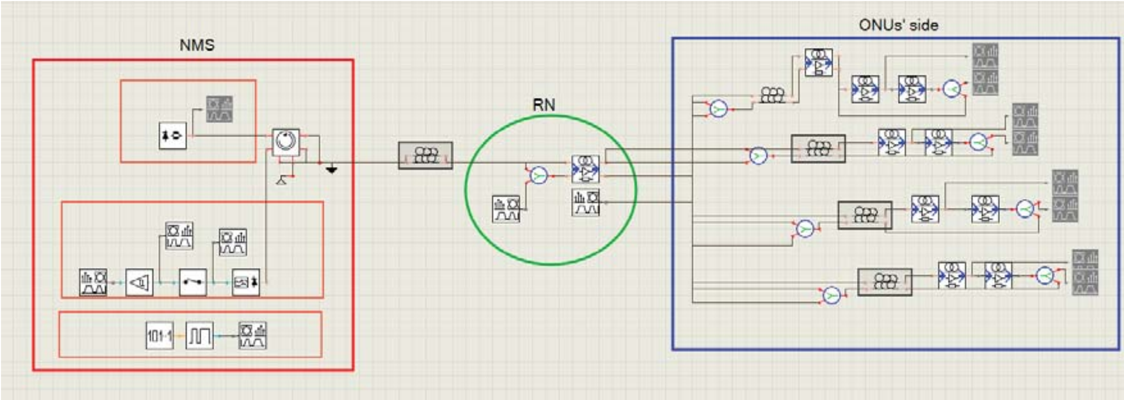

Figure 7-2 VPI model of four ONUs

7.2.1Monitoring Signal Generator

The monitoring signal generator is based on an OOK transmitter, that is available in the VPItransmissionMaker simulator. The interior design of the OOK transmitter is shown in Figure 7-3. The modules used in this OOK transmitter include:

(1) Laser source (LaserCW). This is used to generate a continuous wave (CW) optical signal.

(2) Pseudo Random Binary Sequence generator (PRBS).: This module is used to produce a pseudo random data sequence.

(3) Coder driver OOK. This module is used to produce an electrical signal.

(4) 1x2 Fork. The function of this module is to divide the input into two equal output paths.

(5) Modulator Differential Mach-Zehnder (DiffMZ_DSM).

(6) Add logical channel (LogicAddChannel). This module is used to assign a logical channel to the signal.

(7) DC-Source. This module produces a constant-amplitude electrical signal at a defined value.

(8) Attenuator. This module attenuates the optical signal.

(9) Null sources. This model is used to terminate unused input.

The output of the monitroing signal generator is shown in Figure 7-4. As shown in the Figure, the monitoring signal has a duration of T_c= 1 ns and a power of P_s = 0.00251 W, (4 dBm).

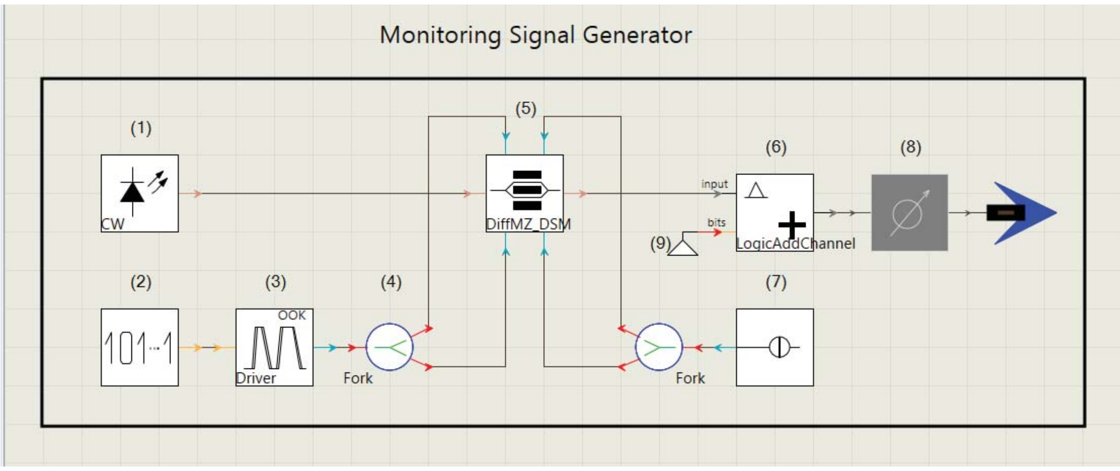

Figure 7-3 VPI OOK transmitter design

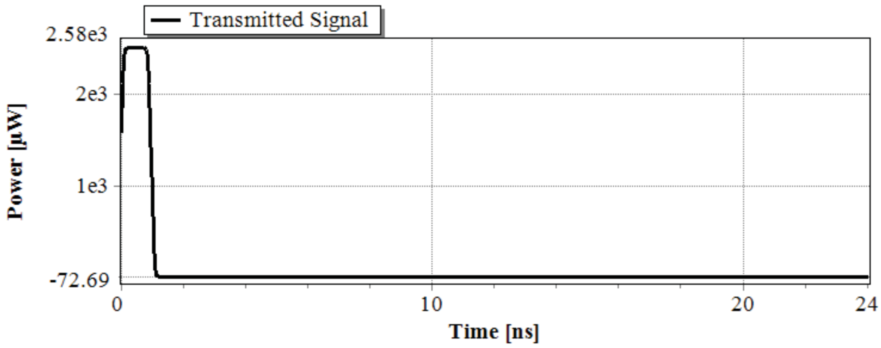

Figure 7-4 Monitoring pulse generator output

7.2.2Remote Node Splitter

The design of the RN is presented in Figure 7-5 and consists of:

(1) 1xN power splitter. Splits the input power into N equal output ports.

(2) Nx1 power combiner. Combines the power coming from N input ports into one output port.

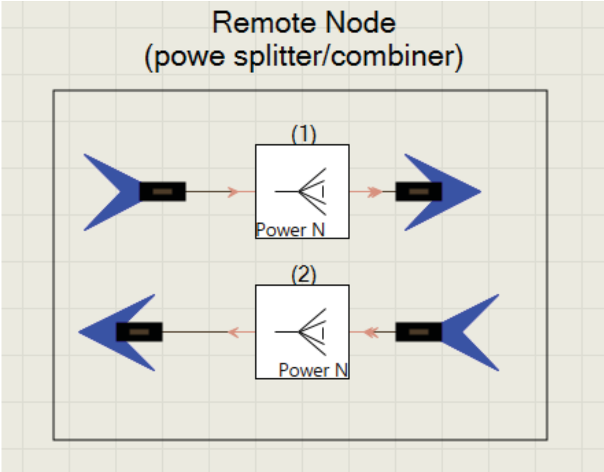

Figure 7-5 VPI splitter and combiner

7.2.3Encoding

The encoder design is presented in Figure 7-6 and consists of:

(1) 1x*N* power splitter.

(2) *N* ODLs, each with a specific delay time corresponding to the encoder's code-word.

(3) *N*x1 power combiner.

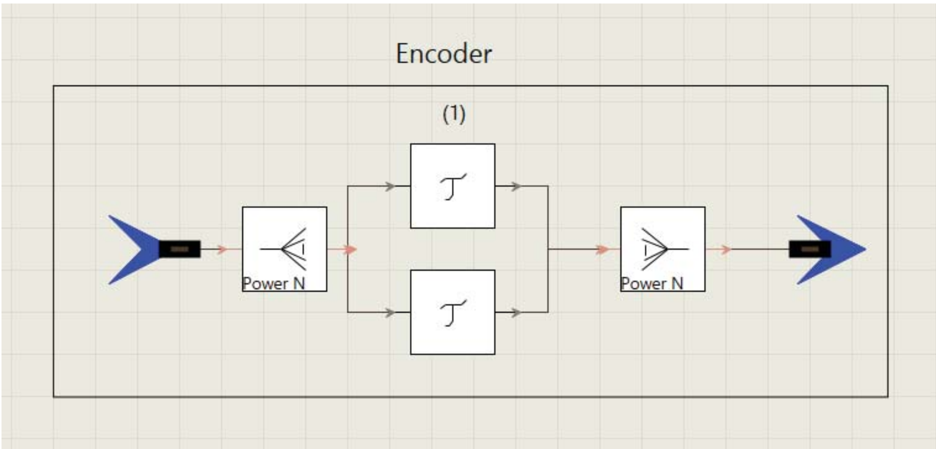

Figure 7-6 VPI encoder design

The outputs of the four encoder showing the *w* sub-pulses locations, in the interval $T = L.T_c$, are presented in Figure 7-7 to Figure 7-10. The time for each sub-pulse is presented in Table 7-1.

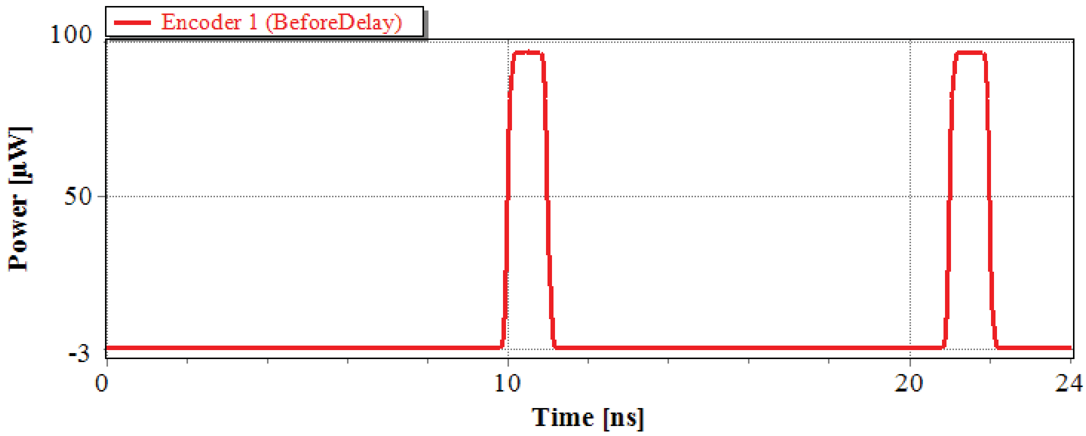

Figure 7-7 Encoder 1 output

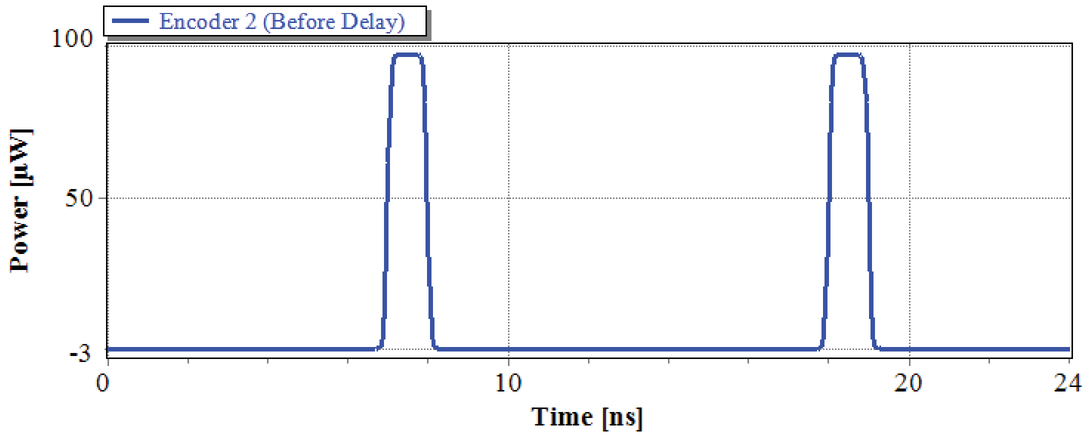

Figure 7-8 Encoder 2 output

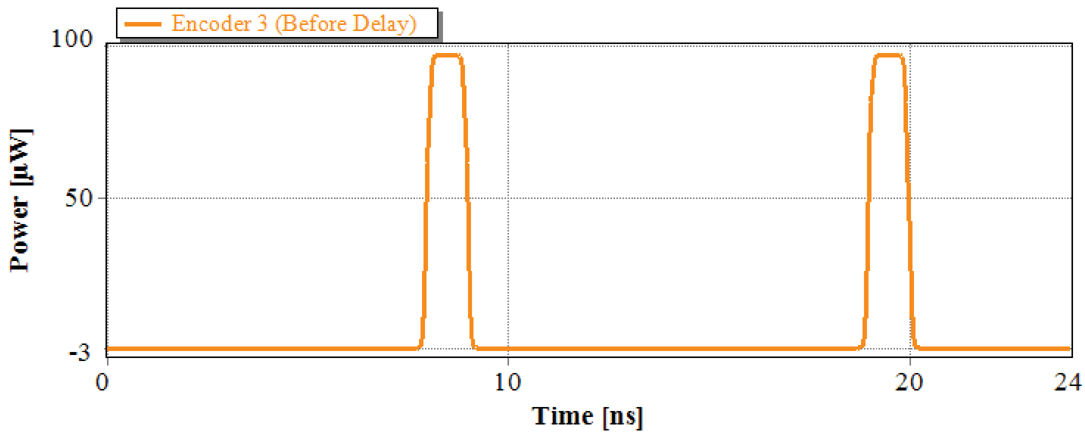

Figure 7-9 Encoder 3 output

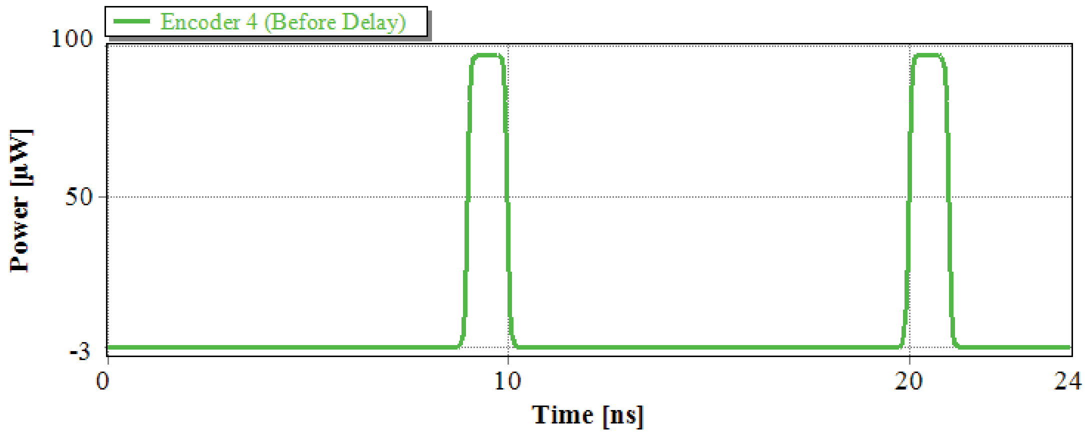

Figure 7-10 Encoder 4 output

Table 7-1 Sub-pulse times for the four encoders

Encoder	Sub-pulse (1) *Tc	Sub-pulse (2) *Tc
Encoder 1	10	21
Encoder 2	7	18
Encoder 3	8	19
Encoder 4	9	20

In this simulation, the distance to the first ONU is set to be 500 m, it then increases by 5 m for each successive ONU. Therefore, according to (6-4), the T_{Δ} between any two successive ONUs is set to be equal to 50 ns. Since T_{Δ} is not assigned to the first ONU, a time that is equal to T_{Δ} has been assigned to ONU_1. Thus, the expected start and end times for the four encoders and their corresponding sub-pulses times are presented in Table 7-2 (see Figure 7-11).

The encoders outputs with their assigned T_{Δ} are shown in Figure 7-12 to Figure 7-15. In addition, a scaling up of the time zones of concern has been conducted in order to obtain more precise values of the sub-pulse times. Results of this scaling up are shown in Figure 7-16 to Figure 7-19.

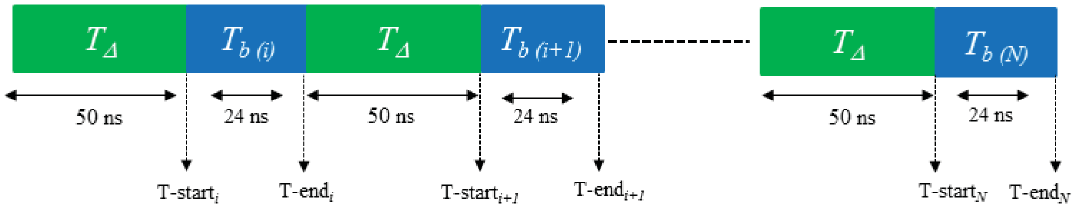

Figure 7-11 Start and end times

Table 7-2 Expected start/end times and sub-pulses times for the ONUs

ONU	Start Time (ns)	End Time (ns)	Sub-pulse (1)	Sub-pulse (2)
ONU1	51	74	60	71
ONU2	124	148	131	142
ONU3	198	222	206	217
ONU4	272	296	281	292

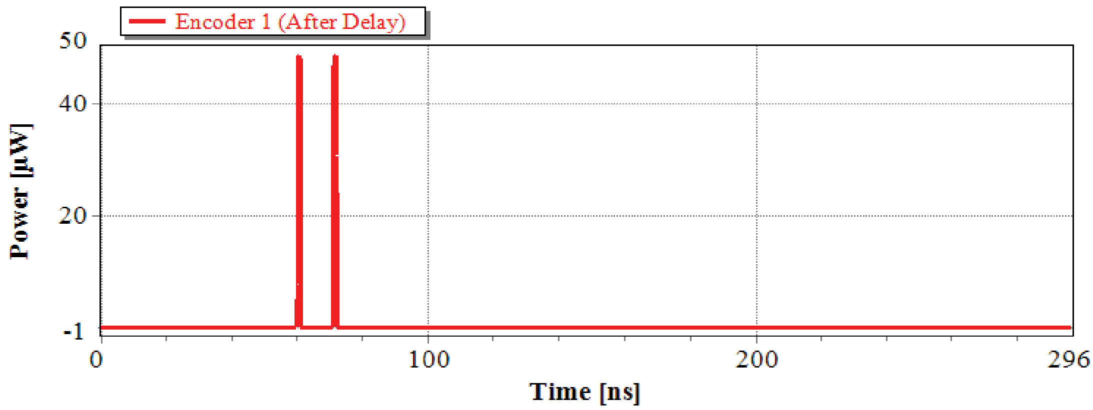

Figure 7-12 Encoder 1 output with delay

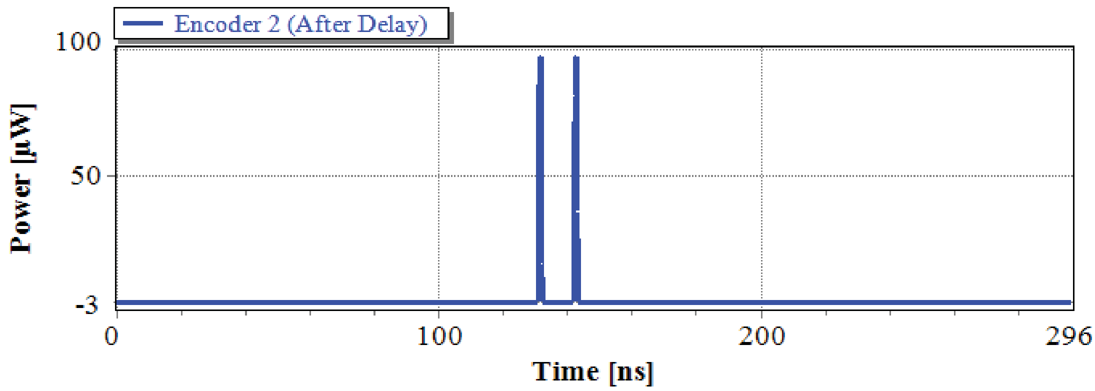

Figure 7-13 Encoder 2 output with delay

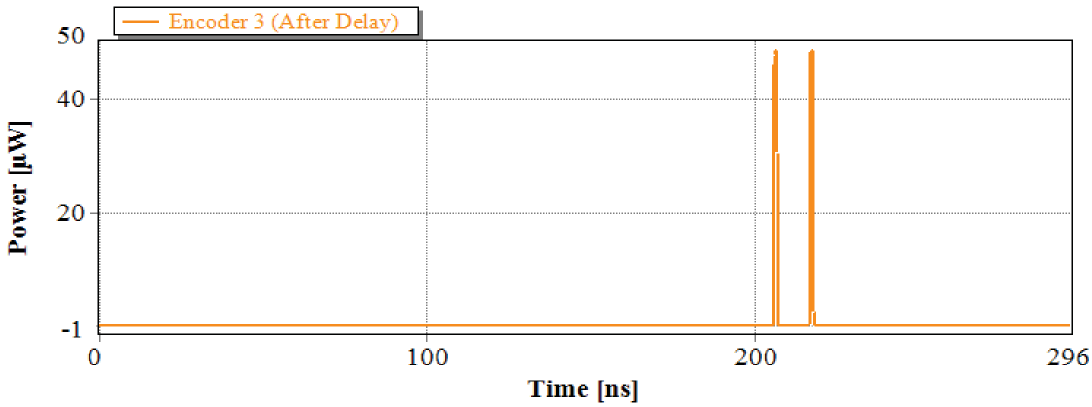

Figure 7-14 Encoder 3 output with delay

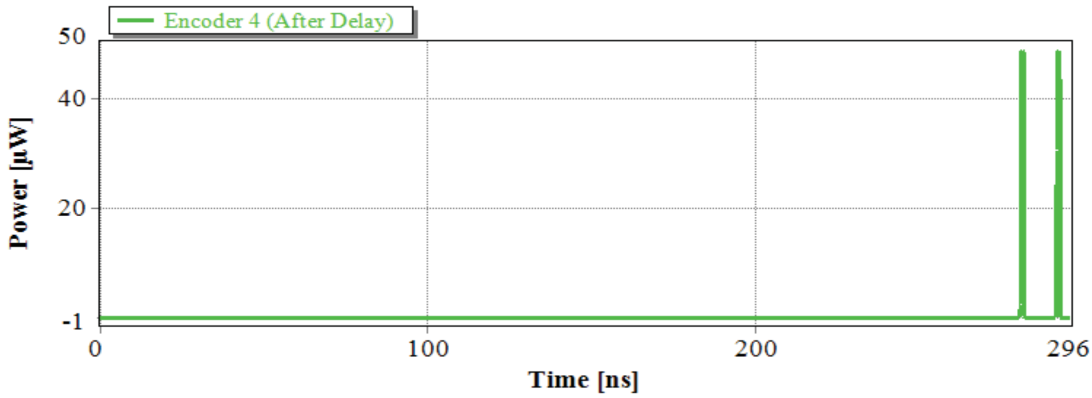

Figure 7-15 Encoder 4 output with delay

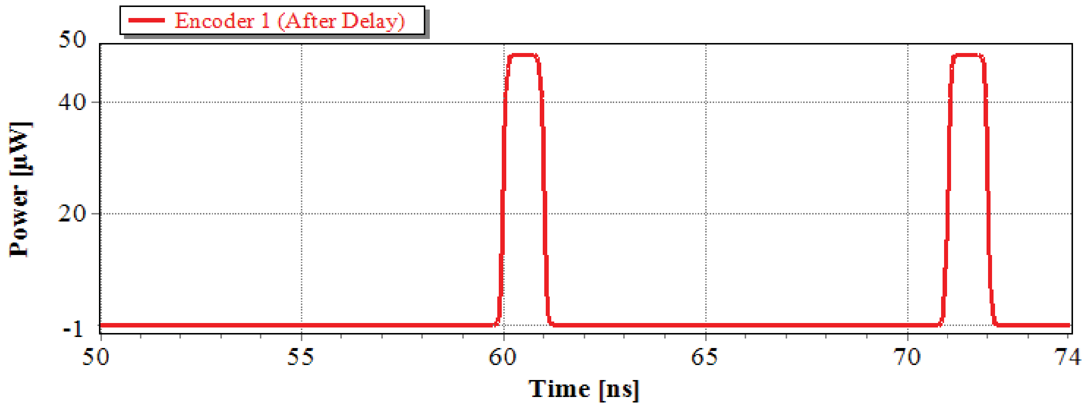

Figure 7-16 Encoder 1 output with delay closeup

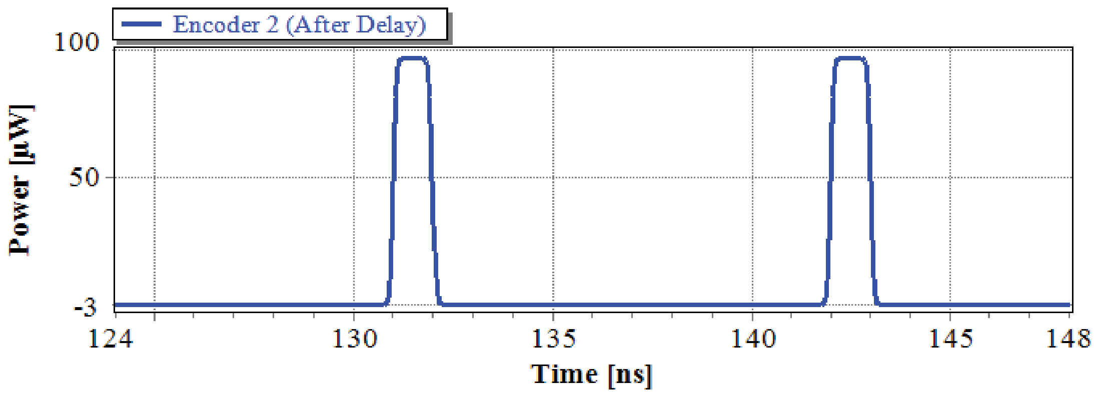

Figure 7-17 Encoder 2 output with delay closeup

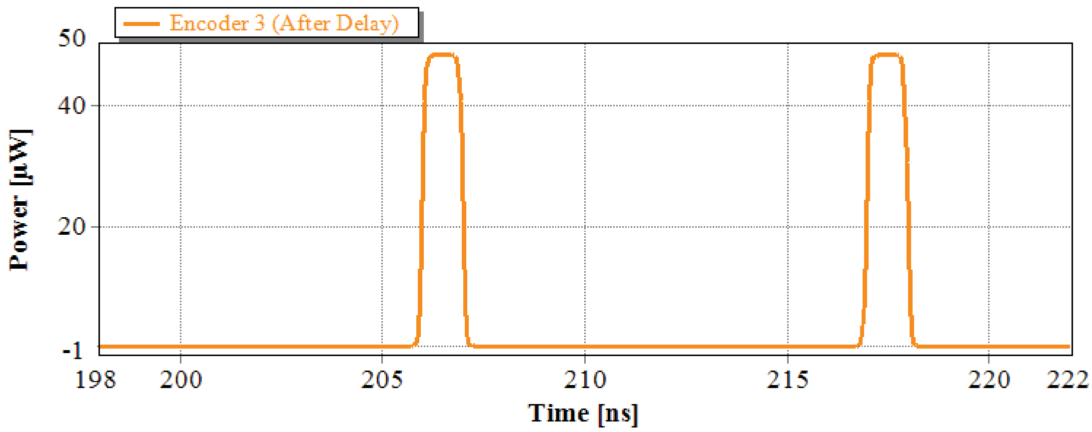

Figure 7-18 Encoder 3 output with delay closeup

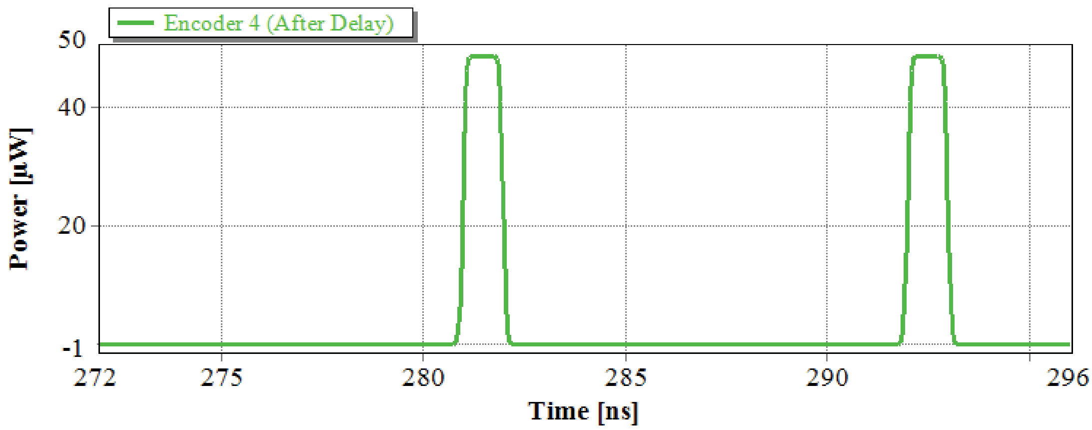

Figure 7-19 Encoder 4 output with delay closeup

7.2.4Remote Node Combiner

Two signal analyzers are used to analyse the combined signal. The first is located before the combiner, where it collects all of the encoded signals and assigns a unique color to each of the signals for ease of identification. The second analyser is located after the combiner to show the encoded signal. The outputs of both analysers are shown in Figure 7-20 and Figure 7-21, respectively. It should be noted that, for the analyser before the combiner, the output of each encoder should be connected to the analyser in the order of their numbers, and in an ascending manner.

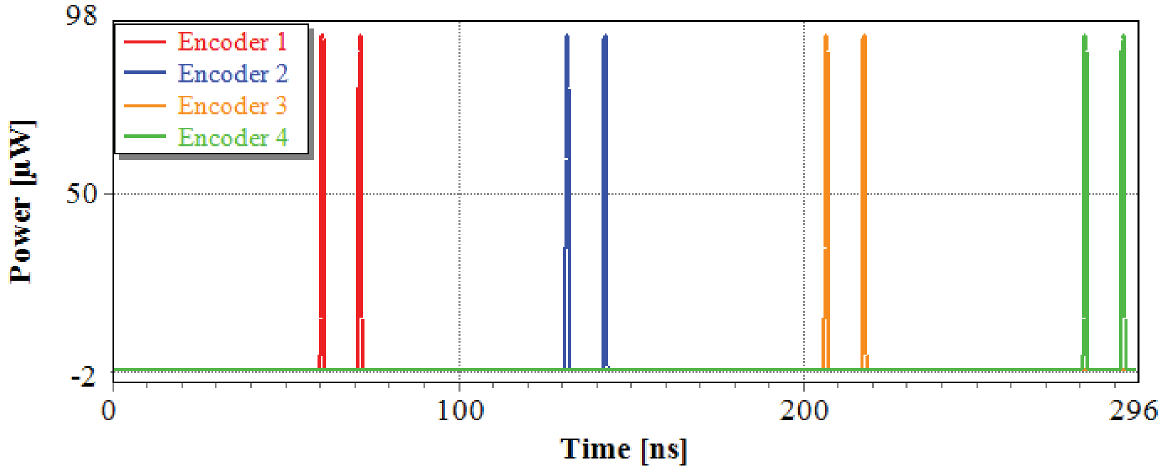

Figure 7-20 Analyser before combiner output

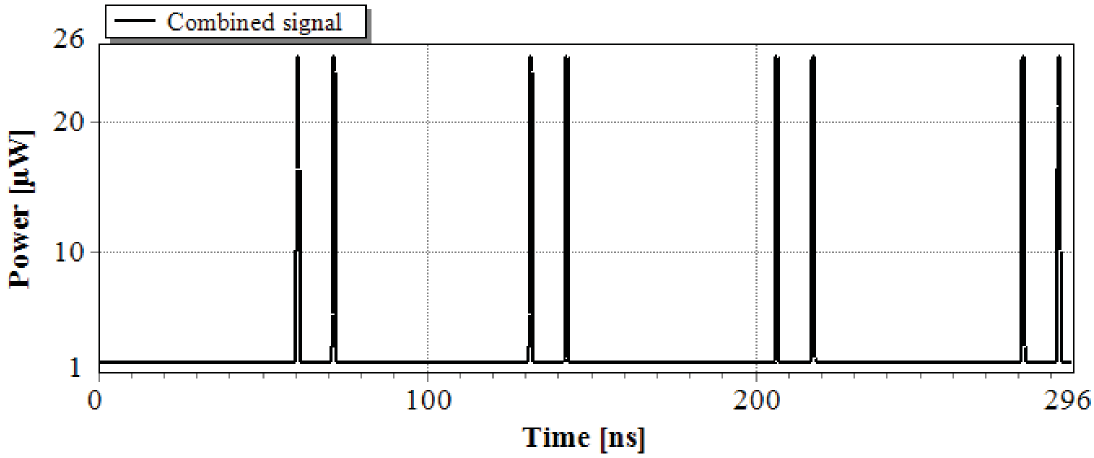

Figure 7-21 Combined signal

7.2.5Fibre Link

After the encoding process, the encoded signal is reflected back to the RN and then transmitted to the NMS. In VPItransmissionMaker, the fibre module available has one input port and one output port. To simulate this structure, a reflector and two fibres (with the same parameters) are used. The reflector is placed between the delay and the second fibre as shown Figure 7-22.

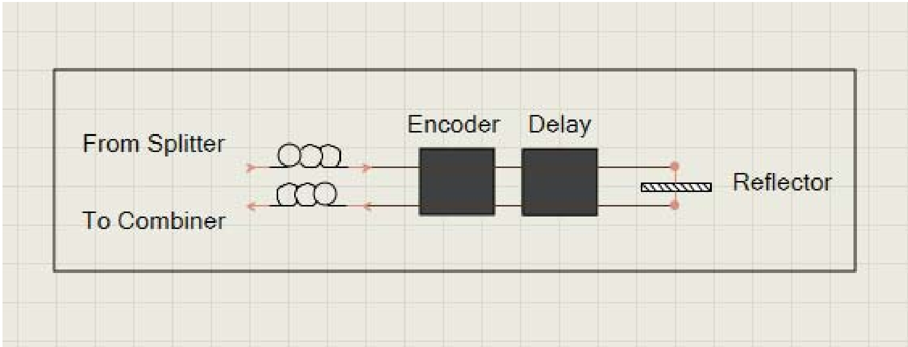

Figure 7-22 Fibre and reflection

7.2.6Decoding and Fault Identification

Fault identification is based on checking the presence/absence of the encoded signal corresponding to each ONU by comparing it to a reference signal that is stored in the NMS. The model of the reference signal and its output for four ONUs are shown in Figure 7-23 and Figure 7-24, respectively.

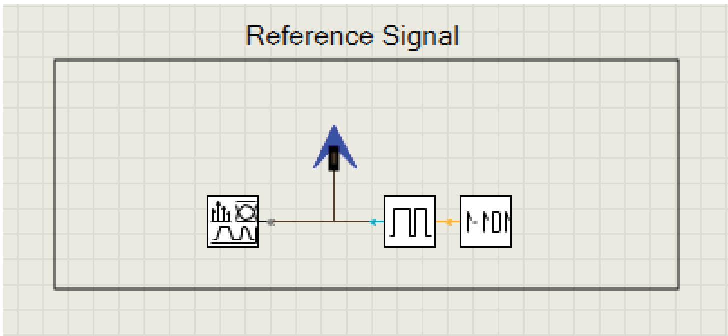

Figure 7-23 Reference signal

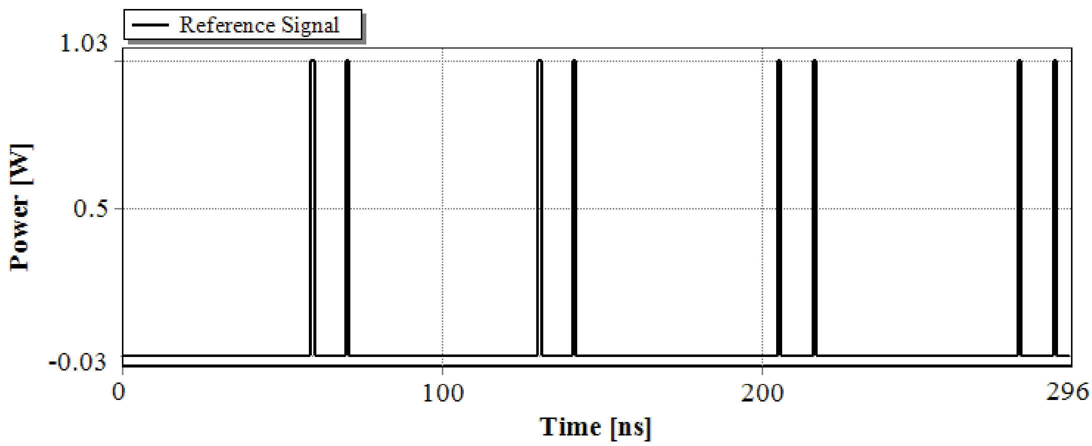

Figure 7-24 Reference signal output

When the encoded signal reaches the NMS, it passes through a photo-diode to convert the optical signal to an electrical signal, and then to a sampler and a thresholder. The NMS will then compare the thresholder output to the reference signal output to determine the status of each fibre link. The fibre to an ONU is healthy if the output of the thresholder matches the output of the reference signal at the time assigned for that ONU, otherwise, it is unhealthy.

The output of the sampler and the thresholder for four ONUs are shown in Figure 7-25 and Figure 7-26, respectively. By comparing the reference signal to the thresholder, it can be noted that all signals are received correctly, indicating a healthy fibre link to the four ONUs.

To increase readability of the results, especially when number of ONUs is 32 or higher, the outputs of each of thresholder and the reference signal are exported to an Excel file, and then processed to produce a table that consists of the ID of each fibre and its corresponding status.

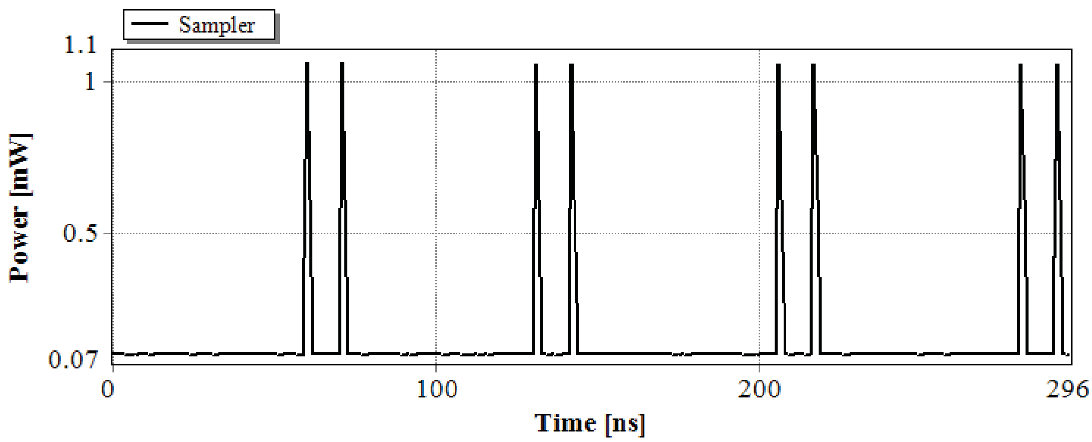

Figure 7-25 Sampler output

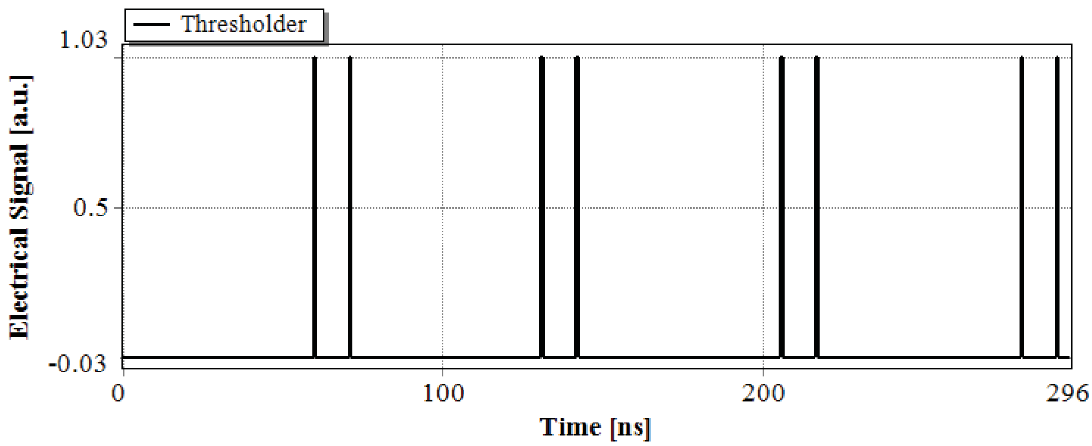

Figure 7-26 Thresholder output

A screenshot of VPI output in a text view for thresholder and reference signal and the exported data to Excel for thresholder and reference signal are presented in Figure 7-27 (a, b, and c, respectively). This figure shows power values corresponding to successive increments of 0.04 ns and 0.0017 ns in time for the reference signal and thresholder respectively. To show results at increments of 1 ns, the data has been filtered. The output of the filtered data for the reference signal and thresholder that shows the time assigned to sub-pulses corresponding to ONU_1 is shown in Figure 7-28 and Figure 7-29, respectively. For more information see Table 7-2. The results of both sets of filtered data are compared to check the status for each fibre link. Comparison results are shown in Table 7-3.

thresholder

Bands

	Thresholder	
	Time(ns)	Electrical Sign...
1	0	0
2	0.00173611111111111	0
3	0.00347222222222222	0
4	0.00520833333333333	0
5	0.00694444444444444	0
6	0.00868055555555556	0
7	0.0104166666666667	0
8	0.0121527777777778	0
9	0.0138888888888889	0
10	0.015625	0
11	0.0173611111111111	0
12	0.0190972222222222	0
13	0.0208333333333333	0
14	0.0225694444444444	0
15	0.0243055555555556	0
16	0.0260416666666667	0
17	0.0277777777777778	0
18	0.0295138888888889	0
19	0.03125	0
20	0.0329861111111111	0
21	0.0347222222222222	0
22	0.0364583333333333	0
23	0.0381944444444444	0
24	0.0399305555555556	0
25	0.0416666666666667	0

reference

Bands

	Input 1	
	Time(ns)	Power(W)
1	0	0
2	0.0416666666666667	0
3	0.0833333333333333	0
4	0.125	0
5	0.166666666666667	0
6	0.208333333333333	0
7	0.25	0
8	0.291666666666667	0
9	0.333333333333333	0
10	0.375	0
11	0.416666666666667	0
12	0.458333333333333	0
13	0.5	0
14	0.541666666666667	0
15	0.583333333333333	0
16	0.625	0
17	0.666666666666667	0
18	0.708333333333333	0
19	0.75	0
20	0.791666666666667	0
21	0.833333333333333	0
22	0.875	0
23	0.916666666666667	0
24	0.958333333333333	0
25	1	0

(a) Screenshot of VPI output (text view) for thresholder and reference signal

4	//TRACE		Thresholder
5	//SampledBand		
6	#Time	Electrical Signal	
7	#(ns)	(a.u.)	
8	0	0	
9	0.001736	0	
10	0.003472	0	
11	0.005208	0	
12	0.006944	0	
13	0.008681	0	
14	0.010417	0	
15	0.012153	0	
16	0.013889	0	
17	0.015625	0	
18	0.017361	0	
19	0.019097	0	
20	0.020833	0	
21	0.022569	0	
22	0.024306	0	
23	0.026042	0	
24	0.027778	0	
25	0.029514	0	
26	0.03125	0	
27	0.032986	0	
28	0.034722	0	
29	0.036458	0	
30	0.038194	0	
31	0.039931	0	
32	0.041667	0	

(b) Thresholder exported data

4	//TRACE		
5	//SampledBand		
6	#Time	Power	Reference Signal
7	#(ns)	(W)	
8	0	0	
9	0.041667	0	
10	0.083333	0	
11	0.125	0	
12	0.166667	0	
13	0.208333	0	
14	0.25	0	
15	0.291667	0	
16	0.333333	0	
17	0.375	0	
18	0.416667	0	
19	0.458333	0	
20	0.5	0	
21	0.541667	0	
22	0.583333	0	
23	0.625	0	
24	0.666667	0	
25	0.708333	0	
26	0.75	0	
27	0.791667	0	
28	0.833333	0	
29	0.875	0	
30	0.916667	0	
31	0.958333	0	
32	1	0	

(c) Reference signal exported data

Figure 7-27 VPI analyser data example for thresholder and reference signal and the exported data in Excel

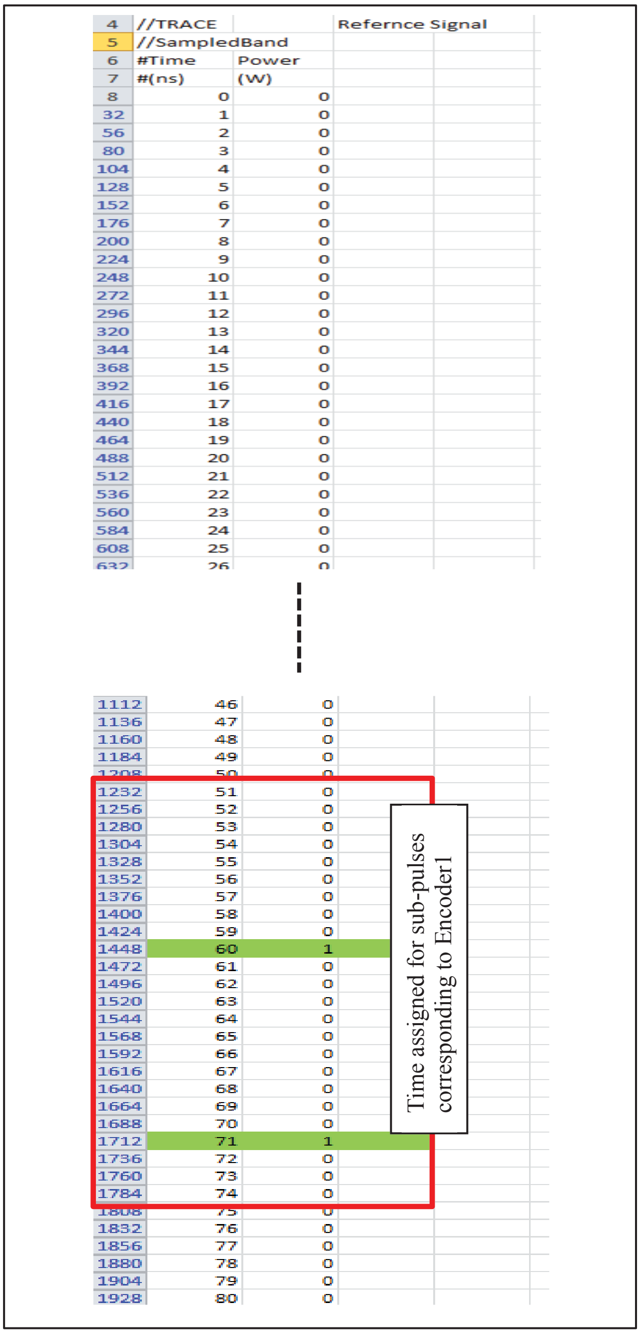

4	//TRACE		Refernce Signal
5	//SampledBand		
6	#Time	Power	
7	#(ns)	(W)	
8	0	0	
32	1	0	
56	2	0	
80	3	0	
104	4	0	
128	5	0	
152	6	0	
176	7	0	
200	8	0	
224	9	0	
248	10	0	
272	11	0	
296	12	0	
320	13	0	
344	14	0	
368	15	0	
392	16	0	
416	17	0	
440	18	0	
464	19	0	
488	20	0	
512	21	0	
536	22	0	
560	23	0	
584	24	0	
608	25	0	
632	26	0	
1112	46	0	
1136	47	0	
1160	48	0	
1184	49	0	
1208	50	0	
1232	51	0	
1256	52	0	
1280	53	0	
1304	54	0	
1328	55	0	
1352	56	0	
1376	57	0	
1400	58	0	
1424	59	0	
1448	60	1	
1472	61	0	
1496	62	0	
1520	63	0	
1544	64	0	
1568	65	0	
1592	66	0	
1616	67	0	
1640	68	0	
1664	69	0	
1688	70	0	
1712	71	1	
1736	72	0	
1760	73	0	
1784	74	0	
1808	75	0	
1832	76	0	
1856	77	0	
1880	78	0	
1904	79	0	
1928	80	0	

Figure 7-28 Filtered data for reference signal

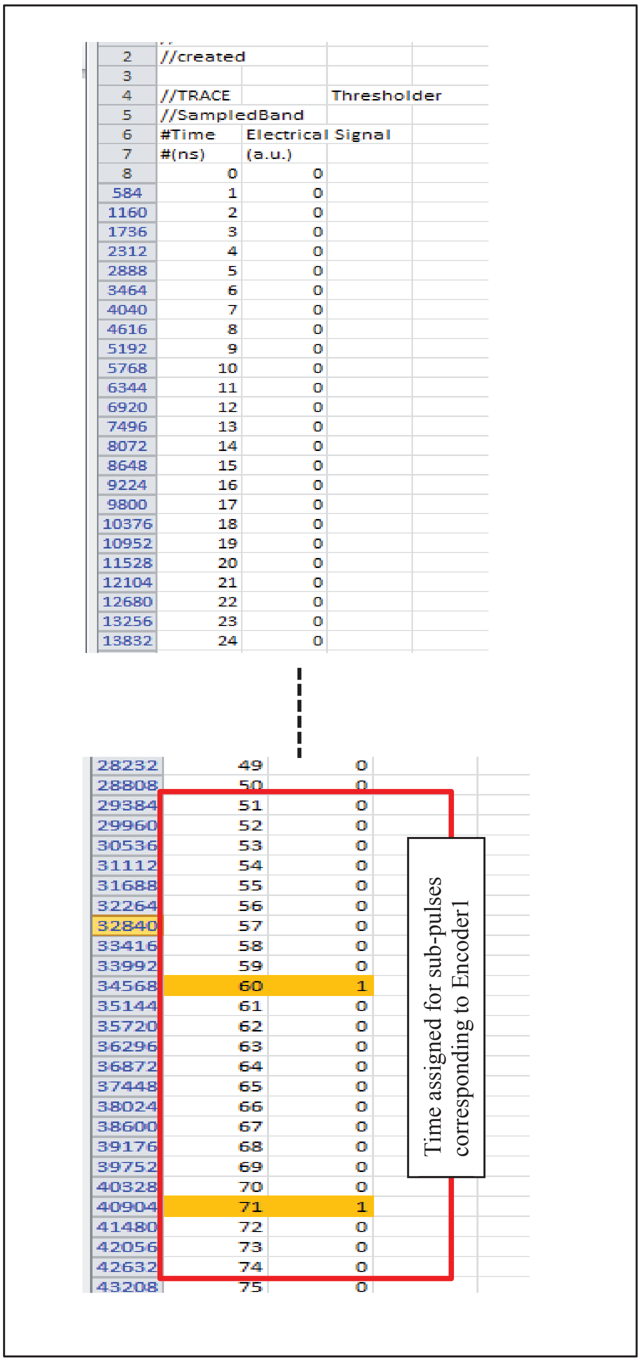

2	//created		
3			
4	//TRACE		Thresholder
5	//SampledBand		
6	#Time	Electrical Signal	
7	#(ns)	(a.u.)	
8	0	0	
584	1	0	
1160	2	0	
1736	3	0	
2312	4	0	
2888	5	0	
3464	6	0	
4040	7	0	
4616	8	0	
5192	9	0	
5768	10	0	
6344	11	0	
6920	12	0	
7496	13	0	
8072	14	0	
8648	15	0	
9224	16	0	
9800	17	0	
10376	18	0	
10952	19	0	
11528	20	0	
12104	21	0	
12680	22	0	
13256	23	0	
13832	24	0	
28232	49	0	
28808	50	0	
29384	51	0	
29960	52	0	
30536	53	0	
31112	54	0	
31688	55	0	
32264	56	0	
32840	57	0	
33416	58	0	
33992	59	0	
34568	60	1	
35144	61	0	
35720	62	0	
36296	63	0	
36872	64	0	
37448	65	0	
38024	66	0	
38600	67	0	
39176	68	0	
39752	69	0	
40328	70	0	
40904	71	1	
41480	72	0	
42056	73	0	
42632	74	0	
43208	75	0	

Figure 7-29 Filtered data for the thresholder

Table 7-3 Fibre ID and status for four ONUs (healthy case)

Fibre ID	Status
1	Healthy
2	Healthy
3	Healthy
4	Healthy

7.2.8 Fibre degradation

Fibre degradation can be simulated by assigning a high attenuation value to the fibre. The model of the fibre with degradation (a break) is presented in Figure 7-30. Each attenuator is assigned an attenuation value of 50 dB.

This section presents results for a break in the fibre to ONU_1. Figure 7-31 shows the output of the encoder, the figure shows no sub-pulses. Figure 7-32 and Figure 7-33 show the output of the analyser before and after the combiner, respectively. It can be noted that, the signal of the encoder corresponding to ONU_1 (red colour) is missing since there are no sub-pulses. Figure 7-34 and Figure 7-35 show the sampler and thresholder outputs, respectively, where the signal corresponding to ONU_1 is missing. Table 7-4 presents the ID of each fibre and its corresponding status.

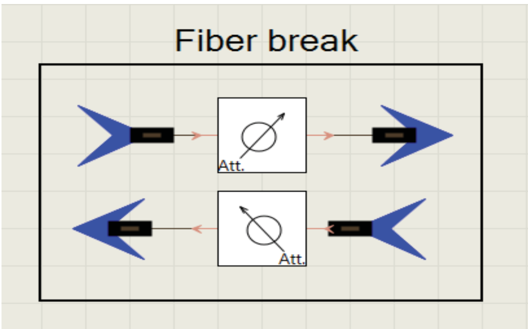

Figure 7-30 Fibre brake module in VPI

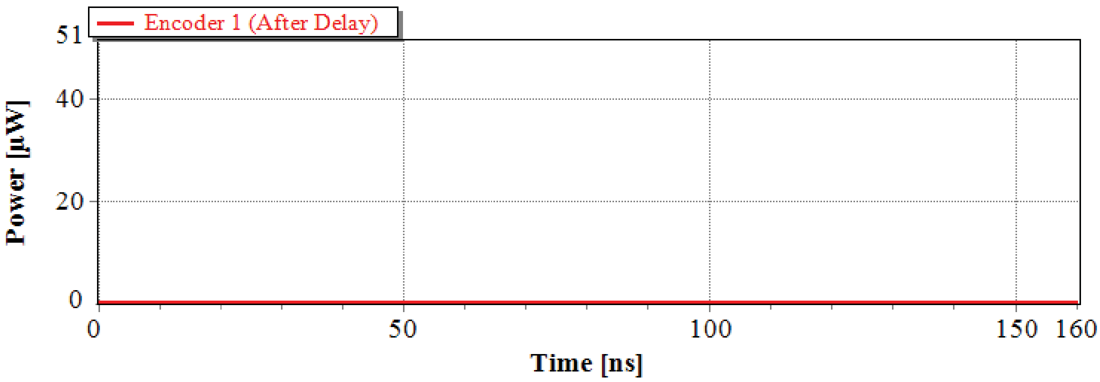

Figure 7-31 Encoder 1 output for a Fault

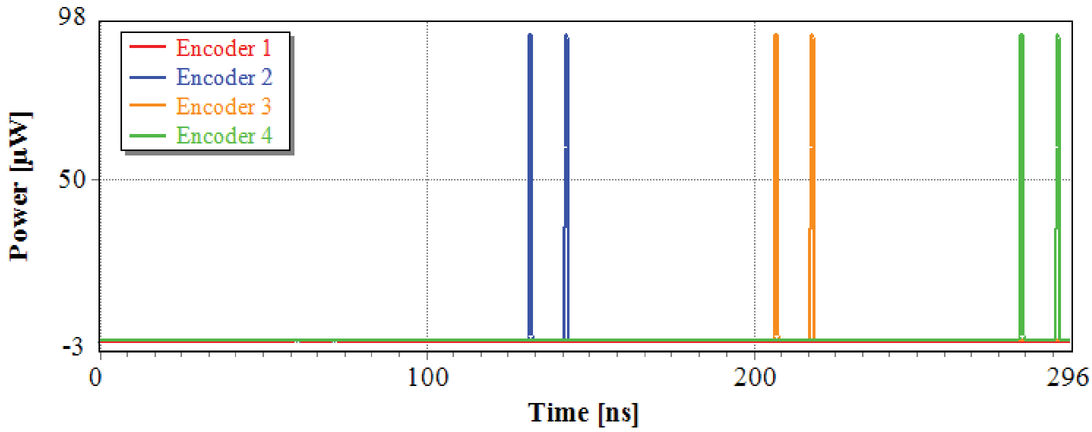

Figure 7-32 Encoded signals for a fibre fault to ONU1 before combiner

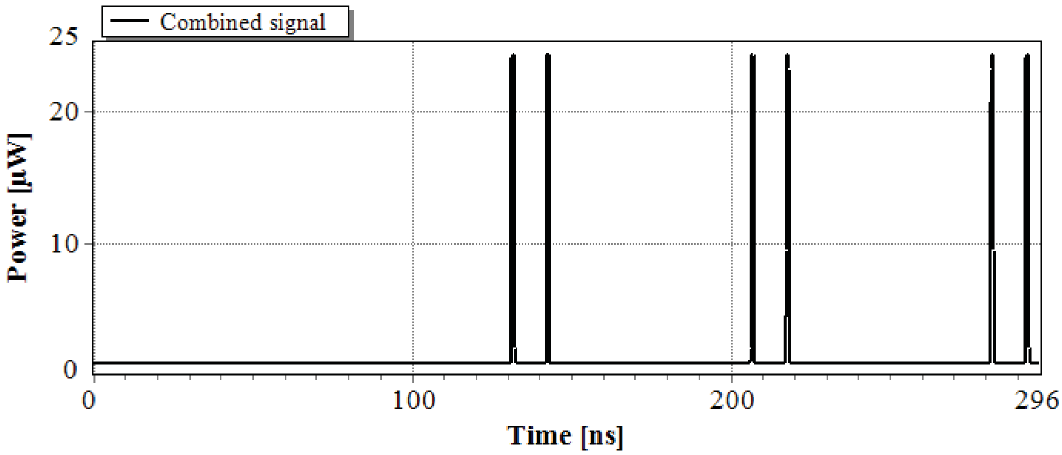

Figure 7-33 Encoded signals for a fibre fault to ONU1 after combiner

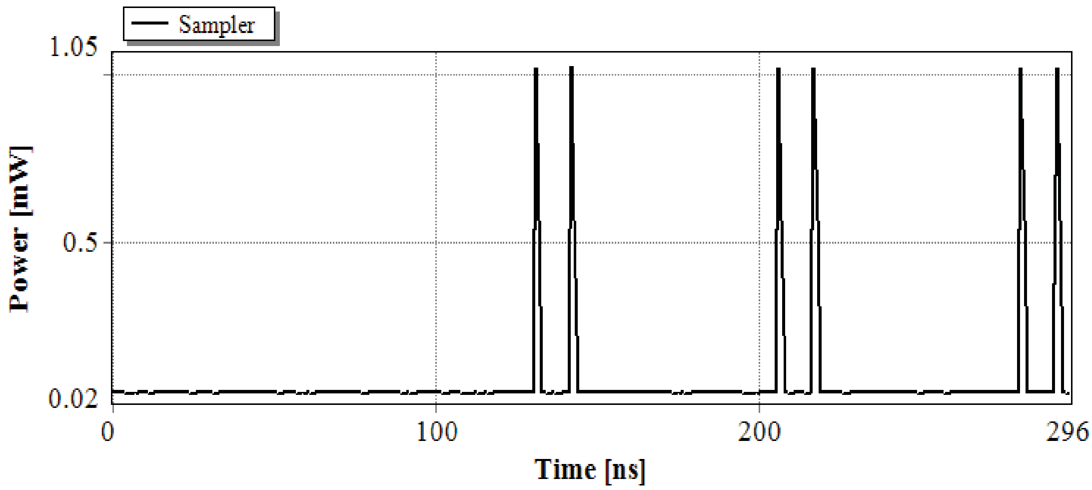

Figure 7-34 Sampler output for a fibre fault to ONU1

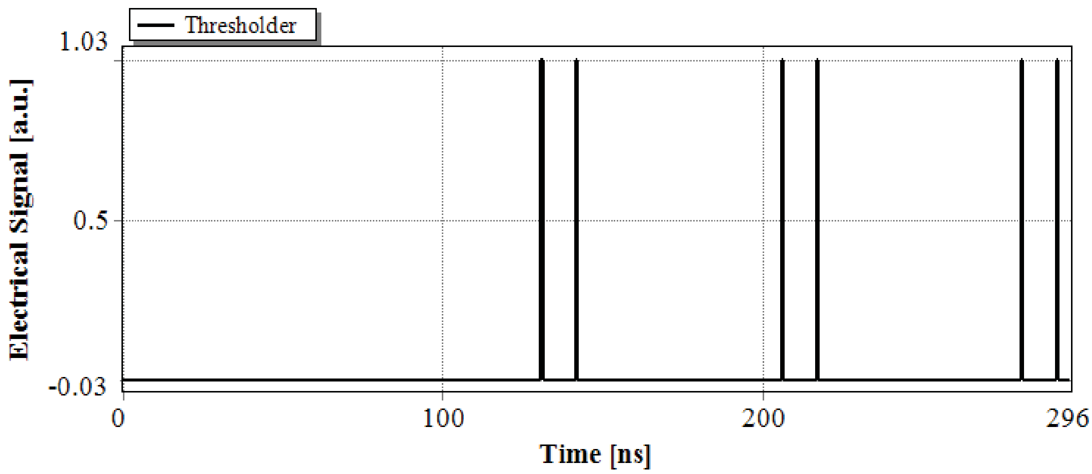

Figure 7-35 Thresholder output for a fibre fault to ONU1

Table 7-4 Fibre ID and status for four ONUs (faulty case)

Fibre ID	Status
1	Faulty
2	Healthy
3	Healthy
4	Healthy

7.3 A Splitting Ratio of 32

The general structure of a system with 32 ONUs is shown in Figure 7-36. The parameters used are presented in the Appendix.

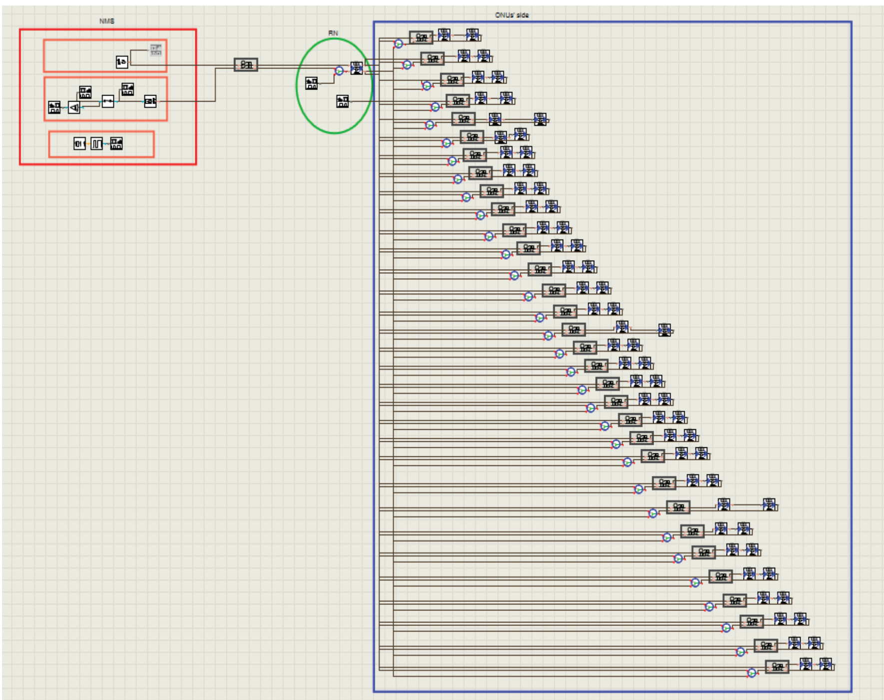

Figure 7-36 VPI model of 32 ONUs

The output of the combiner, sampler, thresholder and the reference signal are shown in Figure 7-37 to Figure 7-40, respectively. From these figures, it can be noted that all signals are received correctly, indicating healthy fibre links to all ONUs as shown in Table 7-5. For a network with 32 ONUs and more, an amplifier has been used to reduce the effect of the noise.

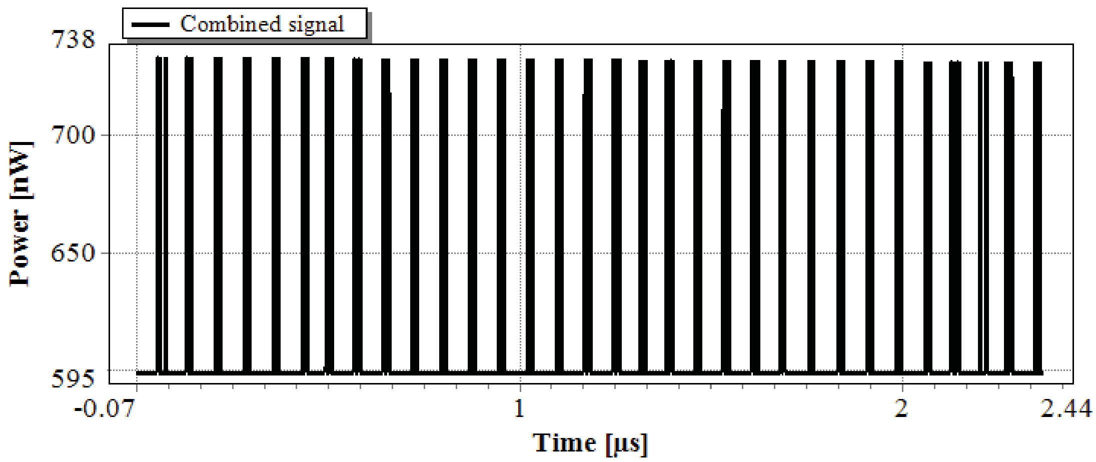

Figure 7-37 Encoded combined signals

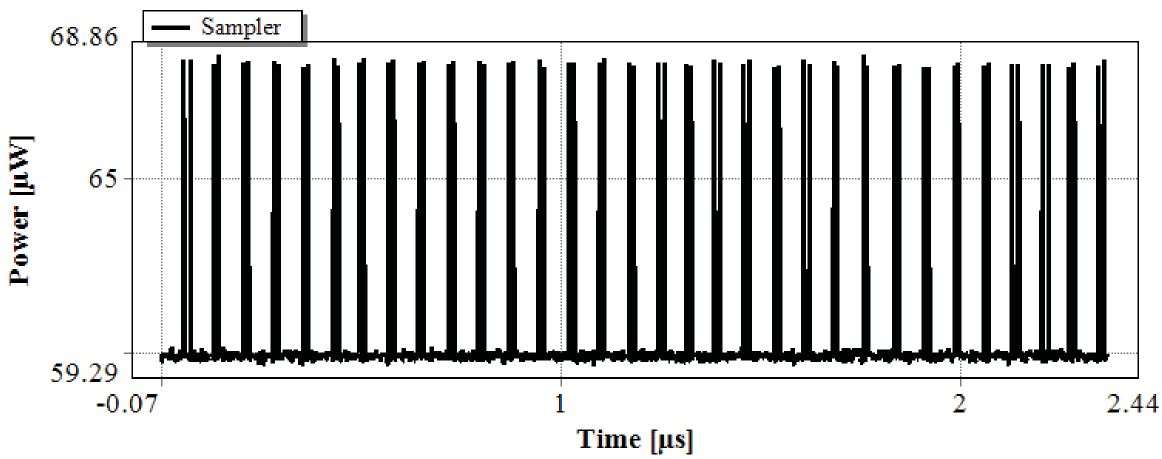

Figure 7-38 Sampler output

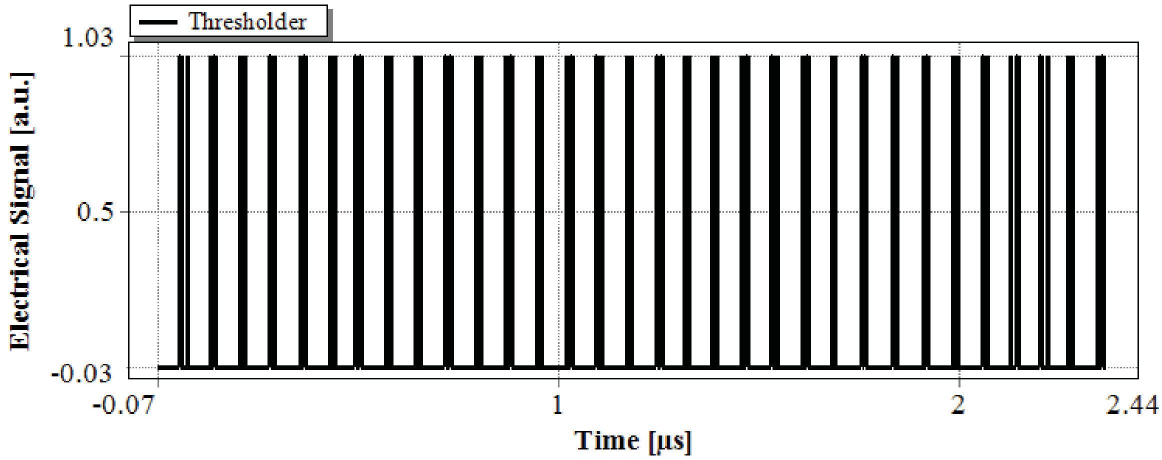

Figure 7-39 Thresholder output

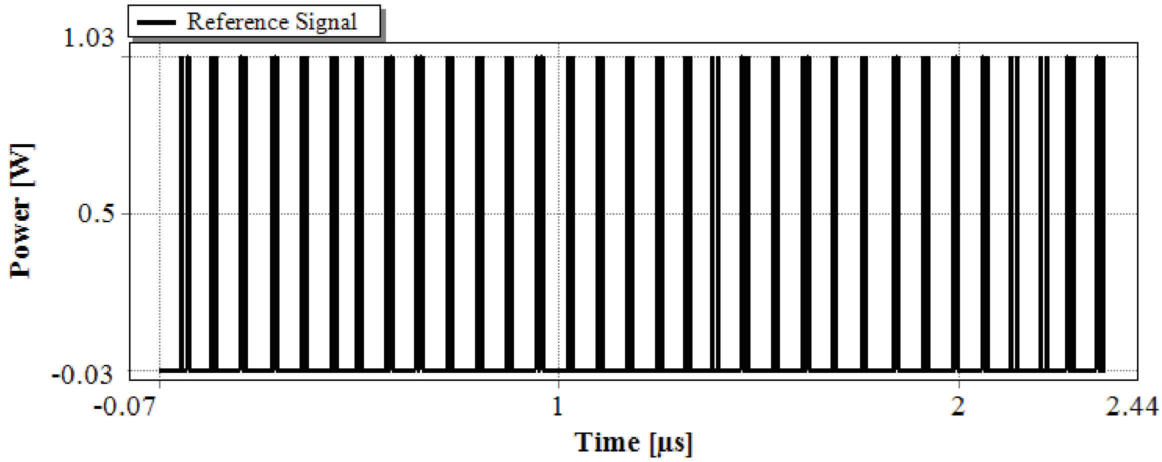

Figure 7-40 Reference signal outputs

Table 7-5 Fibre ID and status (healthy case)

Fibre ID	Status
1	Healthy
2	Healthy
3	Healthy
4	Healthy
5	Healthy
6	Healthy
7	Healthy
8	Healthy
9	Healthy
10	Healthy
11	Healthy
12	Healthy
13	Healthy
14	Healthy
15	Healthy

16	Healthy
17	Healthy
18	Healthy
19	Healthy
20	Healthy
21	Healthy
22	Healthy
23	Healthy
24	Healthy
25	Healthy
26	Healthy
27	Healthy
28	Healthy
29	Healthy
30	Healthy
31	Healthy
32	Healthy

Figure 7-41 to Figure 7-43 show the output of the combiner, sampler and the thresholder, respectively, in the case of a fibre fault to ONU_5, ONU_{16} and ONU_{25}. From these figures, it can be noted that the signals corresponding to the ONUs are missing, indicating a fault in their fibre links as stated in Table 7-6.

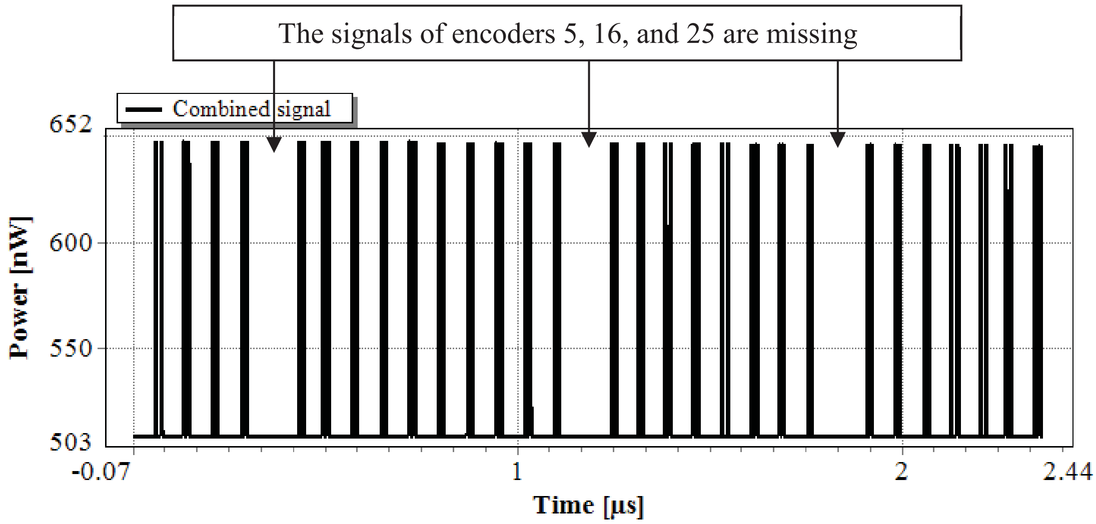

Figure 7-41 Encoded combined signals, (faulty case)

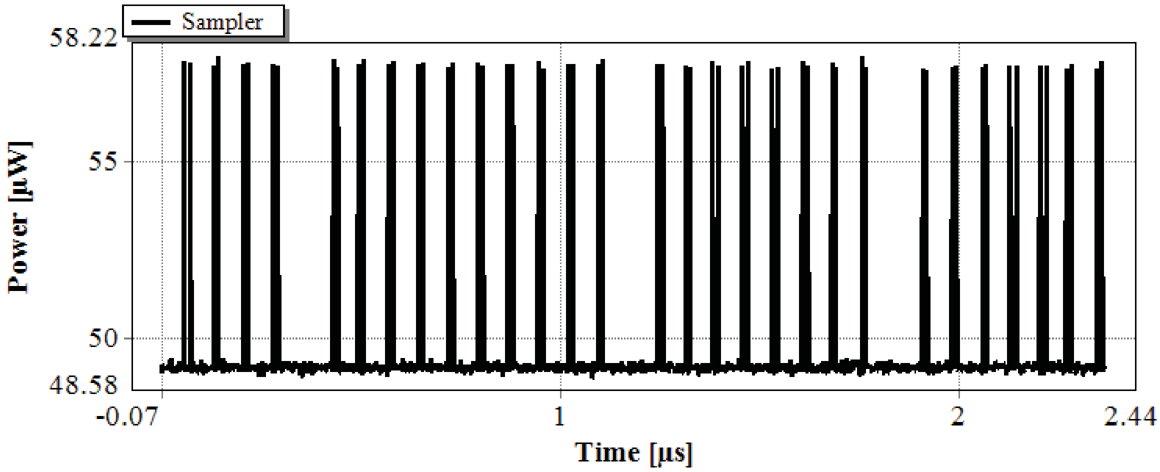

Figure 7-42 Sampler output, (faulty case)

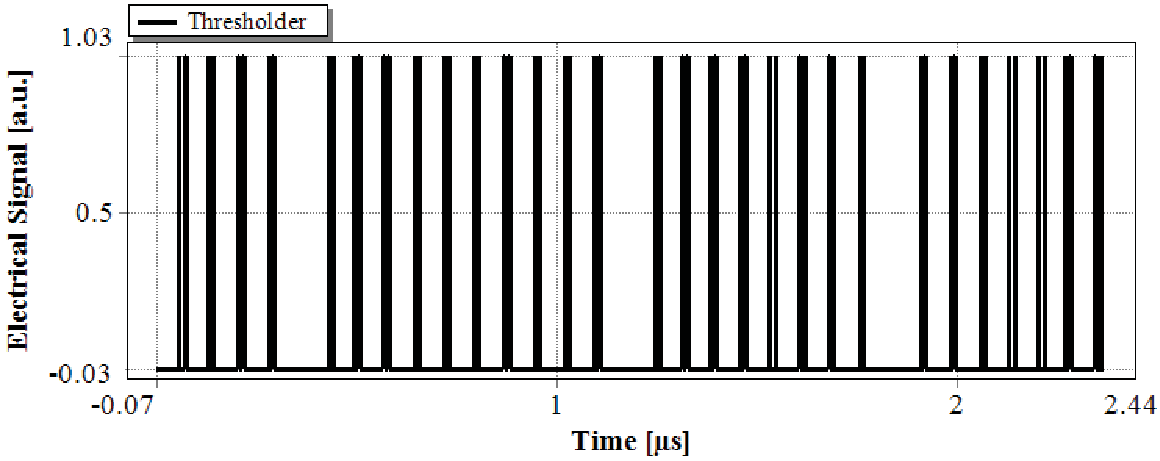

Figure 7-43 Thresholder output, (faulty case)

Table 7-6 Fibre ID and status, (Faulty case)

Fibre ID	Status
1	Healthy
2	Healthy
3	Healthy
4	Healthy
5	Faulty
6	Healthy
7	Healthy
8	Healthy
9	Healthy
10	Healthy
11	Healthy
12	Healthy
13	Healthy
14	Healthy

15	Healthy
16	Faulty
17	Healthy
18	Healthy
19	Healthy
20	Healthy
21	Healthy
22	Healthy
23	Healthy
24	Healthy
24	Healthy
25	Faulty
26	Healthy
27	Healthy
28	Healthy
29	Healthy
30	Healthy
31	Healthy
32	Healthy

7.4 A Splitting Ratio of 64

The general structure of a system with 64 ONUs is shown in Figure 7-44. The parameters used are presented in Appendix.

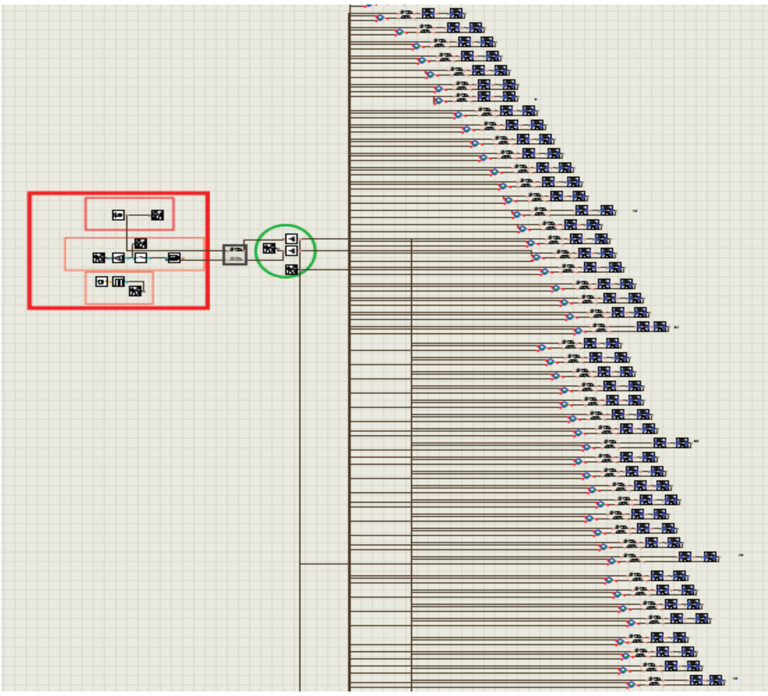

Figure 7-44 VPI model for 64 ONUs

In this scenario, the encoder structure is the same as described in (7.2.3) with an additional ODL. The output of the combiner, sampler, thresholder, and the reference signal are shown in Figure 7-45 to Figure 7-48, respectively. From those figures, it can be noted that all signals are received correctly, indicating a healthy fibre links to all ONUs as shown in Table 7-7

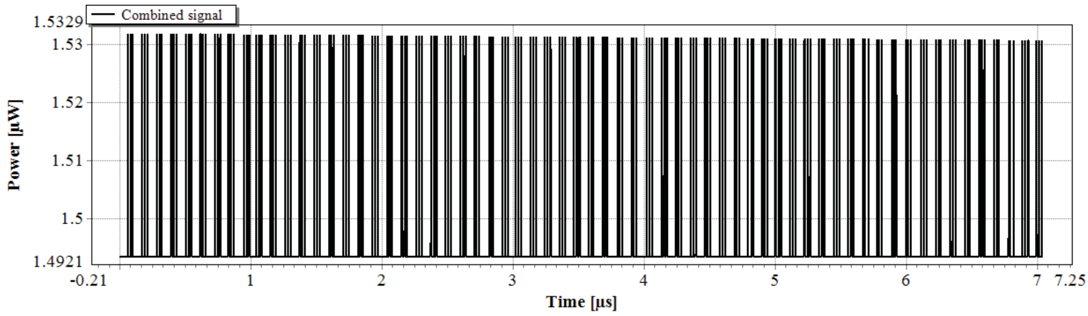

Figure 7-45 Combined signal output for 64 ONUs, (healthy case)

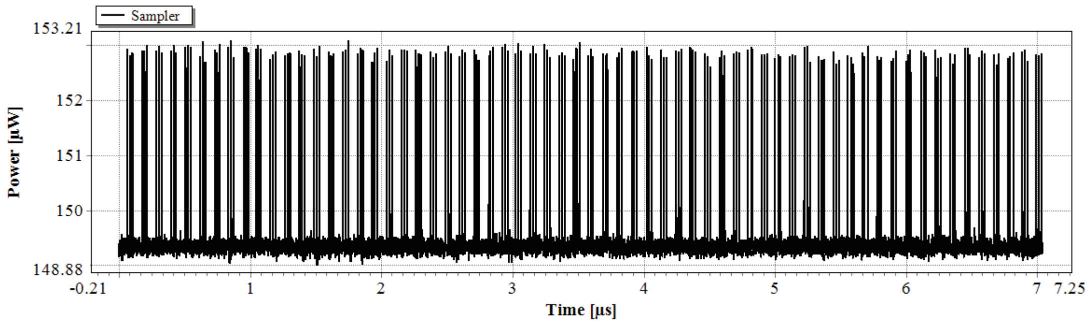

Figure 7-46 Sampler output for 64 ONUs, (healthy case)

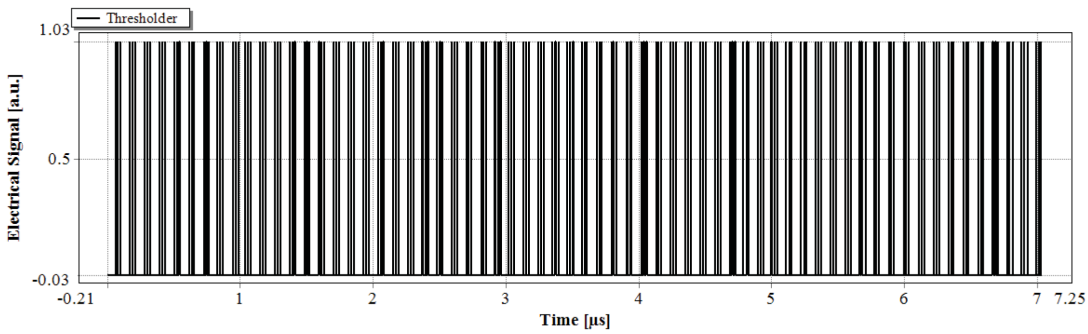

Figure 7-47 Thresholder output for 64 ONUs, (healthy case)

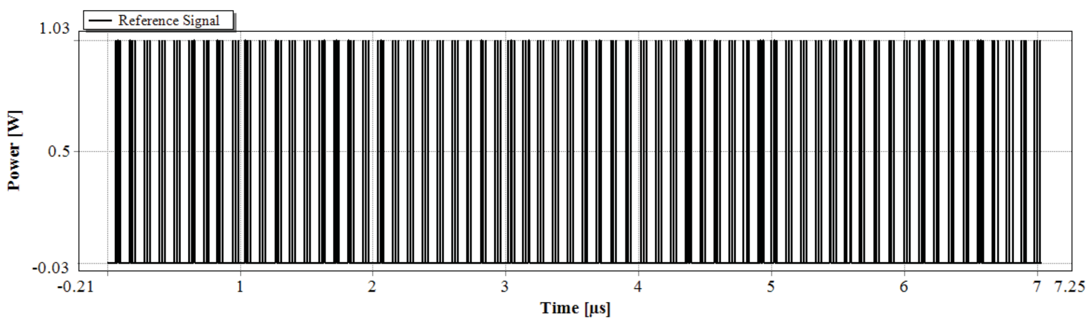

Figure 7-48 Reference signal output for 64 ONUs, (healthy case)

Table 7-7 Fibre ID and status for 64 ONUs, (healthy case)

Fibre ID	Status	Fibre ID	Status
1	Healthy	33	Healthy
2	Healthy	34	Healthy
3	Healthy	35	Healthy
4	Healthy	36	Healthy
5	Healthy	37	Healthy
6	Healthy	38	Healthy
7	Healthy	39	Healthy
8	Healthy	40	Healthy
9	Healthy	41	Healthy
10	Healthy	42	Healthy
11	Healthy	43	Healthy
12	Healthy	44	Healthy
13	Healthy	45	Healthy
14	Healthy	46	Healthy
15	Healthy	47	Healthy
16	Healthy	48	Healthy
17	Healthy	49	Healthy
18	Healthy	50	Healthy
19	Healthy	51	Healthy
20	Healthy	52	Healthy
21	Healthy	53	Healthy
22	Healthy	54	Healthy
23	Healthy	55	Healthy
24	Healthy	56	Healthy
25	Healthy	57	Healthy
26	Healthy	58	Healthy
27	Healthy	59	Healthy
28	Healthy	60	Healthy
29	Healthy	61	Healthy
30	Healthy	62	Healthy
31	Healthy	63	Healthy
32	Healthy	64	Healthy

A scaling up of the time zones for the first three encoders is shown in **Figure 7-49**. The time corresponding to those encoder before and after delay is shown in Figure 7-50.

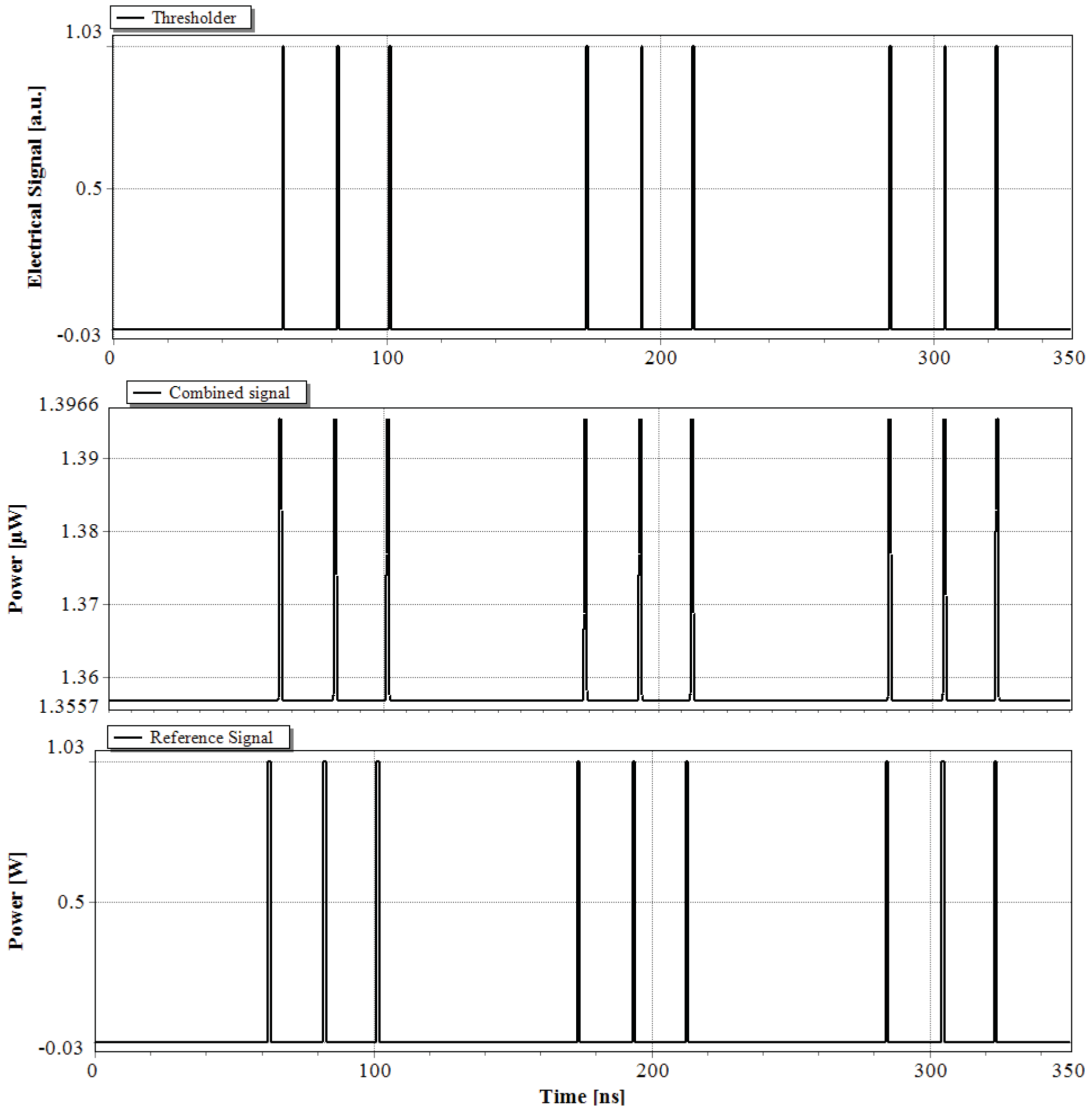

Figure 7-49 **Closeup output of the Combiner, thresholder and reference signal of encoder 1, 2, and 3 with delay**

Encoder	Sub-pulses delay	Before Delay	After delay
1	Delay 1	11	61
	Delay 2	31	81
	Delay 3	50	100
2	Delay 1	12	172
	Delay 2	32	192
	Delay 3	51	211
3	Delay 1	13	283
	Delay 2	33	303
	Delay 3	52	322

Figure 7-50 Sub-pulses times before and after delay

Figure 7-51, Figure 7-52, and Figure 7-53 show the output of the combiner, sampler, and the thresholder, respectively, in case of a fault in the fibre to ONU_{16}, ONU_{48} and ONU_{60}. From these figures, it can be noted that the signals corresponding to the ONUs are missing, indicating a fault in their fibre links as stated in Table 7-8.

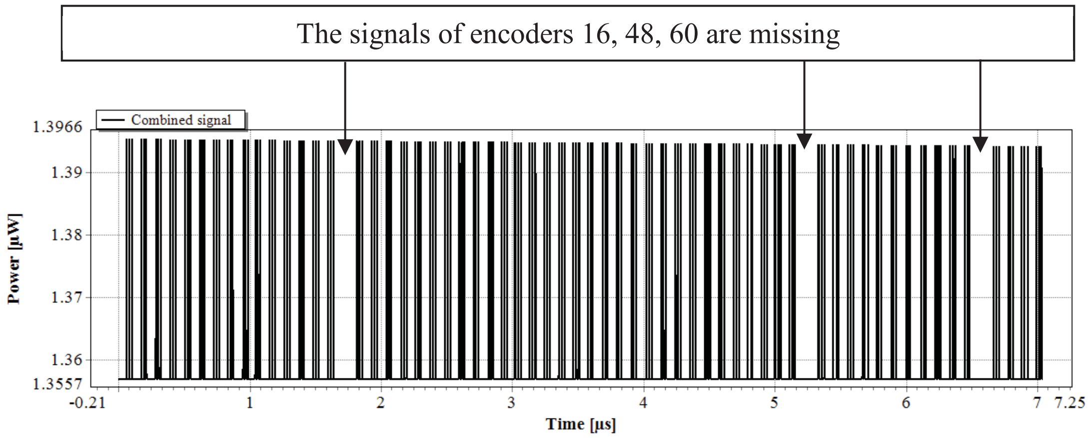

Figure 7-51 Combined signal output for 64 ONUs, (faulty case)

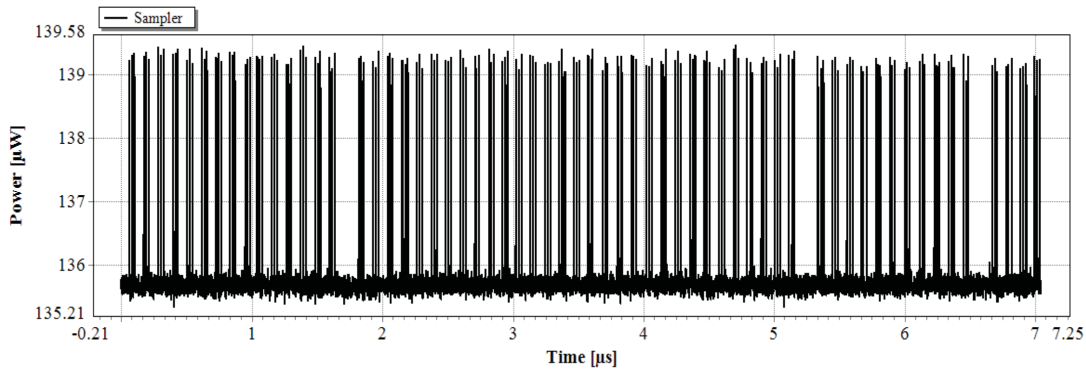

Figure 7-52 Sampler output for 64 ONUs, (faulty case)

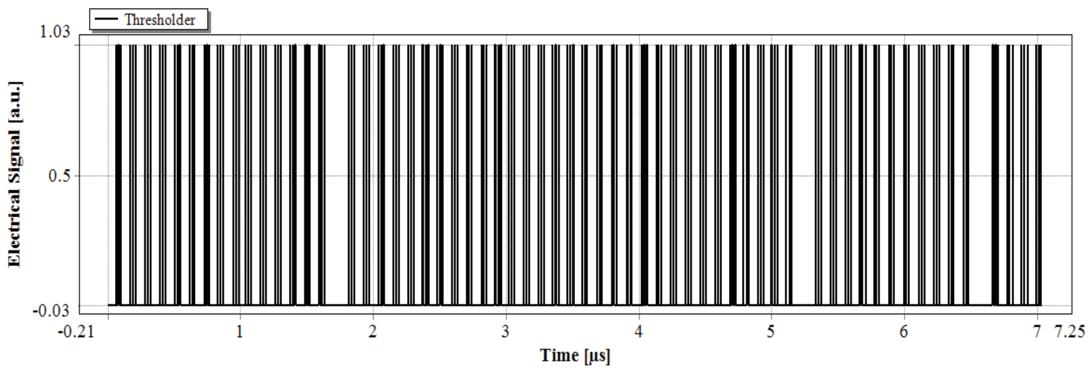

Figure 7-53 Thresholder output for 64 ONUs, (faulty case)

Table 7-8 Fibre ID and status for 64 ONUs, (faulty case)

Fibre ID	Status	Fibre ID	Status
1	Healthy	33	Healthy
2	Healthy	34	Healthy
3	Healthy	35	Healthy
4	Healthy	36	Healthy
5	Healthy	37	Healthy
6	Healthy	38	Healthy
7	Healthy	39	Healthy
8	Healthy	40	Healthy
9	Healthy	41	Healthy
10	Healthy	42	Healthy
11	Healthy	43	Healthy
12	Healthy	44	Healthy
13	Healthy	45	Healthy
14	Healthy	46	Healthy
15	Healthy	47	Healthy
16	Faulty	48	Faulty
17	Healthy	49	Healthy
18	Healthy	50	Healthy
19	Healthy	51	Healthy
20	Healthy	52	Healthy
21	Healthy	53	Healthy
22	Healthy	54	Healthy
23	Healthy	55	Healthy
24	Healthy	56	Healthy
25	Healthy	57	Healthy
26	Healthy	58	Healthy
27	Healthy	59	Healthy
28	Healthy	60	Faulty
29	Healthy	61	Healthy
30	Healthy	62	Healthy
31	Healthy	63	Healthy
32	Healthy	64	Healthy

7.5 A Splitting Ratio of 128

The general structure of a system with 128 ONUs is shown in Figure 7-54. The parameters used are presented in the Appendix.

Due to the large amount of data exported from the analyser, and the limited number of rows permitted in Microsoft Excel, the output of the comparison for the healthy and fault cases in this scenario is displayed for 64 ONUs only. However, Figure 7-55 and Figure 7-56, show the output of the combined signal for 128 for healthy and fault cases, where faults detected in links to ONU_{12}, ONU_{48}, ONU_{96}, and ONU_{128}, respectively. Figure 7-57 shows the output of the reference signal for 128.

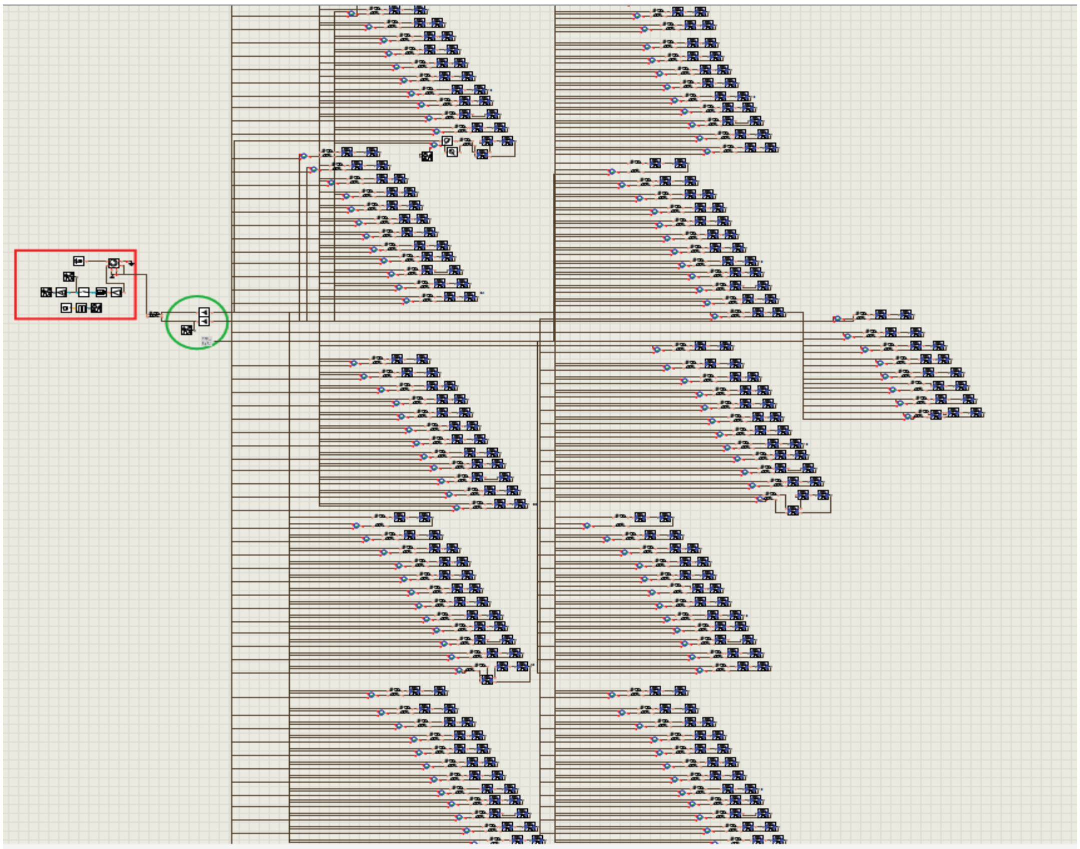

Figure 7-54 VPI model for 128 ONUs

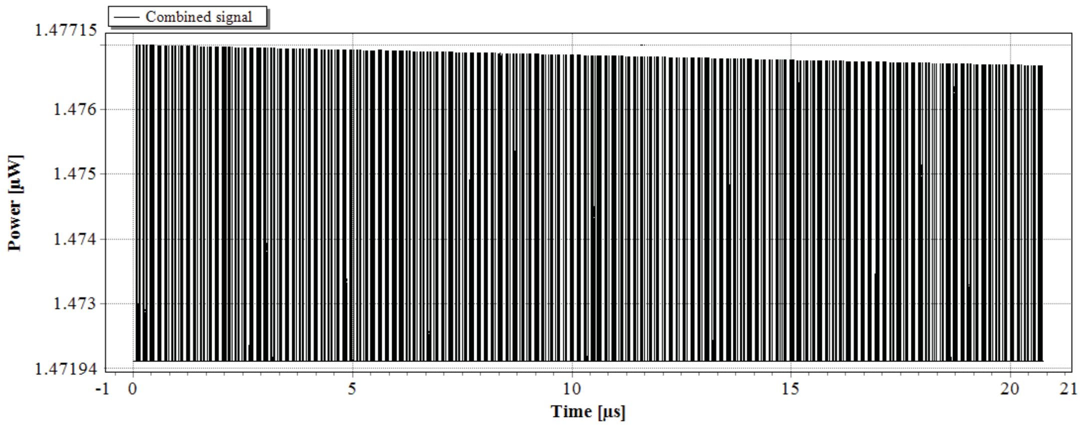

Figure 7-55 Combined signal output for 128 ONUs (healthy case)

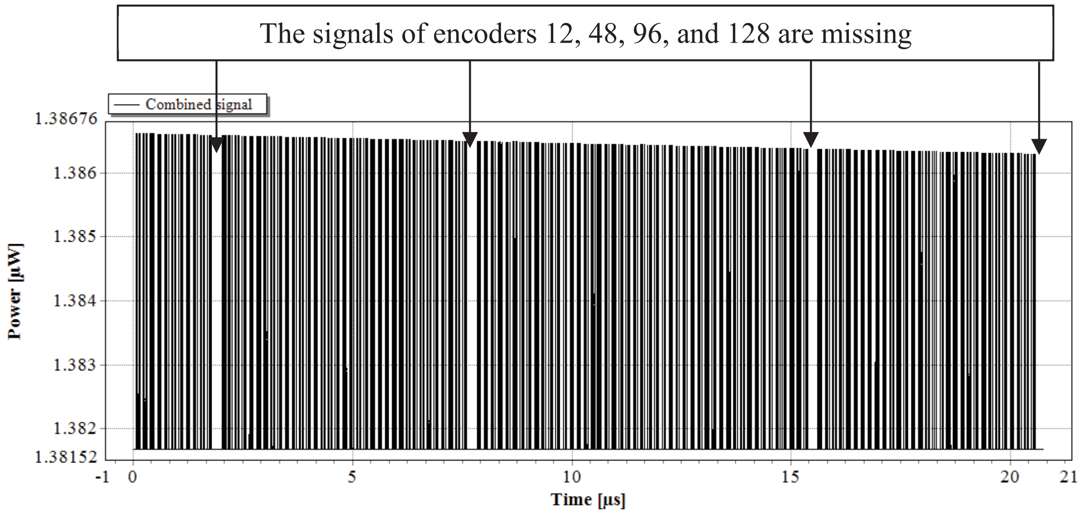

Figure 7-56 Combined signal output for 128 ONUs (faulty case)

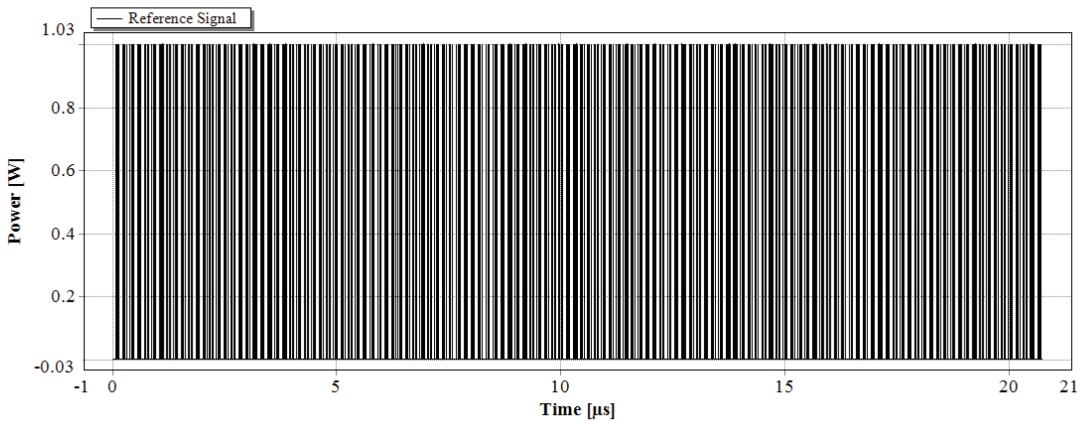

Figure 7-57 Reference signal output for 128 ONUs

The output of the combiner, sampler, thresholder, and the reference signal for 64 ONUs out of 128 are shown in Figure 7-58 to Figure 7-61, respectively. Figure 7-62, Figure 7-63, and Figure 7-64, show the output of the combiner, sampler, and the thresholder, respectively, in case of a fault in ONU_{12} and ONU_{48}. In addition, a scaling up of the time zones for the first three encoders is shown in Figure 7-65, where their corresponding times before and after delay is shown in Figure 7-66. The outputs of the comparison for the healthy and fault cases for 64 ONUs out of 128 are presented in Table 7-9 and

Table 7-10, respectively.

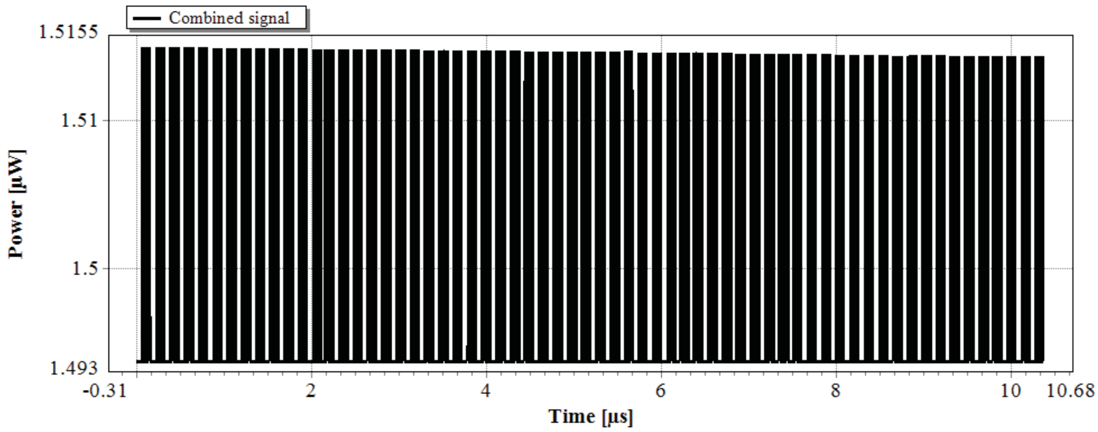

Figure 7-58 Combined signal output for 64 ONUs out of 128, (healthy case)

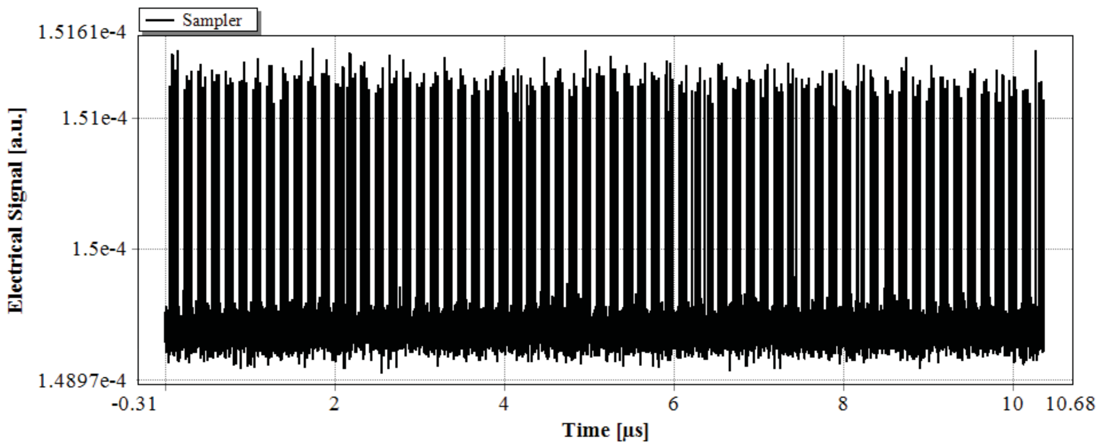

Figure 7-59 Sampler output for 64 ONUs out of 128, (healthy case)

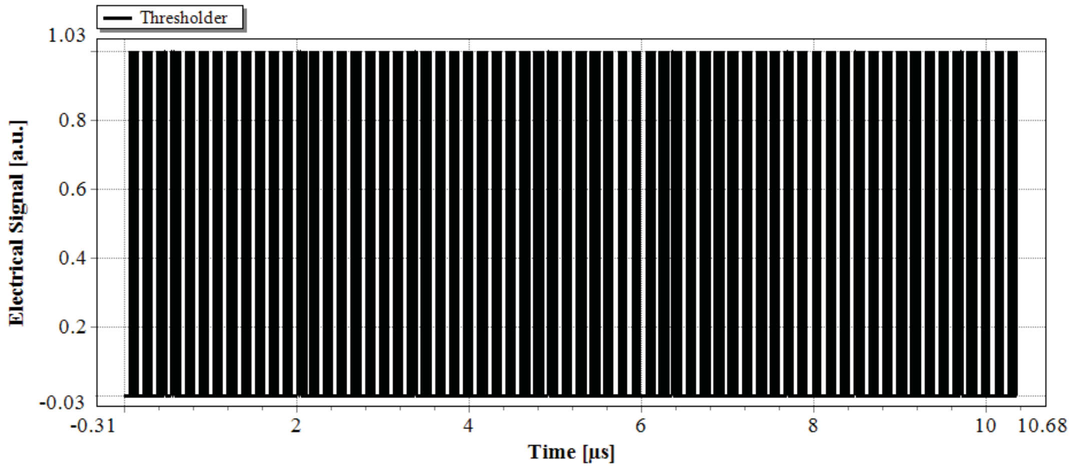

Figure 7-60 Thresholder output for 64 ONUs out of 128, (healthy case)

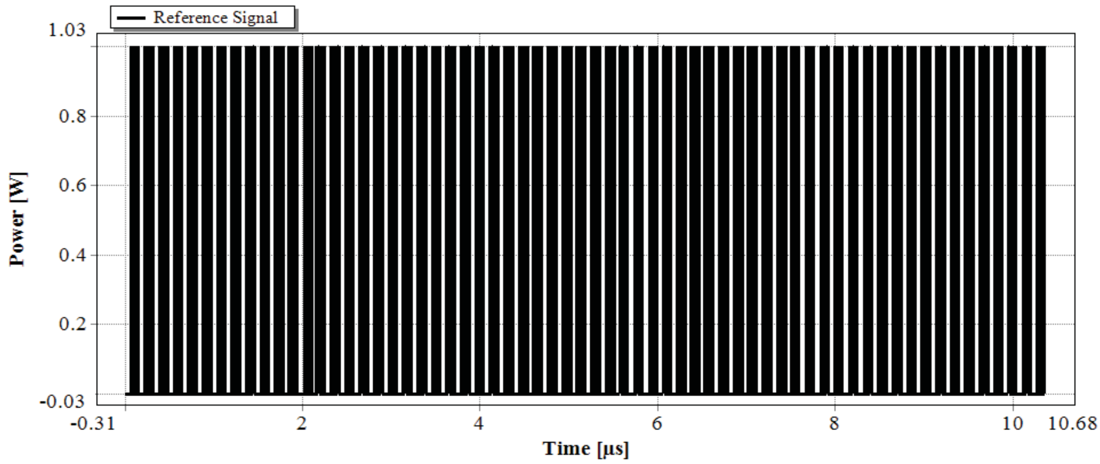

Figure 7-61 Reference signal output for 64 ONUs out of 128

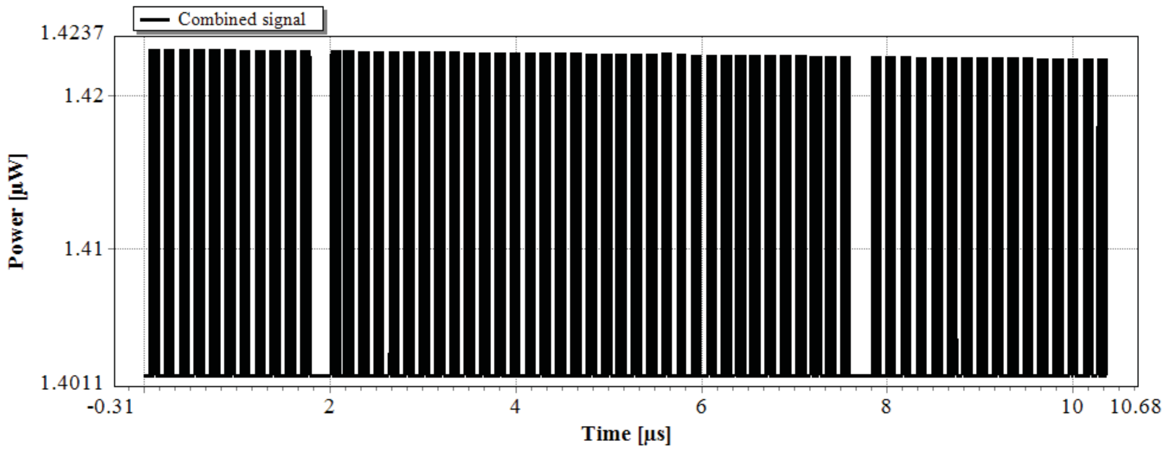

Figure 7-62 Combined signal output for 64 ONUs out of 128, (faulty case)

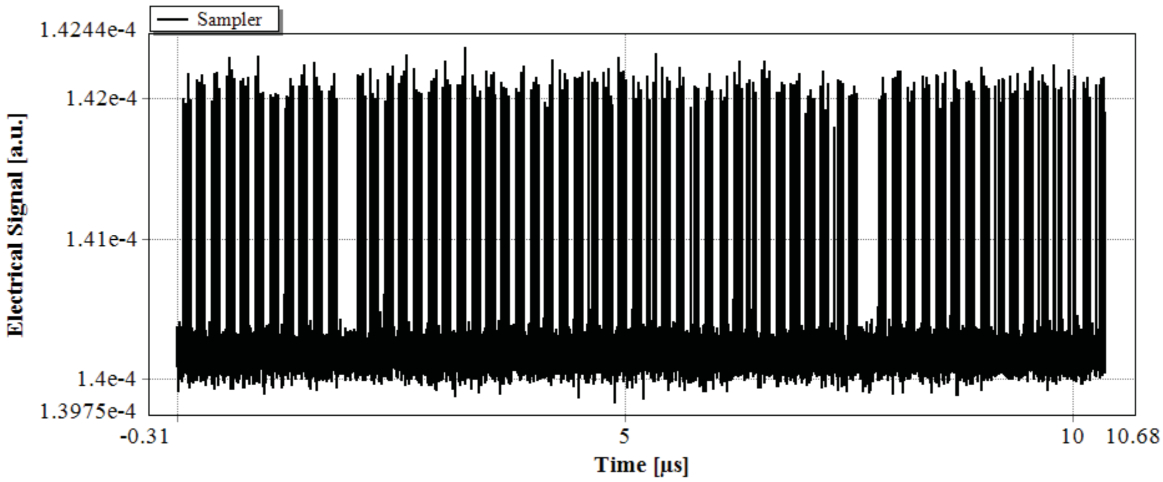

Figure 7-63 Sampler output for 64 ONUs out of 128, (healthy case)

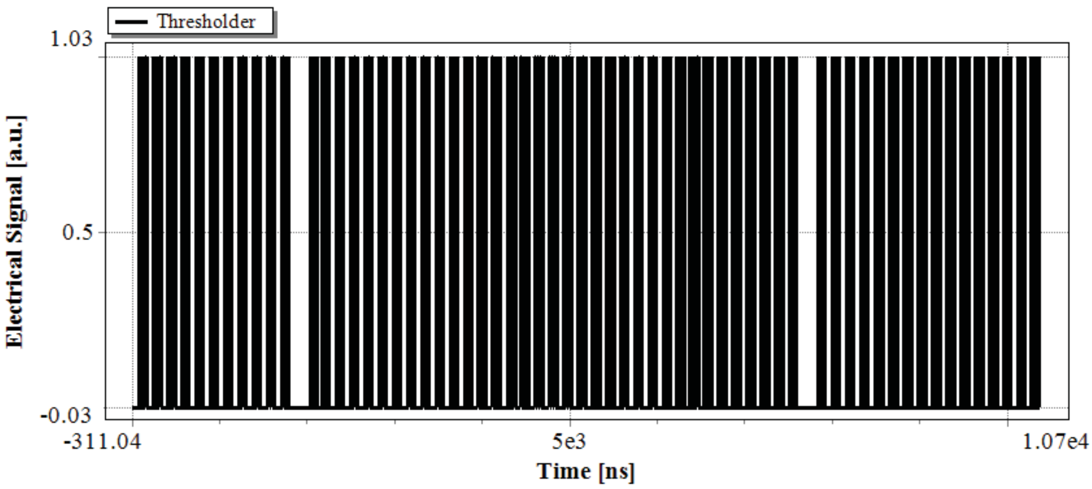

Figure 7-64 Thresholder output for 64 ONUs out of 128, (healthy case)

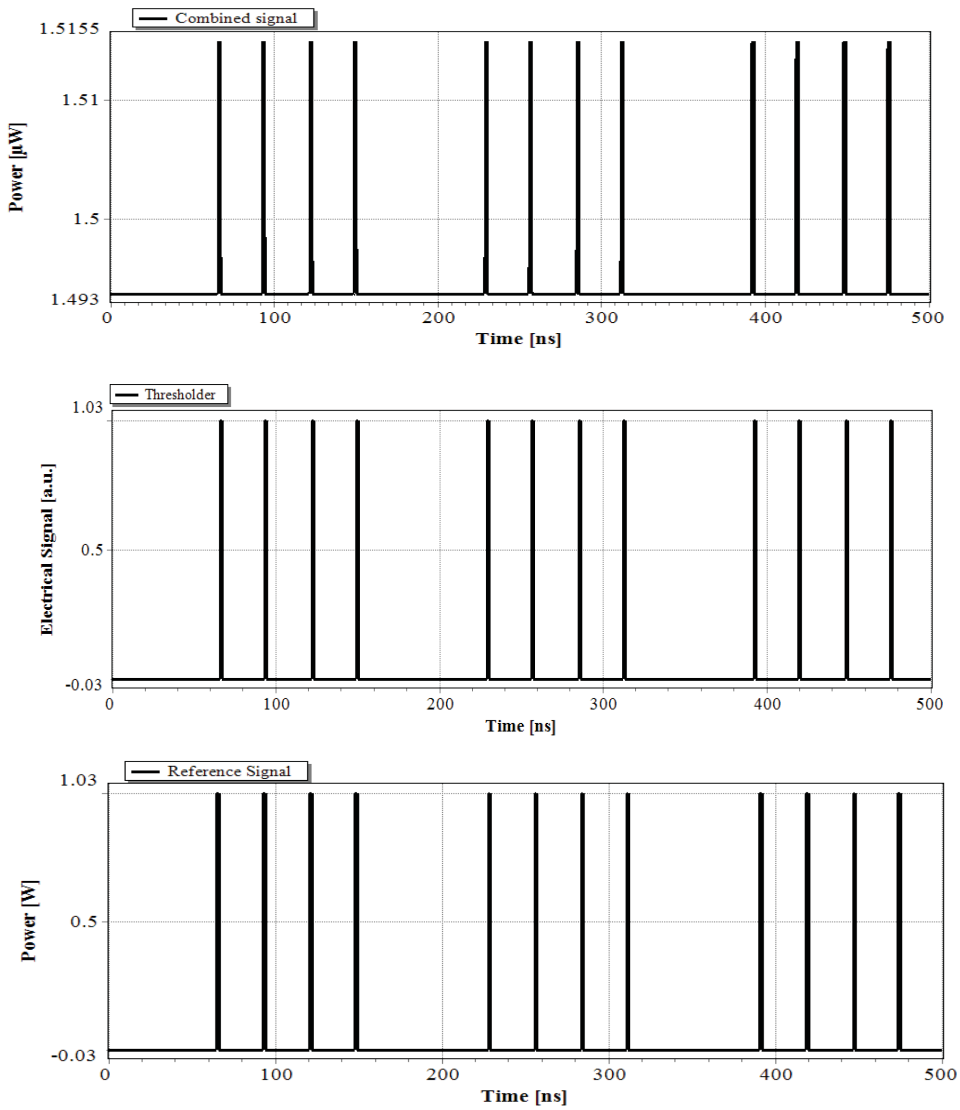

Figure 7-65 Closeup output of the Combiner, thresholder and reference signal of encoder 1, 2, and 3 with delay

Encoder	Sub-pulses delay	Before delay	After delay
1	Delay1	16	66
	Delay2	43	93
	Delay3	72	122
	Delay4	99	149
2	Delay1	17	229
	Delay2	44	256
	Delay3	73	447
	Delay4	100	312
3	Delay1	18	392
	Delay2	45	419
	Delay3	74	448
	Delay4	101	475

Figure 7-66 Sub-pulse delay times after and before delay for encoder1, 2, and 3

Table 7-9 Fibre ID and status for 64 ONUs out of 128 (healthy case)

Fibre ID	Status	Fibre ID	Status	Fibre ID	Status	Fibre ID	Status
1	Healthy	17	Healthy	33	Healthy	49	Healthy
2	Healthy	18	Healthy	34	Healthy	50	Healthy
3	Healthy	19	Healthy	35	Healthy	51	Healthy
4	Healthy	20	Healthy	36	Healthy	52	Healthy
5	Healthy	21	Healthy	37	Healthy	53	Healthy
6	Healthy	22	Healthy	38	Healthy	54	Healthy
7	Healthy	23	Healthy	39	Healthy	55	Healthy
8	Healthy	24	Healthy	40	Healthy	56	Healthy
9	Healthy	25	Healthy	41	Healthy	57	Healthy
10	Healthy	26	Healthy	42	Healthy	58	Healthy
11	Healthy	27	Healthy	43	Healthy	59	Healthy
12	Healthy	28	Healthy	44	Healthy	60	Healthy
13	Healthy	29	Healthy	45	Healthy	61	Healthy
14	Healthy	30	Healthy	46	Healthy	62	Healthy
15	Healthy	31	Healthy	47	Healthy	63	Healthy
16	Healthy	32	Healthy	48	Healthy	64	Healthy

Table 7-10 Fibre ID and status for 64 ONUs out of 128 (faulty case)

Fibre ID	Status	Fibre ID	Status	Fibre ID	Status	Fibre ID	Status
1	Healthy	17	Healthy	33	Healthy	49	Healthy
2	Healthy	18	Healthy	34	Healthy	50	Healthy
3	Healthy	19	Healthy	35	Healthy	51	Healthy
4	Healthy	20	Healthy	36	Healthy	52	Healthy
5	Healthy	21	Healthy	37	Healthy	53	Healthy
6	Healthy	22	Healthy	38	Healthy	54	Healthy
7	Healthy	23	Healthy	39	Healthy	55	Healthy
8	Healthy	24	Healthy	40	Healthy	56	Healthy
9	Healthy	25	Healthy	41	Healthy	57	Healthy
10	Healthy	26	Healthy	42	Healthy	58	Healthy
11	Healthy	27	Healthy	43	Healthy	59	Healthy
12	Faulty	28	Healthy	44	Healthy	60	Healthy
13	Healthy	29	Healthy	45	Healthy	61	Healthy
14	Healthy	30	Healthy	46	Healthy	62	Healthy
15	Healthy	31	Healthy	47	Healthy	63	Healthy
16	Healthy	32	Healthy	48	Faulty	64	Healthy

7.6 Discussion

The demonstration of the monitoring system using 1-D time encoding has shown the capability of the EG-nMPC to accommodate the maximum number of the different splitting ratios of GPON. In addition, the demonstration showed that the use of information gathered from the ranging process can lead to improvement in the performance by easily distinguishing between the codes coming from the multiple ONUs. For fault identification, the received signal of a particular code is compared to a reference signal in order to make a decision about the status of the link. If the signal for a practicular code and the reference signal simultaneously match, then the thresholder returns a peak at the time assigned for that particular code, indicating a healthy link. Otherwise, the link is faulty. In addition, and by utilizing the option of exporting the data into the Excel file, and processing the same using VBA, this chapter provides a readable information about each link, where the healthy link is marked in green and a faulty one in red.

7.7 Summary

This chapter has provided a demonstration of the monitoring system implementation of 1-D EG-nMPC using VPItransmissionMaker. For simplicity and readability, the chapter provided a description of a network simulation with four ONUs. The simulation results for networks with capacities of 32, 64, and 128 splitting ratios were presented based on the results obtained for 4 ONUs.

Chapter 8 CONCLUSION AND FUTURE WORK

8.1 Conclusion

The research has been successfully completed and the research questions identified in Chapter 1 have been answered. The research identified a new and novel monitoring approach for NG-PON and demonstrated the viability of this approach rigorously. The research has resulted in a number of peer reviewed publications.

With the high capacity and wide coverage of NG-PON there is a need to ensure that high network reliability and improved timely fault management can be achieved. Research into monitoring systems and technologies is a key aspect of current research. Applying protection schemes can help in fast traffic restoration when a fault occurs, however, there is a need to identify the location of the fault and eliminate its causes. Therefore, several studies have been proposed in literature for monitoring NG-PONs. It is evident that the features provided by an OC based monitoring technique, such as improved performance, cost-effectiveness, and simplicity, would make it a promising candidate for a future monitoring system. The key requirement of monitoring based OC is the ability of the spreading code to provide a cardinality that is compatible with the number of ONUs under consideration. The main aim of this research was, therefore, to design a spreading code that is able to accommodate the typical PON splitting ratios.

To achieve the research objectives defined in Chapter 1, a new prime code for OCDMA systems has been proposed. In addition, the FIR parameter was used as a criterion to determine the optimal protection scheme. The key achievements of this research are summarised as:

- The code proposed in Chapter 4, has the capability to accommodate the different PON splitting ratios with a smaller prime number when compared to other prime code approaches. In addition, the proposed code requires a lower code weight and shorter code length, leading to a reduction in energy consumption and processing time. In Chapter 4, the construction of the code and its parameters are detailed, as well as the evaluation of its performance using OOK-OCDMA and PPM-OCDMA modulation formats. The proposed code exhibited an improved performance, compared to other codes, when used with an increasing number of channels for both modulation techniques.

- The three protection schemes for ring-and-spur LR-PON presented in Chapter 5 are proposed based on evaluating the FIR parameter for the different network components. The performance of the proposed protection schemes, in terms of availability and cost, are evaluated and compared to the existing protection schemes. It has been shown that the OLT-ring protection scheme, suggested by this research, provides higher availability with a minimal increase in the cost, when compared to ring only protection.

- The significance of utilizing the PON ranging process information, carried out by the OLT at the data layer, to eliminate the interference between the upstream burst at the monitoring layer, is shown in Chapter 6. In addition, Chapter 6 presents a mathematical evaluation of the influence of the different pulse widths on the system SNR and SIR.

- The monitoring system implementation, using the code proposed in Chapter 4, and the T_{Δ} introduced in Chapter 6, are shown in Chapter 7. Chapter 7 presents the details for the design of the system components used in VPItransmissionMaker.

To conclude, the implementation of the proposed code, EG-nMPC, offers better performance than other prime codes when it comes to monitoring PON using an OC based technique. The code reduces the hardware complexity by reducing the code weight required, and consequently the number of ODLs used in encoders and decoders, leading to a reduction in cost and power consumption. In addition, to support the GPON splitting ratios, the proposed code requires shorter code lengths, leading to a reduction in processing time.

8.2 Future work

Research presented in this thesis can be built upon to further improve the performance of the monitoring system. Potential future work is discussed in the following sections.

8.2.1Hybridization of OTDR and OC for LR-PON

As has been shown in Chapter 5, the FF is the most critical part in the network due to its very low availability and high CAF. Therefore, it requires a highly reliable monitoring system. In addition, OTDR has been recommended by the ITU-T for monitoring PON due to its ability to immediately locate faults and analyse the cause. Thus, hybridization of OTDR and OC can be investigated, where OTDR could be used to monitor FF, while an OC technique can be implemented to monitor the drop fibre links.

8.2.2Constructing a 2-D coding using EG-nMPC as one of its dimensions

Although, the proposed 1-D code resulted in a dramatic increase in code cardinality, this code still has the limitation that is needs to be adapted for NG-PON where number of ONUs exceeds 1024. It is important to explore the possibility of constructing a 2-D code, that is based on EG-nMPC as one of the dimensions, if a larger number of ONUs is to be accommodated. Similar to any 2-D coding scheme, this approach requires ONUs and OLT to implement a 2-D encoder and decoder, respectively. It should be noted that, the cardinality of 2-D codes is upper bounded by its parameters. Hence, an additional RN could require changing the coding scheme if the total number of ONUs, after the addition of more ONUs, exceeds that of the available cardinality of the chosen code.

8.2.3Implementing 1D/2D coding in LR-PON

1D/2D coding is a valuable area for further research to provide flexibility when one or more remote nodes are added to the ring. If it is required to add another monitoring wavelength to support the RN then it is appropriate that a broader and more flexible approach be investigated. However, the potential variability in ring-and-spur PON means that additional components such as add/drop filters at the RNs may be needed. In addition, the number of available monitoring wavelengths is dependent on the monitoring band.

BIBLIOGRAPHY

[1] S.-J. Park, C.-H. Lee, K.-T. Jeong, H.-J. Park, J.-G. Ahn, and K.-H. Song, "Fiber-to-the-home services based on wavelength-division-multiplexing passive optical network," *Journal of Lightwave Technology,* vol. 22, p. 2582, 2004.

[2] G. Kramer, B. Mukherjee, and G. Pesavento, "Ethernet PON (ePON): Design and analysis of an optical access network," *Photonic Network Communications,* vol. 3, pp. 307-319, 2001.

[3] S. E. Minzer, "Broadband ISDN and asynchronous transfer mode (ATM)," *IEEE Communications Magazine,* vol. 27, pp. 17-24, 1989.

[4] T. Muciaccia, F. Gargano, and V. Passaro, "Passive Optical Access Networks: State of the Art and Future Evolution," in *Photonics*, 2014, pp. 323-346.

[5] T. Pfeiffer, "An Introduction to PON Technologies," *IEEE Communications Magazine,* p. S18, 2007.

[6] S.-L. Lee, C.-H. Sun, and K.-C. Feng, "Hybrid passive optical networking architecture and techniques for constructing green broadband access networks," 2014.

[7] R. Alvizu, A. Arcia, M. Hernández, M. Huerta, and I. Tafur Monroy, "Hybrid WDM–XDM PON Architectures for Future Proof Access Networks," *International Journal On Advances in Systems and Measurements,* vol. 5, pp. 139-153, 2012.

[8] S. Bindhaiq, A. S. M. Supa, N. Zulkifli, A. B. Mohammad, R. Q. Shaddad, M. A. Elmagzoub, *et al.*, "Recent development on time and wavelength-division multiplexed passive optical network (TWDM-PON) for next-generation passive optical network stage 2 (NG-PON2)," *Optical Switching and Networking,* vol. 15, pp. 53-66, 2015.

[9] E. Wong, "Next-generation broadband access networks and technologies," *Lightwave Technology, Journal of,* vol. 30, pp. 597-608, 2012.

[10] M. Hernandez, A. Arcia, R. Alvizu, and M. Huerta, "A review of XDMA-WDM-PON for Next Generation Optical Access Networks," in *Global Information Infrastructure and Networking Symposium (GIIS), 2012*, 2012, pp. 1-6.

[11] M. A. Esmail and H. Fathallah, "Physical Layer Monitoring Techniques for TDM-Passive Optical Networks: A Survey," *Communications Surveys & Tutorials, IEEE,* vol. 15, pp. 943-958, 2013.

[12] A. M. Ragheb and H. Fathallah, "Performance analysis of next generation-PON (NG-PON) architectures," in *High Capacity Optical Networks and Enabling Technologies (HONET), 2011*, 2011, pp. 339-345.

[13] R. Shaddad, A. Mohammad, S. Al-Gailani, A. Al-hetar, and M. Elmagzoub, "A survey on access technologies for broadband optical and wireless networks," *Journal of Network and Computer Applications,* vol. 41, pp. 459-472, 2014.

[14] I. N. Cano, X. Escayola, A. Peralta, V. Polo, M. C. Santos, and J. Prat, "A study of flexible bandwidth allocation in statistical OFDM-based PON," in *Transparent Optical Networks (ICTON), 2013 15th International Conference on*, 2013, pp. 1-4.

[15] N. Cvijetic, "OFDM for next-generation optical access networks," *Lightwave Technology, Journal of,* vol. 30, pp. 384-398, 2012.

[16] N. Cvijetic, Q. Dayou, and H. Junqiang, "100 Gb/s optical access based on optical orthogonal frequency-division multiplexing," *Communications Magazine, IEEE,* vol. 48, pp. 70-77, 2010.

[17] N. Kataoka, N. Wada, W. Xu, G. Cincotti, and K. Kitayama, "10Gbps-Class, bandwidth-symmetric, OCDM-PON system using hybrid multi-port and SSFBG en/decoder," in *Optical Network Design and Modeling (ONDM), 2010 14th Conference on*, 2010, pp. 1-4.

[18] D. Gutierrez, K. S. Kim, S. Rotolo, F.-T. An, and L. G. Kazovsky, "FTTH standards, deployments and research issues," *Photonics and Networking Research Lab., Proceedings of JCIS '05,* pp. 1358-1361, 2005.

[19] Y. Luo, X. Zhou, F. Effenberger, X. Yan, G. Peng, Y. Qian*, et al.*, "Time-and wavelength-division multiplexed passive optical network (TWDM-PON) for next-generation PON stage 2 (NG-PON2)," *Journal of Lightwave Technology,* vol. 31, pp. 587-593, 2013.

[20] Y. Luo, X. Yan, and F. Effenberger, "Next generation passive optical network offering 40Gb/s or more bandwidth," in *Communications and Photonics Conference (ACP), 2012 Asia*, 2012, pp. 1-3.

[21] J. Prat, J. Lázaro, P. Chanclou, R. Soila, P. Velanas, A. Teixeira*, et al.*, "Passive optical network for long-reach scalable and resilient access," in *Telecommunications, 2009. ConTEL 2009. 10th International Conference on*, 2009, pp. 271-275.

[22] J. Prat, J. A. Lázaro, K. Kanonakis, and I. Tomkos, "New FTTH Architectures for NG-PON-2," in *Access Networks and In-house Communications*, 2010, p. ATuA4.

[23] M. Cen, J. Chen, V. Moeyaert, P. Mégret, and M. Wuilpart, "Full monitoring for long-reach TWDM passive optical networks," *Optics express,* vol. 24, pp. 15782-15797, 2016.

[24] J. Prat, V. Polo, B. Schrenk, J. A. Lazaro, F. Bonada, E. T. Lopez*, et al.*, "Demonstration and field trial of a resilient hybrid NG-PON test-bed," *Optical Fiber Technology,* vol. 20, pp. 537-546, 2014.

[25] S. Jindal and N. Gupta, "OCDMA: Study and Future Aspects," in *Recent Development in Wireless Sensor and Ad-hoc Networks*, ed: Springer, 2015, pp. 125-167.

[26] V. Baby, D. Rand, C.-S. Bres, L. Xu, I. Glesk, and P. R. Prucnal, "Incoherent optical CDMA systems," 2005.

[27] H. Yin and D. J. Richardson, *Optical Code Division Multiple Access Communication Networks:Theory and Applications*, 1 ed., 2009.

[28] C.-S. Bres, I. Glesk, and P. R. Prucnal, "Demonstration of an eight-user 115-Gchip/s incoherent OCDMA system using supercontinuum generation and optical time gating," *IEEE photonics technology letters,* vol. 18, pp. 889-891, 2006.

[29] N. F. Naim, M. S. Ab-Rahman, H. A. Bakarman, and A. A. A. Bakar, "Real-time monitoring in passive optical networks using a superluminescent LED with uniform and phase-shifted fiber Bragg gratings," *Journal of Optical Communications and Networking,* vol. 5, pp. 1425-1430, 2013.

[30] H. Ghafouri-Shiraz and M. M. Karbassian, *Optical CDMA networks: principles, analysis and applications* vol. 38: John Wiley & Sons, 2012.

[31] A. Dixit, B. Lannoo, D. Colle, M. Pickavet, C. Jiajia, and M. Mahloo, "Efficient protection schemes for hybrid WDM/TDM Passive Optical Networks," in *Communications (ICC), 2012 IEEE International Conference on*, 2012, pp. 6220-6224.

[32] "Optical fiber cable network maintenance", ITU-T L.25, ed.

[33] M. Zhu, J. Zhang, D. Wang, and X. Sun, "Optimal Fiber Link Fault Decision for Optical 2D Coding-Monitoring Scheme in Passive Optical Networks," *Journal of Optical Communications and Networking,* vol. 8, pp. 137-147, 2016.

[34] "Optical fibre cable maintenance criteria for in-service fibre testing in access networks", ITU-T Recommendation L.66, ed.

[35] R. F. Moghaddam, Y. Lemieux, and M. Cheriet, "40 Gbps Access for Metro networks: Implications in terms of Sustainability and Innovation from an LCA Perspective," *arXiv preprint arXiv:1504.06262,* 2015.

[36] M. M. Rad, H. A. Fathallah, and L. A. Rusch, "Fiber fault PON monitoring using optical coding: effects of customer geographic distribution," *IEEE transactions on communications,* vol. 58, 2010.
[37] R. Yadav and G. Kaur, "Design and performance analysis of 1D, 2D and 3D prime sequence code family for optical CDMA network," *Journal of Optics,* pp. 1-14, 2016.
[38] "Passive Optical Network Protection Considerations", ITU-T G. Sup 51, ed.
[39] P. Begovic, N. Hadziahmetovic, and D. Raca, "10G EPON vs. XG-PON1 efficiency," in *Ultra Modern Telecommunications and Control Systems and Workshops (ICUMT), 2011 3rd International Congress on*, 2011, pp. 1-9.
[40] "10-Gigabit-capable passive optical networks (XG-PON): Physical media dependent (PMD) layer specification", ITU-T G.987.2.
[41] D. Van Veen, D. Suvakovic, L. Man Fai, H. Krimmel, A. J. de Lind van Wijngaarden, J. Galaro*, et al.*, "Demonstration of a symmetrical 10/10 Gbit/s XG-PON2 system," in *Optical Fiber Communication Conference and Exposition (OFC/NFOEC), 2011 and the National Fiber Optic Engineers Conference*, 2011, pp. 1-3.
[42] J.-i. Kani, "Enabling technologies for future scalable and flexible WDM-PON and WDM/TDM-PON systems," *IEEE Journal of Selected Topics in Quantum Electronics,* vol. 16, pp. 1290-1297, 2010.
[43] D. Nesset, "NG-PON2 technology and standards," *Journal of Lightwave Technology,* vol. 33, pp. 1136-1143, 2015.
[44] A. Banerjee, Y. Park, F. Clarke, H. Song, S. Yang, G. Kramer*, et al.*, "Wavelength-division-multiplexed passive optical network (WDM-PON) technologies for broadband access: a review [Invited]," *Journal of optical networking,* vol. 4, pp. 737-758, 2005.
[45] D. Gutierrez, J. Cho, and L. G. Kazovsky, "TDM-PON security issues: Upstream encryption is needed," in *Optical Fiber Communication and the National Fiber Optic Engineers Conference, 2007. OFC/NFOEC 2007. Conference on*, 2007, pp. 1-3.
[46] N. Sotiropoulos, T. Koonen, and H. de Waardt, "Advanced Differential Modulation Formats for Optical Access Networks," *Lightwave Technology, Journal of,* vol. 31, pp. 2829-2843, 2013.
[47] D. van Veen, D. Suvakovic, H. Chow, V. Houtsma, E. Harstead, P. J. Winzer*, et al.*, "Options for TDM PON beyond 10G," in *Access Networks and In-house Communications*, 2012, p. AW2A. 1.
[48] "40-Gigabit-capable passive optical networks 2 (NG-PON2): Physical media dependent (PMD) layer specification" , ITU-T G989.2, 2015., ed.
[49] S. Yoshima, M. Noda, E. Igawa, S. Shirai, K. Ishii, M. Nogami*, et al.*, "Recent progress of high-speed burst-mode transceiver technologies for TDM-PON systems," in *Wireless and Optical Communications Conference (WOCC), 2012 21st Annual*, 2012, pp. 59-62.
[50] A. Srivastava, "Next generation PON evolution," in *SPIE OPTO*, 2013, pp. 864509-864509-15.
[51] R. Urata, C. Lam, H. Liu, and C. Johnson, "High performance, low cost, colorless ONU for WDM-PON," in *Optical Fiber Communication Conference and Exposition (OFC/NFOEC), 2012 and the National Fiber Optic Engineers Conference*, 2012, pp. 1-3.
[52] S. Biswas and S. Adak, "OFDMA-PON: High Speed PON Access System," *International Journal of Soft Computing,* vol. 1.
[53] J. Armstrong, "OFDM for optical communications," *Journal of Lightwave Technology,* vol. 27, pp. 189-204, 2009.
[54] R. Matsumoto, T. Kodama, S. Shimizu, R. Nomura, K. Omichi, N. Wada*, et al.*,

"40G-OCDMA-PON System With an Asymmetric Structure Using a Single Multi-Port and Sampled SSFBG Encoder/Decoders," *Journal of Lightwave Technology,* vol. 32, pp. 1132-1143, 2014.
[55] L. G. Kazovsky, N. Cheng, W.-T. Shaw, D. Gutierrez, and S.-W. Wong, *Broadband optical access networks*: John Wiley & Sons, 2011.
[56] R. Murano, "Optical component technology options for NGPON2 systems," in *Optical Fiber Communication Conference*, 2014, p. M3I. 1.
[57] N. Cheng, J. Gao, C. Xu, B. Gao, D. Liu, L. Wang*, et al.*, "Flexible TWDM PON system with pluggable optical transceiver modules," *Optics express,* vol. 22, pp. 2078-2091, 2014.
[58] G. Kramer, M. De Andrade, R. Roy, and P. Chowdhury, "Evolution of Optical Access Networks: Architectures and Capacity Upgrades," *Proceedings of the IEEE,* vol. 100, pp. 1188-1196, 2012.
[59] R. Bonk, W. Poehlmann, H. Schmuck, and T. Pfeiffer, "Cross-talk in TWDM-PON beyond NG-PON2," in *Optical Fiber Communication Conference*, 2015, p. Tu3E. 2.
[60] L. Han Hyub, L. Jong Hyun, L. Sang Soo, R. Hee Yeal, Y. Hark, and K. YoonKoo, "Investigation of ONU power leveling method for mitigating inter-channel crosstalk in TWDM-PONs," in *Optical Internet 2014 (COIN), 2014 12th International Conference on*, 2014, pp. 1-2.
[61] A. Buttaboni, M. De Andrade, and M. Tornatore, "New and Improved approaches for Dynamic Bandwidth and Wavelength allocation in LR WDM/TDM PON."
[62] M. I. Dias, D. P. Van, L. Valcarenghi, and E. Wong, "Energy-efficient dynamic wavelength and bandwidth allocation algorithm for TWDM-PONs with tunable VCSEL ONUs," 2014.
[63] M. Dias, D. P. Van, L. Valcarenghi, and E. Wong, "Energy-Efficient Framework for Time and Wavelength Division Multiplexed Passive Optical Networks," *Journal of Optical Communications and Networking,* vol. 7, pp. 496-504, 2015.
[64] J. Segarra, V. Sales, and J. Prat, "OLT design approach for resilient extended PON with OBS dynamic bandwidth allocation sharing the OLT optical resources," in *Transparent Optical Networks, 2008. ICTON 2008. 10th Anniversary International Conference on*, 2008, pp. 139-144.
[65] L. Hui-Tang, H. Zhong-Huan, C. Hung-Chen, and C. Wang-Rong, "SPON: A slotted long-reach PON architecture for supporting internetworking capability," in *Military Communications Conference, 2009. MILCOM 2009. IEEE*, 2009, pp. 1-8.
[66] L. Meng, C. M. Assi, M. Maier, and A. R. Dhaini, "Resource management in STARGATE-based Ethernet passive optical networks (SG-EPONs)," *Journal of Optical Communications and Networking,* vol. 1, pp. 279-293, 2009.
[67] L. Yi, Z. Li, M. Bi, W. Wei, and W. Hu, "Symmetric 40-Gb/s TWDM-PON With 39-dB Power Budget," *IEEE Photonics Technology Letters,* vol. 25, pp. 644-647, 2013.
[68] Z. Li, L. Yi, and W. Hu, "Symmetric 40-Gb/s TWDM-PON with 51-dB loss budget by using a single SOA as preamplifier, booster and format converter in ONU," *Optics express,* vol. 22, pp. 24398-24404, 2014.
[69] M. Bi, S. Xiao, L. Yi, H. He, J. Li, X. Yang*, et al.*, "Power budget improvement of symmetric 40-Gb/s DML-based TWDM-PON system," *Optics express,* vol. 22, pp. 6925-6933, 2014.
[70] Y. Guo, S. Zhu, G. Kuang, Y. Yin, Y. Gao, D. Zhang*, et al.*, "Demonstration of 10G burst-mode DML and EDC in symmetric 40Gbit/s TWDM-PON over 40km passive reach," in *Optical Fiber Communications Conference and Exhibition (OFC), 2014*, 2014, pp. 1-3.
[71] Z. Zhou, M. Bi, S. Xiao, Y. Zhang, and W. Hu, "Experimental Demonstration of

Symmetric 100-Gb/s DML-Based TWDM-PON System," *Photonics Technology Letters, IEEE,* vol. 27, pp. 470-473, 2015.
[72] L. Chengjun, G. Wei, W. Wei, and H. Weisheng, "A novel TWDM-PON architecture with control channel," in *Optical Internet 2014 (COIN), 2014 12th International Conference on*, 2014, pp. 1-2.
[73] I. M. Mohamed and M. S. B. Ab-Rahman, "Options and challenges in next-generation optical access networks (NG-OANs)," *Optik-International Journal for Light and Electron Optics,* vol. 126, pp. 131-138, 2015.
[74] H. Song, B.-W. Kim, and B. Mukherjee, "Long-reach optical access networks: A survey of research challenges, demonstrations, and bandwidth assignment mechanisms," *Communications Surveys & Tutorials, IEEE,* vol. 12, pp. 112-123, 2010.
[75] D. Lavery and S. J. Savory, "Digital coherent technology for long-reach optical access," in *Optical Fiber Communications Conference and Exhibition (OFC), 2014*, 2014, pp. 1-3.
[76] B. Skubic, J. Chen, J. Ahmed, B. Chen, L. Wosinska, and B. Mukherjee, "Dynamic bandwidth allocation for long-reach PON: overcoming performance degradation," *Communications Magazine, IEEE,* vol. 48, pp. 100-108, 2010.
[77] M. De Andrade, M. Maier, M. P. McGarry, and M. Reisslein, "Passive optical network (PON) supported networking," *Optical Switching and Networking,* 2014.
[78] "Gigabit-capable passive optical networks (G-PON):) General characteristics" , ITU-T G.984.1, 2008, ed.
[79] M. S. Ab-Rahman, S. A. C. Aziz, and K. Jumari, "Protection route Mechanism for Survivability in FTTH-PON
Network " *International Journal of Computer Science and Network Security (IJCSNS),* vol. 8, 2008.
[80] C.-Y. Chuang, C.-C. Wei, J.-J. Liu, H.-Y. Wu, H.-M. Nguyen, C.-W. Wang*, et al.*, "A High Loss Budget 400-Gbps WDM-OFDM Long-Reach PON over 60 km Transmission by 10G-class EAM and PIN without In-line or Pre-Amplifier," in *Optical Fiber Communication Conference*, 2017, p. W1K. 3.
[81] M. A. Esmail and H. Fathallah, "Fiber fault management and protection solution for ring-and-spur WDM/TDM long-reach PON," in *Global Telecommunications Conference (GLOBECOM 2011), 2011 IEEE*, 2011, pp. 1-5.
[82] M. A. Esmail and H. Fathallah, "Optical coding for next-generation survivable long-reach passive optical networks," *Optical Communications and Networking, IEEE/OSA Journal of,* vol. 4, pp. 1062-1074, 2012.
[83] S. McGettrick, F. Slyne, N. Kitsuwan, D. B. Payne, and M. Ruffini, "Experimental End-to-End Demonstration of Shared N:1 Dual Homed Protection in Long Reach PON and SDN-Controlled Core," in *Optical Fiber Communication Conference*, Los Angeles, California, 2015, p. Tu2E.5.
[84] M. M. Rad, K. Fouli, H. A. Fathallah, L. A. Rusch, and M. Maier, "Passive optical network monitoring: challenges and requirements," *Communications Magazine, IEEE,* vol. 49, pp. s45-S52, 2011.
[85] T. Zhao, H. Han, J. Zhang, X. Liu, X. Chang, A. Wang*, et al.*, "Precise Fault Location in TDM-PON by Utilizing Chaotic Laser Subject to Optical Feedback," *IEEE Photonics Journal,* vol. 7, pp. 1-9, 2015.
[86] H. Fathallah and M. Esmail, "Performance evaluation of special optical coding techniques appropriate for physical layer monitoring of access and metro optical networks," *Photonic Network Communications,* vol. 30, pp. 223-233, 2015.
[87] D. Pastor, K. Jamshidi, and C.-A. Bunge, "Physical layer monitoring based on 2D-

OCDMA concepts and electronic decoding for high density PON networks," in *2015 17th International Conference on Transparent Optical Networks (ICTON)*, 2015, pp. 1-4.
[88] F. Selmanovic and E. Skaljo, "GPON in Telecommunication Network," in *Ultra Modern Telecommunications and Control Systems and Workshops (ICUMT), 2010 International Congress on*, 2010, pp. 1012-1016.
[89] V. Eržen and B. Batagelj, "NG-PON1: technology presentation, implementation in practice and coexistence with the GPON system."
[90] S. Dahlfort, "Comparison of 10 Gbit/s PON vs WDM-PON," in *Optical Communication, 2009. ECOC'09. 35th European Conference on*, 2009, pp. 1-2.
[91] J. Segarra, V. Sales, and J. Prat, "GPON scheduling disciplines under multi-service bursty traffic and long-reach approach," in *2010 12th International Conference on Transparent Optical Networks*, 2010, pp. 1-6.
[92] I. Cale, A. Salihovic, and M. Ivekovic, "Gigabit passive optical network-GPON," in *Information Technology Interfaces, 2007. ITI 2007. 29th International Conference on*, 2007, pp. 679-684.
[93] O. Marmur and E. Shraga, "GPON: the next big thing in optical access networks," in *Asia-Pacific Optical and Wireless Communications*, 2004, pp. 199-209.
[94] "Gigabit-capable passive optical networks (G-PON): Transmission convergence layer specification", ITU-T G.984.3, 2014, ed.
[95] G. Kramer, "The Problem of Upstream Traffic Synchronization in Passive Optical Networks"," 1999.
[96] M. Radivojević and P. Matavulj, "PON Evolution," in *The Emerging WDM EPON*, ed: Springer, 2017, pp. 67-99.
[97] X.-Z. Qiu, P. Ossieur, J. Bauwelinck, Y. Yi, D. Verhulst, J. Vandewege, *et al.*, "Development of GPON upstream physical-media-dependent prototypes," *Journal of Lightwave Technology,* vol. 22, p. 2498, 2004.
[98] G. Keiser, *FTTX concepts and applications* vol. 91: John Wiley & Sons, 2006.
[99] K. Fouli and M. Maier, "OCDMA and Optical Coding: Principles, Applications, and Challenges [Topics in Optical Communications]," *Communications Magazine, IEEE,* vol. 45, pp. 27-34, 2007.
[100] A. Sayed, L. Jolly, and P. Khot, "Analysis of effect of MAI on an OCDMA system," in *International Conference and Workshop on Emerging Trends in Technology*, 2014, p. 39.
[101] R. C. S. CHAUHAN, "DESIGN OF UNIPOLAR (OPTICAL) ORTHOGONAL CODES AND THEIR MAXIMAL CLIQUE SETS," UTTAR PRADESH TECHNICAL UNIVERSITY, 2015.
[102] S. Han, "Optical CDMA with Optical Orthogonal Code," *Multiuser Wireless Communication (EE381K) Class Project, Fall,* 2002.
[103] H. Abbas and M. Gregory, "OCDM network implementation of 1-D OOC and passive correlation receiver," in *ICAIET 2014*, 2014, pp. 311-318.
[104] L. R. Chen, "Technologies for hybrid wavelength/time optical CDMA transmission," in *Electrical and Computer Engineering, 2001. Canadian Conference on*, 2001, pp. 435-440.
[105] M. E. Marhic, "Trends in optical CDMA," *Proc. Multigigabit Fiber Communication (SPIE),* vol. 1787, pp. 80-98, 1992.
[106] I. Andonovic, L. Tancevski, M. Shabeer, and L. Bazgaloski, "Incoherent all-optical code recognition with balanced detection," *Journal of lightwave technology,* vol. 12, pp. 1073-1080, 1994.
[107] P. Prucnal, M. Santoro, and T. Fan, "Spread spectrum fiber-optic local area network

using optical processing," *Journal of Lightwave Technology,* vol. 4, pp. 547-554, 1986.
[108] F. Liu, M. Karbassian, and H. Ghafouri-Shiraz, "Novel family of prime codes for synchronous optical CDMA," *Optical and quantum electronics,* vol. 39, pp. 79-90, 2007.
[109] J. F. A. Rida, A. Bhardwaj, and A. Jaiswal, "Design optimization of optical communication systems using carbon nanotubes (CNTs) based on optical code division multiple access (OCDMA)," *International Journal of Computer Science and Network Security (IJCSNS),* vol. 14, p. 102, 2014.
[110] H. M. Shalaby, "Cochannel interference reduction in optical PPM-CDMA systems," *IEEE transactions on communications,* vol. 46, pp. 799-805, 1998.
[111] M. A. Esmail and H. Fathallah, "Current and next-generation passive optical networks monitoring solution," in *8th International Conference on High-capacity Optical Networks and Emerging Technologies*, 2011, pp. 334-338.
[112] H. Fathallah and L. A. Rusch, "Code-division multiplexing for in-service out-of-band monitoring of live FTTH-PONs," *Journal of Optical Networking,* vol. 6, pp. 819-829, 2007.
[113] M. Thollabandi, X. Cheng, and Y.-K. Yeo, "Encoded probing technique for detection of the faulty branch in TDM-PON," *IEEE Photonics Technology Letters,* vol. 24, pp. 1610-1613, 2012.
[114] H. Fathallah, M. M. Rad, and L. A. Rusch, "PON monitoring: periodic encoders with low capital and operational cost," *IEEE Photon. Technol. Lett,* vol. 20, pp. 2039-2041, 2008.
[115] M. M. Rad, H. A. Fathallah, M. Maier, L. A. Rusch, and M. Uysal, "A novel pulse-positioned coding scheme for fiber fault monitoring of a PON," *IEEE communications letters,* vol. 15, pp. 1007-1009, 2011.
[116] M. A. Esmail and H. Fathallah, "Novel coding for PON fault identification," *IEEE communications letters,* vol. 15, pp. 677-679, 2011.
[117] M. P. Fernández, P. A. C. Caso, and L. A. B. Rossini, "Design and performance evalauation of an optical coding scheme for PON monitoring," in *Information Processing and Control (RPIC), 2015 XVI Workshop on*, 2015, pp. 1-6.
[118] X. Zhou, F. Zhang, and X. Sun, "Centralized PON monitoring scheme based on optical coding," *IEEE Photonics Technology Letters,* vol. 25, pp. 795-797, 2013.
[119] X. Zhang, S. Chen, F. Lu, X. Zhao, M. Zhu, and X. Sun, "Remote Coding Scheme Using Cascaded Encoder for PON Monitoring," *IEEE Photonics Technology Letters,* vol. 28, pp. 2183-2186, 2016.
[120] M. M. Rad, H. Fathallah, and L. A. Rusch, "Beat Noise Mitigation via Hybrid 1-D/2-D-OCDM: Application to Monitoring of High Capacity PONs," in *Optical Fiber Communication Conference*, 2008, p. OMR7.
[121] T. Tsujioka and H. Yamamoto, "Design of optical orthogonal codes with variable chip rate for flexible optical CDMA systems," in *Advanced Communication Technology (ICACT), 2012 14th International Conference on*, 2012, pp. 1156-1161.
[122] J. A. Salehi, "Code division multiple-access techniques in optical fiber networks. I. Fundamental principles," *IEEE transactions on communications,* vol. 37, pp. 824-833, 1989.
[123] B. Skubic, D. Betou, E. In, T. Ayhan, and S. Dahlfort, "Energy-efficient next-generation optical access networks," *Communications Magazine, IEEE,* vol. 50, pp. 122-127, 2012.
[124] S. De Lausnay, L. De Strycker, J.-P. Goemaere, N. Stevens, and B. Nauwelaers, "Optical CDMA codes for an indoor localization system using VLC," in *Optical*

Wireless Communications (IWOW), 2014 3rd International Workshop in, 2014, pp. 50-54.

[125] J. O. Anaman and S. Prince, "Correlation properties and performance evaluation of 1-dimensional OOC's for OCDMA," in *Devices, Circuits and Systems (ICDCS), 2012 International Conference on*, 2012, pp. 167-171.

[126] G.-C. Yang and W. C. Kwong, "Performance analysis of optical CDMA with prime codes," *Electronics Letters,* vol. 31, pp. 569-570, 1995.

[127] W. C. Kwong, P. A. Perrier, and P. R. Prucnal, "Performance comparison of asynchronous and synchronous code-division multiple-access techniques for fiber-optic local area networks," *IEEE transactions on communications,* vol. 39, pp. 1625-1634, 1991.

[128] M. H. Zoualfaghari, "Co-channel Interference Reduction in
Optical Code Division Multiple Access Systems," School of electronic, electrical and computer engineering, University of Birmingham, 2015.

[129] "Prime Codes with Applications to CDMA Wireless and Optical Networks.(Book Review)(Brief Article)," vol. 26, ed, 2002, p. 188.

[130] M. M. Karbassian and H. Ghafouri-Shiraz, "Capacity enhancement in synchronous optical overlapping PPM-CDMA network by a novel spreading code," in *Global Telecommunications Conference, 2007. GLOBECOM'07. IEEE*, 2007, pp. 2407-2411.

[131] M. Y. Liu and H. W. Tsao, "Cochannel interference cancellation via employing a reference correlator for synchronous optical CDMA systems," *Microwave and Optical Technology Letters,* vol. 25, pp. 390-392, 2000.

[132] M. M. Karbassian and H. Ghafouri-Shiraz, "Fresh prime codes evaluation for synchronous PPM and OPPM signaling for optical CDMA networks," *Journal of Lightwave Technology,* vol. 25, pp. 1422-1430, 2007.

[133] M. M. Karbassian and F. Kueppers, "OCDMA code utilization increase: capacity and spectral efficiency enrichment," in *Global Telecommunications Conference (GLOBECOM 2010), 2010 IEEE*, 2010, pp. 1-5.

[134] M. M. Karbassian and F. Küppers, "Enhancing spectral efficiency and capacity in synchronous OCDMA by transposed-MPC," *Optical Switching and Networking,* vol. 9, pp. 130-137, 2012.

[135] M. M. Karbassian and F. Kueppers, "Synchronous optical CDMA networks capacity increase using transposed modified prime codes," *Journal of Lightwave Technology,* vol. 28, pp. 2603-2610, 2010.

[136] Q. Jin, M. M. Karbassian, and H. Ghafouri-Shiraz, "Energy-Efficient High-Capacity Optical CDMA Networks by Low-Weight Large Code-Set MPC," *Lightwave Technology, Journal of,* vol. 30, pp. 2876-2883, 2012.

[137] I. Garrett, "Towards the fundamental limits of optical-fiber communications," *Journal of Lightwave Technology,* vol. 1, pp. 131-138, 1983.

[138] I. Kaminow and T. Koch, *Optical Fiber Telecommunications III*, 1997.

[139] E. Wong and K.-L. Lee, "Automatic protection, restoration, and survivability of long-reach passive optical networks," in *Communications (ICC), 2011 IEEE International Conference on*, 2011, pp. 1-6.

[140] J. Chen, "Reducing the impact of failures in Next-Generation Optical Access Networks," in *Asia Communications and Photonics Conference*, 2012.

[141] F. J. Effenberger, H. Ichibangase, and H. Yamashita, "Advances in broadband passive optical networking technologies," *IEEE Communications Magazine,* vol. 39, pp. 118-124, 2001.

[142] T. Koonen, "Fiber to the Home/Fiber to the Premises: What, Where, and When?," *Proceedings of the IEEE,* vol. 94, pp. 911-934, 2006.

[143] N. Ghazisaidi, M. Scheutzow, and M. Maier, "Survivability Analysis of Next-Generation Passive Optical Networks and Fiber-Wireless Access Networks," *IEEE Transactions on Reliability,* vol. 60, pp. 479-492, 2011.
[144] (11/08/2017). Available: https://www.cozlink.com
[145] Available: http://www.vpiphotonics.com/Tools/OpticalSystems
[146] E. H. Miguel, "Fiber-based Orthogonal Frequency Division Multiplexing Transmission Systems," 2010.

Appendix A1. Simulation of Four ONUs

A1.1. Simulation parameters of four ONUs

Category	Module	Parameter	Value
Global		Time window	296/1e9
		SampleModeCentreFrequency	184.5e12
		Code-length (L)	24
		Time-Chip (T_c)	1 ns
		T_{Δ}	50 ns
		T_{TDM}	24 ns
		Burst-Duration (T_b)	$L.T_c$ ns
Code-words		$C1$	0 [10] 1 0 [10] 1 0 [2]
		$C2$	0 [7] 1 0 [10] 1 0 [5]
		$C3$	0 [8] 1 0 [10] 1 0 [4]
		$C4$	0 [9] 1 0 [10] 1 0 [3]
		Td	0 [50]
Fibers	Feeder Fiber	ReferenceFrequency	184.5e12
		Length	10 km
		GroupRefractiveIndex	1.47
	Drop fiber 1	ReferenceFrequency	184.5e12
		Length	500 m
		GroupRefractiveIndex	1.47
	Drop fiber 2	ReferenceFrequency	184.5e12
		Length	505 m
		GroupRefractiveIndex	1.47
	Drop fiber 3	ReferenceFrequency	184.5e12
		Length	510 m
		GroupRefractiveIndex	1.47
	Drop fiber 4	ReferenceFrequency	184.5e12

		Length	515 m
		GroupRefractiveIndex	1.47
Monitoring Pulse generator	General	EmissionFrequency	184.5e12
		ModulationType	NRZ
	PRBS	PRBS_Type	CodeWord
		CodeWord	1 0 [295]
Encoding	Encoder 1	SignalDelay 1	10 x T_c
		SignalDelay 2	21 x T_c
	$T_{\Delta 1}$	SignalDelay	1x T_Δ
	Encoder 2	SignalDelay 1	7 x T_c
		SignalDelay 2	18 x T_c
	$T_{\Delta 2}$	SignalDelay	2x T_Δ + T_{TDM}
	Encoder 3	SignalDelay 1	8 x T_c
		SignalDelay 2	19 x T_c
	$T_{\Delta 3}$	SignalDelay	3x T_Δ+ 2xT_{TDM}
	Encoder 4	SignalDelay 1	9 x T_c
		SignalDelay 2	20 x T_c
	$T_{\Delta 4}$	SignalDelay	4x T_Δ+ 3 x T_{TDM}
Reference signal	*PRBS*	CodeWord	Td c1 Td c2 Td c3 Td c4

Appendix A2. A Splitting Ratio of 32

A2.1. Simulation parameters of 32 ONUs

Category	Module	Parameter	Value
Global		Time window	32x (50+L) / BitRateDefault
		BitRateDefault	1e9
		SampleModeCentreFrequency	184.5e12
		Code-length (L)	24
		Time-Chip (T_c)	1 ns
		T_Δ	50 ns
		T_{TDM}	24 ns

		Burst-Duration (T_b)	$L.T_c$ ns
Code-words		*w*	0 [50]
		C1	0 [6] 1 0 [16] 1
		C2	0 [7] 1 0 [10] 1 0 [5]
		C3	0 [8] 1 0 [10] 1 0 [4]
		C4	0 [9] 1 0 [10] 1 0 [3]
		C5	0 [10] 1 0 [10] 1 0 [2]
		C6	0 [11] 1 0 [10] 1 0 [1]
		C7	1 0 [11] 1 0 [11]
		C8	0 [1] 1 0 [11] 1 0 [10]
		C9	0 [2] 1 0 [11] 1 0 [9]
		C10	0 [3] 1 0 [11] 1 0 [8]
		C11	0 [4] 1 0 [11] 1 0 [7]
		C12	0 [5] 1 0 [11] 1 0 [6]
		C13	0 [7] 1 0 [11] 1 0 [4]
		C14	0 [8] 1 0 [11] 1 0 [3]
		C15	0 [9] 1 0 [11] 1 0 [2]
		C16	0 [10] 1 0 [11] 1 0
		C17	0 [11] 1 0 [11] 1
		C18	0 [6] 1 0 [11] 1 0 [5]
		C19	1 0 [13] 1 0 [9]
		C20	0 [1] 1 0 [13] 1 0 [8]
		C21	0 [2] 1 0 [13] 1 0 [7]
		C22	0 [3] 1 0 [13] 1 0 [6]
		C23	0 [4] 1 0 [7] 1 0 [11]
		C24	0 [5] 1 0 [7] 1 0 [10]
		C25	0 [8] 1 0 [9] 1 0 [5]
		C26	0 [9] 1 0 [9] 1 0 [4]
		C27	0 [10] 1 0 [9] 1 0 [3]
		C28	0 [11] 1 0 [9] 1 0 [2]
		C29	0 [6] 1 0 [15] 1 0 [1]
		C30	0 [7] 1 0 [15] 1
		C31	1 0 [12] 1 0 [10]
		C32	0 1 0 [12] 1 0 [9]
Fibers	Feeder Fiber	ReferenceFrequency	184.5e12
		Length	10 km
		GroupRefractiveIndex	1.47
	Drop fibers	ReferenceFrequency	184.5e12
		Length	L1= 500 m Increases by 5 m – L32 = 655 m

		GroupRefractiveIndex	1.47
Monitoring Pulse generator	General	EmissionFrequency	184.5e12
		ModulationType	NRZ
	PRBS	PRBS_Type	CodeWord
		CodeWord	1 0 [2368]
Encoders x T_c	Encoder 1	Signal Delay1	6
		Signal Delay 2	23
	Encoder 2	Signal Delay1	7
		Signal Delay 2	18
	Encoder 3	Signal Delay1	8
		Signal Delay 2	19
	Encoder 4	Signal Delay1	9
		Signal Delay 2	20
	Encoder 5	Signal Delay1	10
		Signal Delay 2	21
	Encoder 6	Signal Delay1	1
		Signal Delay 2	13
	Encoder 7	Signal Delay1	2
		Signal Delay 2	14
	Encoder 8	Signal Delay1	3
		Signal Delay 2	15
	Encoder 9	Signal Delay1	4
		Signal Delay 2	16
	Encoder 10	Signal Delay1	5
		Signal Delay 2	17
	Encoder 11	Signal Delay1	7
		Signal Delay 2	19
	Encoder 12	Signal Delay1	8
		Signal Delay 2	20
	Encoder 13	Signal Delay1	9
		Signal Delay 2	21
	Encoder 14	Signal Delay1	10
		Signal Delay 2	22
	Encoder 15	Signal Delay1	11
		Signal Delay 2	23
	Encoder 16	Signal Delay1	6
		Signal Delay 2	18
	Encoder 17	Signal Delay1	0
		Signal Delay 2	14
	Encoder 18	Signal Delay1	1

		Signal Delay 2	15
	Encoder 19	Signal Delay1	2
		Signal Delay 2	16
	Encoder 20	Signal Delay1	3
		Signal Delay 2	17
	Encoder 21	Signal Delay1	4
		Signal Delay 2	12
	Encoder 22	Signal Delay1	5
		Signal Delay 2	13
	Encoder 23	Signal Delay1	8
		Signal Delay 2	18
	Encoder 24	Signal Delay1	9
		Signal Delay 2	19
	Encoder 25	Signal Delay1	10
		Signal Delay 2	20
	Encoder 26	Signal Delay1	11
		Signal Delay 2	21
	Encoder 27	Signal Delay1	6
		Signal Delay 2	22
	Encoder 28	Signal Delay1	7
		Signal Delay 2	23
	Encoder 29	Signal Delay1	0
		Signal Delay 2	13
	Encoder 30	Signal Delay1	1
		Signal Delay 2	14
	Encoder 31	Signal Delay1	2
		Signal Delay 2	15
	Encoder 32	Signal Delay1	3
		Signal Delay 2	16
Reference signal	*PRBS*	CodeWord	w c1 w c2 w c3 w c4 w c5 w c6 w c7 w c8 w c9 w c10 w c11 w c1 w c13 w c14 w c15 w c16 w c17 w c18 w c19 w c20 w c21 w c22 w c23 w c24 w c25 w c26 w c27 w c28 w c29 w c30 w c31 w c32

A2.2. Sub-pulses times before and after delay

Encoder	Signal Delay	Time (ns)
Encoder 1	Signal Delay1	56

	Signal Delay 2	73
Encoder 2	Signal Delay1	131
	Signal Delay 2	142
Encoder 3	Signal Delay1	206
	Signal Delay 2	217
Encoder 4	Signal Delay1	281
	Signal Delay 2	292
Encoder 5	Signal Delay1	356
	Signal Delay 2	367
Encoder 6	Signal Delay1	421
	Signal Delay 2	433
Encoder 7	Signal Delay1	496
	Signal Delay 2	508
Encoder 8	Signal Delay1	571
	Signal Delay 2	583
Encoder 9	Signal Delay1	646
	Signal Delay 2	658
Encoder 10	Signal Delay1	721
	Signal Delay 2	733
Encoder 11	Signal Delay1	797
	Signal Delay 2	809
Encoder 12	Signal Delay1	872
	Signal Delay 2	884
Encoder 13	Signal Delay1	947
	Signal Delay 2	959
Encoder 14	Signal Delay1	1022
	Signal Delay 2	1034
Encoder 15	Signal Delay1	1097
	Signal Delay 2	1109
Encoder 16	Signal Delay1	1166
	Signal Delay 2	1178
Encoder 17	Signal Delay1	1234
	Signal Delay 2	1248
Encoder 18	Signal Delay1	1309
	Signal Delay 2	1323
Encoder 19	Signal Delay1	1384
	Signal Delay 2	1398
Encoder 20	Signal Delay1	1459
	Signal Delay 2	1473

Encoder 21	Signal Delay1	1534
	Signal Delay 2	1542
Encoder 22	Signal Delay1	1609
	Signal Delay 2	1617
Encoder 23	Signal Delay1	1686
	Signal Delay 2	1696
Encoder 24	Signal Delay1	1761
	Signal Delay 2	1771
Encoder 25	Signal Delay1	1836
	Signal Delay 2	1846
Encoder 26	Signal Delay1	1911
	Signal Delay 2	1921
Encoder 27	Signal Delay1	1980
	Signal Delay 2	1996
Encoder 28	Signal Delay1	2055
	Signal Delay 2	2071
Encoder 29	Signal Delay1	2122
	Signal Delay 2	2135
Encoder 30	Signal Delay1	2197
	Signal Delay 2	2210
Encoder 31	Signal Delay1	2272
	Signal Delay 2	2285
Encoder 32	Signal Delay1	2347
	Signal Delay 2	2360

Appendix A3. A Splitting Ratio of 64

A3.1. Simulation parameters of 64 ONUs

Category	Module	Parameter	Value
Global		Time window	64 x (50+*L*)/ BitRateDefault
		BitRateDefault	1e9
		SampleModeCentreFrequency	184.5e12
		Code-length (*L*)	60
		Time-Chip (*Tc*)	1 ns
		T_{Δ}	50 ns
		T_{TDM}	60 ns
		Burst-Duration (*Tb*)	*L.Tc* ns
Code-words		***w***	0 [50]
		C1	0 [11] 1 0 [19] 1 0 [18] 1 0 [9]

	C2	0 [12] 1 0 [19] 1 0 [18] 1 0 [8]
	C3	0 [13] 1 0 [19] 1 0 [18] 1 0 [7]
	C4	0 [14] 1 0 [19] 1 0 [18] 1 0 [6]
	C5	0 [15] 1 0 [19] 1 0 [18] 1 0 [5]
	C6	0 [16] 1 0 [19] 1 0 [18] 1 0 [4]
	C7	0 [17] 1 0 [19] 1 0 [18] 1 0 [3]
	C8	0 [18] 1 0 [19] 1 0 [18] 1 0 [2]
	C9	0 [19] 1 0 [19] 1 0 [18] 1 0 [1]
	C10	0 [1] 1 0 [19] 1 0 [19] 1 0 [18]
	C11	0 [2] 1 0 [19] 1 0 [19] 1 0 [17]
	C12	0 [3] 1 0 [19] 1 0 [19] 1 0 [16]
	C13	0 [4] 1 0 [19] 1 0 [19] 1 0 [15]
	C14	0 [5] 1 0 [19] 1 0 [19] 1 0 [14]
	C15	0 [6] 1 0 [19] 1 0 [19] 1 0 [13]
	C16	0 [7] 1 0 [19] 1 0 [19] 1 0 [12]
	C17	0 [8] 1 0 [19] 1 0 [19] 1 0 [11]
	C18	0 [9] 1 0 [19] 1 0 [19] 1 0 [10]
	C19	0 [11] 1 0 [21] 1 0 [19] 1 0 [6]
	C20	0 [12] 1 0 [21] 1 0 [19] 1 0 [5]
	C21	0 [13] 1 0 [21] 1 0 [19] 1 0 [4]
	C22	0 [14] 1 0 [21] 1 0 [19] 1 0 [3]
	C23	0 [15] 1 0 [21] 1 0 [19] 1 0 [2]
	C24	0 [16] 1 0 [21] 1 0 [19] 1 0 [1]
	C25	0 [18] 1 0 [11] 1 0 [19] 1 0 [9]
	C26	0 [19] 1 0 [11] 1 0 [19] 1 0 [8]
	C27	0 [10] 1 0 [21] 1 0 [19] 1 0 [7]
	C28	0 [1] 1 0 [21] 1 0 [21] 1 0 [14]
	C29	0 [2] 1 0 [21] 1 0 [21] 1 0 [13]
	C30	0 [3] 1 0 [21] 1 0 [21] 1 0 [12]
	C31	0 [4] 1 0 [21] 1 0 [21] 1 0 [11]
	C32	0 [5] 1 0 [21] 1 0 [21] 1 0 [10]
	C33	0 [6] 1 0 [21] 1 0 [11] 1 0 [19]
	C34	0 [7] 1 0 [21] 1 0 [11] 1 0 [18]
	C35	0 [8] 1 0 [11] 1 0 [21] 1 0 [17]
	C36	0 [9] 1 0 [11] 1 0 [21] 1 0 [16]
	C37	0 [12] 1 0 [18] 1 0 [20] 1 0 [7]
	C38	0 [13] 1 0 [18] 1 0 [20] 1 0 [6]
	C39	0 [14] 1 0 [18] 1 0 [20] 1 0 [5]
	C40	0 [15] 1 0 [18] 1 0 [20] 1 0 [4]
	C41	0 [16] 1 0 [18] 1 0 [20] 1 0 [3]
	C42	0 [17] 1 0 [18] 1 0 [20] 1 0 [2]

		C43	0 [18] 1 0 [18] 1 0 [20] 1 0 [1]
		C44	0 [10] 1 0 [28] 1 0 [10] 1 0 [9]
		C45	0 [11] 1 0 [18] 1 0 [20] 1 0 [8]
		C46	0 [1] 1 0 [23] 1 0 [18] 1 0 [15]
		C47	0 [2] 1 0 [23] 1 0 [18] 1 0 [14]
		C48	0 [3] 1 0 [23] 1 0 [18] 1 0 [13]
		C49	0 [4] 1 0 [23] 1 0 [18] 1 0 [12]
		C50	0 [5] 1 0 [23] 1 0 [18] 1 0 [11]
		C51	0 [6] 1 0 [13] 1 0 [28] 1 0 [10]
		C52	0 [7] 1 0 [13] 1 0 [18] 1 0 [19]
		C53	0 [8] 1 0 [13] 1 0 [18] 1 0 [18]
		C54	0 [9] 1 0 [13] 1 0 [18] 1 0 [17]
		C55	0 [13] 1 0 [20] 1 0 [16] 1 0 [8]
		C56	0 [14] 1 0 [20] 1 0 [16] 1 0 [7]
		C57	0 [15] 1 0 [20] 1 0 [16] 1 0 [6]
		C58	0 [16] 1 0 [20] 1 0 [16] 1 0 [5]
		C59	0 [17] 1 0 [20] 1 0 [16] 1 0 [4]
		C60	0 [18] 1 0 [20] 1 0 [16] 1 0 [3]
		C61	0 [19] 1 0 [10] 1 0 [26] 1 0 [2]
		C62	0 [10] 1 0 [20] 1 0 [26] 1 0 [1]
		C63	0 [12] 1 0 [20] 1 0 [16] 1 0 [9]
		C64	0 [1] 1 0 [20] 1 0 [20] 1 0 [16]
Fibers	Feeder Fiber	ReferenceFrequency	184.5e12
		Length	10 km
		GroupRefractiveIndex	1.47
	Drop fibers	ReferenceFrequency	184.5e12
		Length	$L1$= 500 m Increases by 5 m – $L64$ = 815 m
Monitoring Pulse generator	General	EmissionFrequency	184.5e12
		ModulationType	NRZ
	PRBS	PRBS_Type	CodeWord
		CodeWord	1 0 [7039]
Encoding x Tc	Encoder 1	Signal Delay1	11
		Signal Delay 2	31
		Signal Delay 3	50
	Encoder 2	Signal Delay1	12
		Signal Delay 2	32
		Signal Delay 3	51
	Encoder 3	Signal Delay1	13
		Signal Delay 2	33

		Signal Delay 3	52
	Encoder 4	Signal Delay1	14
		Signal Delay 2	34
		Signal Delay 3	53
	Encoder 5	Signal Delay1	15
		Signal Delay 2	35
		Signal Delay 3	54
	Encoder 6	Signal Delay1	16
		Signal Delay 2	36
		Signal Delay 3	55
	Encoder 7	Signal Delay1	17
		Signal Delay 2	37
		Signal Delay 3	56
	Encoder 8	Signal Delay1	18
		Signal Delay 2	38
		Signal Delay 3	57
	Encoder 9	Signal Delay1	19
		Signal Delay 2	39
		Signal Delay 3	58
	Encoder 10	Signal Delay1	1
		Signal Delay 2	22
		Signal Delay 3	41
	Encoder 11	Signal Delay1	2
		Signal Delay 2	23
		Signal Delay 3	42
	Encoder 12	Signal Delay1	3
		Signal Delay 2	24
		Signal Delay 3	43
	Encoder 13	Signal Delay1	4
		Signal Delay 2	25
		Signal Delay 3	44
	Encoder 14	Signal Delay1	5
		Signal Delay 2	26
		Signal Delay 3	45
	Encoder 15	Signal Delay1	6
		Signal Delay 2	27
		Signal Delay 3	46
	Encoder 16	Signal Delay1	7
		Signal Delay 2	28
		Signal Delay 3	47
	Encoder 17	Signal Delay1	8

		Signal Delay 2	29
		Signal Delay 3	348
	Encoder 18	Signal Delay1	9
		Signal Delay 2	30
		Signal Delay 3	49
	Encoder 19	Signal Delay1	11
		Signal Delay 2	34
		Signal Delay 3	53
	Encoder 20	Signal Delay1	12
		Signal Delay 2	35
		Signal Delay 3	54
	Encoder 21	Signal Delay1	13
		Signal Delay 2	36
		Signal Delay 3	55
	Encoder 22	Signal Delay1	14
		Signal Delay 2	37
		Signal Delay 3	56
	Encoder 23	Signal Delay1	15
		Signal Delay 2	38
		Signal Delay 3	57
	Encoder 24	Signal Delay1	16
		Signal Delay 2	39
		Signal Delay 3	58
	Encoder 25	Signal Delay1	18
		Signal Delay 2	30
		Signal Delay 3	50
	Encoder 26	Signal Delay1	19
		Signal Delay 2	31
		Signal Delay 3	51
	Encoder 27	Signal Delay1	10
		Signal Delay 2	32
		Signal Delay 3	52
	Encoder 28	Signal Delay1	1
		Signal Delay 2	23
		Signal Delay 3	45
	Encoder 29	Signal Delay1	2
		Signal Delay 2	24
		Signal Delay 3	46
	Encoder 30	Signal Delay1	3
		Signal Delay 2	25
		Signal Delay 3	47

	Encoder 31	Signal Delay1	4
		Signal Delay 2	26
		Signal Delay 3	48
	Encoder 32	Signal Delay1	5
		Signal Delay 2	27
		Signal Delay 3	49
	Encoder 33	Signal Delay1	6
		Signal Delay 2	28
		Signal Delay 3	40
	Encoder 34	Signal Delay1	7
		Signal Delay 2	29
		Signal Delay 3	41
	Encoder 35	Signal Delay1	8
		Signal Delay 2	20
		Signal Delay 3	42
	Encoder 36	Signal Delay1	9
		Signal Delay 2	21
		Signal Delay 3	43
	Encoder 37	Signal Delay1	12
		Signal Delay 2	31
		Signal Delay 3	52
	Encoder 38	Signal Delay1	13
		Signal Delay 2	32
		Signal Delay 3	53
	Encoder 39	Signal Delay1	14
		Signal Delay 2	33
		Signal Delay 3	54
	Encoder 40	Signal Delay1	15
		Signal Delay 2	34
		Signal Delay 3	55
	Encoder 41	Signal Delay1	16
		Signal Delay 2	35
		Signal Delay 3	56
	Encoder 42	Signal Delay1	17
		Signal Delay 2	36
		Signal Delay 3	57
	Encoder 43	Signal Delay1	18
		Signal Delay 2	37
		Signal Delay 3	58
	Encoder 44	Signal Delay1	10
		Signal Delay 2	39

		Signal Delay 3	50
	Encoder 45	Signal Delay1	11
		Signal Delay 2	30
		Signal Delay 3	51
	Encoder 46	Signal Delay1	1
		Signal Delay 2	25
		Signal Delay 3	44
	Encoder 47	Signal Delay1	2
		Signal Delay 2	26
		Signal Delay 3	45
	Encoder 48	Signal Delay1	3
		Signal Delay 2	27
		Signal Delay 3	46
	Encoder 49	Signal Delay1	4
		Signal Delay 2	28
		Signal Delay 3	47
	Encoder 50	Signal Delay1	5
		Signal Delay 2	29
		Signal Delay 3	48
	Encoder 51	Signal Delay1	6
		Signal Delay 2	20
		Signal Delay 3	49
	Encoder 52	Signal Delay1	7
		Signal Delay 2	21
		Signal Delay 3	40
	Encoder 53	Signal Delay1	8
		Signal Delay 2	22
		Signal Delay 3	41
	Encoder 54	Signal Delay1	9
		Signal Delay 2	23
		Signal Delay 3	42
	Encoder 55	Signal Delay1	13
		Signal Delay 2	34
		Signal Delay 3	51
	Encoder 56	Signal Delay1	14
		Signal Delay 2	35
		Signal Delay 3	52
	Encoder 57	Signal Delay1	15
		Signal Delay 2	36
		Signal Delay 3	53
	Encoder 58	Signal Delay1	16

		Signal Delay 2	37
		Signal Delay 3	54
	Encoder 59	Signal Delay1	17
		Signal Delay 2	38
		Signal Delay 3	55
	Encoder 60	Signal Delay1	18
		Signal Delay 2	39
		Signal Delay 3	56
	Encoder 61	Signal Delay1	19
		Signal Delay 2	30
		Signal Delay 3	57
	Encoder 62	Signal Delay1	10
		Signal Delay 2	31
		Signal Delay 3	58
	Encoder 63	Signal Delay1	12
		Signal Delay 2	33
		Signal Delay 3	50
	Encoder 64	Signal Delay1	1
		Signal Delay 2	22
		Signal Delay 3	43
Reference signal	*PRBS*	CodeWord	0 [50] c1 w c2 w c3 w c4 w c5 w c6 w c7 w c8 w c9 w c10 w c11 w c1 w c13 w c14 w c15 w c16 w c17 w c18 w c19 w c20 w c21 w c22 w c23 w c24 w c25 w c26 w c27 w c28 w c29 w c30 w c31 w c32 w c33 w c34 w c35 w c36 w c37 w c38 w c39 w c40 w c41 w c42 w c43 w c44 w c45 w c46 w c47 w c48 w c49 w c50 w c51 w c52 w c53 w c54 w c55 w c56 w c57 w c58 w c59 w c60 w c61 w c62 w c63 w c64

A3.2. Binary codes for EG-nMPC, *P* = 5

Binary code-words					
0 0 0 0 0 0 0 0 0 0	1 0 0 0 0 0 0 0 0 0	0 0 0 0 0 0 0 0 0 0	1 0 0 0 0 0 0 0 0 0	0 0 0 0 0 0 0 0 0 0	0 0 0 0 0 0 0 0 0 1
0 0 0 0 0 0 0 0 0 0	0 1 0 0 0 0 0 0 0 0	0 0 0 0 0 0 0 0 0 0	0 1 0 0 0 0 0 0 0 0	0 0 0 0 0 0 0 0 0 0	1 0 0 0 0 0 0 0 0 0
0 0 0 0 0 0 0 0 0 0	0 0 1 0 0 0 0 0 0 0	0 0 0 0 0 0 0 0 0 0	0 0 1 0 0 0 0 0 0 0	0 0 0 0 0 0 0 0 0 0	0 1 0 0 0 0 0 0 0 0
0 0 0 0 0 0 0 0 0 0	0 0 0 1 0 0 0 0 0 0	0 0 0 0 0 0 0 0 0 0	0 0 0 1 0 0 0 0 0 0	0 0 0 0 0 0 0 0 0 0	0 0 1 0 0 0 0 0 0 0
0 0 0 0 0 0 0 0 0 0	0 0 0 0 1 0 0 0 0 0	0 0 0 0 0 0 0 0 0 0	0 0 0 0 1 0 0 0 0 0	0 0 0 0 0 0 0 0 0 0	0 0 0 1 0 0 0 0 0 0
0 0 0 0 0 0 0 0 0 0	0 0 0 0 0 1 0 0 0 0	0 0 0 0 0 0 0 0 0 0	0 0 0 0 0 1 0 0 0 0	0 0 0 0 0 0 0 0 0 0	0 0 0 0 1 0 0 0 0 0

0 0 0 0 0 0 0 0 0 0	0 0 0 0 0 0 1 0 0 0	0 0 0 0 0 0 0 0 0 0	0 0 0 0 0 0 1 0 0 0	0 0 0 0 0 0 0 0 0 0	0 0 0 0 0 1 0 0 0 0
0 0 0 0 0 0 0 0 0 0	0 0 0 0 0 0 0 1 0 0	0 0 0 0 0 0 0 0 0 0	0 0 0 0 0 0 0 1 0 0	0 0 0 0 0 0 0 0 0 0	0 0 0 0 0 0 1 0 0 0
0 0 0 0 0 0 0 0 0 0	0 0 0 0 0 0 0 0 1 0	0 0 0 0 0 0 0 0 0 0	0 0 0 0 0 0 0 0 1 0	0 0 0 0 0 0 0 0 0 0	0 0 0 0 0 0 0 1 0 0
0 0 0 0 0 0 0 0 0 0	0 0 0 0 0 0 0 0 0 1	0 0 0 0 0 0 0 0 0 0	0 0 0 0 0 0 0 0 0 1	0 0 0 0 0 0 0 0 0 0	0 0 0 0 0 0 0 0 1 0
1 0 0 0 0 0 0 0 0 0	0 0 0 0 0 0 0 0 0 0	1 0 0 0 0 0 0 0 0 0	0 0 0 0 0 0 0 0 0 0	1 0 0 0 0 0 0 0 0 0	0 0 0 0 0 0 0 0 0 0
0 1 0 0 0 0 0 0 0 0	0 0 0 0 0 0 0 0 0 0	0 1 0 0 0 0 0 0 0 0	0 0 0 0 0 0 0 0 0 0	0 1 0 0 0 0 0 0 0 0	0 0 0 0 0 0 0 0 0 0
0 0 1 0 0 0 0 0 0 0	0 0 0 0 0 0 0 0 0 0	0 0 1 0 0 0 0 0 0 0	0 0 0 0 0 0 0 0 0 0	0 0 1 0 0 0 0 0 0 0	0 0 0 0 0 0 0 0 0 0
0 0 0 1 0 0 0 0 0 0	0 0 0 0 0 0 0 0 0 0	0 0 0 1 0 0 0 0 0 0	0 0 0 0 0 0 0 0 0 0	0 0 0 1 0 0 0 0 0 0	0 0 0 0 0 0 0 0 0 0
0 0 0 0 1 0 0 0 0 0	0 0 0 0 0 0 0 0 0 0	0 0 0 0 1 0 0 0 0 0	0 0 0 0 0 0 0 0 0 0	0 0 0 0 1 0 0 0 0 0	0 0 0 0 0 0 0 0 0 0
0 0 0 0 0 1 0 0 0 0	0 0 0 0 0 0 0 0 0 0	0 0 0 0 0 1 0 0 0 0	0 0 0 0 0 0 0 0 0 0	0 0 0 0 0 1 0 0 0 0	0 0 0 0 0 0 0 0 0 0
0 0 0 0 0 0 1 0 0 0	0 0 0 0 0 0 0 0 0 0	0 0 0 0 0 0 1 0 0 0	0 0 0 0 0 0 0 0 0 0	0 0 0 0 0 0 1 0 0 0	0 0 0 0 0 0 0 0 0 0
0 0 0 0 0 0 0 1 0 0	0 0 0 0 0 0 0 0 0 0	0 0 0 0 0 0 0 1 0 0	0 0 0 0 0 0 0 0 0 0	0 0 0 0 0 0 0 1 0 0	0 0 0 0 0 0 0 0 0 0
0 0 0 0 0 0 0 0 1 0	0 0 0 0 0 0 0 0 0 0	0 0 0 0 0 0 0 0 1 0	0 0 0 0 0 0 0 0 0 0	0 0 0 0 0 0 0 0 1 0	0 0 0 0 0 0 0 0 0 0
0 0 0 0 0 0 0 0 0 1	0 0 0 0 0 0 0 0 0 0	0 0 0 0 0 0 0 0 0 1	0 0 0 0 0 0 0 0 0 0	0 0 0 0 0 0 0 0 0 1	0 0 0 0 0 0 0 0 0 0
0 0 0 0 0 0 0 0 0 0	0 1 0 0 0 0 0 0 0 0	0 0 0 0 0 0 0 0 0 0	0 0 0 1 0 0 0 0 0 0	0 0 0 0 0 0 0 0 0 0	0 0 0 1 0 0 0 0 0 0
0 0 0 0 0 0 0 0 0 0	0 0 1 0 0 0 0 0 0 0	0 0 0 0 0 0 0 0 0 0	0 0 0 0 1 0 0 0 0 0	0 0 0 0 0 0 0 0 0 0	0 0 0 0 1 0 0 0 0 0
0 0 0 0 0 0 0 0 0 0	0 0 0 1 0 0 0 0 0 0	0 0 0 0 0 0 0 0 0 0	0 0 0 0 0 1 0 0 0 0	0 0 0 0 0 0 0 0 0 0	0 0 0 0 0 1 0 0 0 0
0 0 0 0 0 0 0 0 0 0	0 0 0 0 1 0 0 0 0 0	0 0 0 0 0 0 0 0 0 0	0 0 0 0 0 0 1 0 0 0	0 0 0 0 0 0 0 0 0 0	0 0 0 0 0 0 1 0 0 0
0 0 0 0 0 0 0 0 0 0	0 0 0 0 0 1 0 0 0 0	0 0 0 0 0 0 0 0 0 0	0 0 0 0 0 0 0 1 0 0	0 0 0 0 0 0 0 0 0 0	0 0 0 0 0 0 0 1 0 0
0 0 0 0 0 0 0 0 0 0	0 0 0 0 0 0 1 0 0 0	0 0 0 0 0 0 0 0 0 0	0 0 0 0 0 0 0 0 1 0	0 0 0 0 0 0 0 0 0 0	0 0 0 0 0 0 0 0 1 0
0 0 0 0 0 0 0 0 0 0	0 0 0 0 0 0 0 1 0 0	0 0 0 0 0 0 0 0 0 0	0 0 0 0 0 0 0 0 0 1	0 0 0 0 0 0 0 0 0 0	0 0 0 0 0 0 0 0 0 1
0 0 0 0 0 0 0 0 0 0	0 0 0 0 0 0 0 0 1 0	0 0 0 0 0 0 0 0 0 0	1 0 0 0 0 0 0 0 0 0	0 0 0 0 0 0 0 0 0 0	1 0 0 0 0 0 0 0 0 0
0 0 0 0 0 0 0 0 0 0	0 0 0 0 0 0 0 0 0 1	0 0 0 0 0 0 0 0 0 0	0 1 0 0 0 0 0 0 0 0	0 0 0 0 0 0 0 0 0 0	0 1 0 0 0 0 0 0 0 0
0 0 0 0 0 0 0 0 0 0	1 0 0 0 0 0 0 0 0 0	0 0 0 0 0 0 0 0 0 0	0 0 1 0 0 0 0 0 0 0	0 0 0 0 0 0 0 0 0 0	0 0 1 0 0 0 0 0 0 0
1 0 0 0 0 0 0 0 0 0	0 0 0 0 0 0 0 0 0 0	0 0 1 0 0 0 0 0 0 0	0 0 0 0 0 0 0 0 0 0	0 0 0 0 1 0 0 0 0 0	0 0 0 0 0 0 0 0 0 0
0 1 0 0 0 0 0 0 0 0	0 0 0 0 0 0 0 0 0 0	0 0 0 1 0 0 0 0 0 0	0 0 0 0 0 0 0 0 0 0	0 0 0 0 0 1 0 0 0 0	0 0 0 0 0 0 0 0 0 0
0 0 1 0 0 0 0 0 0 0	0 0 0 0 0 0 0 0 0 0	0 0 0 0 1 0 0 0 0 0	0 0 0 0 0 0 0 0 0 0	0 0 0 0 0 0 1 0 0 0	0 0 0 0 0 0 0 0 0 0
0 0 0 1 0 0 0 0 0 0	0 0 0 0 0 0 0 0 0 0	0 0 0 0 0 1 0 0 0 0	0 0 0 0 0 0 0 0 0 0	0 0 0 0 0 0 0 1 0 0	0 0 0 0 0 0 0 0 0 0
0 0 0 0 1 0 0 0 0 0	0 0 0 0 0 0 0 0 0 0	0 0 0 0 0 0 1 0 0 0	0 0 0 0 0 0 0 0 0 0	0 0 0 0 0 0 0 0 1 0	0 0 0 0 0 0 0 0 0 0
0 0 0 0 0 1 0 0 0 0	0 0 0 0 0 0 0 0 0 0	0 0 0 0 0 0 0 1 0 0	0 0 0 0 0 0 0 0 0 0	0 0 0 0 0 0 0 0 0 1	0 0 0 0 0 0 0 0 0 0
0 0 0 0 0 0 1 0 0 0	0 0 0 0 0 0 0 0 0 0	0 0 0 0 0 0 0 0 1 0	0 0 0 0 0 0 0 0 0 0	1 0 0 0 0 0 0 0 0 0	0 0 0 0 0 0 0 0 0 0
0 0 0 0 0 0 0 1 0 0	0 0 0 0 0 0 0 0 0 0	0 0 0 0 0 0 0 0 0 1	0 0 0 0 0 0 0 0 0 0	0 1 0 0 0 0 0 0 0 0	0 0 0 0 0 0 0 0 0 0
0 0 0 0 0 0 0 0 1 0	0 0 0 0 0 0 0 0 0 0	1 0 0 0 0 0 0 0 0 0	0 0 0 0 0 0 0 0 0 0	0 0 1 0 0 0 0 0 0 0	0 0 0 0 0 0 0 0 0 0
0 0 0 0 0 0 0 0 0 1	0 0 0 0 0 0 0 0 0 0	0 1 0 0 0 0 0 0 0 0	0 0 0 0 0 0 0 0 0 0	0 0 0 1 0 0 0 0 0 0	0 0 0 0 0 0 0 0 0 0
0 0 0 0 0 0 0 0 0 0	0 0 1 0 0 0 0 0 0 0	0 0 0 0 0 0 0 0 0 0	0 1 0 0 0 0 0 0 0 0	0 0 0 0 0 0 0 0 0 0	0 0 1 0 0 0 0 0 0 0
0 0 0 0 0 0 0 0 0 0	0 0 0 1 0 0 0 0 0 0	0 0 0 0 0 0 0 0 0 0	0 0 1 0 0 0 0 0 0 0	0 0 0 0 0 0 0 0 0 0	0 0 0 1 0 0 0 0 0 0
0 0 0 0 0 0 0 0 0 0	0 0 0 0 1 0 0 0 0 0	0 0 0 0 0 0 0 0 0 0	0 0 0 1 0 0 0 0 0 0	0 0 0 0 0 0 0 0 0 0	0 0 0 0 1 0 0 0 0 0
0 0 0 0 0 0 0 0 0 0	0 0 0 0 0 1 0 0 0 0	0 0 0 0 0 0 0 0 0 0	0 0 0 0 1 0 0 0 0 0	0 0 0 0 0 0 0 0 0 0	0 0 0 0 0 1 0 0 0 0
0 0 0 0 0 0 0 0 0 0	0 0 0 0 0 0 1 0 0 0	0 0 0 0 0 0 0 0 0 0	0 0 0 0 0 1 0 0 0 0	0 0 0 0 0 0 0 0 0 0	0 0 0 0 0 0 1 0 0 0
0 0 0 0 0 0 0 0 0 0	0 0 0 0 0 0 0 1 0 0	0 0 0 0 0 0 0 0 0 0	0 0 0 0 0 0 1 0 0 0	0 0 0 0 0 0 0 0 0 0	0 0 0 0 0 0 0 1 0 0
0 0 0 0 0 0 0 0 0 0	0 0 0 0 0 0 0 0 1 0	0 0 0 0 0 0 0 0 0 0	0 0 0 0 0 0 0 1 0 0	0 0 0 0 0 0 0 0 0 0	0 0 0 0 0 0 0 0 1 0
0 0 0 0 0 0 0 0 0 0	0 0 0 0 0 0 0 0 0 1	0 0 0 0 0 0 0 0 0 0	0 0 0 0 0 0 0 0 1 0	0 0 0 0 0 0 0 0 0 0	0 0 0 0 0 0 0 0 0 1
0 0 0 0 0 0 0 0 0 0	1 0 0 0 0 0 0 0 0 0	0 0 0 0 0 0 0 0 0 0	0 0 0 0 0 0 0 0 0 1	0 0 0 0 0 0 0 0 0 0	1 0 0 0 0 0 0 0 0 0

0000000000	0100000000	0000000000	1000000000	0000000000	0100000000
1000000000	0000000000	0000100000	0000000000	0001000000	0000000000
0100000000	0000000000	0000010000	0000000000	0000100000	0000000000
0010000000	0000000000	0000001000	0000000000	0000010000	0000000000
0001000000	0000000000	0000000100	0000000000	0000001000	0000000000
0000100000	0000000000	0000000010	0000000000	0000000100	0000000000
0000010000	0000000000	0000000001	0000000000	0000000010	0000000000
0000001000	0000000000	1000000000	0000000000	0000000001	0000000000
0000000100	0000000000	0100000000	0000000000	1000000000	0000000000
0000000010	0000000000	0010000000	0000000000	0100000000	0000000000
0000000001	0000000000	0001000000	0000000000	0010000000	0000000000
0000000000	0001000000	0000000000	0000100000	0000000000	0100000000
0000000000	0000100000	0000000000	0000010000	0000000000	0010000000
0000000000	0000010000	0000000000	0000001000	0000000000	0001000000
0000000000	0000001000	0000000000	0000000100	0000000000	0000100000
0000000000	0000000100	0000000000	0000000010	0000000000	0000010000
0000000000	0000000010	0000000000	0000000001	0000000000	0000001000
0000000000	0000000001	0000000000	1000000000	0000000000	0000000100
0000000000	1000000000	0000000000	0100000000	0000000000	0000000010
0000000000	0100000000	0000000000	0010000000	0000000000	0000000001
0000000000	0010000000	0000000000	0001000000	0000000000	1000000000
1000000000	0000000000	0100000000	0000000000	0010000000	0000000000
0100000000	0000000000	0010000000	0000000000	0001000000	0000000000
0010000000	0000000000	0001000000	0000000000	0000100000	0000000000
0001000000	0000000000	0000100000	0000000000	0000010000	0000000000
0000100000	0000000000	0000010000	0000000000	0000001000	0000000000
0000010000	0000000000	0000001000	0000000000	0000000100	0000000000
0000001000	0000000000	0000000100	0000000000	0000000010	0000000000
0000000100	0000000000	0000000010	0000000000	0000000001	0000000000
0000000010	0000000000	0000000001	0000000000	1000000000	0000000000
0000000001	0000000000	1000000000	0000000000	0100000000	0000000000
0000000000	0000100000	0000000000	0010000000	0000000000	1000000000
0000000000	0000010000	0000000000	0001000000	0000000000	0100000000
0000000000	0000001000	0000000000	0000100000	0000000000	0010000000
0000000000	0000000100	0000000000	0000010000	0000000000	0001000000
0000000000	0000000010	0000000000	0000001000	0000000000	0000100000
0000000000	0000000001	0000000000	0000000100	0000000000	0000010000
0000000000	1000000000	0000000000	0000000010	0000000000	0000001000
0000000000	0100000000	0000000000	0000000001	0000000000	0000000100
0000000000	0010000000	0000000000	1000000000	0000000000	0000000010
0000000000	0001000000	0000000000	0100000000	0000000000	0000000001
1000000000	0000000000	0001000000	0000000000	0100000000	0000000000
0100000000	0000000000	0000100000	0000000000	0010000000	0000000000

0 0 1 0 0 0 0 0 0 0	0 0 0 0 0 0 0 0 0 0	0 0 0 0 0 1 0 0 0 0	0 0 0 0 0 0 0 0 0 0	0 0 0 1 0 0 0 0 0 0	0 0 0 0 0 0 0 0 0 0
0 0 0 1 0 0 0 0 0 0	0 0 0 0 0 0 0 0 0 0	0 0 0 0 0 0 1 0 0 0	0 0 0 0 0 0 0 0 0 0	0 0 0 0 1 0 0 0 0 0	0 0 0 0 0 0 0 0 0 0
0 0 0 0 1 0 0 0 0 0	0 0 0 0 0 0 0 0 0 0	0 0 0 0 0 0 0 1 0 0	0 0 0 0 0 0 0 0 0 0	0 0 0 0 0 1 0 0 0 0	0 0 0 0 0 0 0 0 0 0
0 0 0 0 0 1 0 0 0 0	0 0 0 0 0 0 0 0 0 0	0 0 0 0 0 0 0 0 1 0	0 0 0 0 0 0 0 0 0 0	0 0 0 0 0 0 1 0 0 0	0 0 0 0 0 0 0 0 0 0
0 0 0 0 0 0 1 0 0 0	0 0 0 0 0 0 0 0 0 0	0 0 0 0 0 0 0 0 0 1	0 0 0 0 0 0 0 0 0 0	0 0 0 0 0 0 0 1 0 0	0 0 0 0 0 0 0 0 0 0
0 0 0 0 0 0 0 1 0 0	0 0 0 0 0 0 0 0 0 0	1 0 0 0 0 0 0 0 0 0	0 0 0 0 0 0 0 0 0 0	0 0 0 0 0 0 0 0 1 0	0 0 0 0 0 0 0 0 0 0
0 0 0 0 0 0 0 0 1 0	0 0 0 0 0 0 0 0 0 0	0 1 0 0 0 0 0 0 0 0	0 0 0 0 0 0 0 0 0 0	0 0 0 0 0 0 0 0 0 1	0 0 0 0 0 0 0 0 0 0
0 0 0 0 0 0 0 0 0 1	0 0 0 0 0 0 0 0 0 0	0 0 1 0 0 0 0 0 0 0	0 0 0 0 0 0 0 0 0 0	1 0 0 0 0 0 0 0 0 0	0 0 0 0 0 0 0 0 0 0

A3.3. Sub-pulses times before and after delay

Encoder	Signal Delay	Time (ns)
Encoder 1	Signal Delay1	61
	Signal Delay 2	81
	Signal Delay 3	100
Encoder 2	Signal Delay1	172
	Signal Delay 2	192
	Signal Delay 3	211
Encoder 3	Signal Delay1	283
	Signal Delay 2	303
	Signal Delay 3	322
Encoder 4	Signal Delay1	394
	Signal Delay 2	414
	Signal Delay 3	433
Encoder 5	Signal Delay1	505
	Signal Delay 2	525
	Signal Delay 3	544
Encoder 6	Signal Delay1	616
	Signal Delay 2	636
	Signal Delay 3	655
Encoder 7	Signal Delay1	727
	Signal Delay 2	747
	Signal Delay 3	766
Encoder 8	Signal Delay1	838
	Signal Delay 2	858
	Signal Delay 3	877
Encoder 9	Signal Delay1	949
	Signal Delay 2	969
	Signal Delay 3	988
Encoder 10	Signal Delay1	1041
	Signal Delay 2	1062
	Signal Delay 3	1081
Encoder 11	Signal Delay1	1152

	Signal Delay 2	1173
	Signal Delay 3	1192
Encoder 12	Signal Delay1	1263
	Signal Delay 2	1284
	Signal Delay 3	1303
Encoder 13	Signal Delay1	1374
	Signal Delay 2	1395
	Signal Delay 3	1414
Encoder 14	Signal Delay1	1485
	Signal Delay 2	1506
	Signal Delay 3	1525
Encoder 15	Signal Delay1	1596
	Signal Delay 2	1617
	Signal Delay 3	1636
Encoder 16	Signal Delay1	1707
	Signal Delay 2	1728
	Signal Delay 3	1747
Encoder 17	Signal Delay1	1818
	Signal Delay 2	1839
	Signal Delay 3	1858
Encoder 18	Signal Delay1	1929
	Signal Delay 2	1950
	Signal Delay 3	1969
Encoder 19	Signal Delay1	2041
	Signal Delay 2	2064
	Signal Delay 3	2083
Encoder 20	Signal Delay1	2152
	Signal Delay 2	2175
	Signal Delay 3	2194
Encoder 21	Signal Delay1	2263
	Signal Delay 2	2286
	Signal Delay 3	2305
Encoder 22	Signal Delay1	2374
	Signal Delay 2	2397
	Signal Delay 3	2416
Encoder 23	Signal Delay1	2485
	Signal Delay 2	2508
	Signal Delay 3	2527
Encoder 24	Signal Delay1	2596
	Signal Delay 2	2619
	Signal Delay 3	2638
Encoder 25	Signal Delay1	2708
	Signal Delay 2	2720

	Signal Delay 3	2740
Encoder 26	Signal Delay1	2819
	Signal Delay 2	2831
	Signal Delay 3	2851
Encoder 27	Signal Delay1	2920
	Signal Delay 2	2942
	Signal Delay 3	2962
Encoder 28	Signal Delay1	3021
	Signal Delay 2	3043
	Signal Delay 3	3065
Encoder 29	Signal Delay1	3132
	Signal Delay 2	3154
	Signal Delay 3	3176
Encoder 30	Signal Delay1	3243
	Signal Delay 2	3265
	Signal Delay 3	3287
Encoder 31	Signal Delay1	3354
	Signal Delay 2	3376
	Signal Delay 3	3398
Encoder 32	Signal Delay1	3465
	Signal Delay 2	3487
	Signal Delay 3	3509
Encoder 33	Signal Delay1	3576
	Signal Delay 2	3598
	Signal Delay 3	3610
Encoder 34	Signal Delay1	3687
	Signal Delay 2	3709
	Signal Delay 3	3721
Encoder 35	Signal Delay1	3798
	Signal Delay 2	3810
	Signal Delay 3	3832
Encoder 36	Signal Delay1	3909
	Signal Delay 2	3921
	Signal Delay 3	3943
Encoder 37	Signal Delay1	4022
	Signal Delay 2	4041
	Signal Delay 3	4062
Encoder 38	Signal Delay1	4133
	Signal Delay 2	4152
	Signal Delay 3	4173
Encoder 39	Signal Delay1	4244
	Signal Delay 2	4263
	Signal Delay 3	4284

Encoder 40	Signal Delay1	4355
	Signal Delay 2	4374
	Signal Delay 3	4395
Encoder 41	Signal Delay1	4466
	Signal Delay 2	4485
	Signal Delay 3	4506
Encoder 42	Signal Delay1	4577
	Signal Delay 2	4596
	Signal Delay 3	4617
Encoder 43	Signal Delay1	4688
	Signal Delay 2	4707
	Signal Delay 3	4728
Encoder 44	Signal Delay1	4790
	Signal Delay 2	4819
	Signal Delay 3	4830
Encoder 45	Signal Delay1	4901
	Signal Delay 2	4920
	Signal Delay 3	4941
Encoder 46	Signal Delay1	5001
	Signal Delay 2	5025
	Signal Delay 3	5044
Encoder 47	Signal Delay1	5112
	Signal Delay 2	5136
	Signal Delay 3	5155
Encoder 48	Signal Delay1	5223
	Signal Delay 2	5247
	Signal Delay 3	5266
Encoder 49	Signal Delay1	5334
	Signal Delay 2	5358
	Signal Delay 3	5377
Encoder 50	Signal Delay1	5445
	Signal Delay 2	5469
	Signal Delay 3	5488
Encoder 51	Signal Delay1	5556
	Signal Delay 2	5570
	Signal Delay 3	5599
Encoder 52	Signal Delay1	5667
	Signal Delay 2	5681
	Signal Delay 3	5700
Encoder 53	Signal Delay1	5778
	Signal Delay 2	5792
	Signal Delay 3	5811
Encoder 54	Signal Delay1	5889

	Signal Delay 2	5903
	Signal Delay 3	5922
Encoder 55	Signal Delay1	6003
	Signal Delay 2	6024
	Signal Delay 3	6041
Encoder 56	Signal Delay1	6114
	Signal Delay 2	6135
	Signal Delay 3	6152
Encoder 57	Signal Delay1	6225
	Signal Delay 2	6246
	Signal Delay 3	6263
Encoder 58	Signal Delay1	6336
	Signal Delay 2	6357
	Signal Delay 3	6374
Encoder 59	Signal Delay1	6447
	Signal Delay 2	6468
	Signal Delay 3	6485
Encoder 60	Signal Delay1	6558
	Signal Delay 2	6579
	Signal Delay 3	6596
Encoder 61	Signal Delay1	6669
	Signal Delay 2	6680
	Signal Delay 3	6707
Encoder 62	Signal Delay1	6770
	Signal Delay 2	6791
	Signal Delay 3	6818
Encoder 63	Signal Delay1	6882
	Signal Delay 2	6903
	Signal Delay 3	6920
Encoder 64	Signal Delay1	6981
	Signal Delay 2	7002
	Signal Delay 3	7023

Appendix A4. A Splitting Ratio of 128

A4.1. Simulation parameters of 128 ONUs

Category	Module	Parameter	Value
Global		Time window	128 x (50+*L*)/ BitRateDefault
		BitRateDefault	1e9
		SampleModeCentreFrequency	184.5e12
		Code-length (*L*)	112

	Time-Chip (T_c)	1 ns
	T_{Δ}	50 ns
	T_{TDM}	112 ns
	Burst-Duration (T_b)	$L.T_c$ ns
Code-words	***C1***	0 [15] 1 0 [27] 1 0 [27] 1 0 [26] 1 0 [13]
	C2	0 [16] 1 0 [27] 1 0 [27] 1 0 [26] 1 0 [12]
	C3	0 [17] 1 0 [27] 1 0 [27] 1 0 [26] 1 0 [11]
	C4	0 [18] 1 0 [27] 1 0 [27] 1 0 [26] 1 0 [10]
	C5	0 [19] 1 0 [27] 1 0 [27] 1 0 [26] 1 0 [9]
	C6	0 [20] 1 0 [27] 1 0 [27] 1 0 [26] 1 0 [8]
	C7	0 [21] 1 0 [27] 1 0 [27] 1 0 [26] 1 0 [7]
	C8	0 [22] 1 0 [27] 1 0 [27] 1 0 [26] 1 0 [6]
	C9	0 [23] 1 0 [27] 1 0 [27] 1 0 [26] 1 0 [5]
	C10	0 [24] 1 0 [27] 1 0 [27] 1 0 [26] 1 0 [4]
	C11	0 [25] 1 0 [27] 1 0 [27] 1 0 [26] 1 0 [3]
	C12	0 [26] 1 0 [27] 1 0 [27] 1 0 [26] 1 0 [2]
	C13	0 [27] 1 0 [27] 1 0 [27] 1 0 [26] 1 0 [1]
	C14	0 [1] 1 0 [27] 1 0 [27] 1 0 [27] 1 0 [26]
	C15	0 [2] 1 0 [27] 1 0 [27] 1 0 [27] 1 0 [25]
	C16	0 [3] 1 0 [27] 1 0 [27] 1 0 [27] 1 0 [24]
	C17	0 [4] 1 0 [27] 1 0 [27] 1 0 [27] 1 0 [23]
	C18	0 [5] 1 0 [27] 1 0 [27] 1 0 [27] 1 0 [22]
	C19	0 [6] 1 0 [27] 1 0 [27] 1 0 [27] 1 0 [21]
	C20	0 [7] 1 0 [27] 1 0 [27] 1 0 [27] 1 0 [20]
	C21	0 [8] 1 0 [27] 1 0 [27] 1 0 [27] 1 0 [19]
	C22	0 [9] 1 0 [27] 1 0 [27] 1 0 [27] 1 0 [18]
	C23	0 [10] 1 0 [27] 1 0 [27] 1 0

		[27] 1 0 [17]
	C24	0 [11] 1 0 [27] 1 0 [27] 1 0 [27] 1 0 [16]
	C25	0 [12] 1 0 [27] 1 0 [27] 1 0 [27] 1 0 [15]
	C26	0 [13] 1 0 [27] 1 0 [27] 1 0 [27] 1 0 [14]
	C27	0 [15] 1 0 [29] 1 0 [29] 1 0 [27] 1 0 [8]
	C28	0 [16] 1 0 [29] 1 0 [29] 1 0 [27] 1 0 [7]
	C29	0 [17] 1 0 [29] 1 0 [29] 1 0 [27] 1 0 [6]
	C30	0 [18] 1 0 [29] 1 0 [29] 1 0 [27] 1 0 [5]
	C31	0 [19] 1 0 [29] 1 0 [29] 1 0 [27] 1 0 [4]
	C32	0 [20] 1 0 [29] 1 0 [29] 1 0 [27] 1 0 [3]
	C33	0 [21] 1 0 [29] 1 0 [29] 1 0 [27] 1 0 [2]
	C34	0 [22] 1 0 [29] 1 0 [29] 1 0 [27] 1 0 [1]
	C35	0 [24] 1 0 [29] 1 0 [15] 1 0 [27] 1 0 [13]
	C36	0 [25] 1 0 [29] 1 0 [15] 1 0 [27] 1 0 [12]
	C37	0 [26] 1 0 [15] 1 0 [29] 1 0 [27] 1 0 [11]
	C38	0 [27] 1 0 [15] 1 0 [29] 1 0 [27] 1 0 [10]
	C39	0 [14] 1 0 [27] 1 0 [31] 1 0 [27] 1 0 [9]
	C40	0 [1] 1 0 [29] 1 0 [29] 1 0 [29] 1 0 [20]
	C41	0 [2] 1 0 [29] 1 0 [29] 1 0 [29] 1 0 [19]
	C42	0 [3] 1 0 [29] 1 0 [29] 1 0 [29] 1 0 [18]
	C43	0 [4] 1 0 [29] 1 0 [29] 1 0 [29] 1 0 [17]
	C44	0 [5] 1 0 [29] 1 0 [29] 1 0 [29] 1 0 [16]
	C45	0 [6] 1 0 [29] 1 0 [29] 1 0 [29] 1 0 [15]
	C46	0 [7] 1 0 [29] 1 0 [29] 1 0 [29] 1 0 [14]
	C47	0 [8] 1 0 [29] 1 0 [29] 1 0 [15] 1 0 [27]
	C48	0 [9] 1 0 [29] 1 0 [29] 1 0

		[15] 1 0 [26]
	C49	0 [10] 1 0 [29] 1 0 [15] 1 0 [29] 1 0 [25]
	C50	0 [11] 1 0 [29] 1 0 [15] 1 0 [29] 1 0 [24]
	C51	0 [12] 1 0 [15] 1 0 [29] 1 0 [29] 1 0 [23]
	C52	0 [13] 1 0 [15] 1 0 [29] 1 0 [29] 1 0 [22]
	C53	0 [16] 1 0 [31] 1 0 [24] 1 0 [28] 1 0 [9]
	C54	0 [17] 1 0 [31] 1 0 [24] 1 0 [28] 1 0 [8]
	C55	0 [18] 1 0 [31] 1 0 [24] 1 0 [28] 1 0 [7]
	C56	0 [19] 1 0 [31] 1 0 [24] 1 0 [28] 1 0 [6]
	C57	0 [20] 1 0 [31] 1 0 [24] 1 0 [28] 1 0 [5]
	C58	0 [21] 1 0 [31] 1 0 [24] 1 0 [28] 1 0 [4]
	C59	0 [22] 1 0 [31] 1 0 [24] 1 0 [28] 1 0 [3]
	C60	0 [23] 1 0 [31] 1 0 [24] 1 0 [28] 1 0 [2]
	C61	0 [24] 1 0 [17] 1 0 [38] 1 0 [28] 1 0 [1]
	C62	0 [26] 1 0 [17] 1 0 [38] 1 0 [14] 1 0 [13]
	C63	0 [27] 1 0 [17] 1 0 [24] 1 0 [28] 1 0 [12]
	C64	0 [14] 1 0 [31] 1 0 [24] 1 0 [28] 1 0 [11]
	C65	0 [15] 1 0 [31] 1 0 [22] 1 0 [30] 1 0 [10]
	C66	0 [1] 1 0 [31] 1 0 [24] 1 0 [31] 1 0 [21]
	C67	0 [2] 1 0 [31] 1 0 [24] 1 0 [31] 1 0 [20]
	c68	0 [3] 1 0 [31] 1 0 [24] 1 0 [31] 1 0 [19]
	C69	0 [4] 1 0 [31] 1 0 [24] 1 0 [31] 1 0 [18]
	C70	0 [5] 1 0 [31] 1 0 [24] 1 0 [31] 1 0 [17]
	C71	0 [6] 1 0 [31] 1 0 [24] 1 0 [31] 1 0 [16]
	C72	0 [7] 1 0 [31] 1 0 [24] 1 0 [31] 1 0 [15]
	C73	0 [8] 1 0 [31] 1 0 [24] 1 0

		[31] 1 0 [14]
	C74	0 [9] 1 0 [31] 1 0 [24] 1 0 [17] 1 0 [27]
	C75	0 [10] 1 0 [17] 1 0 [38] 1 0 [17] 1 0 [26]
	C76	0 [11] 1 0 [17] 1 0 [38] 1 0 [17] 1 0 [25]
	C77	0 [12] 1 0 [17] 1 0 [38] 1 0 [17] 1 0 [24]
	C78	0 [13] 1 0 [17] 1 0 [24] 1 0 [31] 1 0 [23]
	C79	0 [17] 1 0 [26] 1 0 [26] 1 0 [29] 1 0 [10]
	C80	0 [18] 1 0 [26] 1 0 [26] 1 0 [29] 1 0 [9]
	C81	0 [19] 1 0 [26] 1 0 [26] 1 0 [29] 1 0 [8]
	C82	0 [20] 1 0 [26] 1 0 [26] 1 0 [29] 1 0 [7]
	C83	0 [21] 1 0 [26] 1 0 [26] 1 0 [29] 1 0 [6]
	C84	0 [22] 1 0 [26] 1 0 [26] 1 0 [29] 1 0 [5]
	C85	0 [23] 1 0 [26] 1 0 [26] 1 0 [29] 1 0 [4]
	C86	0 [24] 1 0 [26] 1 0 [26] 1 0 [29] 1 0 [3]
	C87	0 [25] 1 0 [26] 1 0 [26] 1 0 [29] 1 0 [2]
	C88	0 [26] 1 0 [26] 1 0 [26] 1 0 [29] 1 0 [1]
	C89	0 [14] 1 0 [40] 1 0 [26] 1 0 [15] 1 0 [13]
	C90	0 [15] 1 0 [26] 1 0 [40] 1 0 [15] 1 0 [12]
	C91	0 [14] 1 0 [28] 1 0 [26] 1 0 [29] 1 0 [11]
	C92	0 [1] 1 0 [33] 1 0 [26] 1 0 [26] 1 0 [22]
	C93	0 [2] 1 0 [33] 1 0 [26] 1 0 [26] 1 0 [21]
	C94	0 [3] 1 0 [33] 1 0 [26] 1 0 [26] 1 0 [20]
	C95	0 [4] 1 0 [33] 1 0 [26] 1 0 [26] 1 0 [19]
	C96	0 [5] 1 0 [33] 1 0 [26] 1 0 [26] 1 0 [18]
	C97	0 [6] 1 0 [33] 1 0 [26] 1 0 [26] 1 0 [17]
	C98	0 [7] 1 0 [33] 1 0 [26] 1 0

		[26] 1 0 [16]
	C99	0 [8] 1 0 [19] 1 0 [40] 1 0 [26] 1 0 [15]
	C100	0 [9] 1 0 [19] 1 0 [26] 1 0 [40] 1 0 [14]
	C101	0 [10] 1 0 [19] 1 0 [26] 1 0 [26] 1 0 [27]
	C102	0 [11] 1 0 [19] 1 0 [26] 1 0 [26] 1 0 [26]
	C103	0 [12] 1 0 [19] 1 0 [26] 1 0 [26] 1 0 [25]
	C104	0 [13] 1 0 [19] 1 0 [26] 1 0 [26] 1 0 [24]
	C105	0 [18] 1 0 [28] 1 0 [28] 1 0 [21] 1 0 [13]
	C106	0 [19] 1 0 [28] 1 0 [28] 1 0 [23] 1 0 [10]
	C107	0 [20] 1 0 [28] 1 0 [28] 1 0 [23] 1 0 [9]
	C108	0 [21] 1 0 [28] 1 0 [28] 1 0 [23] 1 0 [8]
	C109	0 [22] 1 0 [28] 1 0 [28] 1 0 [23] 1 0 [7]
	C110	0 [23] 1 0 [28] 1 0 [28] 1 0 [23] 1 0 [6]
	C111	0 [24] 1 0 [28] 1 0 [28] 1 0 [23] 1 0 [5]
	C112	0 [25] 1 0 [28] 1 0 [28] 1 0 [23] 1 0 [4]
	C113	0 [26] 1 0 [28] 1 0 [14] 1 0 [37] 1 0 [3]
	C114	0 [27] 1 0 [14] 1 0 [28] 1 0 [37] 1 0 [2]
	C115	0 [14] 1 0 [28] 1 0 [28] 1 0 [37] 1 0 [1]
	C116	0 [16] 1 0 [28] 1 0 [28] 1 0 [23] 1 0 [13]
	C117	0 [17] 1 0 [28] 1 0 [28] 1 0 [23] 1 0 [12]
	C118	0 [1] 1 0 [28] 1 0 [28] 1 0 [28] 1 0 [23]
	C119	0 [2] 1 0 [28] 1 0 [28] 1 0 [28] 1 0 [22]
	C120	0 [3] 1 0 [28] 1 0 [28] 1 0 [28] 1 0 [21]
	C121	0 [4] 1 0 [28] 1 0 [28] 1 0 [28] 1 0 [20]
	C122	0 [5] 1 0 [28] 1 0 [28] 1 0 [28] 1 0 [19]
	C123	0 [6] 1 0 [28] 1 0 [28] 1 0

			[28] 1 0 [18]
		C124	0 [7] 1 0 [28] 1 0 [28] 1 0 [28] 1 0 [17]
		C125	0 [8] 1 0 [28] 1 0 [28] 1 0 [28] 1 0 [16]
		C126	0 [9] 1 0 [28] 1 0 [28] 1 0 [28] 1 0 [15]
		C127	0 [10] 1 0 [28] 1 0 [28] 1 0 [28] 1 0 [14]
		C128	0 [11] 1 0 [28] 1 0 [28] 1 0 [14] 1 0 [27]
		w	0 [50]
Fibers	Feeder Fiber	ReferenceFrequency	184.5e12
		Length	10 km
		GroupRefractiveIndex	1.47
	Drop fibers	ReferenceFrequency	184.5e12
		Length	*L*1= 500 m Increases by 5 m – *L*128 = 1135 m
Monitoring Pulse generator	General	BitRate	BitRateDefault
		EmissionFrequency	184.5e12
		ModulationType	NRZ
	PRBS	PRBS_Type	CodeWord
		CodeWord	1 0 [20735]
Encoding x *T*c	Encoder 1	Signal Delay1	16
		Signal Delay 2	43
		Signal Delay 3	72
		Signal Delay 4	99
	Encoder2	Signal Delay1	17
		Signal Delay 2	44
		Signal Delay 3	7573
		Signal Delay 4	100
	Encoder 3	Signal Delay1	18
		Signal Delay 2	45
		Signal Delay 3	74
		Signal Delay 4	101
	Encoder 4	Signal Delay1	19
		Signal Delay 2	46
		Signal Delay 3	75
		Signal Delay 4	102
	Encoder 5	Signal Delay1	20
		Signal Delay 2	47
		Signal Delay 3	76
		Signal Delay 4	103

	Encoder 6	Signal Delay1	21
		Signal Delay 2	48
		Signal Delay 3	77
		Signal Delay 4	104
	Encoder 7	Signal Delay1	22
		Signal Delay 2	49
		Signal Delay 3	78
		Signal Delay 4	105
	Encoder 8	Signal Delay1	23
		Signal Delay 2	50
		Signal Delay 3	79
		Signal Delay 4	106
	Encoder 9	Signal Delay1	24
		Signal Delay 2	51
		Signal Delay 3	80
		Signal Delay 4	107
	Encoder 10	Signal Delay1	25
		Signal Delay 2	52
		Signal Delay 3	81
		Signal Delay 4	108
	Encoder 11	Signal Delay1	26
		Signal Delay 2	53
		Signal Delay 3	82
		Signal Delay 4	109
	Encoder 12	Signal Delay1	27
		Signal Delay 2	54
		Signal Delay 3	83
		Signal Delay 4	110
	Encoder 13	Signal Delay1	28
		Signal Delay 2	55
		Signal Delay 3	84
		Signal Delay 4	111
	Encoder 14	Signal Delay1	2
		Signal Delay 2	30
		Signal Delay 3	58
		Signal Delay 4	86
	Encoder 15	Signal Delay1	3
		Signal Delay 2	31
		Signal Delay 3	59
		Signal Delay 4	87
	Encoder 16	Signal Delay1	4
		Signal Delay 2	32
		Signal Delay 3	60

		Signal Delay 4	88
	Encoder 17	Signal Delay1	5
		Signal Delay 2	33
		Signal Delay 3	61
		Signal Delay 4	89
	Encoder 18	Signal Delay1	6
		Signal Delay 2	34
		Signal Delay 3	62
		Signal Delay 4	90
	Encoder 19	Signal Delay1	7
		Signal Delay 2	35
		Signal Delay 3	63
		Signal Delay 4	91
	Encoder 20	Signal Delay1	8
		Signal Delay 2	36
		Signal Delay 3	64
		Signal Delay 4	92
	Encoder 21	Signal Delay1	9
		Signal Delay 2	37
		Signal Delay 3	65
		Signal Delay 4	93
	Encoder 22	Signal Delay1	10
		Signal Delay 2	38
		Signal Delay 3	66
		Signal Delay 4	94
	Encoder 23	Signal Delay1	11
		Signal Delay 2	39
		Signal Delay 3	67
		Signal Delay 4	95
	Encoder 24	Signal Delay1	12
		Signal Delay 2	40
		Signal Delay 3	68
		Signal Delay 4	96
	Encoder 25	Signal Delay1	13
		Signal Delay 2	41
		Signal Delay 3	69
		Signal Delay 4	97
	Encoder 26	Signal Delay1	14
		Signal Delay 2	42
		Signal Delay 3	70
		Signal Delay 4	98
	Encoder 27	Signal Delay1	16
		Signal Delay 2	46

		Signal Delay 3	76
		Signal Delay 4	104
	Encoder 28	Signal Delay1	17
		Signal Delay 2	47
		Signal Delay 3	77
		Signal Delay 4	105
	Encoder 29	Signal Delay1	18
		Signal Delay 2	48
		Signal Delay 3	78
		Signal Delay 4	106
	Encoder 30	Signal Delay1	19
		Signal Delay 2	49
		Signal Delay 3	79
		Signal Delay 4	107
	Encoder 31	Signal Delay1	20
		Signal Delay 2	50
		Signal Delay 3	80
		Signal Delay 4	108
	Encoder 32	Signal Delay1	21
		Signal Delay 2	51
		Signal Delay 3	81
		Signal Delay 4	109
	Encoder 33	Signal Delay1	22
		Signal Delay 2	52
		Signal Delay 3	82
		Signal Delay 4	110
	Encoder 34	Signal Delay1	23
		Signal Delay 2	53
		Signal Delay 3	83
		Signal Delay 4	111
	Encoder 35	Signal Delay1	25
		Signal Delay 2	55
		Signal Delay 3	71
		Signal Delay 4	90
	Encoder 36	Signal Delay1	26
		Signal Delay 2	56
		Signal Delay 3	72
		Signal Delay 4	100
	Encoder 37	Signal Delay1	27
		Signal Delay 2	43
		Signal Delay 3	73
		Signal Delay 4	101
	Encoder 38	Signal Delay1	28

		Signal Delay 2	44
		Signal Delay 3	74
		Signal Delay 4	102
	Encoder 39	Signal Delay1	15
		Signal Delay 2	45
		Signal Delay 3	75
		Signal Delay 4	103
	Encoder 40	Signal Delay1	2
		Signal Delay 2	32
		Signal Delay 3	62
		Signal Delay 4	92
	Encoder 41	Signal Delay1	3
		Signal Delay 2	33
		Signal Delay 3	63
		Signal Delay 4	93
	Encoder 42	Signal Delay1	4
		Signal Delay 2	34
		Signal Delay 3	64
		Signal Delay 4	94
	Encoder 43	Signal Delay1	5
		Signal Delay 2	35
		Signal Delay 3	65
		Signal Delay 4	95
	Encoder 44	Signal Delay1	6
		Signal Delay 2	36
		Signal Delay 3	66
		Signal Delay 4	96
	Encoder 45	Signal Delay1	7
		Signal Delay 2	37
		Signal Delay 3	67
		Signal Delay 4	97
	Encoder 46	Signal Delay1	8
		Signal Delay 2	38
		Signal Delay 3	68
		Signal Delay 4	98
	Encoder 47	Signal Delay1	9
		Signal Delay 2	39
		Signal Delay 3	69
		Signal Delay 4	85
	Encoder 48	Signal Delay1	10
		Signal Delay 2	40
		Signal Delay 3	70
		Signal Delay 4	86

	Encoder 49	Signal Delay1	11
		Signal Delay 2	41
		Signal Delay 3	57
		Signal Delay 4	87
	Encoder 50	Signal Delay1	12
		Signal Delay 2	42
		Signal Delay 3	58
		Signal Delay 4	88
	Encoder 51	Signal Delay1	13
		Signal Delay 2	29
		Signal Delay 3	58
		Signal Delay 4	89
	Encoder 52	Signal Delay1	14
		Signal Delay 2	30
		Signal Delay 3	60
		Signal Delay 4	90
	Encoder 53	Signal Delay1	17
		Signal Delay 2	49
		Signal Delay 3	74
		Signal Delay 4	103
	Encoder 54	Signal Delay1	18
		Signal Delay 2	50
		Signal Delay 3	75
		Signal Delay 4	104
	Encoder 55	Signal Delay1	19
		Signal Delay 2	51
		Signal Delay 3	76
		Signal Delay 4	105
	Encoder 56	Signal Delay1	20
		Signal Delay 2	52
		Signal Delay 3	77
		Signal Delay 4	106
	Encoder 57	Signal Delay1	21
		Signal Delay 2	53
		Signal Delay 3	78
		Signal Delay 4	107
	Encoder 58	Signal Delay1	22
		Signal Delay 2	54
		Signal Delay 3	79
		Signal Delay 4	108
	Encoder 59	Signal Delay1	23
		Signal Delay 2	55
		Signal Delay 3	80

		Signal Delay 4	109
	Encoder 60	Signal Delay1	24
		Signal Delay 2	56
		Signal Delay 3	81
		Signal Delay 4	110
	Encoder 61	Signal Delay1	25
		Signal Delay 2	43
		Signal Delay 3	82
		Signal Delay 4	111
	Encoder 62	Signal Delay1	27
		Signal Delay 2	45
		Signal Delay 3	84
		Signal Delay 4	99
	Encoder 63	Signal Delay1	28
		Signal Delay 2	46
		Signal Delay 3	71
		Signal Delay 4	100
	Encoder 64	Signal Delay1	15
		Signal Delay 2	47
		Signal Delay 3	72
		Signal Delay 4	101
	Encoder 65	Signal Delay1	16
		Signal Delay 2	48
		Signal Delay 3	73
		Signal Delay 4	102
	Encoder 66	Signal Delay1	2
		Signal Delay 2	34
		Signal Delay 3	59
		Signal Delay 4	91
	Encoder 67	Signal Delay1	3
		Signal Delay 2	35
		Signal Delay 3	60
		Signal Delay 4	92
	Encoder 68	Signal Delay1	4
		Signal Delay 2	36
		Signal Delay 3	61
		Signal Delay 4	93
	Encoder 69	Signal Delay1	5
		Signal Delay 2	37
		Signal Delay 3	62
		Signal Delay 4	94
	Encoder 70	Signal Delay1	6
		Signal Delay 2	38

		Signal Delay 3	63
		Signal Delay 4	95
	Encoder 71	Signal Delay1	7
		Signal Delay 2	39
		Signal Delay 3	64
		Signal Delay 4	96
	Encoder 72	Signal Delay1	8
		Signal Delay 2	40
		Signal Delay 3	65
		Signal Delay 4	97
	Encoder 73	Signal Delay1	9
		Signal Delay 2	41
		Signal Delay 3	66
		Signal Delay 4	98
	Encoder 74	Signal Delay1	10
		Signal Delay 2	42
		Signal Delay 3	67
		Signal Delay 4	85
	Encoder 75	Signal Delay1	11
		Signal Delay 2	29
		Signal Delay 3	68
		Signal Delay 4	86
	Encoder 76	Signal Delay1	12
		Signal Delay 2	30
		Signal Delay 3	69
		Signal Delay 4	87
	Encoder 77	Signal Delay1	13
		Signal Delay 2	31
		Signal Delay 3	70
		Signal Delay 4	88
	Encoder 78	Signal Delay1	14
		Signal Delay 2	32
		Signal Delay 3	57
		Signal Delay 4	89
	Encoder 79	Signal Delay1	18
		Signal Delay 2	45
		Signal Delay 3	72
		Signal Delay 4	102
	Encoder 80	Signal Delay1	19
		Signal Delay 2	46
		Signal Delay 3	73
		Signal Delay 4	103
	Encoder 81	Signal Delay1	20

		Signal Delay 2	47
		Signal Delay 3	74
		Signal Delay 4	104
	Encoder 82	Signal Delay1	21
		Signal Delay 2	48
		Signal Delay 3	75
		Signal Delay 4	105
	Encoder 83	Signal Delay1	22
		Signal Delay 2	49
		Signal Delay 3	76
		Signal Delay 4	106
	Encoder 84	Signal Delay1	23
		Signal Delay 2	50
		Signal Delay 3	77
		Signal Delay 4	107
	Encoder 85	Signal Delay1	24
		Signal Delay 2	51
		Signal Delay 3	78
		Signal Delay 4	108
	Encoder 86	Signal Delay1	25
		Signal Delay 2	52
		Signal Delay 3	79
		Signal Delay 4	109
	Encoder 87	Signal Delay1	26
		Signal Delay 2	53
		Signal Delay 3	80
		Signal Delay 4	110
	Encoder 88	Signal Delay1	27
		Signal Delay 2	54
		Signal Delay 3	81
		Signal Delay 4	111
	Encoder 89	Signal Delay1	15
		Signal Delay 2	56
		Signal Delay 3	83
		Signal Delay 4	99
	Encoder 90	Signal Delay1	16
		Signal Delay 2	43
		Signal Delay 3	84
		Signal Delay 4	100
	Encoder 91	Signal Delay1	17
		Signal Delay 2	44
		Signal Delay 3	71
		Signal Delay 4	101

	Encoder 92	Signal Delay1	2
		Signal Delay 2	36
		Signal Delay 3	63
		Signal Delay 4	90
	Encoder 93	Signal Delay1	3
		Signal Delay 2	37
		Signal Delay 3	64
		Signal Delay 4	91
	Encoder 94	Signal Delay1	4
		Signal Delay 2	38
		Signal Delay 3	65
		Signal Delay 4	92
	Encoder 95	Signal Delay1	5
		Signal Delay 2	39
		Signal Delay 3	66
		Signal Delay 4	93
	Encoder 96	Signal Delay1	6
		Signal Delay 2	40
		Signal Delay 3	67
		Signal Delay 4	94
	Encoder 97	Signal Delay1	7
		Signal Delay 2	41
		Signal Delay 3	68
		Signal Delay 4	95
	Encoder 98	Signal Delay1	8
		Signal Delay 2	42
		Signal Delay 3	69
		Signal Delay 4	96
	Encoder 99	Signal Delay1	9
		Signal Delay 2	29
		Signal Delay 3	70
		Signal Delay 4	97
	Encoder 100	Signal Delay1	10
		Signal Delay 2	30
		Signal Delay 3	57
		Signal Delay 4	98
	Encoder 101	Signal Delay1	11
		Signal Delay 2	31
		Signal Delay 3	58
		Signal Delay 4	85
	Encoder 102	Signal Delay1	12
		Signal Delay 2	32
		Signal Delay 3	59

		Signal Delay 4	86
	Encoder 103	Signal Delay1	13
		Signal Delay 2	33
		Signal Delay 3	59
		Signal Delay 4	87
	Encoder 104	Signal Delay1	14
		Signal Delay 2	34
		Signal Delay 3	61
		Signal Delay 4	88
	Encoder 105	Signal Delay1	19
		Signal Delay 2	48
		Signal Delay 3	77
		Signal Delay 4	99
	Encoder 106	Signal Delay1	20
		Signal Delay 2	49
		Signal Delay 3	78
		Signal Delay 4	102
	Encoder 107	Signal Delay1	21
		Signal Delay 2	50
		Signal Delay 3	79
		Signal Delay 4	103
	Encoder 108	Signal Delay1	22
		Signal Delay 2	51
		Signal Delay 3	80
		Signal Delay 4	104
	Encoder 109	Signal Delay1	23
		Signal Delay 2	52
		Signal Delay 3	81
		Signal Delay 4	105
	Encoder 110	Signal Delay1	24
		Signal Delay 2	53
		Signal Delay 3	82
		Signal Delay 4	106
	Encoder 111	Signal Delay1	25
		Signal Delay 2	54
		Signal Delay 3	83
		Signal Delay 4	107
	Encoder 112	Signal Delay1	26
		Signal Delay 2	55
		Signal Delay 3	84
		Signal Delay 4	108
	Encoder 113	Signal Delay1	27
		Signal Delay 2	56

		Signal Delay 3	71
		Signal Delay 4	109
	Encoder 114	Signal Delay1	28
		Signal Delay 2	43
		Signal Delay 3	72
		Signal Delay 4	110
	Encoder 115	Signal Delay1	15
		Signal Delay 2	44
		Signal Delay 3	73
		Signal Delay 4	111
	Encoder 116	Signal Delay1	17
		Signal Delay 2	46
		Signal Delay 3	75
		Signal Delay 4	99
	Encoder 117	Signal Delay1	18
		Signal Delay 2	47
		Signal Delay 3	76
		Signal Delay 4	100
	Encoder 118	Signal Delay1	2
		Signal Delay 2	31
		Signal Delay 3	60
		Signal Delay 4	89
	Encoder 119	Signal Delay1	3
		Signal Delay 2	32
		Signal Delay 3	61
		Signal Delay 4	90
	Encoder 120	Signal Delay1	4
		Signal Delay 2	33
		Signal Delay 3	62
		Signal Delay 4	91
	Encoder 121	Signal Delay1	5
		Signal Delay 2	34
		Signal Delay 3	63
		Signal Delay 4	92
	Encoder 122	Signal Delay1	6
		Signal Delay 2	35
		Signal Delay 3	64
		Signal Delay 4	93
	Encoder 123	Signal Delay1	7
		Signal Delay 2	36
		Signal Delay 3	65
		Signal Delay 4	94
	Encoder 124	Signal Delay1	8

		Signal Delay 2	37
		Signal Delay 3	66
		Signal Delay 4	95
	Encoder 125	Signal Delay1	9
		Signal Delay 2	38
		Signal Delay 3	67
		Signal Delay 4	96
	Encoder 126	Signal Delay1	10
		Signal Delay 2	39
		Signal Delay 3	68
		Signal Delay 4	97
	Encoder127	Signal Delay1	11
		Signal Delay 2	40
		Signal Delay 3	69
		Signal Delay 4	98
	Encoder128	Signal Delay1	12
		Signal Delay 2	41
		Signal Delay 3	70
		Signal Delay 4	85
Reference signal	*PRBS*	CodeWord	0 [50] c1 w c2 w c3 w c4 w c5 w c6 w c7 w c8 w c9 w c10 w c11 w c12 w c13 w c14 w c15 w c16 w c17 w c18 w c19 w c20 w c21 w c22 w c23 w c24 w c25 w c26 w c27 w c28 w c29 w c30 w c31 w c32 w c33 w c34 w c35 w c36 w c37 w c38 w c39 w c40 w c41 w c42 w c43 w c44 w c45 w c46 w c47 w c48 w c49 w c50 w c51 w c52 w c53 w c54 w c55 w c56 w c57 w c58 w c59 w c60 w c61 w c62 w c63 w c64 w c65 w c66 w c67 w c68 w c69 w c70 w c71 w c72 w c73 w c74 w c75 w c76 w c77 w c78 w c79 w c80 w c81 w c82 w c83 w c84 w c85 w c86 w c87 w c88 w c89 w c90 w c91 w c92 w c93 w c94 w c95 w c96 w c97 w c98 w c99 w c100 w c101 w c102 w c103 w c104 w c105 w c106 w c107 w c108 w c109 w c110 w c111 w c112 w c113 w c114 w c115 w c116 w c117 w c118 w c119 w c120 w c121 w c122 w c123 w c124 w c125 w c126 w c127 w c128

A4.2. Binary codes for EG-nMPC, $P = 7$

Binary code-words for EG-nMPC, $P = 7$							
000000000000 00	100000000000 00	000000000000 00	100000000000 00	000000000000 00	100000000000 00	000000000000 00	000000000000 01
000000000000 00	010000000000 00	000000000000 00	010000000000 00	000000000000 00	010000000000 00	000000000000 00	100000000000 00
000000000000 00	001000000000 00	000000000000 00	001000000000 00	000000000000 00	001000000000 00	000000000000 00	010000000000 00
000000000000 00	000100000000 00	000000000000 00	000100000000 00	000000000000 00	000100000000 00	000000000000 00	001000000000 00
000000000000 00	000010000000 00	000000000000 00	000010000000 00	000000000000 00	000010000000 00	000000000000 00	000100000000 00
000000000000 00	000001000000 00	000000000000 00	000001000000 00	000000000000 00	000001000000 00	000000000000 00	000010000000 00
000000000000 00	000000100000 00	000000000000 00	000000100000 00	000000000000 00	000000100000 00	000000000000 00	000001000000 00
000000000000 00	000000010000 00	000000000000 00	000000010000 00	000000000000 00	000000010000 00	000000000000 00	000000100000 00
000000000000 00	000000001000 00	000000000000 00	000000001000 00	000000000000 00	000000001000 00	000000000000 00	000000010000 00
000000000000 00	000000000100 00	000000000000 00	000000000100 00	000000000000 00	000000000100 00	000000000000 00	000000001000 00
000000000000 00	000000000010 00	000000000000 00	000000000010 00	000000000000 00	000000000010 00	000000000000 00	000000000100 00
000000000000 00	000000000001 00	000000000000 00	000000000001 00	000000000000 00	000000000001 00	000000000000 00	000000000010 00
000000000000 00	000000000000 10	000000000000 00	000000000000 10	000000000000 00	000000000000 10	000000000000 00	000000000001 00
000000000000 00	000000000000 01	000000000000 00	000000000000 01	000000000000 00	000000000000 01	000000000000 00	000000000000 10
100000000000 00	000000000000 00	100000000000 00	000000000000 00	100000000000 00	000000000000 00	100000000000 00	000000000000 00
010000000000 00	000000000000 00	010000000000 00	000000000000 00	010000000000 00	000000000000 00	010000000000 00	000000000000 00
001000000000 00	000000000000 00	001000000000 00	000000000000 00	001000000000 00	000000000000 00	001000000000 00	000000000000 00
000100000000 00	000000000000 00	000100000000 00	000000000000 00	000100000000 00	000000000000 00	000100000000 00	000000000000 00
000010000000 00	000000000000 00	000010000000 00	000000000000 00	000010000000 00	000000000000 00	000010000000 00	000000000000 00
000001000000 00	000000000000 00	000001000000 00	000000000000 00	000001000000 00	000000000000 00	000001000000 00	000000000000 00
000000100000 00	000000000000 00	000000100000 00	000000000000 00	000000100000 00	000000000000 00	000000100000 00	000000000000 00
000000010000 00	000000000000 00	000000010000 00	000000000000 00	000000010000 00	000000000000 00	000000010000 00	000000000000 00
000000001000 00	000000000000 00	000000001000 00	000000000000 00	000000001000 00	000000000000 00	000000001000 00	000000000000 00
000000000100 00	000000000000 00	000000000100 00	000000000000 00	000000000100 00	000000000000 00	000000000100 00	000000000000 00
000000000010 00	000000000000 00	000000000010 00	000000000000 00	000000000010 00	000000000000 00	000000000010 00	000000000000 00
000000000001 00	000000000000 00	000000000001 00	000000000000 00	000000000001 00	000000000000 00	000000000001 00	000000000000 00
000000000000 10	000000000000 00	000000000000 10	000000000000 00	000000000000 10	000000000000 00	000000000000 10	000000000000 00
000000000000 01	000000000000 00	000000000000 01	000000000000 00	000000000000 01	000000000000 00	000000000000 01	000000000000 00
000000000000 00	010000000000 00	000000000000 00	000100000000 00	000000000000 00	000001000000 00	000000000000 00	000001000000 00
000000000000 00	001000000000 00	000000000000 00	000010000000 00	000000000000 00	000000100000 00	000000000000 00	000000100000 00
000000000000 00	000100000000 00	000000000000 00	000001000000 00	000000000000 00	000000010000 00	000000000000 00	000000010000 00
000000000000 00	000010000000 00	000000000000 00	000000100000 00	000000000000 00	000000001000 00	000000000000 00	000000001000 00
000000000000 00	000001000000 00	000000000000 00	000000010000 00	000000000000 00	000000000100 00	000000000000 00	000000000100 00
000000000000 00	000000100000 00	000000000000 00	000000001000 00	000000000000 00	000000000010 00	000000000000 00	000000000010 00
000000000000 00	000000010000 00	000000000000 00	000000000100 00	000000000000 00	000000000001 00	000000000000 00	000000000001 00
000000000000 00	000000001000 00	000000000000 00	000000000010 00	000000000000 00	000000000000 10	000000000000 00	000000000000 10
000000000000 00	000000000100 00	000000000000 00	000000000001 00	000000000000 00	000000000000 01	000000000000 00	000000000000 01
000000000000 00	000000000010 00	000000000000 00	000000000000 10	000000000000 00	100000000000 00	000000000000 00	100000000000 00
000000000000 00	000000000001 00	000000000000 00	000000000000 01	000000000000 00	010000000000 00	000000000000 00	010000000000 00

000000000000 00	000000000000 10	000000000000 00	100000000000 00	000000000000 00	001000000000 00	000000000000 00	001000000000 00
000000000000 00	000000000000 01	000000000000 00	010000000000 00	000000000000 00	000100000000 00	000000000000 00	000100000000 00
000000000000 00	100000000000 00	000000000000 00	100000000000 00	000000000000 00	000010000000 00	000000000000 00	000010000000 00
100000000000 00	000000000000 00	001000000000 00	000000000000 00	000010000000 00	000000000000 00	000000100000 00	000000000000 00
010000000000 00	000000000000 00	000100000000 00	000000000000 00	000001000000 00	000000000000 00	000000010000 00	000000000000 00
001000000000 00	000000000000 00	000010000000 00	000000000000 00	000000100000 00	000000000000 00	000000001000 00	000000000000 00
000100000000 00	000000000000 00	000001000000 00	000000000000 00	000000010000 00	000000000000 00	000000000100 00	000000000000 00
000010000000 00	000000000000 00	000000100000 00	000000000000 00	000000001000 00	000000000000 00	000000000010 00	000000000000 00
000001000000 00	000000000000 00	000000010000 00	000000000000 00	000000000100 00	000000000000 00	000000000001 00	000000000000 00
000000100000 00	000000000000 00	000000001000 00	000000000000 00	000000000010 00	000000000000 00	000000000000 10	000000000000 00
000000010000 00	000000000000 00	000000000100 00	000000000000 00	000000000001 00	000000000000 00	000000000000 01	000000000000 00
000000001000 00	000000000000 00	000000000010 00	000000000000 00	000000000000 10	000000000000 00	100000000000 00	000000000000 00
000000000100 00	000000000000 00	000000000001 00	000000000000 00	000000000000 01	000000000000 00	010000000000 00	000000000000 00
000000000010 00	000000000000 00	000000000000 10	000000000000 00	100000000000 00	000000000000 00	001000000000 00	000000000000 00
000000000001 00	000000000000 00	000000000000 01	000000000000 00	010000000000 00	000000000000 00	000100000000 00	000000000000 00
000000000000 10	000000000000 00	100000000000 00	000000000000 00	001000000000 00	000000000000 00	000010000000 00	000000000000 00
000000000000 01	000000000000 00	010000000000 00	000000000000 00	000100000000 00	000000000000 00	000001000000 00	000000000000 00
---	---	---	---	---	---	---	---
000000000000 00	001000000000 00	000000000000 00	000000100000 00	000000000000 00	000100000000 00	000000000000 00	000010000000 00
000000000000 00	000100000000 00	000000000000 00	000000010000 00	000000000000 00	000010000000 00	000000000000 00	000001000000 00
000000000000 00	000010000000 00	000000000000 00	000000001000 00	000000000000 00	000001000000 00	000000000000 00	000000100000 00
000000000000 00	000001000000 00	000000000000 00	000000000100 00	000000000000 00	000000100000 00	000000000000 00	000000010000 00
000000000000 00	000000100000 00	000000000000 00	000000000010 00	000000000000 00	000000010000 00	000000000000 00	000000001000 00
000000000000 00	000000010000 00	000000000000 00	000000000001 00	000000000000 00	000000001000 00	000000000000 00	000000000100 00
000000000000 00	000000001000 00	000000000000 00	000000000000 10	000000000000 00	000000000100 00	000000000000 00	000000000010 00
000000000000 00	000000000100 00	000000000000 00	000000000000 01	000000000000 00	000000000010 00	000000000000 00	000000000001 00
000000000000 00	000000000010 00	000000000000 00	100000000000 00	000000000000 00	000000000001 00	000000000000 00	000000000000 10
000000000000 00	000000000001 00	000000000000 00	010000000000 00	000000000000 00	000000000000 10	000000000000 00	000000000000 01
000000000000 00	000000000000 10	000000000000 00	001000000000 00	000000000000 00	000000000000 01	000000000000 00	100000000000 00
000000000000 00	000000000000 01	000000000000 00	000100000000 00	000000000000 00	100000000000 00	000000000000 00	010000000000 00
000000000000 00	100000000000 00	000000000000 00	000010000000 00	000000000000 00	010000000000 00	000000000000 00	001000000000 00
000000000000 00	010000000000 00	000000000000 00	000001000000 00	000000000000 00	100000000000 00	000000000000 00	000100000000 00
100000000000 00	000000000000 00	000010000000 00	000000000000 00	010000000000 00	000000000000 00	000001000000 00	000000000000 00
010000000000 00	000000000000 00	000001000000 00	000000000000 00	001000000000 00	000000000000 00	000000100000 00	000000000000 00
001000000000 00	000000000000 00	000000100000 00	000000000000 00	000100000000 00	000000000000 00	000000010000 00	000000000000 00
000100000000 00	000000000000 00	000000010000 00	000000000000 00	000010000000 00	000000000000 00	000000001000 00	000000000000 00
000010000000 00	000000000000 00	000000001000 00	000000000000 00	000001000000 00	000000000000 00	000000000100 00	000000000000 00
000001000000 00	000000000000 00	000000000100 00	000000000000 00	000000100000 00	000000000000 00	000000000010 00	000000000000 00
000000100000 00	000000000000 00	000000000010 00	000000000000 00	000000010000 00	000000000000 00	000000000001 00	000000000000 00
000000010000 00	000000000000 00	000000000001 00	000000000000 00	000000001000 00	000000000000 00	000000000000 10	000000000000 00
000000001000 00	000000000000 00	000000000000 10	000000000000 00	000000000100 00	000000000000 00	000000000000 01	000000000000 00
000000000100 00	000000000000 00	000000000000 01	000000000000 00	000000000010 00	000000000000 00	100000000000 00	000000000000 00
000000000010 00	000000000000 00	100000000000 00	000000000000 00	000000000001 00	000000000000 00	010000000000 00	000000000000 00
000000000001 00	000000000000 00	010000000000 00	000000000000 00	000000000000 10	000000000000 00	001000000000 00	000000000000 00
000000000000 10	000000000000 00	001000000000 00	000000000000 00	000000000000 01	000000000000 00	000100000000 00	000000000000 00

000000000000 01	000000000000 00	000100000000 00	000000000000 00	100000000000 00	000000000000 00	000010000000 00	000000000000 00
000000000000 00	000100000000 00	000000000000 00	001000000000 00	000000000000 00	010000000000 00	000000000000 00	000100000000 00
000000000000 00	000010000000 00	000000000000 00	000100000000 00	000000000000 00	001000000000 00	000000000000 00	000010000000 00
000000000000 00	000001000000 00	000000000000 00	000010000000 00	000000000000 00	000100000000 00	000000000000 00	000001000000 00
000000000000 00	000000100000 00	000000000000 00	000001000000 00	000000000000 00	000010000000 00	000000000000 00	000000100000 00
000000000000 00	000000010000 00	000000000000 00	000000100000 00	000000000000 00	000001000000 00	000000000000 00	000000010000 00
000000000000 00	000000001000 00	000000000000 00	000000010000 00	000000000000 00	000000100000 00	000000000000 00	000000001000 00
000000000000 00	000000000100 00	000000000000 00	000000001000 00	000000000000 00	000000010000 00	000000000000 00	000000000100 00
000000000000 00	000000000010 00	000000000000 00	000000000100 00	000000000000 00	000000001000 00	000000000000 00	000000000010 00
000000000000 00	000000000001 00	000000000000 00	000000000010 00	000000000000 00	000000000100 00	000000000000 00	000000000001 00
000000000000 00	000000000000 10	000000000000 00	000000000001 00	000000000000 00	000000000010 00	000000000000 00	000000000000 10
000000000000 00	000000000000 01	000000000000 00	000000000000 10	000000000000 00	000000000001 00	000000000000 00	000000000000 01
000000000000 00	100000000000 00	000000000000 00	000000000000 01	000000000000 00	000000000000 10	000000000000 00	100000000000 00
000000000000 00	010000000000 00	000000000000 00	100000000000 00	000000000000 00	000000000000 01	000000000000 00	010000000000 00
000000000000 00	100000000000 00	000000000000 00	010000000000 00	000000000000 00	100000000000 00	000000000000 00	001000000000 00
100000000000 00	000000000000 00	000000100000 00	000000000000 00	000001000000 00	000000000000 00	000010000000 00	000000000000 00
010000000000 00	000000000000 00	000000010000 00	000000000000 00	000000100000 00	000000000000 00	000001000000 00	000000000000 00
001000000000 00	000000000000 00	000000001000 00	000000000000 00	000000010000 00	000000000000 00	000000100000 00	000000000000 00
000100000000 00	000000000000 00	000000000100 00	000000000000 00	000000001000 00	000000000000 00	000000010000 00	000000000000 00
000010000000 00	000000000000 00	000000000010 00	000000000000 00	000000000100 00	000000000000 00	000000001000 00	000000000000 00
000001000000 00	000000000000 00	000000000001 00	000000000000 00	000000000010 00	000000000000 00	000000000100 00	000000000000 00
000000100000 00	000000000000 00	000000000000 10	000000000000 00	000000000001 00	000000000000 00	000000000010 00	000000000000 00
000000010000 00	000000000000 00	000000000000 01	000000000000 00	000000000000 10	000000000000 00	000000000001 00	000000000000 00
000000001000 00	000000000000 00	100000000000 00	000000000000 00	000000000000 01	000000000000 00	000000000000 10	000000000000 00
000000000100 00	000000000000 00	010000000000 00	000000000000 00	100000000000 00	000000000000 00	000000000000 01	000000000000 00
000000000010 00	000000000000 00	001000000000 00	000000000000 00	010000000000 00	000000000000 00	100000000000 00	000000000000 00
000000000001 00	000000000000 00	000100000000 00	000000000000 00	001000000000 00	000000000000 00	010000000000 00	000000000000 00
000000000000 10	000000000000 00	000010000000 00	000000000000 00	000100000000 00	000000000000 00	001000000000 00	000000000000 00
000000000000 01	000000000000 00	000001000000 00	000000000000 00	000010000000 00	000000000000 00	000100000000 00	000000000000 00
000000000000 00	000010000000 00	000000000000 00	000001000000 00	000000000000 00	000000100000 00	000000000000 00	100000000000 00
000000000000 00	000001000000 00	000000000000 00	000000100000 00	000000000000 00	000000010000 00	000000000000 00	000100000000 00
000000000000 00	000000100000 00	000000000000 00	000000010000 00	000000000000 00	000000001000 00	000000000000 00	000010000000 00
000000000000 00	000000010000 00	000000000000 00	000000001000 00	000000000000 00	000000000100 00	000000000000 00	000001000000 00
000000000000 00	000000001000 00	000000000000 00	000000000100 00	000000000000 00	000000000010 00	000000000000 00	000000100000 00
000000000000 00	000000000100 00	000000000000 00	000000000010 00	000000000000 00	000000000001 00	000000000000 00	000000010000 00
000000000000 00	000000000010 00	000000000000 00	000000000001 00	000000000000 00	000000000000 10	000000000000 00	000000001000 00
000000000000 00	000000000001 00	000000000000 00	000000000000 10	000000000000 00	000000000000 01	000000000000 00	000000000100 00
000000000000 00	000000000000 10	000000000000 00	000000000000 01	000000000000 00	100000000000 00	000000000000 00	000000000010 00
000000000000 00	000000000000 01	000000000000 00	100000000000 00	000000000000 00	010000000000 00	000000000000 00	000000000001 00
000000000000 00	100000000000 00	000000000000 00	010000000000 00	000000000000 00	001000000000 00	000000000000 00	000000000000 10
000000000000 00	010000000000 00	000000000000 00	001000000000 00	000000000000 00	000100000000 00	000000000000 00	000000000000 01
000000000000 00	001000000000 00	000000000000 00	000100000000 00	000000000000 00	000010000000 00	000000000000 00	100000000000 00
000000000000 00	000100000000 00	000000000000 00	000010000000 00	000000000000 00	000001000000 00	000000000000 00	010000000000 00
100000000000 00	000000000000 00	010000000000 00	000000000000 00	001000000000 00	000000000000 00	000100000000 00	000000000000 00

010000000000 00	000000000000 00	001000000000 00	000000000000 00	000100000000 00	000000000000 00	000010000000 00	000000000000 00
001000000000 00	000000000000 00	000100000000 00	000000000000 00	000010000000 00	000000000000 00	000001000000 00	000000000000 00
000100000000 00	000000000000 00	000010000000 00	000000000000 00	000001000000 00	000000000000 00	000000100000 00	000000000000 00
000010000000 00	000000000000 00	000001000000 00	000000000000 00	000000100000 00	000000000000 00	000000010000 00	000000000000 00
000001000000 00	000000000000 00	000000100000 00	000000000000 00	000000010000 00	000000000000 00	000000001000 00	000000000000 00
000000100000 00	000000000000 00	000000010000 00	000000000000 00	000000001000 00	000000000000 00	000000000100 00	000000000000 00
000000010000 00	000000000000 00	000000001000 00	000000000000 00	000000000100 00	000000000000 00	000000000010 00	000000000000 00
000000001000 00	000000000000 00	000000000100 00	000000000000 00	000000000010 00	000000000000 00	000000000001 00	000000000000 00
000000000100 00	000000000000 00	000000000010 00	000000000000 00	000000000001 00	000000000000 00	000000000000 10	000000000000 00
000000000010 00	000000000000 00	000000000001 00	000000000000 00	000000000000 10	000000000000 00	000000000000 01	000000000000 00
000000000001 00	000000000000 00	000000000000 10	000000000000 00	000000000000 01	000000000000 00	100000000000 00	000000000000 00
000000000000 10	000000000000 00	000000000000 01	000000000000 00	100000000000 00	000000000000 00	010000000000 00	000000000000 00
000000000000 01	000000000000 00	100000000000 00	000000000000 00	010000000000 00	000000000000 00	100000000000 00	000000000000 00
000000000000 00	000001000000 00	000000000000 00	010000000000 00	000000000000 00	000010000000 00	000000000000 00	010000000000 00
000000000000 00	000000100000 00	000000000000 00	001000000000 00	000000000000 00	000001000000 00	000000000000 00	001000000000 00
000000000000 00	000000010000 00	000000000000 00	000100000000 00	000000000000 00	000000100000 00	000000000000 00	000100000000 00
000000000000 00	000000001000 00	000000000000 00	000010000000 00	000000000000 00	000000010000 00	000000000000 00	000010000000 00
000000000000 00	000000000100 00	000000000000 00	000001000000 00	000000000000 00	000000001000 00	000000000000 00	000001000000 00
000000000000 00	000000000010 00	000000000000 00	000000100000 00	000000000000 00	000000000100 00	000000000000 00	000000100000 00
000000000000 00	000000000001 00	000000000000 00	000000010000 00	000000000000 00	000000000010 00	000000000000 00	000000010000 00
000000000000 00	000000000000 10	000000000000 00	000000001000 00	000000000000 00	000000000001 00	000000000000 00	000000001000 00
000000000000 00	000000000000 01	000000000000 00	000000000100 00	000000000000 00	000000000000 10	000000000000 00	000000000100 00
000000000000 00	100000000000 00	000000000000 00	000000000010 00	000000000000 00	000000000000 01	000000000000 00	000000000010 00
000000000000 00	010000000000 00	000000000000 00	000000000001 00	000000000000 00	100000000000 00	000000000000 00	000000000001 00
000000000000 00	001000000000 00	000000000000 00	000000000000 10	000000000000 00	010000000000 00	000000000000 00	000000000000 10
000000000000 00	000100000000 00	000000000000 00	000000000000 01	000000000000 00	001000000000 00	000000000000 00	000000000000 01
000000000000 00	000010000000 00	000000000000 00	100000000000 00	000000000000 00	000100000000 00	000000000000 00	100000000000 00
100000000000 00	000000000000 00	000100000000 00	000000000000 00	000000100000 00	000000000000 00	001000000000 00	000000000000 00
010000000000 00	000000000000 00	000010000000 00	000000000000 00	000000010000 00	000000000000 00	000100000000 00	000000000000 00
001000000000 00	000000000000 00	000001000000 00	000000000000 00	000000001000 00	000000000000 00	000010000000 00	000000000000 00
000100000000 00	000000000000 00	000000100000 00	000000000000 00	000000000100 00	000000000000 00	000001000000 00	000000000000 00
000010000000 00	000000000000 00	000000010000 00	000000000000 00	000000000010 00	000000000000 00	000000100000 00	000000000000 00
000001000000 00	000000000000 00	000000001000 00	000000000000 00	000000000001 00	000000000000 00	000000010000 00	000000000000 00
000000100000 00	000000000000 00	000000000100 00	000000000000 00	000000000000 10	000000000000 00	000000001000 00	000000000000 00
000000010000 00	000000000000 00	000000000010 00	000000000000 00	000000000000 01	000000000000 00	000000000100 00	000000000000 00
000000001000 00	000000000000 00	000000000001 00	000000000000 00	100000000000 00	000000000000 00	000000000010 00	000000000000 00
000000000100 00	000000000000 00	000000000000 10	000000000000 00	010000000000 00	000000000000 00	000000000001 00	000000000000 00
000000000010 00	000000000000 00	000000000000 01	000000000000 00	001000000000 00	000000000000 00	000000000000 10	000000000000 00
000000000001 00	000000000000 00	100000000000 00	000000000000 00	000100000000 00	000000000000 00	000000000000 01	000000000000 00
000000000000 10	000000000000 00	010000000000 00	000000000000 00	000010000000 00	000000000000 00	100000000000 00	000000000000 00
000000000000 01	000000000000 00	100000000000 00	000000000000 00	000001000000 00	000000000000 00	010000000000 00	000000000000 00
000000000000 00	000000100000 00	000000000000 00	000010000000 00	000000000000 00	001000000000 00	000000000000 00	100000000000 00
000000000000 00	000000010000 00	000000000000 00	000001000000 00	000000000000 00	000100000000 00	000000000000 00	010000000000 00
000000000000 00	000000001000 00	000000000000 00	000000100000 00	000000000000 00	000010000000 00	000000000000 00	001000000000 00

000000000000 00	000000000100 00	000000000000 00	000000010000 00	000000000000 00	000001000000 00	000000000000 00	000100000000 00
000000000000 00	000000000010 00	000000000000 00	000000001000 00	000000000000 00	000000100000 00	000000000000 00	000010000000 00
000000000000 00	000000000001 00	000000000000 00	000000000100 00	000000000000 00	000000010000 00	000000000000 00	000001000000 00
000000000000 00	000000000000 10	000000000000 00	000000000010 00	000000000000 00	000000001000 00	000000000000 00	000000100000 00
000000000000 00	000000000000 01	000000000000 00	000000000001 00	000000000000 00	000000000100 00	000000000000 00	000000010000 00
000000000000 00	100000000000 00	000000000000 00	000000000000 10	000000000000 00	000000000010 00	000000000000 00	000000001000 00
000000000000 00	010000000000 00	000000000000 00	000000000000 01	000000000000 00	000000000001 00	000000000000 00	000000000100 00
000000000000 00	001000000000 00	000000000000 00	100000000000 00	000000000000 00	000000000000 10	000000000000 00	000000000010 00
000000000000 00	000100000000 00	000000000000 00	010000000000 00	000000000000 00	000000000000 01	000000000000 00	000000000001 00
000000000000 00	000010000000 00	000000000000 00	001000000000 00	000000000000 00	100000000000 00	000000000000 00	000000000000 10
000000000000 00	000001000000 00	000000000000 00	000100000000 00	000000000000 00	010000000000 00	000000000000 00	000000000000 01
100000000000 00	000000000000 00	000001000000 00	000000000000 00	000100000000 00	000000000000 00	010000000000 00	000000000000 00
010000000000 00	000000000000 00	000000100000 00	000000000000 00	000010000000 00	000000000000 00	001000000000 00	000000000000 00
001000000000 00	000000000000 00	000000010000 00	000000000000 00	000001000000 00	000000000000 00	000100000000 00	000000000000 00
000100000000 00	000000000000 00	000000001000 00	000000000000 00	000000100000 00	000000000000 00	000010000000 00	000000000000 00
000010000000 00	000000000000 00	000000000100 00	000000000000 00	000000010000 00	000000000000 00	000001000000 00	000000000000 00
000001000000 00	000000000000 00	000000000010 00	000000000000 00	000000001000 00	000000000000 00	000000100000 00	000000000000 00
000000100000 00	000000000000 00	000000000001 00	000000000000 00	000000000100 00	000000000000 00	000000010000 00	000000000000 00
000000010000 00	000000000000 00	000000000000 10	000000000000 00	000000000010 00	000000000000 00	000000001000 00	000000000000 00
000000001000 00	000000000000 00	000000000000 01	000000000000 00	000000000001 00	000000000000 00	000000000100 00	000000000000 00
000000000100 00	000000000000 00	100000000000 00	000000000000 00	000000000000 10	000000000000 00	000000000010 00	000000000000 00
000000000010 00	000000000000 00	010000000000 00	000000000000 00	000000000000 01	000000000000 00	000000000001 00	000000000000 00
000000000001 00	000000000000 00	001000000000 00	000000000000 00	100000000000 00	000000000000 00	000000000000 10	000000000000 00
000000000000 10	000000000000 00	000100000000 00	000000000000 00	010000000000 00	000000000000 00	000000000000 01	000000000000 00
000000000000 01	000000000000 00	000010000000 00	000000000000 00	100000000000 00	000000000000 00	100000000000 00	000000000000 00

A4.3. Sub-pulses times after delay

Encoder	Signal Delay	Time (ns)
Encoder 1	Signal Delay1	66
	Signal Delay 2	93
	Signal Delay 3	122
	Signal Delay 4	149
Encoder2	Signal Delay1	229
	Signal Delay 2	256
	Signal Delay 3	447
	Signal Delay 4	312
Encoder 3	Signal Delay1	392
	Signal Delay 2	419
	Signal Delay 3	448
	Signal Delay 4	475
Encoder 4	Signal Delay1	555
	Signal Delay 2	582

	Signal Delay 3	611
	Signal Delay 4	638
Encoder 5	Signal Delay1	718
	Signal Delay 2	745
	Signal Delay 3	774
	Signal Delay 4	801
Encoder 6	Signal Delay1	881
	Signal Delay 2	908
	Signal Delay 3	937
	Signal Delay 4	964
Encoder 7	Signal Delay1	1044
	Signal Delay 2	1071
	Signal Delay 3	1100
	Signal Delay 4	1127
Encoder 8	Signal Delay1	1207
	Signal Delay 2	1234
	Signal Delay 3	1263
	Signal Delay 4	1290
Encoder 9	Signal Delay1	1370
	Signal Delay 2	1397
	Signal Delay 3	1426
	Signal Delay 4	1453
Encoder 10	Signal Delay1	1533
	Signal Delay 2	1560
	Signal Delay 3	1589
	Signal Delay 4	1616
Encoder 11	Signal Delay1	1696
	Signal Delay 2	1723
	Signal Delay 3	1752
	Signal Delay 4	1779
Encoder 12	Signal Delay1	1859
	Signal Delay 2	1886
	Signal Delay 3	1915
	Signal Delay 4	1942
Encoder 13	Signal Delay1	2022
	Signal Delay 2	2049
	Signal Delay 3	2078
	Signal Delay 4	2105
Encoder 14	Signal Delay1	2158
	Signal Delay 2	2186
	Signal Delay 3	2214
	Signal Delay 4	2242
Encoder 15	Signal Delay1	2321

	Signal Delay 2	2349
	Signal Delay 3	2377
	Signal Delay 4	2405
Encoder 16	Signal Delay1	2484
	Signal Delay 2	2512
	Signal Delay 3	2540
	Signal Delay 4	2568
Encoder 17	Signal Delay1	2647
	Signal Delay 2	2675
	Signal Delay 3	2703
	Signal Delay 4	2731
Encoder 18	Signal Delay1	2810
	Signal Delay 2	2838
	Signal Delay 3	2866
	Signal Delay 4	2894
Encoder 19	Signal Delay1	2973
	Signal Delay 2	3001
	Signal Delay 3	3029
	Signal Delay 4	3057
Encoder 20	Signal Delay1	3136
	Signal Delay 2	3164
	Signal Delay 3	3192
	Signal Delay 4	3220
Encoder 21	Signal Delay1	3299
	Signal Delay 2	3327
	Signal Delay 3	3355
	Signal Delay 4	3383
Encoder 22	Signal Delay1	3462
	Signal Delay 2	3490
	Signal Delay 3	3518
	Signal Delay 4	3546
Encoder 23	Signal Delay1	3625
	Signal Delay 2	3653
	Signal Delay 3	3681
	Signal Delay 4	3709
Encoder 24	Signal Delay1	3788
	Signal Delay 2	3816
	Signal Delay 3	3844
	Signal Delay 4	3872
Encoder 25	Signal Delay1	3951
	Signal Delay 2	3979
	Signal Delay 3	4007
	Signal Delay 4	4035

Encoder 26	Signal Delay1	4114
	Signal Delay 2	4142
	Signal Delay 3	4170
	Signal Delay 4	4198
Encoder 27	Signal Delay1	4278
	Signal Delay 2	4308
	Signal Delay 3	4338
	Signal Delay 4	4366
Encoder 28	Signal Delay1	4441
	Signal Delay 2	4471
	Signal Delay 3	4501
	Signal Delay 4	4529
Encoder 29	Signal Delay1	4604
	Signal Delay 2	4634
	Signal Delay 3	4664
	Signal Delay 4	4692
Encoder 30	Signal Delay1	4767
	Signal Delay 2	4797
	Signal Delay 3	4827
	Signal Delay 4	4855
Encoder 31	Signal Delay1	4930
	Signal Delay 2	4960
	Signal Delay 3	4990
	Signal Delay 4	5018
Encoder 32	Signal Delay1	5093
	Signal Delay 2	5123
	Signal Delay 3	5153
	Signal Delay 4	5181
Encoder 33	Signal Delay1	5256
	Signal Delay 2	5286
	Signal Delay 3	5316
	Signal Delay 4	5344
Encoder 34	Signal Delay1	5419
	Signal Delay 2	5449
	Signal Delay 3	5479
	Signal Delay 4	5507
Encoder 35	Signal Delay1	5583
	Signal Delay 2	5613
	Signal Delay 3	5629
	Signal Delay 4	5648
Encoder 36	Signal Delay1	5746
	Signal Delay 2	5776
	Signal Delay 3	5792

	Signal Delay 4	5820
Encoder 37	Signal Delay1	5909
	Signal Delay 2	5925
	Signal Delay 3	5955
	Signal Delay 4	5983
Encoder 38	Signal Delay1	6072
	Signal Delay 2	6088
	Signal Delay 3	6118
	Signal Delay 4	6146
Encoder 39	Signal Delay1	6221
	Signal Delay 2	6251
	Signal Delay 3	6281
	Signal Delay 4	6309
Encoder 40	Signal Delay1	6370
	Signal Delay 2	6400
	Signal Delay 3	6430
	Signal Delay 4	6460
Encoder 41	Signal Delay1	6533
	Signal Delay 2	6563
	Signal Delay 3	6593
	Signal Delay 4	6623
Encoder 42	Signal Delay1	6696
	Signal Delay 2	6726
	Signal Delay 3	6756
	Signal Delay 4	6786
Encoder 43	Signal Delay1	6859
	Signal Delay 2	6889
	Signal Delay 3	6919
	Signal Delay 4	6949
Encoder 44	Signal Delay1	7022
	Signal Delay 2	7052
	Signal Delay 3	7082
	Signal Delay 4	7112
Encoder 45	Signal Delay1	7185
	Signal Delay 2	7215
	Signal Delay 3	7245
	Signal Delay 4	7275
Encoder 46	Signal Delay1	7348
	Signal Delay 2	7378
	Signal Delay 3	7408
	Signal Delay 4	7438
Encoder 47	Signal Delay1	7511
	Signal Delay 2	7541

	Signal Delay 3	7571
	Signal Delay 4	7587
Encoder 48	Signal Delay1	7674
	Signal Delay 2	7704
	Signal Delay 3	7734
	Signal Delay 4	7750
Encoder 49	Signal Delay1	7837
	Signal Delay 2	7867
	Signal Delay 3	7883
	Signal Delay 4	7913
Encoder 50	Signal Delay1	8000
	Signal Delay 2	8030
	Signal Delay 3	8046
	Signal Delay 4	8076
Encoder 51	Signal Delay1	8163
	Signal Delay 2	8179
	Signal Delay 3	8208
	Signal Delay 4	8239
Encoder 52	Signal Delay1	8326
	Signal Delay 2	8342
	Signal Delay 3	8372
	Signal Delay 4	8402
Encoder 53	Signal Delay1	8491
	Signal Delay 2	8523
	Signal Delay 3	8548
	Signal Delay 4	8577
Encoder 54	Signal Delay1	8654
	Signal Delay 2	8686
	Signal Delay 3	8711
	Signal Delay 4	8740
Encoder 55	Signal Delay1	8817
	Signal Delay 2	8849
	Signal Delay 3	8874
	Signal Delay 4	8903
Encoder 56	Signal Delay1	8980
	Signal Delay 2	9012
	Signal Delay 3	9037
	Signal Delay 4	9066
Encoder 57	Signal Delay1	9143
	Signal Delay 2	9175
	Signal Delay 3	9200
	Signal Delay 4	9229
Encoder 58	Signal Delay1	9306

	Signal Delay 2	9338
	Signal Delay 3	9363
	Signal Delay 4	9392
Encoder 59	Signal Delay1	9469
	Signal Delay 2	9501
	Signal Delay 3	9526
	Signal Delay 4	9555
Encoder 60	Signal Delay1	9632
	Signal Delay 2	9664
	Signal Delay 3	9689
	Signal Delay 4	9718
Encoder 61	Signal Delay1	9795
	Signal Delay 2	9813
	Signal Delay 3	9852
	Signal Delay 4	9881
Encoder 62	Signal Delay1	9959
	Signal Delay 2	9977
	Signal Delay 3	10016
	Signal Delay 4	10031
Encoder 63	Signal Delay1	10122
	Signal Delay 2	10140
	Signal Delay 3	10165
	Signal Delay 4	10194
Encoder 64	Signal Delay1	10271
	Signal Delay 2	10303
	Signal Delay 3	10328
	Signal Delay 4	10357
Encoder 65	Signal Delay1	10434
	Signal Delay 2	10466
	Signal Delay 3	10491
	Signal Delay 4	10520
Encoder 66	Signal Delay1	10582
	Signal Delay 2	10614
	Signal Delay 3	10639
	Signal Delay 4	10671
Encoder 67	Signal Delay1	10745
	Signal Delay 2	10777
	Signal Delay 3	10802
	Signal Delay 4	10834
Encoder 68	Signal Delay1	10908
	Signal Delay 2	10940
	Signal Delay 3	10965
	Signal Delay 4	10997

Encoder 69	Signal Delay1	11071
	Signal Delay 2	11103
	Signal Delay 3	11128
	Signal Delay 4	11160
Encoder 70	Signal Delay1	11234
	Signal Delay 2	11266
	Signal Delay 3	11291
	Signal Delay 4	11323
Encoder 71	Signal Delay1	11397
	Signal Delay 2	11429
	Signal Delay 3	11454
	Signal Delay 4	11486
Encoder 72	Signal Delay1	11560
	Signal Delay 2	11592
	Signal Delay 3	11617
	Signal Delay 4	11649
Encoder 73	Signal Delay1	11723
	Signal Delay 2	11755
	Signal Delay 3	11780
	Signal Delay 4	11812
Encoder 74	Signal Delay1	11886
	Signal Delay 2	11918
	Signal Delay 3	11943
	Signal Delay 4	11961
Encoder 75	Signal Delay1	12049
	Signal Delay 2	12067
	Signal Delay 3	12106
	Signal Delay 4	12124
Encoder 76	Signal Delay1	12212
	Signal Delay 2	12230
	Signal Delay 3	12269
	Signal Delay 4	12287
Encoder 77	Signal Delay1	12375
	Signal Delay 2	12393
	Signal Delay 3	12432
	Signal Delay 4	12450
Encoder 78	Signal Delay1	12538
	Signal Delay 2	12556
	Signal Delay 3	12581
	Signal Delay 4	12613
Encoder 79	Signal Delay1	12704
	Signal Delay 2	12731
	Signal Delay 3	12758

	Signal Delay 4	12788
Encoder 80	Signal Delay1	12867
	Signal Delay 2	12894
	Signal Delay 3	12921
	Signal Delay 4	12951
Encoder 81	Signal Delay1	13030
	Signal Delay 2	13057
	Signal Delay 3	13084
	Signal Delay 4	13114
Encoder 82	Signal Delay1	13193
	Signal Delay 2	13220
	Signal Delay 3	13247
	Signal Delay 4	13277
Encoder 83	Signal Delay1	13356
	Signal Delay 2	13383
	Signal Delay 3	13410
	Signal Delay 4	13440
Encoder 84	Signal Delay1	13519
	Signal Delay 2	13546
	Signal Delay 3	13573
	Signal Delay 4	13603
Encoder 85	Signal Delay1	13682
	Signal Delay 2	13709
	Signal Delay 3	13736
	Signal Delay 4	13604
Encoder 86	Signal Delay1	13845
	Signal Delay 2	13872
	Signal Delay 3	13899
	Signal Delay 4	13929
Encoder 87	Signal Delay1	14008
	Signal Delay 2	14035
	Signal Delay 3	14062
	Signal Delay 4	14092
Encoder 88	Signal Delay1	14171
	Signal Delay 2	14198
	Signal Delay 3	14225
	Signal Delay 4	14255
Encoder 89	Signal Delay1	14321
	Signal Delay 2	14362
	Signal Delay 3	14389
	Signal Delay 4	14405
Encoder 90	Signal Delay1	14484
	Signal Delay 2	14511

	Signal Delay 3	14552
	Signal Delay 4	14568
Encoder 91	Signal Delay1	14647
	Signal Delay 2	14674
	Signal Delay 3	14701
	Signal Delay 4	14731
Encoder 92	Signal Delay1	14794
	Signal Delay 2	14828
	Signal Delay 3	14855
	Signal Delay 4	14882
Encoder 93	Signal Delay1	14957
	Signal Delay 2	14991
	Signal Delay 3	15018
	Signal Delay 4	15045
Encoder 94	Signal Delay1	15120
	Signal Delay 2	15154
	Signal Delay 3	15181
	Signal Delay 4	15208
Encoder 95	Signal Delay1	15283
	Signal Delay 2	15317
	Signal Delay 3	15344
	Signal Delay 4	15371
Encoder 96	Signal Delay1	15446
	Signal Delay 2	15480
	Signal Delay 3	15507
	Signal Delay 4	15534
Encoder 97	Signal Delay1	15609
	Signal Delay 2	15643
	Signal Delay 3	15670
	Signal Delay 4	15697
Encoder 98	Signal Delay1	15772
	Signal Delay 2	15806
	Signal Delay 3	15833
	Signal Delay 4	15860
Encoder 99	Signal Delay1	15935
	Signal Delay 2	15955
	Signal Delay 3	15996
	Signal Delay 4	16023
Encoder 100	Signal Delay1	16098
	Signal Delay 2	16118
	Signal Delay 3	16145
	Signal Delay 4	16186
Encoder 101	Signal Delay1	16261

	Signal Delay 2	16281
	Signal Delay 3	16308
	Signal Delay 4	16335
Encoder 102	Signal Delay1	16424
	Signal Delay 2	16444
	Signal Delay 3	16471
	Signal Delay 4	16498
Encoder 103	Signal Delay1	16587
	Signal Delay 2	16607
	Signal Delay 3	16633
	Signal Delay 4	16661
Encoder 104	Signal Delay1	16750
	Signal Delay 2	16770
	Signal Delay 3	16797
	Signal Delay 4	16824
Encoder 105	Signal Delay1	16917
	Signal Delay 2	16946
	Signal Delay 3	16975
	Signal Delay 4	16997
Encoder 106	Signal Delay1	17080
	Signal Delay 2	17109
	Signal Delay 3	17138
	Signal Delay 4	17162
Encoder 107	Signal Delay1	17243
	Signal Delay 2	17272
	Signal Delay 3	17301
	Signal Delay 4	17325
Encoder 108	Signal Delay1	17406
	Signal Delay 2	17435
	Signal Delay 3	17464
	Signal Delay 4	17488
Encoder 109	Signal Delay1	17569
	Signal Delay 2	17598
	Signal Delay 3	17627
	Signal Delay 4	17651
Encoder 110	Signal Delay1	17732
	Signal Delay 2	17761
	Signal Delay 3	17790
	Signal Delay 4	17814
Encoder 111	Signal Delay1	17895
	Signal Delay 2	17924
	Signal Delay 3	17953
	Signal Delay 4	17977

Encoder 112	Signal Delay1	18058
	Signal Delay 2	18087
	Signal Delay 3	18116
	Signal Delay 4	18140
Encoder 113	Signal Delay1	18221
	Signal Delay 2	18250
	Signal Delay 3	18265
	Signal Delay 4	18303
Encoder 114	Signal Delay1	18384
	Signal Delay 2	18399
	Signal Delay 3	18428
	Signal Delay 4	18466
Encoder 115	Signal Delay1	18533
	Signal Delay 2	18562
	Signal Delay 3	18591
	Signal Delay 4	18629
Encoder 116	Signal Delay1	18697
	Signal Delay 2	18726
	Signal Delay 3	18755
	Signal Delay 4	18779
Encoder 117	Signal Delay1	18860
	Signal Delay 2	18889
	Signal Delay 3	18918
	Signal Delay 4	18942
Encoder 118	Signal Delay1	19006
	Signal Delay 2	19035
	Signal Delay 3	19064
	Signal Delay 4	19093
Encoder 119	Signal Delay1	19169
	Signal Delay 2	19198
	Signal Delay 3	19227
	Signal Delay 4	19256
Encoder 120	Signal Delay1	19332
	Signal Delay 2	19361
	Signal Delay 3	19390
	Signal Delay 4	19419
Encoder 121	Signal Delay1	19495
	Signal Delay 2	19524
	Signal Delay 3	19553
	Signal Delay 4	19582
Encoder 122	Signal Delay1	19658
	Signal Delay 2	19687
	Signal Delay 3	19716

	Signal Delay 4	19745
Encoder 123	Signal Delay1	19821
	Signal Delay 2	19850
	Signal Delay 3	19879
	Signal Delay 4	19908
Encoder 124	Signal Delay1	19984
	Signal Delay 2	20013
	Signal Delay 3	20042
	Signal Delay 4	20071
Encoder 125	Signal Delay1	20147
	Signal Delay 2	20176
	Signal Delay 3	20205
	Signal Delay 4	20234
Encoder 126	Signal Delay1	20310
	Signal Delay 2	20339
	Signal Delay 3	20368
	Signal Delay 4	20397
Encoder127	Signal Delay1	20473
	Signal Delay 2	20502
	Signal Delay 3	20531
	Signal Delay 4	20560
Encoder128	Signal Delay1	20636
	Signal Delay 2	20665
	Signal Delay 3	20694
	Signal Delay 4	20709